

**APPLICATION OF ARTIFICIAL NEURAL NETWORKS  
TO  
DISTANCE PROTECTION**

---

By  
**WEIGUO QI**

*B.Sc., Jiangxi University of Technology, China, 1982*  
*M.Sc., Nanjing Automation Research Institute, China, 1984*

A Thesis Submitted to the  
**The Faculty of Graduate Studies**  
in partial fulfillment of the requirements for the degree of  
**DOCTOR OF PHILOSOPHY**

**Department of Electrical and Computer Engineering**  
**The University of Manitoba**  
**Winnipeg, Manitoba, Canada**

© WEIGUO QI, May, 1996



National Library  
of Canada

Bibliothèque nationale  
du Canada

Acquisitions and  
Bibliographic Services Branch

Direction des acquisitions et  
des services bibliographiques

395 Wellington Street  
Ottawa, Ontario  
K1A 0N4

395, rue Wellington  
Ottawa (Ontario)  
K1A 0N4

*Your file* *Votre référence*

*Our file* *Notre référence*

**The author has granted an irrevocable non-exclusive licence allowing the National Library of Canada to reproduce, loan, distribute or sell copies of his/her thesis by any means and in any form or format, making this thesis available to interested persons.**

**L'auteur a accordé une licence irrévocable et non exclusive permettant à la Bibliothèque nationale du Canada de reproduire, prêter, distribuer ou vendre des copies de sa thèse de quelque manière et sous quelque forme que ce soit pour mettre des exemplaires de cette thèse à la disposition des personnes intéressées.**

**The author retains ownership of the copyright in his/her thesis. Neither the thesis nor substantial extracts from it may be printed or otherwise reproduced without his/her permission.**

**L'auteur conserve la propriété du droit d'auteur qui protège sa thèse. Ni la thèse ni des extraits substantiels de celle-ci ne doivent être imprimés ou autrement reproduits sans son autorisation.**

ISBN 0-612-16235-4

**Canada**

Name \_\_\_\_\_

*Dissertation Abstracts International* and *Masters Abstracts International* are arranged by broad, general subject categories. Please select the one subject which most nearly describes the content of your dissertation or thesis. Enter the corresponding four-digit code in the spaces provided.

0544

UMI

SUBJECT TERM

SUBJECT CODE

## Subject Categories

## THE HUMANITIES AND SOCIAL SCIENCES

**COMMUNICATIONS AND THE ARTS**  
 Architecture ..... 0729  
 Art History ..... 0377  
 Cinema ..... 0900  
 Dance ..... 0378  
 Fine Arts ..... 0357  
 Information Science ..... 0723  
 Journalism ..... 0391  
 Library Science ..... 0399  
 Mass Communications ..... 0708  
 Music ..... 0413  
 Speech Communication ..... 0459  
 Theater ..... 0465

**EDUCATION**  
 General ..... 0515  
 Administration ..... 0514  
 Adult and Continuing ..... 0516  
 Agricultural ..... 0517  
 Art ..... 0273  
 Bilingual and Multicultural ..... 0282  
 Business ..... 0688  
 Community College ..... 0275  
 Curriculum and Instruction ..... 0727  
 Early Childhood ..... 0518  
 Elementary ..... 0524  
 Finance ..... 0277  
 Guidance and Counseling ..... 0519  
 Health ..... 0680  
 Higher ..... 0745  
 History of ..... 0520  
 Home Economics ..... 0278  
 Industrial ..... 0521  
 Language and Literature ..... 0279  
 Mathematics ..... 0280  
 Music ..... 0522  
 Philosophy of ..... 0998  
 Physical ..... 0523

Psychology ..... 0525  
 Reading ..... 0535  
 Religious ..... 0527  
 Sciences ..... 0714  
 Secondary ..... 0533  
 Social Sciences ..... 0534  
 Sociology of ..... 0340  
 Special ..... 0529  
 Teacher Training ..... 0530  
 Technology ..... 0710  
 Tests and Measurements ..... 0288  
 Vocational ..... 0747

## LANGUAGE, LITERATURE AND LINGUISTICS

**LANGUAGE**  
 General ..... 0679  
 Ancient ..... 0289  
 Linguistics ..... 0290  
 Modern ..... 0291

**LITERATURE**  
 General ..... 0401  
 Classical ..... 0294  
 Comparative ..... 0295  
 Medieval ..... 0297  
 Modern ..... 0298  
 African ..... 0316  
 American ..... 0591  
 Asian ..... 0305  
 Canadian (English) ..... 0352  
 Canadian (French) ..... 0355  
 English ..... 0593  
 Germanic ..... 0311  
 Latin American ..... 0312  
 Middle Eastern ..... 0315  
 Romance ..... 0313  
 Slavic and East European ..... 0314

## PHILOSOPHY, RELIGION AND THEOLOGY

Philosophy ..... 0422  
 Religion  
 General ..... 0318  
 Biblical Studies ..... 0321  
 Clergy ..... 0319  
 History of ..... 0320  
 Philosophy of ..... 0322  
 Theology ..... 0469

## SOCIAL SCIENCES

American Studies ..... 0323  
 Anthropology  
 Archaeology ..... 0324  
 Cultural ..... 0326  
 Physical ..... 0327  
 Business Administration  
 General ..... 0310  
 Accounting ..... 0272  
 Banking ..... 0770  
 Management ..... 0454  
 Marketing ..... 0338  
 Canadian Studies ..... 0385  
 Economics  
 General ..... 0501  
 Agricultural ..... 0503  
 Commerce-Business ..... 0505  
 Finance ..... 0508  
 History ..... 0509  
 Labor ..... 0510  
 Theory ..... 0511  
 Folklore ..... 0358  
 Geography ..... 0366  
 Gerontology ..... 0351  
 History  
 General ..... 0578

Ancient ..... 0579  
 Medieval ..... 0581  
 Modern ..... 0582  
 Black ..... 0328  
 African ..... 0331  
 Asia, Australia and Oceania ..... 0332  
 Canadian ..... 0334  
 European ..... 0335  
 Latin American ..... 0336  
 Middle Eastern ..... 0333  
 United States ..... 0337  
 History of Science ..... 0585  
 Law  
 American Studies ..... 0398  
 Political Science  
 General ..... 0615  
 International Law and  
 Relations ..... 0616  
 Public Administration ..... 0617  
 Recreation ..... 0814  
 Social Work ..... 0452  
 Sociology  
 General ..... 0626  
 Criminology and Penology ..... 0627  
 Demography ..... 0938  
 Ethnic and Racial Studies ..... 0631  
 Individual and Family  
 Studies ..... 0628  
 Industrial and Labor  
 Relations ..... 0629  
 Public and Social Welfare ..... 0630  
 Social Structure and  
 Development ..... 0700  
 Theory and Methods ..... 0344  
 Transportation ..... 0709  
 Urban and Regional Planning ..... 0999  
 Women's Studies ..... 0453

## THE SCIENCES AND ENGINEERING

## BIOLOGICAL SCIENCES

Agriculture  
 General ..... 0473  
 Agronomy ..... 0285  
 Animal Culture and  
 Nutrition ..... 0475  
 Animal Pathology ..... 0476  
 Food Science and  
 Technology ..... 0359  
 Forestry and Wildlife ..... 0478  
 Plant Culture ..... 0479  
 Plant Pathology ..... 0480  
 Plant Physiology ..... 0817  
 Range Management ..... 0777  
 Wood Technology ..... 0746

Biology  
 General ..... 0306  
 Anatomy ..... 0287  
 Biostatistics ..... 0308  
 Botany ..... 0309  
 Cell ..... 0379  
 Ecology ..... 0329  
 Entomology ..... 0353  
 Genetics ..... 0369  
 Limnology ..... 0793  
 Microbiology ..... 0410  
 Molecular ..... 0307  
 Neuroscience ..... 0317  
 Oceanography ..... 0416  
 Physiology ..... 0433  
 Radiation ..... 0821  
 Veterinary Science ..... 0778  
 Zoology ..... 0472

Biophysics  
 General ..... 0786  
 Medical ..... 0760

Geodesy ..... 0370  
 Geology ..... 0372  
 Geophysics ..... 0373  
 Hydrology ..... 0388  
 Mineralogy ..... 0411  
 Paleobotany ..... 0345  
 Paleocology ..... 0426  
 Paleontology ..... 0418  
 Paleozoology ..... 0985  
 Palynology ..... 0427  
 Physical Geography ..... 0368  
 Physical Oceanography ..... 0415

## HEALTH AND ENVIRONMENTAL SCIENCES

Environmental Sciences ..... 0768  
 Health Sciences  
 General ..... 0566  
 Audiology ..... 0300  
 Chemotherapy ..... 0992  
 Dentistry ..... 0567  
 Education ..... 0350  
 Hospital Management ..... 0769  
 Human Development ..... 0758  
 Immunology ..... 0982  
 Medicine and Surgery ..... 0564  
 Mental Health ..... 0347  
 Nursing ..... 0569  
 Nutrition ..... 0570  
 Obstetrics and Gynecology ..... 0380  
 Occupational Health and  
 Therapy ..... 0354  
 Ophthalmology ..... 0381  
 Pathology ..... 0571  
 Pharmacology ..... 0419  
 Pharmacy ..... 0572  
 Physical Therapy ..... 0382  
 Public Health ..... 0573  
 Radiology ..... 0574  
 Recreation ..... 0575

Speech Pathology ..... 0460  
 Toxicology ..... 0383  
 Home Economics ..... 0386

## PHYSICAL SCIENCES

**Pure Sciences**  
 Chemistry  
 General ..... 0485  
 Agricultural ..... 0749  
 Analytical ..... 0486  
 Biochemistry ..... 0487  
 Inorganic ..... 0488  
 Nuclear ..... 0738  
 Organic ..... 0490  
 Pharmaceutical ..... 0491  
 Physical ..... 0494  
 Polymer ..... 0495  
 Radiation ..... 0754  
 Mathematics ..... 0405

Physics  
 General ..... 0605  
 Acoustics ..... 0986  
 Astronomy and  
 Astrophysics ..... 0606  
 Atmospheric Science ..... 0608  
 Atomic ..... 0748  
 Electronics and Electricity ..... 0607  
 Elementary Particles and  
 High Energy ..... 0798  
 Fluid and Plasma ..... 0759  
 Molecular ..... 0609  
 Nuclear ..... 0610  
 Optics ..... 0752  
 Radiation ..... 0756  
 Solid State ..... 0611  
 Statistics ..... 0463

**Applied Sciences**  
 Applied Mechanics ..... 0346  
 Computer Science ..... 0984

**Engineering**  
 General ..... 0537  
 Aerospace ..... 0538  
 Agricultural ..... 0539  
 Automotive ..... 0540  
 Biomedical ..... 0541  
 Chemical ..... 0542  
 Civil ..... 0543  
 Electronics and Electrical ..... 0544  
 Heat and Thermodynamics ..... 0348  
 Hydraulic ..... 0545  
 Industrial ..... 0546  
 Marine ..... 0547  
 Materials Science ..... 0794  
 Mechanical ..... 0548  
 Metallurgy ..... 0743  
 Mining ..... 0551  
 Nuclear ..... 0552  
 Packaging ..... 0549  
 Petroleum ..... 0765  
 Sanitary and Municipal ..... 0554  
 System Science ..... 0790  
 Geotechnology ..... 0428  
 Operations Research ..... 0796  
 Plastics Technology ..... 0795  
 Textile Technology ..... 0994

## PSYCHOLOGY

General ..... 0621  
 Behavioral ..... 0384  
 Clinical ..... 0622  
 Developmental ..... 0620  
 Experimental ..... 0623  
 Industrial ..... 0624  
 Personality ..... 0625  
 Physiological ..... 0989  
 Psychobiology ..... 0349  
 Psychometrics ..... 0632  
 Social ..... 0451

## EARTH SCIENCES

Biogeochemistry ..... 0425  
 Geochemistry ..... 0996

THE UNIVERSITY OF MANITOBA  
FACULTY OF GRADUATE STUDIES  
COPYRIGHT PERMISSION

APPLICATION OF ARTIFICIAL NEURAL NETWORKS  
TO DISTANCE PROTECTION

BY

WEIGUO QI

A Thesis/Practicum submitted to the Faculty of Graduate Studies of the University of Manitoba in partial fulfillment of the requirements for the degree of

DOCTOR OF PHILOSOPHY

Weiguo Qi     © 1996

Permission has been granted to the LIBRARY OF THE UNIVERSITY OF MANITOBA to lend or sell copies of this thesis/practicum, to the NATIONAL LIBRARY OF CANADA to microfilm this thesis/practicum and to lend or sell copies of the film, and to UNIVERSITY MICROFILMS INC. to publish an abstract of this thesis/practicum..

This reproduction or copy of this thesis has been made available by authority of the copyright owner solely for the purpose of private study and research, and may only be reproduced and copied as permitted by copyright laws or with express written authorization from the copyright owner.



# Dedication

---

To

My wife Xing Li

and

My Daughter Mengdi Qi

# Abstract

---

Artificial neural network(ANN) strategy was developed as a method of using a large number of simple parallel processors to recognize preprogrammed, or “learned”, patterns. This approach can be adapted to recognizing learned patterns of behavior in electric power systems where exact functional relationships are neither well defined nor easily computable, and is able to compute the answer quickly by using associations learned from previous experience. Certain problems in power systems, with their inherent nonlinear and complex nature, seem amenable to solutions through trained ANNs.

A distance relay is an important protective relay with its excellent performance for transmission line protection. However, the suitability of conventional distance relays to adapt to change in source impedance and to the effect of remote infeed and nonlinear arcing fault resistance is still unsatisfied. Utilization of artificial neural networks is a good strategy for those problems, using pattern recognition, a basic function of distance relays.

The goal of this thesis is concentrated on creating more selective ground fault detection by using artificial neural networks. Two applications of artificial neural networks to distance protection are presented in this thesis, one for nonlinear arcing fault resistance and another for remote infeed. At the current stage

of research, only single-line-to-ground faults are considered because most faults in power system transmission lines are line-to-ground faults.

In the case concerning the effect of remote source infeed, research was focused on creating more sensitive ground fault detection in spite of pre-fault loading in either direction, variable source impedance and variable ground fault resistance. A matured power system simulator named Electromagnetic Transients Simulation Program (EMTDC), was utilized to create the training and testing cases with varying system parameters. The proposed neural network was **trained** using many load and fault cases, **tested** using cases with different system conditions and **run** using more detailed fault cases along the whole transmission line.

In the case concerning the nonlinear nature of arcing fault resistance, research was focused on creating more sensitive arcing fault detection, especially for radial distribution lines where arc resistance can be a significant part of the zero sequence impedance. A neural network was **trained, tested** and **run** by three sets of pattern vectors with different system conditions. A simple power system model and a nonlinear arcing fault resistance model were used to collect training, testing and running patterns for the proposed neural network. A new operating characteristic based on fault voltage instead of fault resistance was devised.

The prospective ANN distance relays showed very good performance in detecting a single-line-to-ground fault with the effect of remote source infeed, or with nonlinear arcing resistance along the whole transmission line. Basic prin-

principles learned from this investigation of application of ANN's to power system protection will be of value to future advances in this direction.

# Acknowledgements

---

I wish to express my deep appreciation and gratitude to my supervisor, Professor Glenn W. Swift at Department of Electrical and Computer Engineering, The University of Manitoba, for his guidance, council and encouragement throughout the course of this research work.

I also wish to thank Professor Peter G. McLaren for his discussions and assistance in the study of this project. Special thanks are due to Dr. Bahman S. Kermanshahi, a visiting scholar at Department of Electrical and Computer Engineering, The University of Manitoba, for his discussions and assistance on the application of artificial neural networks.

The author would like to acknowledge the financial support provided by the research committee of Manitoba Hydro, and owes special thanks to Mr. Adrian V. Castro, a protection specialist at Stations Department, Engineering Division, Manitoba Hydro, for his discussions, suggestions and supply of necessary power system data which were important to the success of this project.

I also wish to express my sincere thanks to all professors, colleagues and technical staff at Department of Electrical and Computer Engineering, The University of Manitoba, for their support, assistance and friendship during the course of this study.

Finally, I wish to express my greatest thanks to my wife and daughter for their contributions, sacrifice, as well as their continuous support and encouragement, for which I am deeply debted. Also, special thanks to my mother for her support and encouragement of my study in Canada.

WEIGUO QI

# Contents

---

<b>ABSTRACT</b> .....	<i>i</i>
<b>ACKNOWLEDGEMENT</b> .....	<i>iv</i>
<b>CONTENTS</b> .....	<i>v</i>
<b>LIST OF FIGURES</b> .....	<i>viii</i>
<b>LIST OF TABLES</b> .....	<i>xi</i>
<b>CHAPTER ONE : Introduction</b> .....	<i>1</i>
1.1 The Suitability of Artificial Neural Networks for Power System Protection .....	<i>2</i>
1.2 Previous Research Efforts on Applications of Artificial Neural Networks to Power System Protection .....	<i>3</i>
1.2.1 Application of ANN to High Impedance Arcing Fault Detection .....	<i>4</i>
1.2.2 Application of ANN to Transmission Line Protection .....	<i>6</i>
1.2.3 Application of an ANN to Busbar Protection .....	<i>9</i>
1.2.4 Application of ANN to Autoreclosure .....	<i>10</i>
1.2.5 Application of ANN to Fault Identification in An AC-DC System .....	<i>11</i>
1.2.6 Application of ANN to Alarm Processing and Fault Diagnosis .....	<i>12</i>
1.2.7 Application of ANNs to Signal Processing .....	<i>16</i>
1.2.8 Application of ANNs to Transformer Protection .....	<i>17</i>
1.3 Summary of The Application of ANNs to Power System Protection ...	<i>18</i>
1.4 Research Objectives .....	<i>20</i>
1.5 The Scope of This Thesis .....	<i>21</i>

---

<b>CHAPTER TWO : Distance Protection Systems</b> .....	<b>24</b>
2.1 Introduction .....	24
2.2 Overview of Distance Protection .....	25
2.3 Operating Principles of Distance Protection .....	26
2.4 Operating Characteristics of Distance Protection .....	30
2.5 Fault Resistance Tolerance of Distance Protection .....	33
<b>CHAPTER THREE : Some Problems of Distance Protection</b> .....	<b>35</b>
3.1 Introduction .....	35
3.2 Inappropriate Settings .....	36
3.3 Load Encroachment .....	39
3.4 Effect of Pre-fault Load Flow .....	40
3.5 Nonlinearity of Arcing Fault Resistance .....	46
<b>CHAPTER FOUR : Simulation of Transmission Line Faults</b> .....	<b>48</b>
4.1 Introduction .....	48
4.2 Simulating The Kelsey-Thompson Line .....	49
4.2.1 Simulating System Structure .....	49
4.2.2 Equivalent Source Impedance .....	51
4.2.3 Modelling of The Transmission Line .....	52
4.2.4 Data-acquisition Subsystem for Pattern Generation .....	53
4.2.5 Sample Outputs .....	56
<b>CHAPTER FIVE : Artificial Neural Networks</b> .....	<b>59</b>
5.1 Introduction .....	59
5.2 General Description of A Neural Network .....	60
5.3 Artificial Model of The Neurons .....	62
5.4 Multilayer Feedforward Networks .....	64
5.5 Necessary Number of Hidden Neurons .....	66
5.6 Back Propagation Learning Algorithm .....	67
5.7 Pattern Classification by Artificial Neural Network .....	71
5.8 An Artificial Neural Network Simulator : Xerion .....	74
<b>CHAPTER SIX : Application of ANNs to Distance Protection</b>	
Part I : The Suitability to The Problem of Remote Infeed and Varying Source Impedances .....	77

6.1	Introduction .....	77
6.2	Proposed ANN Construction .....	78
6.3	The Sigmoid Function .....	81
6.4	Operating Characteristic Definition for an ANN Distance Relay .....	84
6.5	Selection of Training Patterns .....	85
6.6	Training of The Proposed ANN .....	85
6.7	Testing of The Proposed ANN .....	90
6.8	Running of The Proposed ANN .....	90
6.9	Comparison Concerning Underreach/Overreach Error .....	95
6.10	Summary .....	96
<b>CHAPTER SEVEN : Application of ANNs to Distance Protection</b>		
Part II : The Suitability to The Problem of Non-linear		
	Arcing Fault Resistance .....	<b>98</b>
7.1	Introduction .....	98
7.2	Investigation of Arcing Fault Resistance Nonlinearity .....	99
7.3	Arc Length of A Ground Fault .....	101
7.4	The Model for Arc Resistance .....	103
7.5	Structure of The Suggested ANN .....	105
7.6	Operating Characteristic Defining for ANN Distance Relay .....	107
7.7	Selection of Training, Testing and Running Patterns .....	109
7.8	Training and Testing Details .....	110
7.9	Running Performance of The Proposed ANN .....	112
7.10	Comparison with Conventional Distance Relay .....	115
7.11	Summary .....	117
<b>CHAPTER EIGHT : Conclusions</b> .....		<b>119</b>
<b>CHAPTER NINE : Future Work</b> .....		<b>121</b>
<b>REFERENCES</b> .....		<b>122</b>
<b>APPEDIX A : DRAFTs of Simulation Systems</b> .....		<b>128</b>
<b>APPEDIX B : Transmission Line Parameters</b> .....		<b>136</b>
<b>APPEDIX C : FORTRAN Programs</b> .....		<b>148</b>
<b>APPEDIX D : Training, Testing and Running Patterns</b> .....		<b>156</b>



# List of Figures

---

Fig. 2.1	Typical distance relay characteristic .....	27
Fig. 2.2	Fault measurements .....	29
Fig. 2.3	Distance relay characteristics .....	31
Fig. 2.4	Typical distance system .....	32
Fig. 2.5	Phase angle biasing of Mho relay ( $\psi-\theta$ ) to increase tolerance of fault resistance .....	33
Fig. 2.6	Two distance relays with better fault resistance tolerance .....	34
Fig. 3.1	Effect of source impedance on distance relay .....	38
Fig. 3.2	Load conditions superimposed on impedance polar diagram .....	40
Fig. 3.3	A power system with a single line-to-ground fault .....	41
Fig. 3.4	Effect of remote fault infeed on measuring accuracy .....	42
Fig. 3.5	Effect of fault resistance on measured impedance (no real power flow) .....	42
Fig. 3.6	Effect of ground fault resistance on measured impedance (power flow from $S$ to $R$ ) .....	43
Fig. 3.7	Effect of ground fault resistance on measured impedance (power flow from $R$ to $S$ ) .....	44

---

Fig. 3.8	Characteristics of adaptive distance relay .....	45
Fig. 4.1	System model on PSCAD/EMTDC .....	50
Fig. 4.2	Pattern generation subsystem .....	55
Fig. 4.3	Simulation of the transmission line .....	57
Fig. 5.1	Model of $j$ th neuron .....	63
Fig. 5.2	Topology of a three layer feedforward network .....	65
Fig. 5.3	Error back-propagation in a three-layer network .....	68
Fig. 5.4	Principle of pattern classification by ANN .....	72
Fig. 5.5	Block diagram of pattern classification system .....	72
Fig. 5.6	Separability of patterns .....	73
Fig. 6.1	Proposed neural network architecture .....	79
Fig. 6.2	Sigmoid function .....	82
Fig. 6.3	A general picture of pattern distribution .....	83
Fig. 6.4	Data selection and categories recognized by ANN .....	84
Fig. 6.5	Minimization of the error $E$ as a function of single weight .....	87
Fig. 6.6	Training performance of the proposed ANN .....	89
Fig. 6.7	Link weights of a successful training .....	91
Fig. 6.8	ANN distance relay performance with varying transmitted load, Run #1 ( $R_F = 6 \Omega$ ) .....	92
Fig. 6.9	ANN distance relay performance with varying transmitted load, Run #2 ( $R_F = 16 \Omega$ ) .....	93
Fig. 6.10	ANN distance relay performance with varying transmitted load, Run #3 ( $\alpha = 0.4$ ) .....	94

---

Fig. 7.1	Current and arc voltage with 48-inch series arc .....	100
Fig. 7.2	Volt-ampere characteristic of an arc with length 48 inches .....	100
Fig. 7.3	Independence of current through the arc in a simple system .....	101
Fig. 7.4	Modelling metal oxide surge arrester .....	104
Fig. 7.5	Simulation system considering nonlinear arc resistance .....	105
Fig. 7.6	Simulation outcomes .....	106
Fig. 7.7	Proposed neural network structure .....	107
Fig. 7.8	ANN training and testing patterns .....	108
Fig. 7.9	The final weights and biases of a successful training .....	111
Fig. 7.10	ANN distance relay performance with varying transmitted load, Run #1 ( $V_F = 0.02$ ) .....	112
Fig. 7.11	ANN distance relay performance with varying transmitted load, Run #2 ( $V_F = 0.08$ ) .....	113
Fig. 7.12	ANN distance relay performance with varying transmitted load, Run #3 ( $\alpha = 0.4$ ) .....	114
Fig. 7.13	Comparison of conventional relay and ANN relay for low source impedance and $\delta = -30^\circ$ .....	116
Fig. 7.14	Comparison of conventional relay and ANN Relay for high source impedance and $\delta = 30^\circ$ .....	117

# List of Tables

---

Table 4.1	Subtransient source impedance $X''d (\Omega)$ .....	51
Table 4.2	Transient source impedance $X'd (\Omega)$ .....	51
Table 4.3	Kelsey-Thompson line parameters .....	54
Table 6.1	Selection of system parameters .....	86
Table 7.1	Typical line insulation .....	102
Table 7.2	ASEA XAP-A I-V characteristic .....	104
Table 7.3	Selection of system parameters .....	109
Table 7.4	Per km impedance of Kelsey-Thompson line .....	115

# Chapter One

## Introduction

---

The capital investment involved in a power system for the generation, transmission and distribution of electrical power is so great that proper precautions must be taken to ensure that the equipment not only operates as nearly as possible to peak efficiency, but also that it is protected from accidents. The purpose of protective relays and relaying systems is to operate the correct circuit breakers, so as to disconnect only the faulty equipment, such as generator, transformer, busbar, or transmission line, from the system as quickly as possible, thus minimizing the trouble and damage caused by faults when they do occur.

As power systems increase in size and complexity, a desire for a more accurate and faster power system protection method and protective devices is always present among relay engineers. Modern protection systems have become more and more complicated due to increased requirements for sensitivity and selectivity. In the past few decades, there has been explosive growth in studies and applications of artificial neural networks for engineering problems. Engineers are naturally attracted to finding ways to use artificial neural networks for solving complex protection problems.

## **1.1 The Suitability of Artificial Neural Networks for Power System Protection**

Artificial neural networks (ANNs) have been studied for many years with the hope of achieving human-like performance in solving certain problems in speech and image processing. There has been a recent resurgence in the field of neural networks due to the introduction of new network topologies, training algorithms and VLSI implementation techniques. The potential benefits of neural networks such as parallel distributed processing, high computation rates, fault tolerance, and adaptive capability have lured researchers from other fields such as controls, robotics and energy systems to seek neural network solutions to some of their more difficult problems.

Artificial neural network strategy was developed as a method for using a large number of simple parallel processors to recognize preprogrammed, or "learned", patterns. This procedure is called pattern recognition, and defined as an abstract formulation of the categorization of tasks in pattern classification, which is the dominating field of the applications of neural networks. This approach can be adapted to recognizing learned patterns of behavior in an electric power system where exact functional relationships are neither well defined nor easily computable. It is able to compute the answer quickly by using associations learned from previous experience. Certain problems in power systems, with their inherent nonlinear and complex nature, seem amenable to solutions through trained ANNs.

In electric power system protection, the relays make decisions depending on input information (voltage and current patterns) and separate decisions into two categories: normal operation and fault. Neural networks appear to offer features which coincide well with the requirements of protective relays. Distance protection can be conceptualized as a pattern classification problem which involves the association of patterns of input data representing the behavior of the power system into one of these two categories.

## **1.2 Previous Research Efforts on Applications of Artificial Neural Networks to Power System Protection**

Artificial neural networks have been recently proposed as an alternative method for solving certain traditional problems in power systems where conventional techniques have not achieved the desired speed, accuracy or efficiency.

Neural network applications that have been proposed in the literature can be categorized under three main areas: Regression, Classification and Combinatorial Optimization[1]. The applications involving regression include transient stability, load forecasting, synchronous machine modelling, contingency screening and harmonic evaluation. Applications involving classification include harmonic load identification, fault diagnosis and alarm processing, static security assessment and dynamic security assessment. In the area of combinatorial optimization, there are topological observability and capacitor control. In this section, an overview of the reported neural networks applications to power system protection is provided.

### **1.2.1 Application of ANN to High Impedance Arcing Faults Detection**

A high impedance fault (HIF) on a power system distribution line could be due to a downed conductor, and is a dangerous situation because the current may be too small to be detected by conventional relays. Such faults do not cause significant trouble for the integrity of the electric power system, but an energized conductor lying on ground has the potential to injure human and animal as well as cause property damage.

#### **The University of Manitoba[2][3]**

Research at The University of Manitoba has played a leading role in the detection of arcing high impedance faults using artificial neural networks.

Based on the study of the nature of HIF, waveforms of high impedance faults as well as loads that behave or appear like high impedance faults were collected and processed. The detection parameters used in a number of existing high impedance fault detection algorithms were extracted. Then, a feed-forward three-layer artificial neural network was trained by high impedance fault, fault-like, and normal load current patterns, using the back-propagation training algorithm. The neural network parameters were embodied in a high impedance arcing fault detection algorithm.

The ANN based algorithm was tested by traces of normal load current disturbed by currents of faults on dry and wet grassy soil, arc welder, computer, fluorescent light, and sinusoidal loads. The results of this study indicated that



the neural network was able to reach a general solution of the problem for the available training patterns.

A high impedance fault detector was implemented later on, based on above ANN algorithm in a PC environment. The performance of this detector was very good[4].

### **North Carolina State University[5]**

It was concluded that the neural network approach has potential to detect high impedance faults. A typical distribution system with capacitors and induction motors fed from power electronic circuit was simulated by using the Electromagnetic Transients Program(EMTP). Capacitors were included in the feeder model for demonstrating the switching events that must be distinguished from faults. Induction motors were set up to provide HIF detector current harmonic samples generated in normal operation and the possible arcing faults. Twenty parameters were computed for each 512 sample-per-cycle-per-phase window to represent the status of the system undergoing a transient. A preprocessor extracts pertinent information on the state of the feeder over 10 cycles of operation for neural network. A proposed neural network, containing 200 input neurons, 200 first hidden layer neurons, 400 second hidden layer neurons and one output neuron, was trained by a 50-vector training set in 38 iterations using the back-propagation algorithm. A detection set, consisting of 100 input vectors representing feeder operation, was collected and then passed to the detector. In most cases the neural network responded correctly.

For a practical implementation of a high impedance fault detector, a fault data library obtained from measurements in the field would have to be used to train the network. The parameters used to characterize the current waveforms and the number of data windows which were used to show time-varying effects also need to be re-examined.

### **University of New Brunswick[6]**

Detection of High Impedance Faults using artificial neural networks was developed in a novel approach at The University of New Brunswick. The ANN based detector utilizes a discriminant vector of low order harmonics, namely 2nd, 3rd and 5th of the sampled and transformed three phase residual voltage, current and power at the substation feeder distribution transformer secondary. The three-layer neural network consists of 18 input nodes, 17 hidden nodes and one output node. Digital simulation was performed using ATP-EMTP for different variations of fault types, fault location, equivalent loading, capacitor and line switching, etc. The arcing high impedance fault was modeled as two sets (positive and negative) of diodes in series with a resistance and a DC source. This detector provides robust and precise detection by tolerating high noise content in the acquired signals.

#### **1.2.2 Application of ANN to Transmission Line Protection**

### **Delft University of Technology, The Netherlands[7]**

The adaptation of a distance relay to the power system state could be achieved by correcting the relaying settings with a nonlinear factor which was

---

traced by a neural network. The faults in a weakened power system often caused serious power system disturbances. Over-tripping of relays and sympathy trips easily happen due to inappropriate settings. The calculation of the fault distance by a distance relay was hampered by inappropriate settings because of the dynamic character of the power system. These included changes in load and generation, and change in the topology of the power system. Simulation of a double-circuit line showed that the locus of measuring impedance by a distance relay was a nonlinear curve which was caused by the zero sequence current. An artificial neural network was introduced to trace this nonlinear effect and form a correction factor to compensate the inappropriate settings. After learning many examples, the ANN could compute the nonlinear correction factor based on local measurements on-line, so that the performance of the distance relay was optimized.

### **Indian Institute of Technology, India[8]**

The research work at Indian Institute of Technology confirms the feasibility of using ANNs as relays because the relay could be envisaged as a pattern classifying device. The neural network could perform the pattern classification in excellent fashion so that it could work as a relay. The feasibility of using an ANN in protection of transmission lines was found by keeping the microprocessor relay framework intact. The training was performed in off-line mode and the converged weight matrix was stored for on-line use, and so a neural relay could be realized in its simplest form. The proposed scheme considered two inputs viz. voltage and current values so that the decision space was V-I plane rather than the R-X plane. The relay setting could be changed by changing link weights, and time delay

---

settings could be achieved, too. But the implementation of the feature of ANN parallel computation was not shown clearly in this paper.

### **University of Bath, UK[9,10]**

A novel adaptive protection scheme for a series compensated transmission system was achieved at University of Bath by using a neural network approach. The application of series compensation was widely applied to long distance transmission systems to improve power transfer. The Metal Oxide Varistor(MOV) used as the overvoltage protection device for the series capacitor had a non-linear resistance characteristic and posed problems for conventional distance protection. The simulation by EMTP showed that the conduction of the MOV was not symmetrical during the unbalanced fault and the effect of conduction through the MOV on the impedance of the transmission line was different at different fault locations, so that the impedance relationship between the MOV and transmission line was non-linear. A neural network was applied to solve this problem. The proposed ANN for each phase was composed of 12 input nodes, 20 hidden nodes and 2 output nodes. The voltage at the busbar and line current, each with 6 samples at a sampling time of 1.4ms, were used as input feature signals. One of the outputs indicated fault or no-fault, another one indicated the fault location. Training and testing results showed that this adaptive protection scheme was particularly suitable for a series compensated EHV transmission system where traditional distance protection scheme might have difficulties.

Another application of a neural network to a Controllable Series Compensated EHV Transmission System at University of Bath was considered with

---

the effect of a CVT (Capacitor Voltage Transducer)[10]. The input vector was composed of 25 nodes. The first 24 nodes represented the 8 sample values of three phase instantaneous voltages respectively while the last node indicated the firing angle of the controllable series compensation. In the two proposed ANNs, one network had the ability to detect different faults at different locations, load and incipience conditions, whereas another network had the ability to detect the fault type.

### **1.2.3 Application of an ANN to Busbar Protection**

#### **University of Stuttgart, F. R. of Germany[11]**

The study at University of Stuttgart showed that the application of a neural network to restore distorted current values was possible in principle. The saturation of the current transducers(CTs) is an important consideration in the design of the numerical busbar protection algorithm. The possibility of using a neural network for preprocessing the data and restoring the distorted signals needed to be investigated. Best results suggested a medium sized three-layer-network with 10/3/1 neurons in the input/hidden/output layers. The proposed neural network was trained by a set of typical distorted and undistorted current waveshapes as input signals and minimizing the mean square error with the undistorted values as target function. The training procedure showed that the output waveshape of ANN roughly coincides with the desired current waveshape for the high values but not yet for the small ones after 200 training steps. After 600 iterations, this matched the desired function quite well and almost restored the desired signals after 7000 training steps. An implementation in hardware for

this strategy may easily be programmed into existing NN hardware. However, it is still unclear how the proposed ANN adapts to the magnitude of distorted input current.

#### **1.2.4 Application of ANN to Autoreclosure**

##### **University of Bath, UK[12,13]**

An adaptive circuit breaker control system using neural networks was proposed at the University of Bath. It is well known that the current practice of auto reclosure with a fixed time delay could arise problems. During transient faults, a restrike of a fault due to insufficient time for the fault path to deionize fully can compromise system stability and reliability and, in the case of a permanent fault a second shock to the system can cause irreparable damage to expensive equipment. Using the EMTP software simulation package, an extensive series of voltage waveforms, either permanent faults or transient faults, was created. The frequency spectra analysis by Fast Fourier Transform(FFT) was applied to the waveforms to extract five features for neural networks which are good at performing pattern recognition. The features used in this application were found by comparing the spectra of the transient and permanent faults for distinguishing between permanent and transient faults, and by comparing the pre and post secondary arc frequency spectra for estimating when the secondary arc has extinguished in a transient fault.

The proposed three-layer neural network had five input neurons corresponding to five features and two output neurons that represented the fault, permanent or transient, and when to close. Of the neurons in the hidden layer,

some were fully linked to all of the inputs. The others was connected to only some input neurons, and only a few of the hidden nodes was connected to output neurons. A set of 104 training cases was utilized to train the network, and a set of 44 test cases was applied for testing of the trained network. The results from the network were very accurate, and the network correctly classified the waveforms irrespective of changes in the line length, system source and load capacity, and the position of the fault on the transmission line. However, the network was only trained to distinguish between two types of faults, and all the faults were single phase to ground faults.

### **1.2.5 Application of ANN to Fault Identification in An AC-DC System**

#### **Concordia University[14]**

The research at Concordia University explored the possibility of using neural networks to identify faults that may have occurred in an AC-DC power system. Because of the fast control response of HVDC systems, the stability of attached AC systems was greatly enhanced if proper control measures were taken when a fault occurred anywhere on the AC-DC system. Foundation of such fast reacting controls was the capability to distinguish what type of fault occurred, its severity and its location. Time domain simulations performed with EMTDC simulation package were used to provide the training samples for the neural networks. Three different neural network architectures were proposed to distinguish between different types of faults on the AC-DC system. The first network included 4 input nodes, 22 hidden nodes and 6 output nodes. The three phase voltages (rms values) were selected as the 4 inputs, and six output neurons

showed the fault types. The second network was a multi-network: three Phase Detector networks and a Main network. Each phase detector network was three-layer network. The input layer had three nodes for rms phase voltage and angles between the phase and other two phases. The outputs of phase detector networks were then connected to the main network whose outputs tell the fault types. Similar to the second network, the third network is also a multi-network, but the sampled instantaneous values of the phase voltages were used as inputs for each phase detector network instead of phase angles.

These three networks could distinguish the highest number of fault types but some confusion still occurred in distinguishing a line to line fault from a remote AC fault. Based on the ability of these networks to distinguish the reliably between different types of faults, appropriate control measures could be taken to improve the dynamic performance of the AC-DC power system.

### **1.2.6 Application of ANN to Alarm Processing and Fault Diagnosis**

#### **University of Washington[15]**

The control centers of a power system are continuously interpreting a large number of alarms signals to determine the status of the system components and to evaluate the power system operation. This process is very complex for two key reasons:

1. Alarm patterns are not unique to a given power system problem. Same faults may manifest in different alarm patterns based on the current topology and operating status of the power system.



2. Alarm patterns are likely to be contaminated with noise due to equipment problems, incorrect relay settings, interference, or miscalibrated meters.

Expert system techniques have been widely tested for analyzing alarm signals. The formulation of rules, however, requires a precise definition of the power system and its operational strategies which may widely vary depending on the utility. Therefore, neural networks, with their ability to classify noisy patterns, seemed a logical choice for alarm processing.

The ANN developed at The University of Washington was also capable of associating different alarm patterns to the same system fault by training the ANN with a set of *information rich* data that represents different operating scenarios. The training set was generated by first creating a credible set of contingencies and then deriving the possible alarm patterns under each fault. These patterns were generated by relay protection schemes and power flow analyses. The concept was tested on a 115kV/12kV substation for 65 different fault conditions with 99 bit alarm patterns. It was also tested on the IEEE 30 bus system for 72 different bus and line fault conditions with 112 bit alarm patterns. Results showed that the trained ANN was able to correctly classify all noiseless input patterns and some of the noisy patterns.

### **Indian Institute of Science, India[16]**

Artificial neural networks were applied to real-time Fault Detection and Diagnosis at Indian Institute of Science. Traditional systems performed diagnosis by mapping fault symptoms to generated hypothesis to reach at diagnostic con-

clusions. The expert systems were also inadequate because knowledge acquisition and search processes were time consuming. Artificial neural networks had great advantages over expert systems in terms of knowledge acquisition, addition of new knowledge, performance and speed, and appeared to offer characters which coincide well with the requirements of *pattern-based diagnosis*.

The proposed three-layer neural network was trained by using the back propagation algorithm until the error in the weights between successive iterations was less than a specified minimum value. The neural network was trained off-line for 53 different types of faults and used on-line. The neural network was designed so that it captured the behavior of the power system represented in the form of signals from relays and circuit breakers. This resulted in the neural network consisting of 35 input nodes and 10 output nodes corresponding to the various components of the power system. It was found that 18 nodes in the hidden layer gave the optimum and satisfactory performance in terms of generalization and recall performance of the neural network. The neural network diagnostic system was found to be able to diagnose correctly even in the presence of faulty operation of the relays of the power system and during disturbances. This system trained for single faults was able to precisely diagnose abnormal behavior resulting from simultaneous multiple faults.

**National Cheng Kung University, Taiwan[17]**

A similar fault section estimation system based on the information of relay operation and circuit breaker status was suggested at National Cheng Kung University, Taiwan. Actually, it was more like an expert system because the inputs

of neural network came from a SCADA system. It was capable of locating the sections of single or multiple faults even subject to failure operation of relay or breaker, or existence of error in the data transmission of SCADA system. Because it possessed a friendly User Interface, the proposed diagnostic system could automatically learn new fault scenarios by adding sample data into its training set, and could make reasonable generalization of learned scenarios.

### **National Sun Yat-Sen University, Taiwan[18]**

Artificial neural networks were employed in trouble call analysis at National Sun Yat-Sen University. Customers often estimated the quality of their power supplier by the service interruption they suffer. To minimize the duration of service interruption it was essential to locate the problem as soon as possible. Expert system techniques had been applied for assisting the dispatchers in service restoration but most of the expert systems were only suitable for assessing the fault section on transmission lines or on the primary distribution system. This suggested the use of an ANN approach for trouble call analysis.

The ANN was used for fast pattern recognition and classification of trouble calls so that the time and effort needed for service restoration could be reduced. To generate the training patterns, a 1:600 paper map which covered a 400m x 250m area and geographic information of trouble calls and system facilities was divided into 1000 squares and each square covered a 10m x 10m area. A square in the map was described by two numbers, one corresponds to the X-axis, and the other one corresponds to the Y-axis. A square with 1's in both X and Y coordinates indicated that a trouble call was made from that area. The output

node that had an output value close to 1 was the most likely outaged device. Approximately 7000 service interruption cases were used to train the network. Experience had shown that the proposed system allowed the utility to restore service quickly, kept consumers informed regarding the status of the outages, spotted recurrent system problems, and facilitated reporting requirements.

### **1.2.7 Application of ANNs to Signal Processing**

#### **( 1 ) Harmonic Identification and Evaluation[19]**

It was necessary to analyze and predict the behavior of current and voltage harmonics so that appropriate action could be taken to reduce their adverse effects. Model based analysis had been inaccurate and time consuming because of the nonlinearity of the harmonic components, the random behavior of harmonic signals and the wide variety of harmonic profiles of all solid state circuits.

A three-layer neural network was used to identify the type of harmonic load from among a set of pre-specified selections. The training patterns for the ANNs were generated by monitoring the current waveforms corresponding to each specific type of harmonic load. The Fast Fourier Transform (FFT) of the digitized current waveform was used to produce the harmonic frequency spectrum. Different combinations of harmonic magnitudes and phases were then fed to the ANN as inputs with the corresponding load type as the output. The ability to correctly classify the load based on the harmonic currents was investigated for

the three cases, and several ANN architectures with different numbers of hidden layers were used to find the optimal ANN design.

## **( 2 ) Real-time Estimation of Basic Waveforms[20]**

For the control and protection of electrical power systems, it was necessary to estimate in real-time the parameters of the basic waveforms of voltages and currents. Different digital algorithms had been proposed based on the Fourier technique or Kalman filtering but they were not parallel, therefore the speed of processing was limited. New algorithms and new architectures for analogue neuron-like adaptive processors for on-line estimation of parameters (magnitudes and frequency) of sinusoidal signals, distorted by higher harmonics and corrupted by noise, were proposed at Technical University of Warsaw, Poland.

The problem was expressed as an optimization problem and solved by using the steepest descent continuous-time optimization algorithm. An artificial neuron-like network consisted of basic computing units: integrators, summers, multipliers, signum activation functions, and trigonometric (sin,cos) function generators. Extensive computer simulation experiments confirmed that the neural networks represented a very realistic and promising approach for high speed estimation of parameters of signals.

### **1.2.8 Application of ANNs to Transformer Protection[21]**

A feed forward neural network was used as an alternative method to discriminate between inrush magnetizing current and internal faults in power

transformers at Washington State University. The effect of magnetizing inrush current was important to any power transformer protective scheme. The classic methods delaying trip or blocking relay according to the harmonic content were not desirable or sufficient because of the potential danger of incorrect operation of relays during internal faults.

The ANN strategy detected inrush current based on recognizing its wave shape by differentiating its wave shape from the fault wave shapes. The feed forward neural network consisted of 12 input neurons, because the wave shape recognition was based on 12 data samples per 60Hz cycle, and one output neuron showed the appearance of inrush currents.

The inrush cases were measured in the laboratory by energizing, at random, a small power transformer of 50 VA, 120/240 V. The fault cases were generated by the electromagnetic transients program EMTP. The trained neural network responded well, performing the discrimination function between inrush and fault currents correctly for most cases. The percentage of correct classification was above 94% for the inrush examples and fault plus inrush artificial examples.

### **1.3 Summary of The Application of ANNs to Power System Protection**

The application of artificial neural network to power system protection could be characterized as follows:

- **Suitability of ANNs to Power System Protection**

Artificial neural networks are particularly well suited for solving those protection problems that are inherently non-linear and complex in

nature, and are too difficult for conventional protection schemes.

- **Key function of ANNs**

Excellent performance of artificial neural networks on pattern recognition or classification is the basis of all applications. The development of adaptive protection can be treated as a problem of pattern recognition, like waveforms recognition.

- **Necessity of Feature Extraction**

Feature extraction is an important issue in neural networks. Different features of a system can be used as input signals to a neural network, as calculated by a pre-processor. Usually, the selected features will determine the number of neurons in the input layer of the neural network.

- **Source of Training and Testing Patterns for ANNs**

In most applications, the training and/or testing patterns for the proposed neural network come from the computation of Electromagnetic Transients Programs such as EMTP or EMTDC. Some of the training samples comes from laboratory experiments and some come from field measurements.

- **Role of ANNs in A Protection System**

In most feasibility studies of neural network application, the proposed neural network plays a sole role in taking responsibility for the suggested task. In real-time or on-line applications, the proposed neural network usually plays an accessory role to assist the protective relay to

adapt to complex system conditions.

- **Selection of The Neuron Number in Hidden Layer of Network**

In general, the number of hidden layers in the neural network is determined dynamically, depending on the complexity of the relationship between the inputs and outputs, and the optimum and satisfactory performance in terms of generalization and recall performance of the neural network.

- **Selection of architecture of an ANN and its learning algorithm**

The most popular architecture of neural network is the three-layer feed forward network and the most popular learning algorithm is the error back-propagation rule, which is a steepest descent method for finding the minimum of error function. In some cases, multiple neural networks are applied to a certain problem.

#### **1.4 Research Objectives**

This research had two major tasks. One was to use artificial neural networks for special problems in distance protection. The second was to investigate the feasibility of applying neural networks to the non-linear nature of arcing fault resistance.

The goal of the first task was to create more selective ground fault detection in spite of pre-fault loading in either direction, variable source impedance, and variable ground fault resistance. Although some aspects of these special distance protection problems have been studied previously, the solutions are still



not satisfactory. This research suggests a novel neural network solution to these problems.

The goal of the second task was to create more selective arcing fault detection, especially for radial distribution lines where arc resistance could be a significant part of the zero sequence impedance and has non-linear characteristics. ANNs were well suited to problems where there were neither well defined nor obvious relationships existing between inputs and outputs. The study involved:

- Investigation of the non-linear nature of arcing fault resistance,
- Establishment of a non-linear arcing fault resistance model, and
- Search for a neural network solution.

### **1.5 The Scope of This Thesis**

This thesis consists of five major parts with nine chapters. The first part, which includes Chapters 2 and 3, is the introduction of distance protection and its problems. The second part, Chapter 4, is the simulation of a transmission line. The third part, Chapter 5, is the introduction of artificial neural networks. The fourth part, Chapter 6 to Chapter 7, is the application of artificial neural networks to distance protection. Chapter 8 and Chapter 9 contain the fifth part outlining the main achievements and conclusions of this research work, as well as some suggested future research. The contents of these chapters are briefly described as follows:

- 1). Chapter 1 : Introduction. (This chapter)
- 2). Chapter 2 : The distance protection system is briefly introduced. The

---

operating principles, measuring equations and operating characteristics of conventional distance relays are presented first and then, the fault resistance tolerance of distance relays is defined.

- 3). Chapter 3 : Some problems of distance protection are raised in this chapter. Several topics are discussed here, including the problem of inappropriate settings because of the variation of source impedances, the load encroachment problem, the pre-fault load flow effect problem and nonlinearity of arcing fault resistance.
- 4). Chapter 4 : The simulation of transmission line faults is presented in this chapter. An actual Manitoba Hydro transmission line, a 138kV line from Kelsey to Thompson in northern Manitoba, is modelled on PSCAD/EMTDC.
- 5). Chapter 5 : Artificial neural networks are briefly introduced in this chapter. The artificial model of a neuron is given first, and then multilayer feedforward networks are shown. Second, an emphasis is put on the Back Propagation Learning Algorithm. Finally, the basic principle of pattern classification using artificial neural networks is presented.
- 6). Chapter 6 : An application of artificial neural networks to distance protection is proposed in this chapter. The emphasis here is on creating more selective ground fault detection in spite of pre-fault loading in either direction, variable source impedance, and variable ground fault resistance. The performance of a prospective ANN dis-

tance relay in detecting single line-to-ground faults is described at the end of the chapter.

- 7). Chapter 7 : Another application of artificial neural networks to distance protection is proposed in this chapter. The research here was concentrated on creating more selective arcing fault detection, especially for radial distribution lines where arc resistance can be a significant part of the zero sequence impedance, in spite of pre-fault loading in either direction and variable source impedance. A new operating characteristic is devised, and the performance of the proposed ANN distance relay on detecting single line-to-ground faults with nonlinear arcing resistance along the whole transmission line is shown at the end of the chapter.
- 8). Chapter 8 : The achievements and conclusions of this research work are presented in this chapter.
- 9). Chapter 9 : Suggestions of future works on this project are given in this chapter.

## Chapter Two

# Distance Protection Systems

---

### 2.1 Introduction

“An electric power system is a network of interconnected components designed to continuously convert non-electric energy into the electric form, transport the electrical energy over potentially great distances and transform the electric energy into a specific form subject to close tolerances.”[23]

After the first small power systems were built up, the requirement to add automatic protection was realized soon. An electric power system should ensure the reliability and availability of electric energy without interruption to users. The normal path of the electric current is from the power source through conductors in the generators, transformers and transmission lines to the load and it is confined to this path by insulation. The insulation, however, may break down, either by the effect of temperature and age or by a physical accident. When this happens the current follows an abnormal path generally known as a short-circuit or fault. Whenever this occurs the enormous energy of the power system may cause expensive damage to equipment, severe drop in voltage and loss of revenue because of interruption of service. Once a fault arises in a power system, that fault must be isolated as quickly as possible from all live supplies in order (a) to retain system stability and (b) to reduce the damage at the point of fault,

because of fire and explosion, and in the parts of the system carrying the fault current, due to overheating[24].

Protection is the art or science of detecting the presence of a fault and initiating the correct tripping of the circuit breakers so as to disconnect only the faulty equipment from the system, thus minimizing the trouble and damage caused by faults when they do occur. An ideal protection system would detect and isolate faults as quickly as possible at any point in the system and accomplish this while keeping as much of the system interconnected as possible. A basic protection system comprises instrument transducers, protective relays with their associated wiring and circuit breakers.

A complete power system is divided into zones: an alternator, a transformer, a busbar section, a feeder. Each zone has one or more co-ordinated protective systems connected to it. Since the objective of this thesis is mainly concerned with the feeder protection, the distance protection will be described in brief in the following sections.

## **2.2 Overview of Distance Protection[22, 24-28]**

Distance relays were invented in 1923 in an effort to solve the application problems associated with graded time overcurrent relaying. The operation of distance protection depends on the basic fact that on the occurrence of a fault, the distance between any point in the power system and the fault is proportional to the ratio of voltage to current at that point. The following benefits of distance protection make it widely applicable to power system transmission line protections:

- It offers fast and discriminative protection for all faults occurring on the feeder.
- It offers some measure of back-up protection (zone 2 and zone 3) for other feeders and plant at remote stations and, often, on reverse reach of zone 3 at its own substation.
- It does not need an input signal from a remote station in order to trip, even though the lack of such input signal may delay tripping.

The principle of impedance measurement and the engineering of basic impedance measuring elements into schemes of distance protection has always formed an important part of power system feeder protection. The importance of its role is reflected in the fact that this form of protection more than any other has long been the subject of rapid and continuous development necessary to meet the ever increasing demands typical of modern power systems. Such development has, for many years, seen little change in operating principle (discounting computer-based techniques) although the methods of implementation vary considerably largely because of the degrees of freedom allowed by modern developments in technologies of all kinds. However, although implementation of the principle is subject to continuous change through development, there are basic design concepts which are almost universally established and are important in understanding the principles of application.

### **2.3 Operating Principles of Distance Protection[25,26,27]**

The operating principle of distance protection is based on the knowledge that, at any measuring point in a power system, the line impedance to a fault can be decided by measuring the voltage and current at the measuring point. Actually,

the measuring relay is organized to have balance point which is specified by the relay impedance setting,  $Z_R$ . Therefore, the relay either trips or restrains, depending on if the fault impedance is less than or greater than the relay setting. Those relays can be applied to various points on the system and by arranging the relays so that those closer to the fault operate faster than those more remote, discriminative tripping of the circuit breakers controlling the various feeders can be accomplished. Such discrimination needs, in addition to impedance measurement, a directional character and a time-dependent character. Fig. 2.1 shows a combination of distance relays with a stepped time-distance characteristic.

The relay at A has a zone 1 distance range which is set to operate immediately and trip the related breaker when a fault happens within the first 80% of feeder 1 and only when the fault current is in the direction shown. The zone 2 setting of the same relay is set to cover the whole of feeder 1 and usually

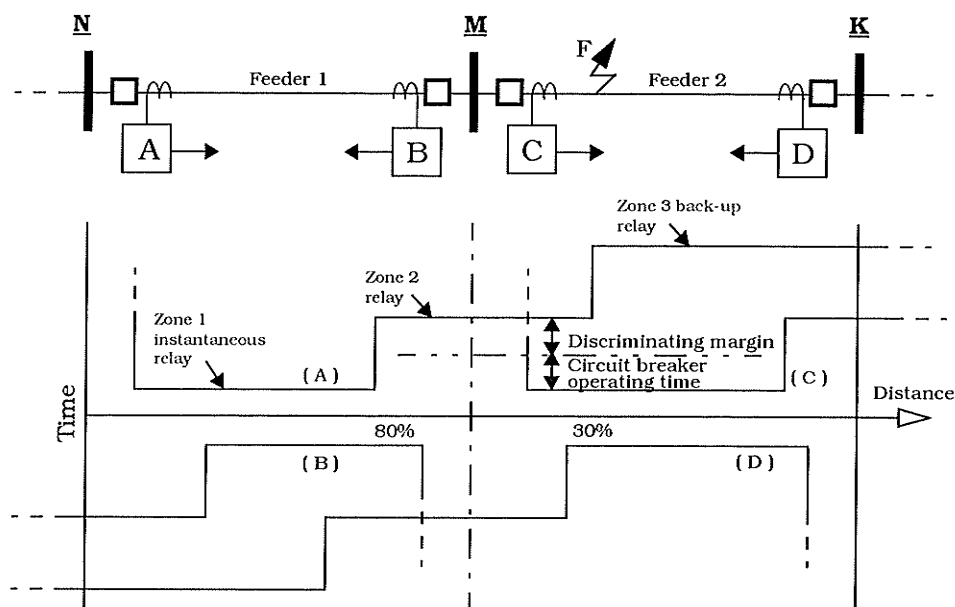


**Fig. 2.1** Typical distance relay characteristic

the first 20-30% of feeder 2 but tripping is delayed for only a short time. The zone 3 setting is set to include faults in feeders 1 and 2 and possibly beyond with tripping after a further time delay. Combining these zones of measurement and superimposing those of relays B, C and D relative to the two feeders and with direction of measurement indicated by the arrows, results in the overall time-distance characteristic shown in Fig. 2.1.

It is necessary for a distance protection to adapt to the variety of power system faults (three-phase, phase-to-phase, phase-to-ground, two-phase-to-ground and three-phase-to-ground) by arranging that the appropriate relays measure the same impedance for all fault types. It can be implemented by selecting the correct voltage and current quantities from the power system suitable to the type of fault condition. Therefore, for faults involving more than one phase the appropriate phase-to-phase voltage is used for the relay with the difference of the phase currents. In this way, the measured impedance for phase-to-phase and three-phase faults is the positive sequence impedance  $\alpha Z_1$  and also this impedance is measured for a double-ground fault condition [24].

Measurement for a single phase-to-ground fault condition is a little more complicated even for the simple system illustrated in Fig. 2.2. To utilize phase-to-phase voltage and the difference of phase currents, like in the case of phase-fault measurement, produces a complex impedance which is not only in excess of the positive sequence impedance of the line but also varies with zero and positive sequence source impedance. In order to achieve correct measurement of positive sequence impedance, phase-to-neutral voltage with a combination of line and



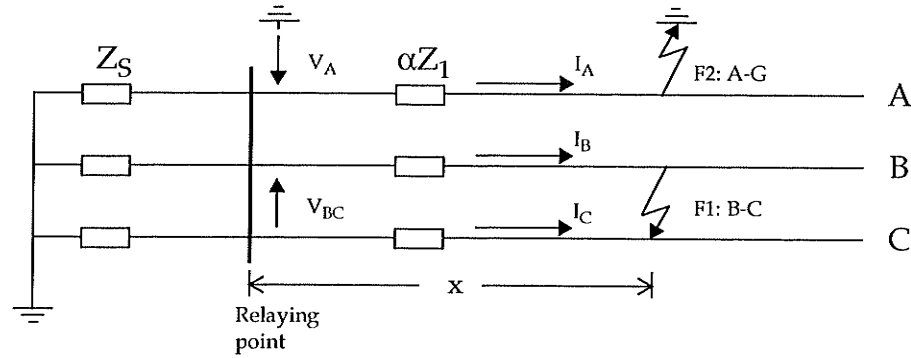


**Fig. 2.2** Fault measurements

neutral currents are applied to the relay. From the sequence network for a single phase-to-ground fault the voltage at the relaying point is:

$$V_A = I_{A1} \alpha Z_{L1} + I_{A0} \alpha Z_{L0} + I_{A2} \alpha Z_{L2} \quad (2.1)$$

where  $V_A$ : the voltage of phase A at relaying point.

$I_{A1}$ ,  $I_{A2}$ ,  $I_{A0}$ : the positive, negative and zero sequence current of phase A.

$$I_A = I_{A1} + I_{A0} + I_{A2} \quad (2.2)$$

$Z_{L1}$ ,  $Z_{L2}$ ,  $Z_{L0}$ : the positive, negative and zero sequence impedance of line.

$\alpha$ : the fractional fault distance, defined as fault distance  $x$  over line length  $L$ :  $\alpha = \frac{x}{L}$ .

Assuming  $Z_{L1} = Z_{L2}$ ,

$$\begin{aligned} V_A &= (I_{A1} + I_{A0} + I_{A2}) \alpha Z_{L1} + I_{A0} \alpha Z_{L0} - I_{A0} \alpha Z_{L1} \\ &= I_A \alpha Z_{L1} + I_{A0} \left( \frac{Z_{L0}}{Z_{L1}} - 1 \right) \alpha Z_{L1} \end{aligned} \quad (2.3)$$

Thus

$$\alpha Z_{L1} = \frac{V_A}{I_A + I_{A0} \left( \frac{Z_{L0}}{Z_{L1}} - 1 \right)} = \frac{V_A}{I_A + \frac{I_N}{3} \left( \frac{Z_{L0}}{Z_{L1}} - 1 \right)} \quad (2.4)$$

where  $I_N = I_{A0} + I_{B0} + I_{C0}$  is the neutral current. Since  $I_N = 3I_{A0}$ ,

$$\alpha Z_{L1} = \frac{V_A}{I_A + \frac{k}{3}I_N} \quad (2.5)$$

where

$$k = \frac{Z_{L0} - Z_{L1}}{Z_{L1}} \quad (2.6)$$

(zero sequence compensation factor)

Note that different relaying quantities are necessary to distinguish between phase and ground faults, common practice being to provide two separate sets of (zone 1) relays for these faults, one set for phase faults and the other set for ground faults. Each set consists of three relays because multi-phase faults may involve any pair of phases and similarly any single phase can be faulted to ground. Zone 2 impedance measurement may use zone 1 relays, the settings of which are increased after a zone 2 time-delay, or may use six separate relays. Zone 3 measurement uses six separate relays.

## 2.4 Operating Characteristics of Distance Protection[22,26]

The principles outlined above suggest that a distance relay can have a balance point specified by impedance setting  $Z_R$  so that operation occurs for line impedances less than the setting value of the relay, i.e.,

$$|Z| \leq |Z_R| \quad (2.7)$$

The locus of (2.7) yields a circular characteristic on  $R$ - $X$  plane, the centre at the origin (relaying point) and radius the setting  $|Z_R|$  as shown in Fig. 2.3(a). This plain impedance relay is non-directional and measures only the magnitude of

the fault-loop impedance (regardless of phase angle). Obviously, this plain impedance relay has the disadvantage of allowing incorrect operation for reverse faults within the relay setting  $Z_R$ . This problem can be overcome by a *directional relay*.

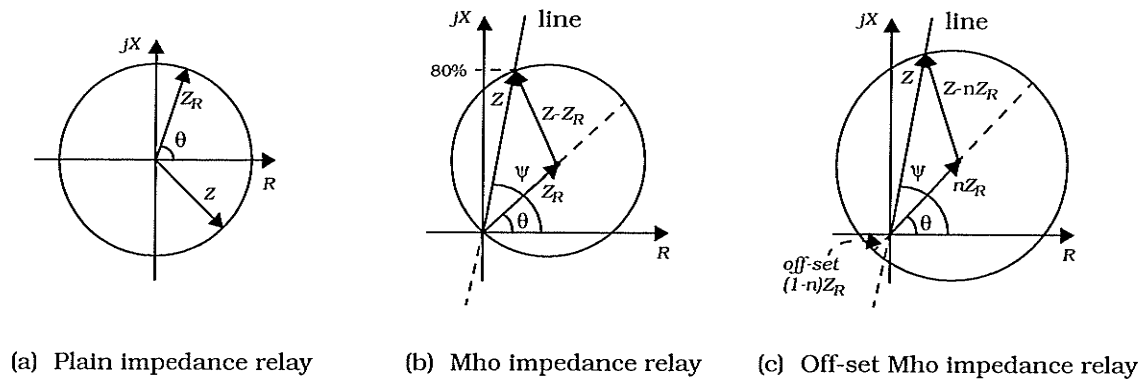


**Fig. 2.3** Distance relay characteristics

The Mho distance relay is defined by [24]:

$$|Z - Z_R| \leq |Z_R| \quad (2.8)$$

A directional relay and its characteristic, shown in Fig. 2.3(b), is a circle passing through the origin (relaying point). It can still operate with close-up fault by introducing a voltage called the polarizing voltage which is obtained from a pair of healthy phases.

The Off-set Mho distance relay is defined by:

$$|Z - nZ_R| \leq |Z_R| \quad (2.9)$$

It is also directional and the off-set is given by  $(1-n)Z_R$ , where the fraction  $n < 1$ . Its characteristic is shown in Fig. 2.3(c). The Off-set mho relay offers good operation under close-up faults, even close-up three-phase faults. It will also oper-

ate for faults a short distance behind itself, i.e. it gives some back-up protection (zone 3) for the busbars. A typical value of the off-set is 10% ( $n=0.9$ ) of the protected zone length.

The Mho family is most widely applied because it is inherently directional. It provides the best fault coverage and is relatively immune to high load conditions and power swings [26]. In Fig. 2.3,  $\psi$  is the line-impedance angle and  $\theta$  is the characteristic angle of the distance relay.

Based on the principles of relay arrangement and distance relays outlined above, a distance protection system for the transmission system shown in Fig. 2.1 has been established in Fig. 2.4. Zone 1 is a mho distance relay set to about 80% of the length of the protected line  $NM$ . It is converted, after about 0.3 s, into the zone 2 relay when its setting is about 1.3 zones ahead. The zone 3 relay, an entirely separate relay, is an off-set mho relay, set to about 2.25 zones ahead, which, for a fault within its reach, starts two timer-relays. The first timer-relay converts zone 1 to zone 2 measurement about 0.3 s while the second trips the circuit breaker at N about 0.6 s after fault initiation.

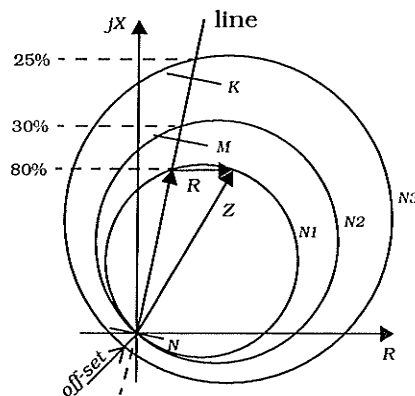


**Fig. 2.4** Typical distance system

## 2.5 Fault Resistance Tolerance of Distance Protection[26,28]

Of fundamental importance in assessing the effectiveness of the available polar characteristics of impedance-measuring relay is the range of fault resistances. The fault resistance has two components: arc resistance and ground resistance. Those resistances are non-linear and the arc fault resistance will be discussed in detail later.

In the mho operating characteristic shown in Fig. 2.3, the characteristic angle of the relay,  $\theta$ , is defined by the angle of impedance setting  $Z_R$ , between  $R$ -axis and the diameter of the characteristic circle which passes through the relaying point, as shown in Fig. 2.5. From Fig. 2.5, it is clear that the fault resistance tolerance of the distance relay can be adjusted by changing the phase angle difference ( $\psi - \theta$ ) at a sacrifice of less vulnerability to power swings.

However, as shown in Fig. 2.5, the tolerance of a mho relay is still limited because its characteristic is restricted to a circular shape. Reactance relays were introduced to overcome the problem of arc resistance at the point of fault.

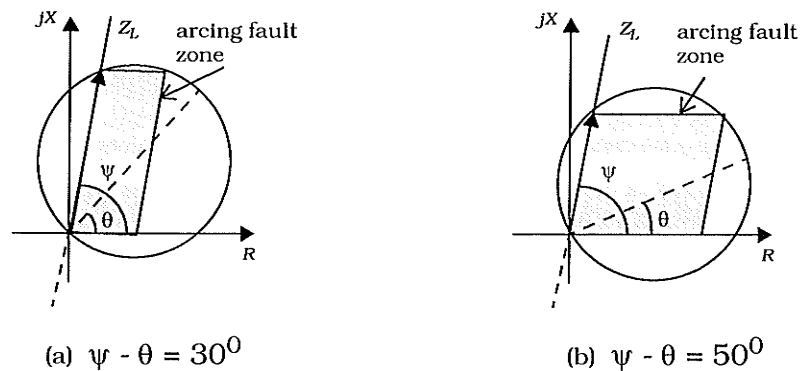


**Fig. 2.5** Phase angle biasing of Mho relay ( $\psi - \theta$ ) to increase tolerance of fault resistance

The effect was particularly severe for short lines where the vector addition of arc resistance and faulted line impedance could cause the resultant impedance to fall outside the relay impedance reach. Its characteristic, being parallel to the resistance axis and offsetting the reactance of the protected section from the origin, is shown in Fig. 2.6(a). The relay trips when the measured impedance lies below the characteristic. It is evident from Fig. 2.6(a) that the reactance relay is non-directional and susceptible to operation under load conditions and power swings.

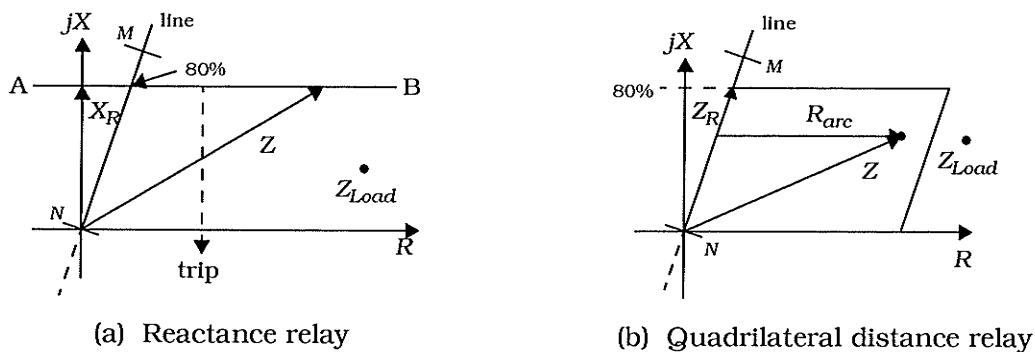


**Fig. 2.6** Two distance relays with better fault resistance tolerance

The distance relay with a quadrilateral characteristic, Fig. 2.6(b), has been used widely in computer relaying because microprocessors can be used to achieve independent control of resistance and reactance components of characteristic impedance. This relay is directional and has significant extension of the resistive reach under unbalanced fault conditions. It is a compromise between maximum resistive coverage and the avoidance of load and power swing encroachment.

In this thesis, the discussion is concentrated on the distance relay with a quadrilateral characteristic.

## Chapter Three

# Some Problems Of Distance Protection

---

### 3.1 Introduction

The increase in line lengths and power transmitted has introduced a number of new problems in relation to protection. New techniques have become necessary to tackle these problems and the stringent requirements associated with them. Firstly it has become necessary to see that lines are not unnecessarily disconnected (which leads to the loss of a portion of the power transmitted), but at the same time shorter operating times from protective relays are demanded on faulted sections to preserve the system stability. Moreover, extreme variations of fault current are often encountered with long lines necessitating that protective relays take this into account.

The establishment of electronic and computerizing methods has provided a much greater design flexibility. This is reflected mainly in the development of new types of techniques having more complex characteristics.

However, the suitability of distance relays to adapt to variation of source impedance, pre-fault loading in either direction, and variable ground fault resistance, especially for non-linear arc resistance, is still unsatisfied. In this chapter, some problems considered in this thesis are presented and some corresponding solutions are introduced. Even though some so-called adaptive relays appearing

in recent years are well suited to some of the existing problems, they are still quite complex procedures.

### **3.2 Inappropriate Settings**

Serious power system disturbances are often caused by faults in a weak power system. In these cases, mis-operation easily happens because of inappropriate settings. A system avalanche of outages can be caused by relays which have inappropriate settings for the prevailing system conditions. Such a situation is worsened because transmission system margins for contingencies are lessening, resulting from several factors such as difficulties with obtaining right of way, generation deferrals and uneven load growth. With this situation transmission protection reliability becomes increasingly important. Since they remove additional circuits along with the loss of the faulted system component, the mis-operation of relays represents a major source of concern to the planner and operator [30].

Neglecting measuring inaccuracies, the computation of the fault distance by a distance relay is affected by inappropriate settings because of the dynamic character of the power system. These would include changes in load and generation, and changes in the topology of the power system. These factors are usually dealt with by determining the relay settings according to off-line worst case studies. This results in fixed settings with great safety margins, depending on the compromise between security and dependability. Thus, distance relay settings seem to almost never be appropriate, as worst case scenarios are not likely to occur frequently [7].



Fault arc resistance is nonlinear (discussed in detail later) because it is essentially *a constant voltage* element rather than *a constant resistance* element. This means that if a distance relay is set to measure it correctly at a fault current calculated for a given source impedance, the fault arc resistance will appear high if the source impedance increases (because the fault current will decrease and  $\text{resistance} = \text{voltage}/\text{current}$ ). Conversely, if the source impedance decreases (at high generation day time conditions, for example), the fault arc resistance will appear low. Thus an impedance relay might underreach in the former case, and overreach in the latter case. For example, under low system impedance which the relay's settings are based on, if there is an arc resistance located inside the relay tripping zone, Fig. 3.1 (a), the same fault will cause relay mis-operation when the system impedance goes higher, as shown in Fig. 3.1 (b). Note that simply increasing the resistance reach of the relay might encroach on the load region.

Relays based on microprocessors are often used for protection purposes. They provide remarkable benefits such as flexibility, reliability and communication ability. Adaptive conceptual solutions have been introduced to improve the performance of power system transmission line protective relaying and, hence, the reliability of power system operation has been enhanced [30]. Information about the actual state of the power system is collected from substations equipment, and then forwarded to the control center.

Source equivalent impedance could be developed at the substation using a locally available system impedance data base and circuit-out information from local event and from remote computers[30].

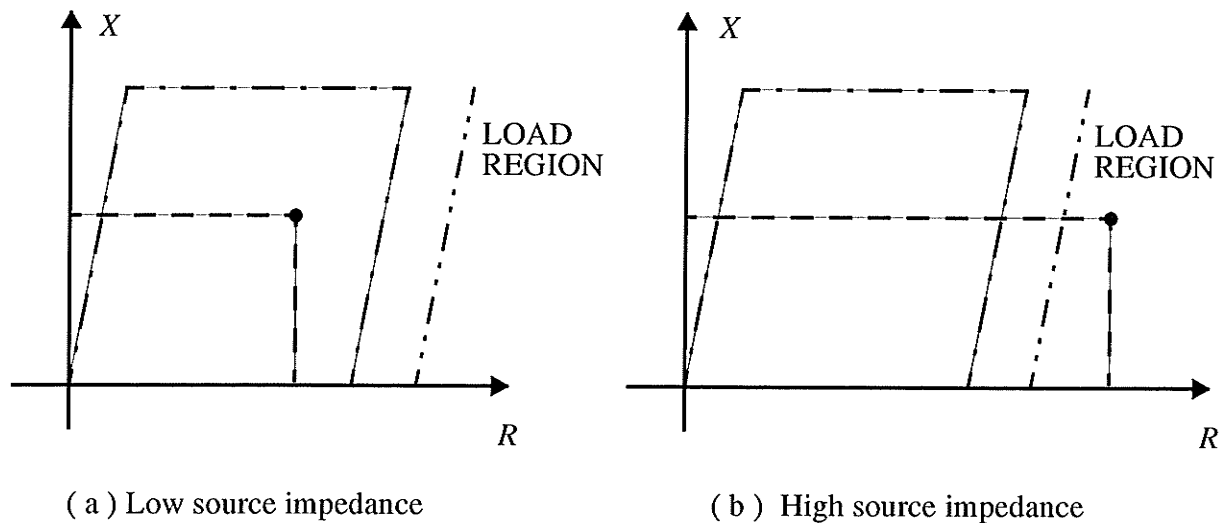


**Fig. 3.1** Effect of source impedance on distance relay

An approximate impedance model can be updated based on conditions within the substation. Open circuit breakers or undercurrent conditions can recognize the opening of lines connected to the station. Distinctive load flow manners may claim an outage of a nearby generator. Upon detection of a configuration change, the substation host computer provides an update of the impedance model, using pre-loaded system equivalents and local circuit impedances. The accuracy of the impedance model improves with better knowledge of the status of the system beyond the substation.

Therefore, inappropriate settings can be avoided by adjusting the settings of the relay according to changes in the power system state because the status of the complete system is available. Such an adaptive relay can be thought of as a protection device whose characteristics or functions are altered on the basis of external information [31]. The local available information is used to adapt

the relays to the actual power system state and maintain appropriate settings. Relays that can change settings adaptively reduce the necessary safety margins, and are therefore more selective because they keep track of the power system state. Relays are adapted to the prevailing power system state, and their misoperations are reduced.

However, adaptive processing is a complex procedure for microcomputer based relays.

### **3.3 Load Encroachment**

Application of impedance-measuring relays requires adequate discrimination against maximum circuit load conditions. The protection impedance characteristic must avoid load impedance encroachment, Fig. 3.1(b). This is not a problem by applying zone-1 and zone-2 relays but can be a significant practical problem in setting the zone-3 reach for circuits comprising very long bundle-conductor lines.

In practice, considerations of circuit loading must take account of maximum circuit rating as dictated by the sending-end to receiving-end busbar-voltage ratio and the corresponding angular displacement. These factors affect the boundary of load conditions in the way shown in Fig. 3.2. The change of angular displacement between busbar voltages for unity voltage ratio between ends generates the load varying trace ABC. The effect of variation in the ratio of busbar voltages is seen to produce the curvilinears A'B'C' and A''B''C'', and the two sets  $P_1$  and  $P_2$  being for receiving and sending conditions, respectively. It is clear that maximum circuit loading can present an impedance to the distance

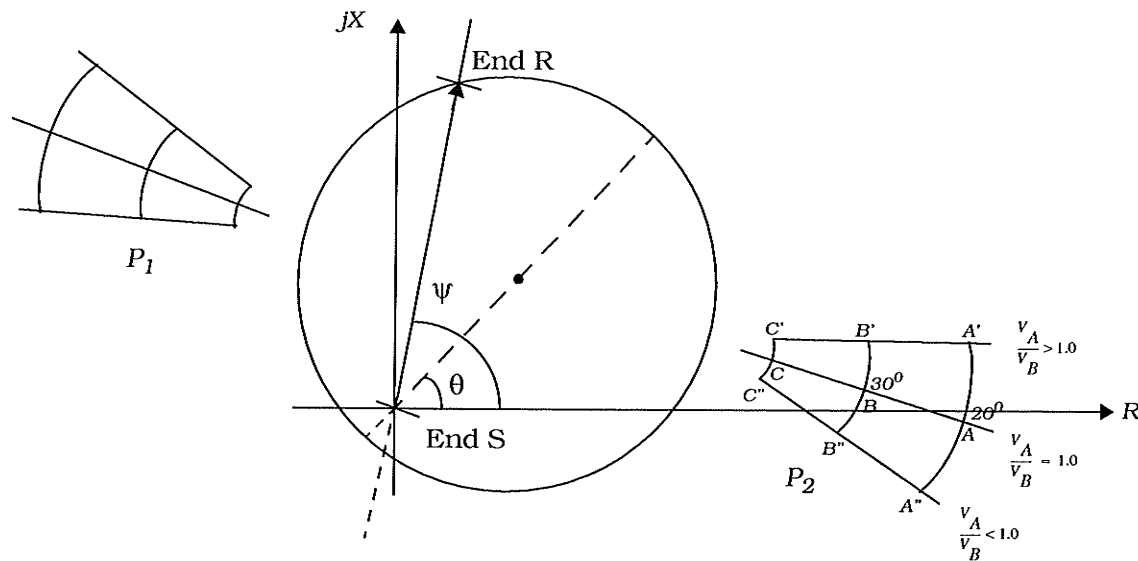


**Fig. 3.2** Load conditions superimposed on impedance polar diagram

relay which encroaches on its boundary and this may lead to a limitation on relay settings.

In a transmission system, the fault resistance of a line-to-ground fault is dominated by ground resistance which could be much bigger than arcing fault resistance. However, in a distribution system, the arcing fault resistance will be the main part of the fault resistance and could be bigger than the load resistance, as shown in Fig. 3.1 (b).

### 3.4 Effect of Pre-fault Load Flow[26,32]

Fig. 3.3 shows a typical single-line diagram of a power system with ground fault. The system has a source at each end of the line and some details

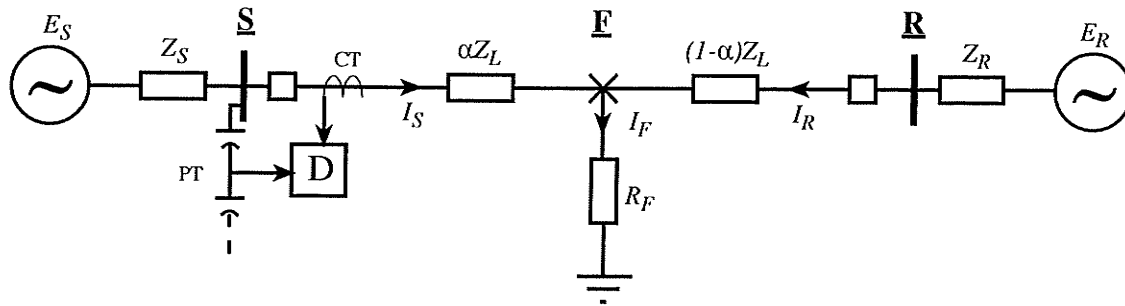
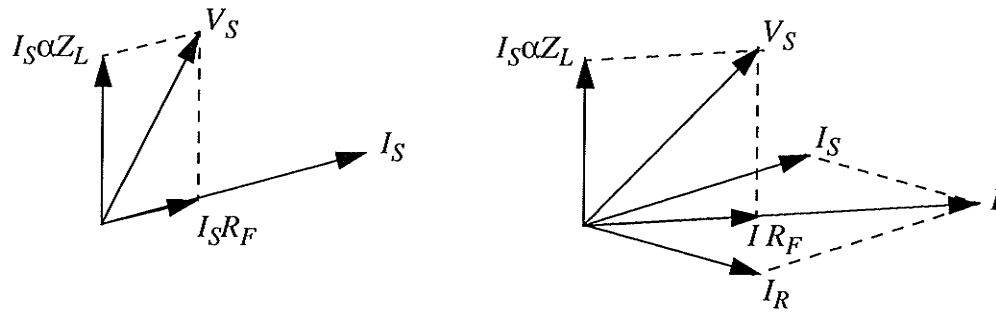


**Fig. 3.3** A power system with a single line-to-ground fault

on the transmission line are shown in the figure. A single line-to-ground fault occurs between phase and ground at  $F$ , a fraction  $\alpha$  of the total distance  $L$  from bus  $S$  to bus  $R$ . A distance relay located at bus  $S$  monitors the voltage phasor and current phasor to determine the value of the fault impedance. The measured impedance is given in the form of equation (2.5). For the ground fault distance relay, there is a basic problem of accommodating fault resistance, the value of which as seen by the relay may differ from the real value as a result of remote infeeds. The problem is illustrated by Fig. 3.4. It is simplified by assuming that source impedances at  $S$  and  $R$  are significantly larger than  $\alpha Z_L$ ,  $(1-\alpha)Z_L$  and  $R_F$ . For a fault fed only from  $S$ , the relay at end  $S$ , supplied with  $V_S$  and  $I_S$ , would see the true resistance with the drop across  $R_F$  being in-phase with  $I_S$  (Fig. 3.4(a)). For a fault fed from  $S$  and  $R$ , fault currents  $I_S$  and  $I_R$  will have a phase shift determined by the prefault load transfer conditions (Fig. 3.4(b)). In this case, the remote source infeed to the fault branch may significantly modify the apparent impedance presented to the relay at the local end. The fault current from both local and remote terminals causes a voltage drop in the fault branch if it is not in phase with the local fault current. It gives a reactance effect and shifts the fault

locus up or down in the impedance plane. The shift direction and magnitude for



(a) Phasor diagram for single-end feed      (b) Phasor diagram for double-end feed

**Fig. 3.4** Effect of remote fault infeed on measuring accuracy

the fault locus is dependent upon the system power flow at pre-fault.

Consider a distance relay with a quadrilateral characteristic, as shown in Fig. 3.5. In the case if there is no power flow through the transmission line,

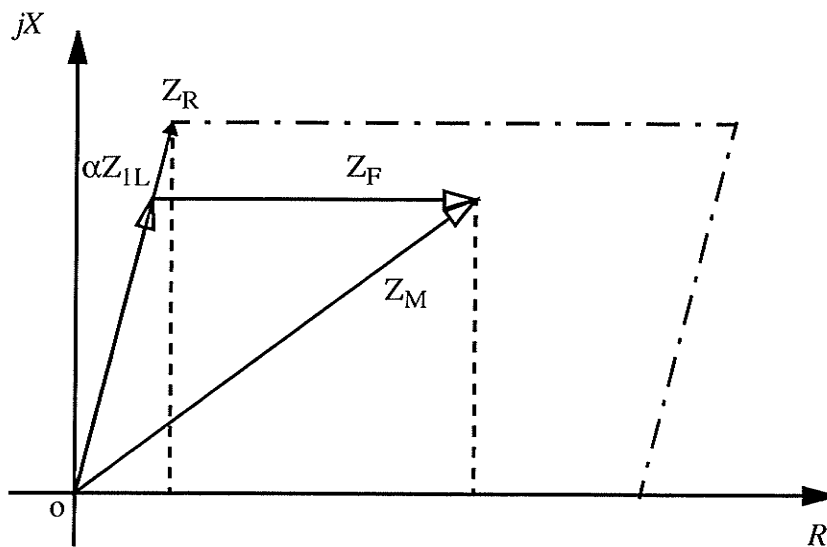


**Fig. 3.5** Effect of fault resistance on measured impedance  
( no real power flow )

the fault voltage and the relay current will be in phase and provide a pure resistance effect as shown in Fig. 3.5.

In the case if there is a power flow from bus  $S$  to bus  $R$  (Fig 3.3), the fault voltage will lag the relay current and shift the fault impedance locus downward on the impedance plane, as shown in Fig. 3.6, which causes a possible overreach error.

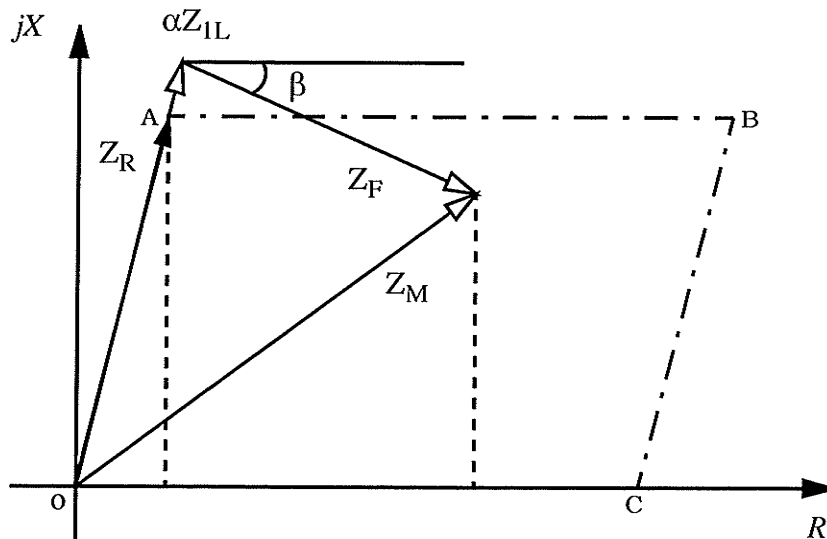


**Fig. 3.6** Effect of ground fault resistance on measured impedance  
( power flow from  $S$  to  $R$  )

In the case if there is a power flow from bus  $R$  to bus  $S$  (Fig 3.3), the fault voltage will lead the relay current and shift the fault impedance locus upward on the impedance plane, as shown in Fig. 3.7, which causes a possible underreach error.

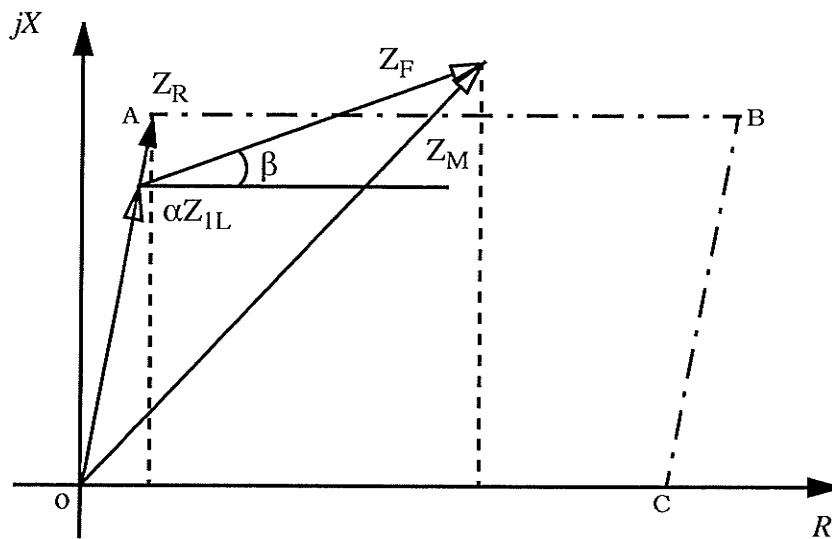
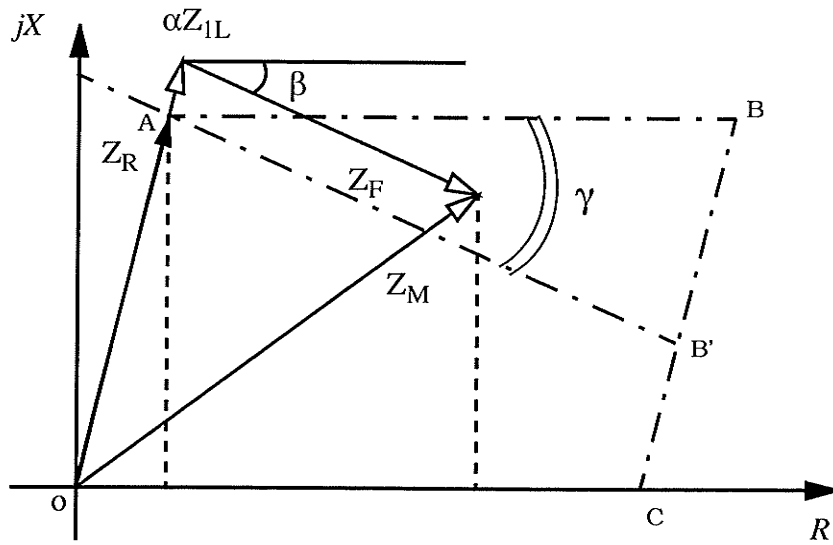


**Fig. 3.7** Effect of ground fault resistance on measured impedance  
( power flow from R to S )

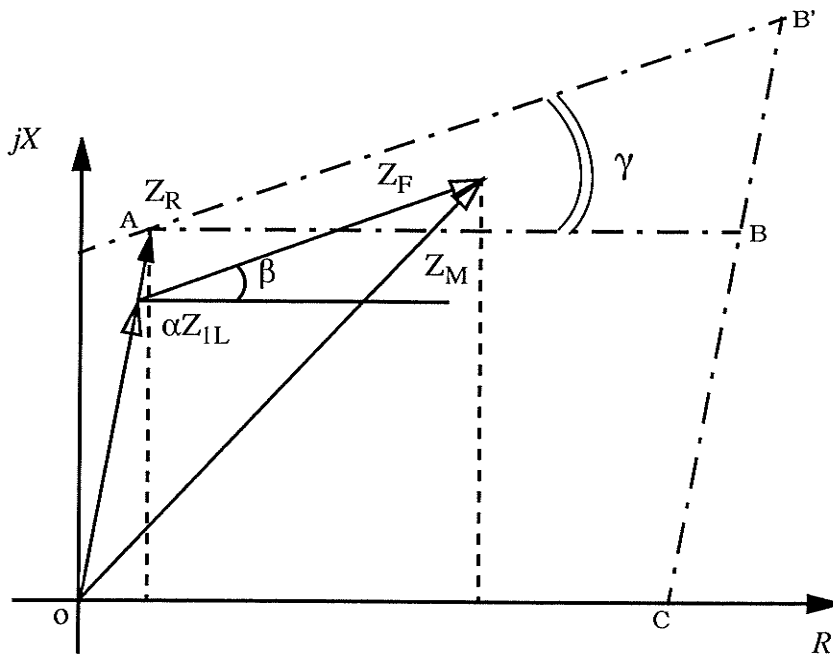
In order to compensate the errors caused by ground fault resistance and remote infeed, an adaptive scheme for single line-to-ground fault protection is suggested in [33]. It is believed that this adaptive scheme can provide the digital impedance relay the ability to automatically adjust its operating characteristic so that the relay can more closely follow the locus of the measured impedance associated with variable pre-fault load flow conditions.

Taking account of Fig.3.6 and Fig 3.7, if the boundary AB of the distance relay operating characteristic can be rotated through the angle  $\gamma$  around the reference point A as center, then the operating boundary ABCO will be rearranged as a new quadrilateral AB'CO, as shown in Fig. 3.8. By this means, the misoperation of the distance relay can be avoided and the elimination of the negative influence of the fault resistance is feasible.





(a) Adaptive operating characteristic ( power flow from S to R )



(b) Adaptive operating characteristic ( power flow from R to S )

**Fig. 3.8** Characteristics of adaptive distance relay

Although the above method is a great idea, its implementation is still a complex procedure because the remote source impedance is not known.

### **3.5 Nonlinearity of Arcing Fault Resistance**

For faults involving ground, fault impedance is generally understood to include the impedance in the path of the fault current between a phase conductor at the fault point and ground, including local ground resistance. Only the non-linearity of arcing fault resistance is covered in this thesis but not the ground resistance because of the complex inherently nonlinear characteristics of soil [34].

Short circuits on transmission lines and at terminals of high voltage power equipment usually take place through long arcs in air between conductor and ground (in the case of wires falling on the earth), in tower footings, in a foreign object between conductor and tower (or ground) or in some combination of these factors. Fault impedance, in general, appears to be predominantly resistive. It may be constant throughout the duration of a fault or it may vary continuously, as in the case of an arc which is blown out to gradual extinction by the wind.

The drop across the arc will affect the phase angle between voltage and current in directional types of relays. Of fundamental importance in estimating the effectiveness of the available polar characteristics of impedance-measuring circuits is the range of fault resistances likely to occur in practice. Most of primary system faults are accompanied by a fault arc when phase conductors clash or co-ordinating gaps flash-over. The resistance of the arc is nonlinear with the most generally accepted expression for its value due to Van Warrington [24]:

$$R_F = \frac{2613L}{I^{1.4}} \quad (3.1)$$

where  $L$  is the length of arc in still air in meters and  $I$  is the fault current in amps.  $L$  will be initialized with the conductor spacing but it increases with the presence of a cross wind because the arc has no inertia.

Obviously, considering a given length of arc (due, for example, to a specific co-ordinating gap length) the fault arc resistance increases nonlinearly as the fault MVA reduces, i.e. as the source impedance ratio increases. Usually, the fault arc resistance in an earthed construction line will be unlikely to exceed about  $0.5 \Omega$  which could be significant for distribution lines for which fault arc resistance imposes an application limit.

The investigation of the nature of arcing fault resistance is an old topic and was studied by a few early researchers about a half century ago. The characteristics of fault resistance are described and the neutral-current wave traces are presented in [36]. Based largely on statistical and oscillographic study of power system fault currents for five power systems, the reasonable values of fault resistance for a line-to-ground fault are given by [37]. The most frequently occurring values of "apparent fault resistance" (which includes the arc resistance) for the systems studied ranged from  $5$  to  $25 \Omega$ . Those determined for faults at substations were generally less than for faults on lines. The data indicate that, where fault resistance is to be allowed for in fault current computations,  $20 \Omega$  for line and  $5 \Omega$  for substation ground-faults are reasonable values to use.

## Chapter Four

# Simulation of Transmission Line Faults

---

### 4.1 Introduction

As stated in the previous chapter, the distance relay is one of the most important relays for transmission or distribution lines. To demonstrate the performance of a distance relay with new concepts, strategies or algorithms, the most important step is to put it in a field test. However, it is hard to develop a distance relay, especially one using artificial neural networks for which few efficient hardware or computing frames are available. Because of the availability of the artificial neural network simulator, Xerion, in the department of Electrical and Computer Engineering at the University of Manitoba, the digital simulation of power system transmission line faults is favored in this research.

A power system simulator, PSCAD/EMTDC\* (Electromagnetic Transients Simulation Program) has been developed by The Manitoba HVDC Research Centre. It is a powerful tool for solving large systems and analyzing specific problems in power systems. It can model AC machines, transformers, distributed transmission lines/cables, DC inversion/conversion, and many other elements in actual power systems. It has a user-friendly graphical user interface so that the systems studied can be built quickly and the simulation can be handled easily.

---

\*. PSCAD: Graphic User Interfaces for EMTDC

Users can create their own models, functions or algorithms of dynamic systems through the construction and use of subroutines[45].

An actual Manitoba Hydro transmission line, a 138kV line from Kelsey to Thompson in northern Manitoba, is here modelled on PSCAD/EMTDC.

In this chapter, details about the Kelsey-Thompson line are described. A traditional distance relay defined by Eq. (2.5) and (2.6) was also built up and simulated with this line model to create training, testing and running patterns for artificial neural networks.

## **4.2 Simulating The Kelsey-Thompson Line**

The Kelsey-Thompson line, designated K24W, is a transmission line designed for 230kV but actually operates at a 138kV voltage level. It is 97.77km long and located in northern Manitoba. Its length was extended to 100km for convenience.

Most faults in power system transmission lines are single line-to-ground faults. This work, therefore, focuses on such cases. More complex fault conditions will be considered in future work.

### **4.2.1 Simulating System Structure**

The system modelled is shown in Fig. 4.1. It consists of equivalent sources at each end, two sets of circuit breakers as well as their control logic, three transmission line sections, and a fault branch with its control logic.

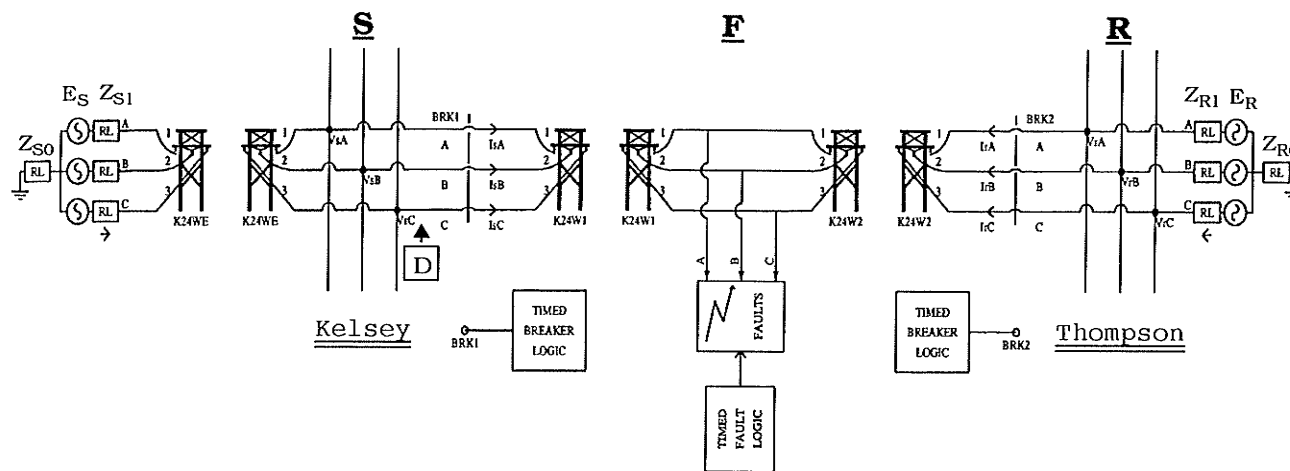


**Fig. 4.1** System model on PSCAD/EMTDC

In the system shown, a single line-to-ground fault (phase A to ground) is located at  $F$  through a fault resistance  $R_F$  and controlled by timed fault logic which specifies the time to apply the fault and the duration of the fault. The circuit breaker sets keep on conducting even during the single line-to-ground faults in order to sample the fault signals. The simulated line has been divided into three distinct sections: K24WE, 10km long, is for the simulation of reverse faults; K24W1 is for the line section between the relay location and fault location; and K24W2 is for the rest of the transmission line. The length of K24W1 plus K24W2 is 100km. Note that each of the three transmission line sections is implied between the identically labeled tower symbols.

### 4.2.2 Equivalent Source Impedances

As shown in Fig. 4.1, the systems at both ends are condensed into two equivalent sources. Each source has equivalent source impedances including positive, negative and zero sequence impedances. Table 4.1 and Table 4.2 list the equivalent source impedances provided by Manitoba Hydro. There are two types

**Table 4.1** *Subtransient source impedance  $X''d$  ( $\Omega$ )*

Minimum generation

	Kelsey	Thompson
Positive Sequence	$1.29 + j 19.11 = 19.15 \angle 86.1^{\circ}$	$3.08 + j 27.03 = 27.20 \angle 83.5^{\circ}$
Negative Sequence	$1.57 + j 21.70 = 21.75 \angle 85.9^{\circ}$	$3.13 + j 28.23 = 28.40 \angle 83.7^{\circ}$
Zero Sequence	$0.52 + j 11.93 = 11.94 \angle 87.5^{\circ}$	$0.30 + j 4.69 = 4.70 \angle 86.4^{\circ}$

Maximum generation

	Kelsey	Thompson
Positive Sequence	$1.06 + j 16.26 = 16.30 \angle 86.3^{\circ}$	$2.82 + j 24.49 = 24.65 \angle 83.4^{\circ}$
Negative Sequence	$1.12 + j 16.90 = 16.94 \angle 86.2^{\circ}$	$2.82 + j 24.72 = 24.88 \angle 83.5^{\circ}$
Zero Sequence	$0.52 + j 11.93 = 11.94 \angle 87.5^{\circ}$	$0.30 + j 4.69 = 4.70 \angle 86.4^{\circ}$

**Table 4.2** *Transient source impedance  $X'd$  ( $\Omega$ )*

Minimum generation

	Kelsey	Thompson
Positive Sequence	$1.68 + j 26.10 = 26.16 \angle 86.3^{\circ}$	$3.18 + j 31.03 = 31.19 \angle 84.1^{\circ}$
Negative Sequence	$1.51 + j 23.24 = 23.28 \angle 86.3^{\circ}$	$3.07 + j 28.97 = 29.13 \angle 84.0^{\circ}$
Zero Sequence	$0.52 + j 11.93 = 11.94 \angle 87.5^{\circ}$	$0.30 + j 4.69 = 4.70 \angle 86.4^{\circ}$

Maximum generation

	Kelsey	Thompson
Positive Sequence	$1.19 + j 18.41 = 18.45 \angle 86.3^{\circ}$	$2.86 + j 25.75 = 25.90 \angle 83.7^{\circ}$
Negative Sequence	$1.12 + j 16.91 = 16.95 \angle 86.2^{\circ}$	$2.81 + j 24.75 = 24.91 \angle 83.5^{\circ}$
Zero Sequence	$0.52 + j 11.93 = 11.94 \angle 87.5^{\circ}$	$0.30 + j 4.69 = 4.70 \angle 86.4^{\circ}$

of fault source impedance: sub-transient and transient, which occur under minimum and maximum generation conditions. To demonstrate a relay's performance, the sub-transient source impedances should be used for transmission line fault simulations. At the current period of research, however, only steady state components of fault quantities are used, implying transient source impedances. Table 4.2 also shows that the positive and negative source impedances are quite close so that it is reasonable to set  $Z_2 = Z_1$  as is a common assumption. The zero sequence source impedances are independent of generation modes because the grounding points of the system are fixed no matter how many generators are operating.

Note that the source  $E_S$  in Fig. 4.1 is selected as zero phase reference.  $Z_{S1}$  and  $Z_{R1}$  are positive sequence source impedances and  $Z_{S0}$  and  $Z_{R0}$  are zero sequence source impedances.

### 4.2.3 Modelling of The Transmission Line

Generally, in electromagnetic transients simulations, a distributed transmission line is most suited for transient line response modelling using a digital computer. A distributed model operates on the principle of travelling waves. A voltage disturbance will travel along a conductor at its propagation velocity (near the speed of light), until it is reflected at the line's end. A transmission line is a delay function. Whatever is fed into one end will appear at the other end, perhaps slightly distorted, after some delay. However, there are some other considerations which must be dealt with which include mutual coupling with other conductors, and wave-shape attenuation as it travels along the line.



In EMTDC, the Frequency-Dependent Line Model is applied as the transmission line modelling technique. It is basically a distributed R-L-C travelling wave model which incorporates the frequency dependence of all parameters, and is necessary for studies requiring a very detailed representation of the line over a wide frequency range [46].

The PSCAD T-LINE program is used to generate the data required by the EMTDC line models. Only the conductor properties (resistance, radius ...) and geometry (horizontal and vertical tower dimensions) are required to model the line. The T-LINE program then stores the solved line constants data in named batch files. The DRAFT program copies the appropriate data from the batch files into the EMTDC data file.

The conductor properties and geometry of Kelsey-Thompson line are listed on Table 4.3.

#### 4.2.4 Data-acquisition Subsystem for Pattern Generation

In Fig. 4.1, a distance relay  $\square$  is located at bus S (Kelsey). The measured impedance  $Z_m$  from  $\square$  to the fault is of the form of Eq. (2.5), copied as follows:

$$Z_m = \frac{V_A}{I_A + \frac{k}{3}I_N} \quad (4.1)$$

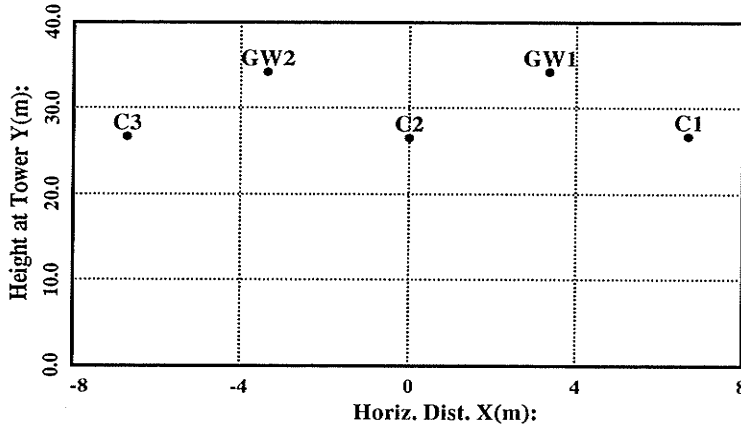
where

$$k = \frac{Z_{L0} - Z_{L1}}{Z_{L1}} \quad (4.2)$$

(zero sequence compensation factor)

**Table 4.3** Kelsey-Thompson line parameters**PS-CAD - Transmission Line Analysis Program**

Version 1.0  
Thu Aug 31 12:35:19 1995

**Summary of Main Data**

Line Name: K24W  
Line Length(km): 100.0  
Gnd Resist.(ohm-m): 100.0  
Low Freq(Hz): 5  
High Freq(Hz): 1e+06  
Ideally-Transposed Conductors  
Travel Times are Interpolated  
Transform Freq.(Hz): 60

**Summary of Conductor Data**

Conductor # ( 1 - 3 ) ---->	1	2	3
Conductor Name:	1272ACSR	1272ACSR	1272ACSR
Conductor Type (AC/DC):	AC	AC	AC
V(kV)(AC:L-L,rms/DC:L-G,pk):	138.0	138.0	138.0
V Phase(Deg.):	0.0	-120.0	120.0
Line I (kA)(AC:rms/DC:pk):	1.2	1.2	1.2
Line I Phase(Deg.):	-20.0	-140.0	100.0
# of Sub-Conductors:	1	1	1
Sub-Cond Radius(cm):	1.43077	1.43077	1.43077
Sub-Cond Spacing(cm):	45.72	45.72	45.72
Horiz. Dist. X(m):	6.706	0.0	-6.706
Height at Tower Y(m):	26.670	26.542	26.670
Sag at Midspan(m):	18.898	18.898	18.898
DC Resistance(ohms/km):	0.04305	0.04305	0.04305

**Summary of Ground Wire Data**

Ground Wire # ( 1 - 2 ) ---->	1	2
Conductor Name:	7/16 Steel	7/16 Steel
Cond Radius(cm):	0.48077	0.48077
Horiz. Dist. X(m):	3.353	-3.353
Height at Tower Y(m):	34.107	34.107
Sag at Midspan(m):	14.630	14.630
DC Resistance(ohms/km):	2.29956	2.29956

- $Z_{L1}$  : positive sequence impedance of the line.
- $Z_{L0}$  : zero sequence impedance of the line.
- $V_A$  : the faulted phase voltage at relay location.
- $I_A$  : the faulted phase current at relay location.
- $I_N$  : the neutral current at relay location.

The voltages and currents in (4.1) are the stable state fundamental components after faults and they need to be extracted from the voltages and currents at the relay location. FFT and sequence quantity extraction are applied as shown in Fig. 4.2.

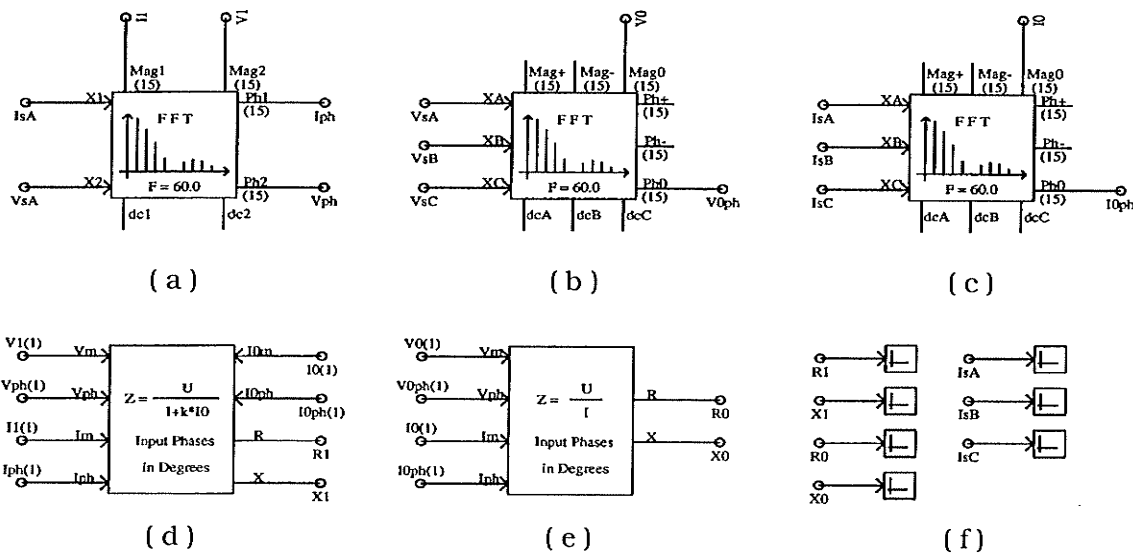


**Fig. 4.2** Pattern generation subsystem

Fig. 4.2(a) presents a fundamental component extractor whose inputs are faulted phase voltage  $V_{SA}$  and current  $I_{SA}$  while its outputs are the fundamental components of input voltage and current represented by their magnitudes and phase angles. Fig. 4.2 (b) and (c) show the sequence component extractor whose

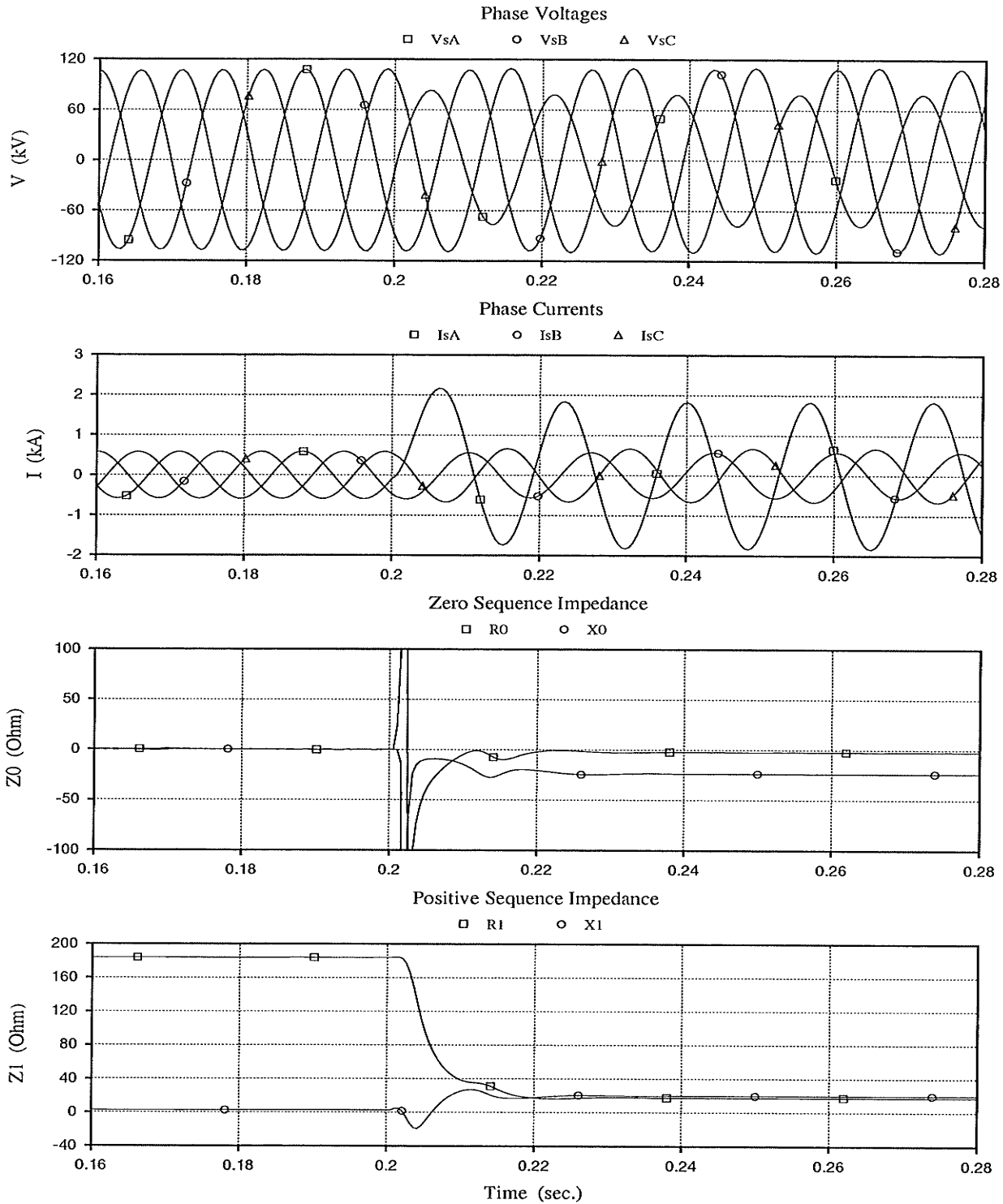
inputs are voltages and currents at the relay location while the outputs are the magnitudes and phase angles of zero sequence voltage and current.

Fig. 4.2 (d) forms a distance relay function of (4.1) and the FORTRAN subroutine is referred in APPENDIX C. This block produces measured impedance  $Z_m = R_1 + j X_1$ , which is the fault impedance of the transmission line from relay location to fault location at the fault period while it should be the load impedance during pre-fault. Fig. 4.2 (e) gives a impedance relay function which provides the zero sequence impedance  $Z_0 = R_0 + j X_0$  at relay location. Its FORTRAN subroutine is referred in APPENDIX C. Fig. 4.2 (f) will illustrate the current waveforms and impedance outputs.

The pattern generation procedure is implemented by a set of signal processing units as shown in Fig. 4.2. The reasons for selecting  $R_1$ ,  $X_1$ ,  $R_0$ ,  $X_0$  as input patterns will be discussed for details in Chapter 6.

#### 4.2.5 Sample Outputs

Let us consider a case when the source at each end of the line is at maximum generation, i.e.  $Z_{S1} = 1.19 + j 18.41 \Omega$ ,  $Z_{S0} = 0.52 + j 11.93 \Omega$  and  $Z_{R1} = 2.86 + j 25.75 \Omega$ ,  $Z_{R0} = 0.30 + j 4.69 \Omega$ . Assuming that the load angle  $\delta = -30^\circ$  and the phase A to ground fault happens at 50% of the line with a fault resistance  $R_F = 15 \Omega$ . The outputs for a single line-to-ground fault are shown in Fig. 4.3.



**Fig. 4.3** Simulation of the transmission line

In Fig. 4.3, the single line-to-ground fault happens at 0.2 seconds at which time, the  $V_{SA}$  decreases and  $I_{SA}$  increases. Note that the impedance outputs are unstable during the fault transients and thus, they can not be used for the fault distance measurement. The reason for this is that the time-decaying transient DC component significantly affects the FFT accuracy. As a result, the impedance outputs two cycles after the fault will be used here for the fault location computation.

## Chapter Five

# Artificial Neural Networks<sup>[39-43]</sup>

---

### 5.1 Introduction

The recent re-emergence of network-based approaches to artificial intelligence (“artificial neural networks”) has been accomplished by a virtual explosion of research, spanning a range of disciplines perhaps wider than any other contemporary intellectual endeavor. Researchers from such diverse fields as cognitive science, physics, neuro-science, computer science, economics, medicine, engineering, statistics, philosophy and mathematics are making substantial contributions daily to the understanding, development and application of artificial systems that mimic certain aspects of the formulation and functionality of animal and human intelligence.

The resurgence of interest in artificial neural networks has its own roots in the recognition that the human brain performs computations in a different manner than do conventional digital computers. Computers are very fast and precise at executing sequences of instructions that have been formulated for them. A human information processing system is composed of neurons switching at speeds about a million times slower than computer gates. Yet humans are more efficient than computers at computationally complex tasks such as speech understanding and visual information recognition.

Programmed computation has its base on decision rules and algorithms transformed to the form of computer programs. The algorithms and program-controlled computation which the conventional computers require have their counterparts in the learning rules and information recall procedures of an artificial neural network. However, these are not precise counterparts because artificial neural networks go above digital computers since they can progressively change their processing construction corresponding to the information received.

***“Artificial neural networks (ANNs) are physical cellular systems which can acquire, store, and utilize experiential knowledge. The knowledge is in the form of stable states or mappings embedded in networks that can be recalled in response to the presentation of cues.”***[41]

An artificial neural network as a computing system is made up of a number of simple and highly interconnected processing units which handle information by its dynamic state response to input from the external world. The study of the ANN models is gaining rapid and increasing importance because of their potential to offer solutions to some of the problems which have been intractable so far by standard serial computers in the areas of computer science and artificial intelligence. The fundamentals of artificial neural network theory and algorithms for information acquisition and retrieval will be introduced in this chapter.

## **5.2 General Description of A Neural Network**

An artificial neural network's capability to perform computations is based on the hope that we can duplicate some of the flexibility and power of the human brain by artificial measure. Network computation is performed by a dense



mesh of calculating nodes and links. They work collectively and simultaneously on most or all data and inputs. The basic processing components of neural networks are called *neurons*, or *nodes*. Neurons work as summing and nonlinear mapping junctions. They can be considered as threshold nodes that fire after their total input exceeds certain bias levels. Neurons usually operate in parallel and are configured in regular architectures. They are often constructed in layers, and feedback link strength is expressed by a numerical value called a *weight*, which can be changed.

Artificial neural networks function as parallel distributed computing systems. Their most fundamental feature is their architecture. A few of the networks provides instantaneous responses. Other networks require time to respond and are featured by their time-domain behavior, which is referred to as *dynamics*. Neural networks also differ from one another in their learning methods. There are many learning rules that establish when and how the link weights change. Finally, networks show a variety of speeds and efficiency of learning. Therefore, they also differ in their capability to precisely respond to the cues presented as the input.

Unlike conventional computers, programmed to implement specific tasks, neural networks must be taught, or trained. They learn new patterns, and new functional relationships. *Learning corresponds to parameter alterations*. Learning rules and algorithms applied to experiential training of networks replace the programming needed for conventional computation. Application engineer do not specify an algorithm to be executed by each computing node as would programmers of a more traditional machine. Instead, they choose what in their opin-

ion is the best architecture, define the features of the neurons and initial weights, and select the training algorithm for the network. Proper inputs are then used for the network so that it can acquire knowledge from the environment. As a result of such procedure, the network digests the information that can later be reproduced by the user.

### 5.3 Artificial Model of The Neurons

The *elementary nerve cell (neuron)* is the fundamental building block of the biological neural network. A typical cell has three major regions: the cell body, the *axon*, and the *dendrites*. Dendrites form a dendritic tree and receive information from neurons through axons. An axon is a long, cylindrical connection that carries impulses from the neuron. The axon-dendrite contact organ is called a *synapse*. The synapse is where the neuron introduces its signal to the neighboring neuron. The receiving neuron either generates an impulse to its axon, or produces no response, depending on the conditions necessary for firing to be fulfilled.

Incoming impulses can be *excitatory* if they cause the firing, or *inhibitory* if they hinder the firing of the response. A more precise condition for firing is that the excitation should exceed the inhibition by the amount called the *threshold* of the neuron. Since a synaptic connection causes the excitatory or inhibitory reactions of the receiving neuron, it is practical to assign positive and negative unity weight values respectively, to such connections. The neuron fires when the total of the weights to receive impulses exceeds the threshold value.

A general neuron model is represented in Fig. 5.1. This artificial neuron consists of inputs, summation, activation function and a single output. The signal flow of neuron inputs,  $x_i$ , is considered to be unidirectional as indicated by arrows.

Each neuron can have multiple inputs, while there can be only one output. Inputs

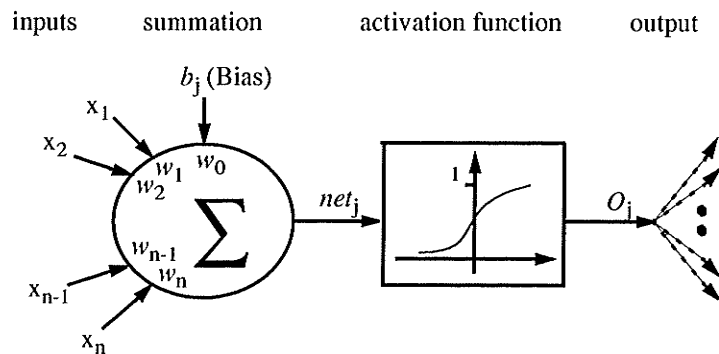


**Fig. 5.1** Model of  $j$ th neuron

to a neuron could be from external stimuli or from the output of other neurons. Each of the inputs to the neuron is multiplied by an associated weight, and these weighted inputs are summed with a bias, which can be also seen as an extra input to the neuron. This summation is presented to the activation function which determines the output value of the neuron, i.e.

$$O_j = g(net_j) = g\left(\sum_{i=1}^n w_i \cdot x_i + b_j\right) \quad (5.1)$$

where  $w_i$  is weight vector,  $x_i$  is input vector and  $b_j$  is the bias. The function  $g(x)$  is referred to as an activation function. Typical activation functions used are non-linear functions:

$$g(net_j) = \frac{1}{1 + \exp(-net_j)} \quad (0 < net_j < 1) \quad (5.2)$$

$$g(net_j) = \tanh(net_j) = \frac{\exp(net_j) - \exp(-net_j)}{\exp(net_j) + \exp(-net_j)} \quad (-1 < net_j < 1) \quad (5.3)$$

(5.2) is the sigmoid function with its unipolar feature and (5.3) is the hyperbolic tangent function with bipolar feature.

## 5.4 Multilayer Feedforward Networks

Biologically, the human brain is made up of billions of neurons. Each neuron performs like a computer with very limited capabilities. They communicate with each other by means of electrical impulses through a connecting network of axons and synapses. The vast neural network has an elaborate structure with very complex interconnections. The input to the network is provided by sensory receptors. Receptors deliver stimuli both from within the body, as well as from sense organs when the stimuli originate in the external world. The stimuli are in the form of electrical impulses that convey the information into the network of neurons. As a result of information processing in the central nervous systems, the effectors are controlled and give human responses in the form of diverse actions.

Similarly, an artificial neural network represents a new class of computing systems formed by simulated neurons connected to each other in much the same way as the brain neurons and working as a parallel distributed processing system. Fig. 5.2 shows the structure of a generic feedforward network which is the most commonly used ANN model.

An ANN consists basically of several layers: input layer, output layer and one or more hidden layers. The neurons in the input layer have a linear activation function, not a nonlinear one. Theoretically, a network can have any specifically chosen connection structure depending on the actual problem being addressed, where each neuron in any given layer may be connected to any neuron in any layer, including being connected to itself. If there are no connections leading from a neuron to neurons in previous layers, nor to other neurons in the same

layer, nor to neurons more than one layer ahead, and every neuron feeds only

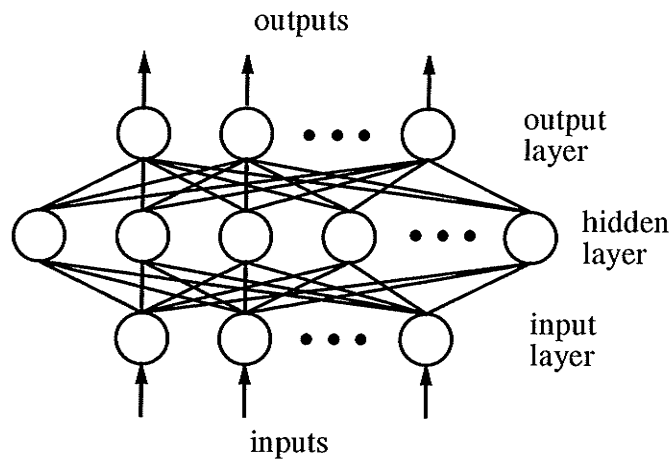


**Fig. 5.2** Topology of a three layer feedforward network

the neurons in the next layer, this neuron network is called feedforward network, or perceptrons. Fig. 5.2 shows a three layer feedforward network, where connections are unidirectional, so that a signal is presented to the input layer, and propagates through the hidden layers to the output layer.

In general, forward propagation consists of passing weighted and summed input signals through a chosen nonlinearity, i.e.

$$net_j(l+1) = \sum_{i=1}^N w_{ji}(l+1) \cdot O_i(l) + b_j(l+1) \quad (5.4)$$

$$O_j(l+1) = g[net_j(l+1)] \quad (5.5)$$

where  $O_j(l+1)$  is the output of the  $j$ th neuron of the  $(l+1)$ th layer;  $net_j(l+1)$  is the net input to the  $j$ th neuron in the  $(l+1)$ th layer;  $w_{ji}(l+1)$  is the weight between  $j$ th neuron of  $(l+1)$ th layer and  $i$ th neuron of  $l$ th layer;  $b_j(l+1)$  is the bias of the  $j$ th neuron of  $(l+1)$ th layer;  $g(x)$  is activation function. Once the activation function is chosen, a neural network is completely described by its weights and biases.

Since a given neural network solves a specific problem, finding weights and biases for the network is equivalent to finding the input/output relationship that describes the problem.

“Multilayer networks can implement arbitrary complex input/output mappings or decision surfaces separating pattern classes. The most important attribute of a multilayer feedforward network is that it can learn a mapping of any complexity. The network learning is based on repeated presentations of the training samples. The trained network often produces surprising results and generalizations in applications where explicit derivation of mappings and discovery of relationships is almost impossible.” [41]

### **5.5 Necessary Number of Hidden Neurons**

The size of a hidden layer is a most important consideration to solve real problems using multilayer feedforward networks. The problem of the size selection is under intensive research without conclusive answers available for many tasks. The precise analysis of the issue is difficult due to the complexity of the network mapping and the nondeterministic characteristic of many successfully finished training procedures.

“Single hidden-layer networks can form arbitrary decision regions in  $n$ -dimensional input pattern space. There exist certain useful solutions as to the number  $J$  of hidden neurons needed for the network to perform properly. [41]

Reference [41] suggests two formulas for estimating the number of hidden neurons. Assume that the  $n$ -dimensional nonaugmented input space is lin-

early separable into  $M$  disjoint regions with boundaries being parts of hyperplanes. The hidden layer neurons  $J$  needed to achieve classification constitutes the solution of the equation:

$$M = 1 + J + \frac{J(J-1)}{2!} + \frac{J(J-1)(J-2)}{3!} + \frac{J(J-1) \cdot \cdot \cdot (J-n+1)}{n!} \quad (5.6)$$

for  $J > n$

For the case  $J \leq n$  we have simply

$$J = \log_2 M \quad (5.7)$$

## 5.6 Back Propagation Learning Algorithm [39]

The back propagation learning algorithm is the most frequently used method in training the neural network. This algorithm finds the values of all of the weights that minimize the error function using a method of gradient descent. That is, after each pattern has been presented, the error on that pattern is computed and each weight is moved down the error gradient towards its minimum value for that pattern.

The iterative determination of the weights is usually initiated by setting the weights to some small random values. The weight adjustments are then made by applying the generalized delta rule which is based on the well-known gradient minimization method. If pattern  $\mu$  is presented to the network, the inputs are always clamped to particular values, as shown in Fig. 5.3. We mark different patterns by a superscript  $\mu$ , then input  $k$  is set to  $\xi_k^\mu$  if pattern  $\mu$  is being presented. The  $\xi_k^\mu$  can be binary or continuous-valued.  $N$  is used for the number of input

units and  $p$  for the number of input pattern ( $\mu=1,2, \dots , p$ ). A differentiable function  $g(x)$  is chosen as activation function for all units.

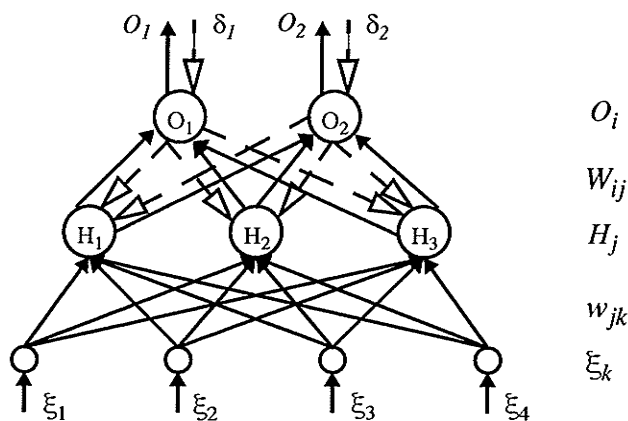


**Fig. 5.3** Error back-propagation in a three-layer network

— Forward propagation of signals  
 - - - Backward propagation of errors

For a given pattern  $\mu$ , hidden unit  $j$  has a net input

$$h_j^\mu = \sum_k w_{jk} \xi_k^\mu \tag{5.8}$$

and generates output

$$H_j^\mu = g(h_j^\mu) = g\left(\sum_k w_{jk} \xi_k^\mu\right) \tag{5.9}$$

Therefore, output unit  $i$  has

$$o_i^\mu = \sum_j W_{ij} H_j^\mu = \sum_j W_{ij} \cdot g\left(\sum_k w_{jk} \xi_k^\mu\right) \tag{5.10}$$

and reaches the final output

$$O_i^\mu = g(o_i^\mu) = g\left(\sum_j W_{ij} H_j^\mu\right) = g\left(\sum_j W_{ij} \cdot g\left(\sum_k w_{jk} \xi_k^\mu\right)\right) \tag{5.11}$$



The bias terms have been omitted here because they can be taken care of by an extra input unit connected to all units in the network.

The error function  $E$  is actually defined by

$$E = \frac{1}{2} \sum_{\mu} \sum_i (T_i^{\mu} - O_i^{\mu})^2 \quad (5.12)$$

where  $T_i^{\mu}$  is the target output of unit  $k$ .

$O_i^{\mu}$  is the actual output of unit  $k$ .

The idea behind gradient descent is to make a change in the weight proportional to the negative of the derivative of the error, as measured in the current pattern, with respect to each weight. Thus to readily complete the derivative of the error function with respect to any weight in the network. We change the weight according to following rule

$$\Delta w = -\eta \frac{\partial E}{\partial w} \quad (5.13)$$

For the hidden-to-output connections the gradient rule gives

$$\Delta W_{ij} = -\eta \frac{\partial E}{\partial W_{ij}} = \eta \sum_{\mu} \delta_i^{\mu} H_j^{\mu} \quad (5.14)$$

and 
$$\delta_i^{\mu} = g'(h_i^{\mu}) [T_i^{\mu} - O_i^{\mu}] \quad (5.15)$$

where  $\eta$  is learning rate constant

For the input-to-hidden connection  $\Delta w_{jk}$ , we must differentiate with respect to the  $\Delta w_{jk}$ 's :

$$\Delta w_{jk} = -\eta \frac{\partial E}{\partial w_{jk}} = -\eta \sum_{\mu} \frac{\partial E}{\partial H_j^{\mu}} \cdot \frac{\partial H_j^{\mu}}{\partial w_{jk}} = \eta \sum_{\mu} \delta_j^{\mu} \cdot \xi_k^{\mu} \quad (5.16)$$

$$\delta_j^{\mu} = g'(h_j^{\mu}) \sum_i w_{ij} \cdot \delta_i^{\mu} \quad (5.17)$$

It is interesting that (5.16) has the same format as (5.14), but with a different definition of  $\delta$ 's. Generally, with an arbitrary number of layers, the weight update rule can always be written in the form

$$\Delta w_{pq} = \eta \sum_{\text{patterns}} \delta_{\text{output}} \times H_{\text{input}} \quad (5.18)$$

where *output* and *input* refer to the ends  $p$  and  $q$  of the link concerned, and  $H$  represents for the appropriate input-end activation from a hidden unit or a real input. The form of  $\delta$  depends on the layer concerned; for the last layer of connections it is given by (5.15), while for all other layers it is given by an equation like (5.17).

Usually, a sigmoid function is selected as the activation function  $g(x)$ . The derivatives of this function are readily expressed in terms of the function itself as  $g'(x) = g(1-g)$ . Thus (5.15) is often written as

$$\delta_i^{\mu} = O_i^{\mu} (1 - O_i^{\mu}) (T_i^{\mu} - O_i^{\mu}) \quad (5.19)$$

The convergence rate can be improved by adding a momentum term to (5.18)

$$\Delta w_{pq}(n+1) = \eta \sum_{\text{patterns}} \delta_{\text{output}} \times H_{\text{input}} + \alpha \Delta w_{pq}(n) \quad (5.20)$$

where  $\alpha$  is the momentum constant to determine the effect of past weight changes.  $n$  is the iteration number.

(5.17) allows us to determine the  $\delta$  for a given hidden unit  $H_j$  in terms of the  $\delta$ 's of units  $O_i$  that it feeds. The coefficients are just the usual "forward"  $W_{ij}$ 's, but here they are propagating errors backwards instead of signals forwards as shown in Fig. 5.3: hence the name error back-propagation or just back-propagation.

## 5.7 Pattern Classification by Artificial Neural Network

Pattern recognition, defined as an abstract formulation of the categorization tasks in pattern classification, is the dominating field of the applications of neural networks. A *pattern* is the quantitative description of an object or phenomenon. The goal of pattern classification is to assign a physical object or phenomenon to one of the prespecified *classes* (or *categories*). Despite the lack of any formal theory of pattern perception and classification, human beings and animals have performed these tasks since the beginning of their existence.

In general, the concept of pattern classification may be expressed as a mapping from  $N$  dimensional feature space  $\mathfrak{R}$  to decision space  $\mathfrak{C}$ , as shown in Fig. 5.4. The input to the pattern recognition system is a feature vector and the output is the decision as to the category in which the input pattern belongs. Given an input pattern, consisting of  $N$  measured patterns, it is possible to extract some of the inherent characteristics in the input pattern which are hard to be derived and to provide a meaningful categorization of input data content.

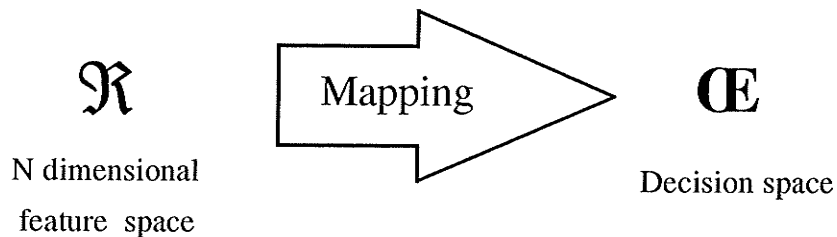


**Fig. 5.4** Principle of pattern classification by ANN

A pattern classification system is generally considered as a two stage device, The first stage is **feature extraction** and the second stage is **classification**, as shown in Fig. 5.5. Feature extraction corresponds to selection of a defi-

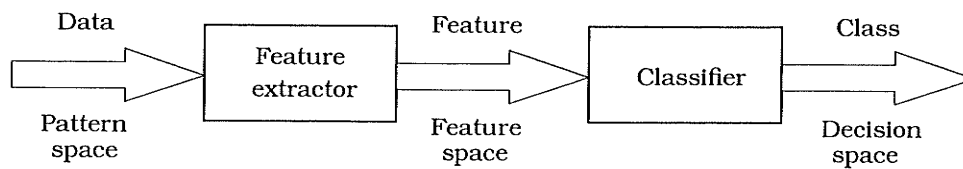


**Fig. 5.5** Block diagram of pattern classification system

nite characteristic of the input pattern. The classifier is supplied with the list of measured features. The task is to map these input patterns onto a classification state, that is, given the input features, the classifier must decide which type class category they must match closely. The classifiers typically rely on distance metrics and probability theories to perform the above task. They are designed to learn the proper decision rule using a training set. The training set consists of feature vectors of known classification. During the training phase, the system is given the feature vectors one by one and is told what the classification should be. The system uses this information in a learning algorithm to learn the decision rules needed.

To demonstrate the working principle of a classifier, let us consider a

simple example where there are only two inputs to the neural network,  $x_1$  and  $x_2$ . In this case, the pattern space reduces to be a plane with the inputs  $x_1$  and  $x_2$  being the coordinates of the plane, as shown in Fig. 5.6. Each point on the

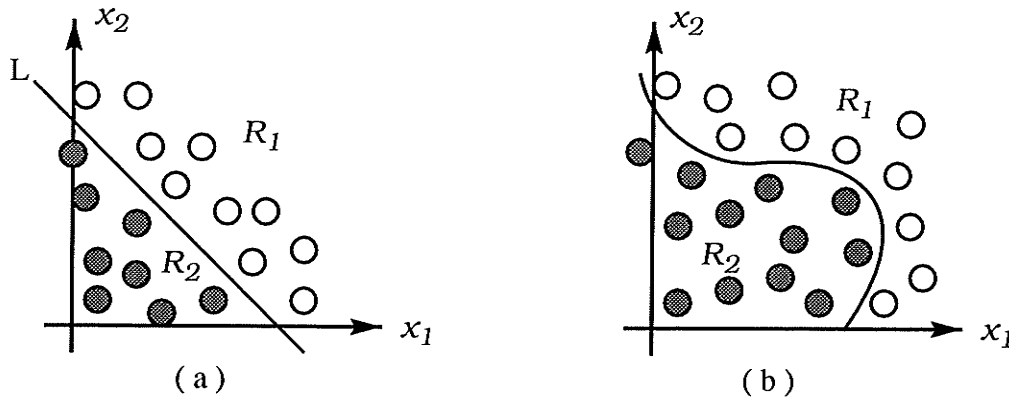


**Fig. 5.6** Separability of patterns

plane corresponds to an input pattern. If the relationship between input and output is linear, a linear function, such as threshold function, can be chosen as the activation function. There exists exactly a straight line to separate the input patterns into two categories,  $R_1$  and  $R_2$ , shown as in Fig. 5.6 (a) and ( 5.4 ) and ( 5.5 ) become:

$$L : w_1 \cdot x_1 + w_2 \cdot x_2 + b = 0 \quad (5.21)$$

$$R_1 : w_1 \cdot x_1 + w_2 \cdot x_2 + b > 0 \quad (5.22)$$

$$R_2 : w_1 \cdot x_1 + w_2 \cdot x_2 + b < 0 \quad (5.23)$$

In fact, problems in a power system are mostly nonlinear. A nonlinear function, such as a sigmoid function, can be chosen as the activation function, and hidden neurons can be added to the network. There should be a curve existing to map the input patterns to output categories, like in Fig. 5.6(b).

Actually, the number of neural network inputs,  $N$ , is usually more than two. Hence, the pattern feature space  $\mathfrak{R}$  can be divided into expected classes by a set of hyperplanes which can be used to represent the connection weights between neurons. Thus, updating connection weights in the training process is equivalent to moving the weight hyperplanes in pattern space  $\mathfrak{R}$ .

In electric power system protection, relays make decisions depending on input information (voltage and current patterns) and separate these decisions into two categories: normal operation and fault. Neural networks appear to offer features which coincide well with the requirements of protective relays. Distance protection can be conceptualized as a pattern classification problem which involves the association of patterns of input data representing the behaviour of the power system into one of two categories.

### **5.8 An Artificial Neural Network Simulator: Xerion [44]**

A powerful artificial neural network simulator, Xerion, developed by the Department of Computer Science, University of Toronto, was installed on the SUN-station system at Department of Electrical and Computer Engineering, The University of Manitoba. Xerion is a collection of C libraries that can be used to implement many different neural network models. It has a command line interface for creating and training the ANN, examining and modifying data structures, redirecting the output using streams, as well as miscellaneous utilities. It also has a graphical interface for displaying network activations and examining connection weights. Several simulators have been built with Xerion. Among them, a Boltzmann Machine, Mean Field Theory Machine, a Kohonen Network, Back Propagation and Recurrent Back Propagation Network.

Networks in Xerion are composed of sets of objects. Building a network requires creating these objects and connecting them together in the proper order to create a single network. A unit is an object that has an input, an output and a function for transferring the input to the output (i.e. a neuron model). Units are connected to one another by links. Links have modifiable connection weights, derivatives for the weights, and a function for calculating these derivatives. Through a set of commands, you can specify layers of the network, units (neurons) in each layer, and the links between neurons, so that a neural network is created. Note that when a new network is created, a bias group is automatically created. It has a single unit in it whose output is always 1.

Once the network is built, the most important thing is to initialize the weights in the network on the range (-1, 1). Patterns for training, testing and validation are put in separate files with a special format. A system command, *addExamples*, takes a mask describing the type of patterns to add and the name of the file containing these patterns, and then adds them into the simulator. The network, thus, is ready to be trained. Training command, *minimize*, is a complex command. It can train a network using: steepest descent, momentum descent, delta-bar-delta, quick-pop, and conjugate gradient with various line searches. Once a network has been built and trained, the weights in the network can be saved to the file you specified.

When Xerion is started, it pops up a window with several push buttons on it. Each of these buttons opens another window (display) which allows you to view or modify the network learning methods or simulator variables:

Activity Display : to view the activations of the network and process individual patterns.

Connection Display : to view the connection weights of the network.

Learning Methods : to select the learning method and set parameters that affect it.

Graphs : to plot values as they change during training.

System Variables : to view and modified a list of system wide variables used by the simulator.



## Chapter Six

# Application of ANNs to Distance Protection

### Part I: The Suitability to The Problem of Remote Infeed and Varying Source Impedances

---

#### 6.1 Introduction

Even though the conventional distance relay is one of the most important relays for the transmission or distribution line protection, its suitability to adapt to variations of source impedances and remote infeed is still a problem, as presented in Chapter 3. For the case of source impedance variation, a varying fault arc resistance will lead to mis-operation because the fault arc resistance is non-linear in that it is essentially a constant voltage element rather than a constant resistance element. For the case of remote end infeed, the current into the fault branch may significantly modify the impedance presented to the relay at the local end and lead again to a possible overreach/underreach error.

Artificial neural networks are well-suited to the above problems where exact functional relationships are neither well defined nor easily computable.

The application of artificial neural networks to distance protection is presented in this chapter. The PSCAD/EMTDC tool is utilized to create the training and testing cases with varying system parameters. The ANN is *trained* using many load and fault cases, *tested* using cases with different system conditions and *run* using more detailed fault cases along the whole transmission line.

The emphasis here is on creating more selective ground fault detection in spite of pre-fault loading in either direction, variable source impedance, and variable arcing fault resistance. The prospective ANN distance relay shows very good performance in identifying single line-to-ground faults. Basic principles learned from this investigation of application of an ANN to power system protection will be of value to future advances in this direction.

## **6.2 Proposed ANN Construction**

It is proposed that a feedforward neural network consisting of input, hidden and output layers is well suited to the problem to be solved here.

The input vectors represent a *feature space* which is necessary to implement an expected transfer function by a neural network. For this application, it seems logical to choose variables (after pre-processing) related to impedance.

Too many inputs to a network implies that the input vector contains too much information, whereas too few inputs means that the input vector contains too little information. In other words, some trial-and-error compromises have to be made to reach a successful implementation.

For a distance relay, the problem is one of designing a feedforward network that, given a set of samples, can classify the input pattern into two categories: normal and fault. In this case it was chosen that the network's output be 1 when the applied pattern is a fault pattern, and 0, when it is a normal pattern.

Consider the neural network in Fig. 6.1. It is a fully connected three-layer feedforward neural network that classifies the input patterns into expected categories.

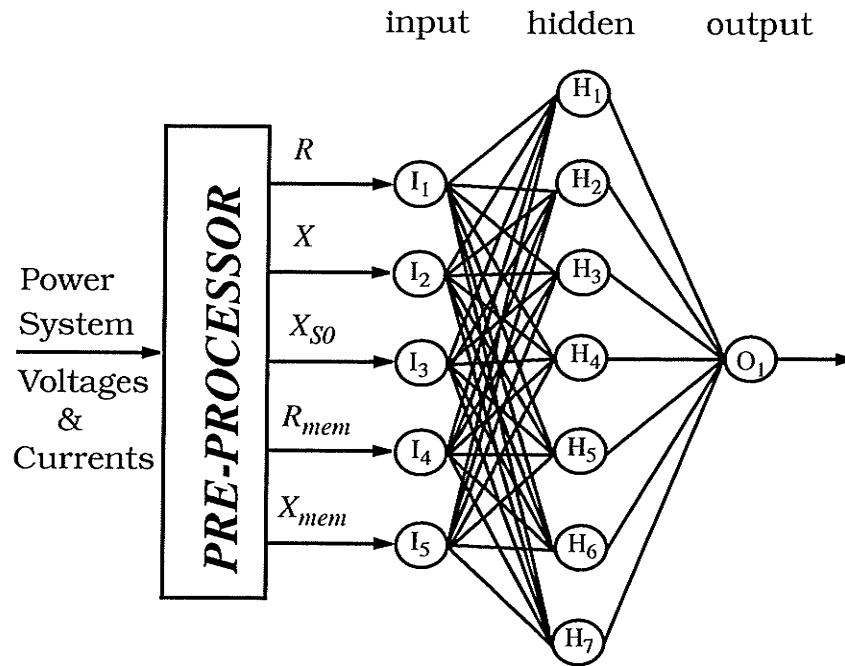


**Fig. 6.1** Proposed neural network architecture

There are five input signals required at the input layer :  $R$ ,  $X$ ,  $X_{S0}$ ,  $R_{mem}$  and  $X_{mem}$ .

$R$  and  $X$  are the measured apparent impedance of the faulted transmission line at the relay location  $D$  (Fig. 4.1) using Eq. (2.5), the same components that a conventional distance relay uses to detect the fault location. Inputting the magnitude and phase angle of the measured impedance is another option, but it needs much more computation in the preprocessor and results in a time delay of relay trip and a burden for the preprocessor.

$R_{mem}$  and  $X_{mem}$  are the memory impedance, for example, 5 cycles before the fault. They define the pre-fault conditions of the transmission line such as direction and magnitude of load current so that the relay based on ANN can adapt to the effect of pre-fault load flow. The load current magnitude and phase angle as well as the phase difference between the voltage and current can also be used as inputs to represent the pre-fault conditions, but again much more calculation is required. On the other hand, the load impedance,  $R_{mem}$  and  $X_{mem}$ , has already been calculated for earlier impedance measurement even under normal load conditions. Therefore it does not increase the computation time.

$X_{S0}$  is the equivalent zero sequence source reactance behind the relay and can be obtained from the imaginary part of  $-V_0/I_0$ . This allows the distance relay to be more sensitive because only small zero sequence quantities exist during normal operation [47] and the grounding points are relatively fixed so that the impedance of the zero sequence network can be used to identify the system structure. In other words, the introduction of  $X_{S0}$  makes it possible for the distance relay to adapt to changes in system structure, i.e., system impedance.

As shown in Fig. 6.1, a *pre-processor* performs the above calculation.

The output layer consists of only one neuron which has a continuous-value output in the range [0, 1]. Outputs bigger than 0.5 indicate tripping, otherwise non-tripping. A continuous-value output is preferred at this stage in order to see the decisiveness of the output. It is easy to get the necessary binary output, 0 or 1, by adding an extra neuron with a bias of -0.5 and threshold activation function to this output neuron.

The hidden layer here plays a very important role. Sometimes two hidden layers are used, but it has been proven that only one hidden layer is sufficient to approximate any continuous function[39]. The utility of these results depends, of course, on how many hidden neurons are necessary, and this is not known in general. In many cases it may grow exponentially with the number of input units. Thus, selecting the number of hidden neurons is critical to the success of the network. If too few hidden neurons are selected, the network will not be able to learn all of the patterns correctly. But too many hidden neurons will result in the network tending to memorize the patterns instead of learning to detect the global features of the patterns[39].

Reference [41] suggests Eq. (5.6) and Eq. (5.7) from Chapter 5 for estimating the number of hidden neurons. In this case, the 5-dimensional input space is expected to be linearly separable into 2 disjoint regions: normal and fault. The formulas indicate that only one hidden neuron is required. Obviously, this can not be true. Our experience indicates that the number of hidden units selected at first should be around (number of input units + number of output units)/2 and then increased or decreased dynamically in order to achieve an optimal configuration. In the proposed ANN shown in Fig. 6.1, **seven** hidden neurons allow the training algorithm to easily find the values of a set of the weights that minimizes the error function, and allows the ANN to have an excellent generalizing ability.

### **6.3 The Sigmoid Function**

The sigmoid function of Eq. (5.2) is a popular continuous function used as the activation function of neurons. Specifically, this function provides more

information than the binary output of the thresholding element (see Chapter 5). The derivative  $f'(net)$  of the activation function serves as a multiplying factor in building components of the so-called error signal vectors. Thus, the shape of the sigmoid function would strongly affect the speed of network learning. The default activation function of neurons in Xerion is a sigmoid function of the form:

$$f(net) = \frac{1}{1 + e^{-net}} \quad (6.1)$$

Its shape is shown in Fig. 6.2. Notice that the output takes on values in the range (0, 1).

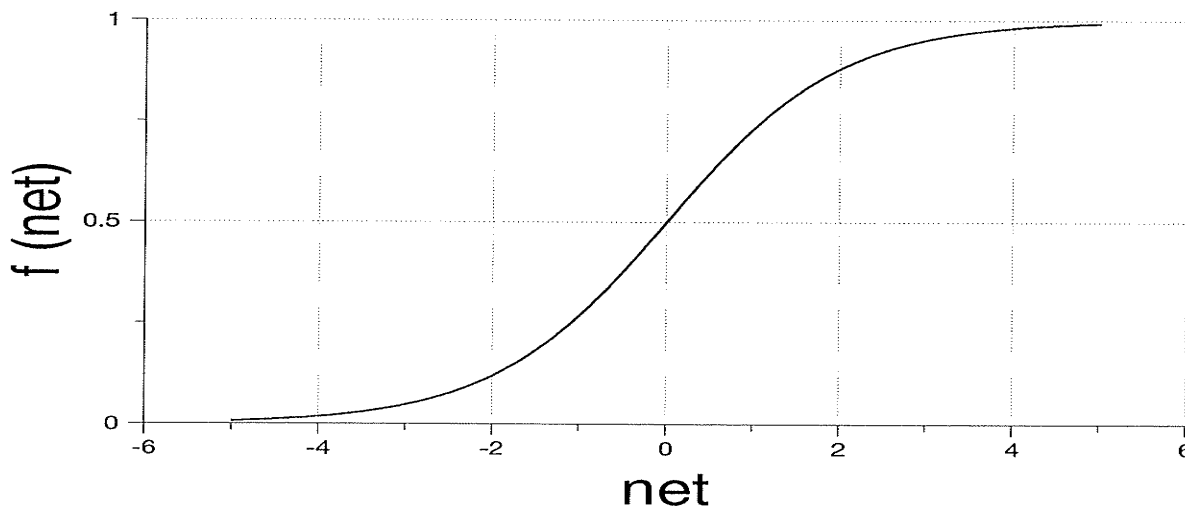


**Fig. 6.2** Sigmoid function

The input patterns are the quantitative description of a phenomenon. In order to make use of the nonlinearity of a sigmoid function such that the neuron's output lies on the range (0, 1) and, ultimately, permit the network to reach a successful classification, it is required that the input patterns have to be normalized into the range (0, 1) before they are applied to the neural network for

training. Supposing that an input of network,  $\bar{x}$ , has a minimum value of  $x_{min}$  and a maximum value of  $x_{max}$  the normalized value of an input  $x$  should be of the form:

$$x' = 1.0 - \frac{x_{max} - x}{x_{max} - x_{min}} \quad (6.2)$$

This raises a question as to how to select the minimum  $x_{min}$  and the maximum  $x_{max}$  because a 'raw' variable might have a large range. However, for most real-world problems, the principle distribution of digitalized patterns which describe the problem will be in a relatively fixed range, as shown in Fig. 6.3,

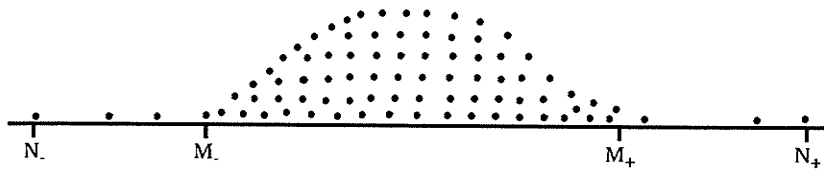


**Fig. 6.3** A general picture of pattern distribution

where the maximum number is  $N_+$  and the minimum number is  $N_.$  It is clear that most patterns are distributed in the range  $(M., M_+)$  and only a few extreme cases locate at the range  $(N_., N_+)$ . If  $N_+$  was selected as  $x_{max}$  and  $N_.$  as  $x_{min}$ , the training of a neural network is probably convergent but it is not in most cases because, usually,  $(N_+ - N_.)$  is too large a number. The normalization which converts the patterns into the range  $(0, 1)$  will greatly compress the useful information so that the useful features are hard to extract during the training procedure. Based on above consideration,  $M_+$  is selected as  $x_{max}$  and  $M_.$  is selected as  $x_{min}$ .

## 6.4 Operating Characteristic Definition for an ANN Distance Relay

In Chapter 2, it was stated that a distance relay with a quadrilateral characteristic has been used widely in computer relaying because it is directional and has significant extension of the resistive reach under unbalanced fault conditions. The quadrilateral operating characteristic for the ANN distance relay is shown in Fig. 6.4.

In order to identify the fault location easily, the fractional distance along the line from the relay location,  $\alpha$ , instead of reactance  $X$  is introduced as one of the axes while the fault resistance  $R_F$  is another. In general, it is expected that the relay trips only if the faults are less than 80% of the transmission line length

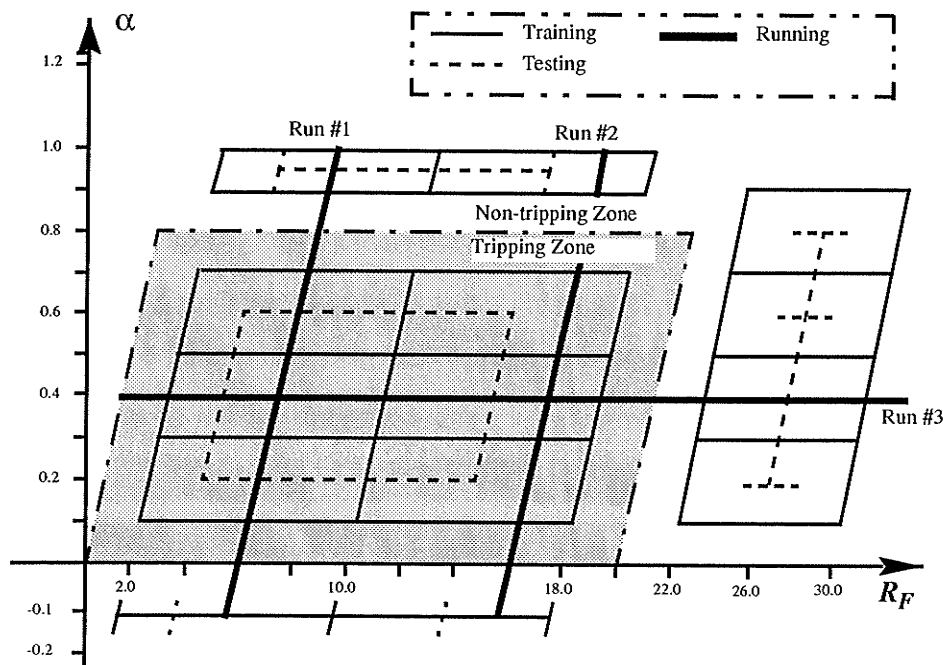


**Fig. 6.4** Data selection and categories recognized by ANN



( $\alpha = 0.8$ ). As suggested in [37], the most frequently occurring values of “apparent fault resistance” range from  $5 \Omega$  to  $25 \Omega$ . Thus  $20 \Omega$  is a reasonable value for one of the tripping region boundaries. A quadrilateral protection zone is therefore assigned to the prospective ANN distance relay as the shaded area in Fig. 6.4:

$$0 < \alpha \leq 0.80 \quad (6.3)$$

$$0.0 < R_F \leq 20.0 \quad (6.4)$$

Note that the target of the ANN output is set to 1 if a training pattern is located in the tripping-zone, otherwise to 0.

## 6.5 Selection of Training Patterns

Training patterns come from PSCAD/EMTDC simulation of the system shown in Fig. 4.1 of Chapter 4. The selection of training patterns should cover most possible cases, including varying source impedances, pre-fault load conditions, fault locations and fault resistances. In the simulation, therefore, five variables are chosen to be adjustable, as seen in Table 6.1 and in Fig. 6.4 as the intersections of the solid lines. Totally, there are 488 cases listed in APPENDIX D, including loads and faults, used to train the ANN.

## 6.6 Training of The Proposed ANN

The proposed neural network is trained using the above input/output patterns under the *error backpropagation learning algorithm*. The back-propagation learning algorithm allows experimental acquisition of input/output mapping knowledge within the multilayer network. If a pattern is submitted and its classification is determined to be erroneous, the synaptic weights as well as the

**Table 6.1 : Selection of system parameters**

$$E_S = E_R = 138.0 \angle 0^\circ \text{ kV}, \quad E_R = 138.0 \angle \delta \text{ kV}$$

$$\text{Source Impedance : Kelsey : } Z_{S-\max G} = 18.45 \angle 86.3^\circ, Z_{S-\min G} = 26.16 \angle 86.3^\circ, Z_{S-\text{zero}} = 11.94 \angle 87.5^\circ$$

$$\text{Thompson : } Z_{R-\max G} = 25.90 \angle 84.0^\circ, Z_{R-\min G} = 31.19 \angle 86.3^\circ, Z_{R-\text{zero}} = 4.70 \angle 86.4^\circ$$

	TRAINING	TESTING	RUNNING		
			Run #1	Run #2	Run #3
$\alpha$	-0.1, 0.1, 0.3, 0.5, 0.7, 0.9, 1.0	-0.1, 0.2, 0.6, (0.8), 0.95	-0.1 ~ 1.0		0.4
$R_F$	2.0, 10.0, 18.0 22.0, 30.0	4.0, 14.0, 26.0	6.0	16.0	0.0 ~ 40.0
<i>Kelsey</i>	$Z_{S1} = Z_{S-\max G}, Z_{S0} = Z_{S-\text{zero}} ;$ $Z_{S1} = Z_{S-\min G}, Z_{S0} = Z_{S-\text{zero}} .$	$Z_{S1} = 24.50 \angle 86.3^\circ,$ $Z_{S0} = Z_{S-\text{zero}}$	$Z_{S1} = 20.66 \angle 86.3^\circ, Z_{S0} = Z_{S-\text{zero}}$		
<i>Thompson</i>	$Z_{R1} = Z_{R-\max G}, Z_{R0} = Z_{R-\text{zero}} ;$ $Z_{R1} = Z_{R-\min G}, Z_{R0} = Z_{R-\text{zero}} .$	$Z_{R1} = 27.40 \angle 84.0^\circ,$ $Z_{R0} = Z_{R-\text{zero}}$	$Z_{R1} = 29.89 \angle 84.0^\circ, Z_{R0} = Z_{R-\text{zero}}$		
$\delta$	-30 <sup>0</sup> , -10 <sup>0</sup> , 10 <sup>0</sup> , 30 <sup>0</sup>	-20 <sup>0</sup> , 20 <sup>0</sup>	-25 <sup>0</sup> , -15 <sup>0</sup> , 15 <sup>0</sup> , 25 <sup>0</sup>		

$\alpha$  the fractional distance along the line from the relay location.

$R_F$  the fault resistance.

$Z_S$  the source impedance at the relay end (Kelsey).

$Z_R$  the source impedance at the remote end (Thompson).

$\delta$  the load angle of Thompson end with respect to Kelsey end.

thresholds are adjusted so that the current least mean-square classification error is reduced. The input/output mapping, comparison of target and actual values, and adjustment continue and training examples are presented to network randomly and repeatedly until all mapping examples from training set are learned within an acceptable overall error.

The error back-propagation learning algorithm in which synaptic strengths are systematically modified so that the response of the network increasingly approximates the desired response can be interpreted as an optimization problem. The generic criterion function optimization algorithm is simply a negative gradient descent with a fixed step size. Its essence is the evaluation of the contribution of each particular weight to the output error.

Gradient descent and other optimization techniques can become stuck in *local minima* of the error function [39]. Fig. 6.5 shows a typical cross section of an error space in a single weight dimension. In practice, however, the learning would be considered successful for  $E$  below an acceptable minimum  $E_{min}$  value. The error function shown in Fig. 6.5 possesses one global minimum below the  $E_{min}$ , but it also has two local minima at  $w_{l1}$  and  $w_{l2}$ . The learning procedure will stop prematurely if it starts at point 2 or 3; thus the trained network will be unable to produce the desired performance in terms of its acceptable terminal error. To ensure convergence of a satisfactory minimum the starting point should be changed to 1. This is why the training has to be reprocessed many times to find

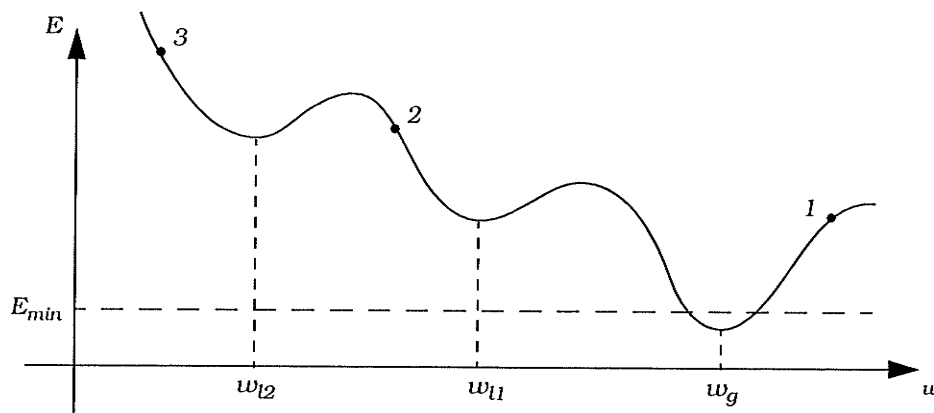


**Fig. 6.5** Minimization of the error  $E$  as a function of single weight

the global minimum. An appropriate choice of the learning parameters should guarantee that a good quality solution is found within a reasonable period of computing time. There is a set of parameters available in Xerion to be adjustable.

The weights of the network to be trained are typically initialized at small random values. The initialization strongly affects the ultimate solution. If all weights start out with equal weight values, and if the solution requires that unequal weights be developed, the network may not train properly. Unless the network is disturbed by random factors or the random character of input patterns during training, the internal representation may continuously result in symmetric weights.

Also, the network may fail to learn the set of training examples with the error stabilizing or even increasing as the learning continues. In fact, many empirical studies of the algorithm point out that continuing training beyond a certain low-error plateau results in the undesirable drift of weights [41]. This causes the error to increase and the quality of mapping implemented by the network decreases. To counteract the drift problem, network learning should be restarted with other random weights.

The effectiveness and convergence of the error back-propagation learning algorithm depend significantly on the value of the learning rate  $\eta$ . In general, however, the optimum value of  $\eta$  depends on the problem being solved, and there is no single learning rate value suitable for different training cases. When broad minima yield small gradient values, then a larger value of  $\eta$  will result in a more rapid convergence. However, for problems with steep and narrow minima, a small

value of  $\eta$  must be chosen to avoid overshooting the solution. This leads to the conclusion that  $\eta$  should indeed be chosen experimentally for each problem. Usually, small learning rates guarantee a true gradient descent, but the price is an increased total number of learning steps needed to reach the satisfactory solution.

The training patterns are re-presented to the ANN to inspect its operation after training. Fig. 6.6 shows that the performance is satisfactory. A solid node  $\bullet$  represents a tripping output and an oval  $\circ$  represents a non-tripping output. The neural network learns the training patterns very well and follows exactly what it was told.

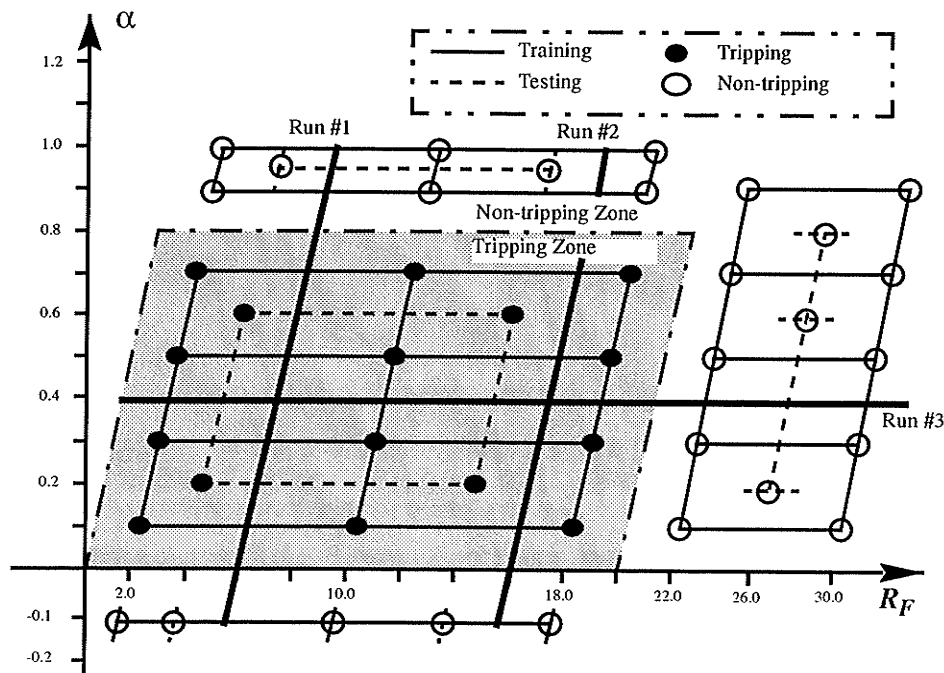


**Fig. 6.6** Training performance of the proposed ANN

Fig. 6.7 shows a set of weights for the problem studied here, which has the least learning error and very good generalizing capability.

## 6.7 Testing of The Proposed ANN

In order to check the ability of this network to generalize after training, a set of 22 **testing patterns** (which were never presented to the network before) was applied to the ANN. If the network has begun to memorize the training data and lost the ability to generalize, such training has to restart until the performance on both training data and testing data is acceptable and then the training is finished. Selection of testing patterns is also shown in Table 6.1 and Fig. 6.4. The performance of the network on these testing patterns is shown in Fig. 6.6.

## 6.8 Running of The Proposed ANN

One of the distinct strengths of neural networks is their ability to generalize. The network is said to generalize well when it sensibly interpolates input patterns that are new to the network. For the testing patterns, the network generalized in very "sensible" ways. But it is important to be clear just what it is we are expecting the network to do when we look for generalization.

In our case, after successful presentation of training data and testing data, the third set of patterns, **running data**, was used to determine whether or not the trained network met our acceptance criteria. The running cases were made to pass through the whole tripping region and non-tripping region with many more samples than training and testing, as shown by the lines *Run #1*, *Run #2* and *Run #3* in Fig. 6.4, about 528 cases listed in APPENDIX D. The selection

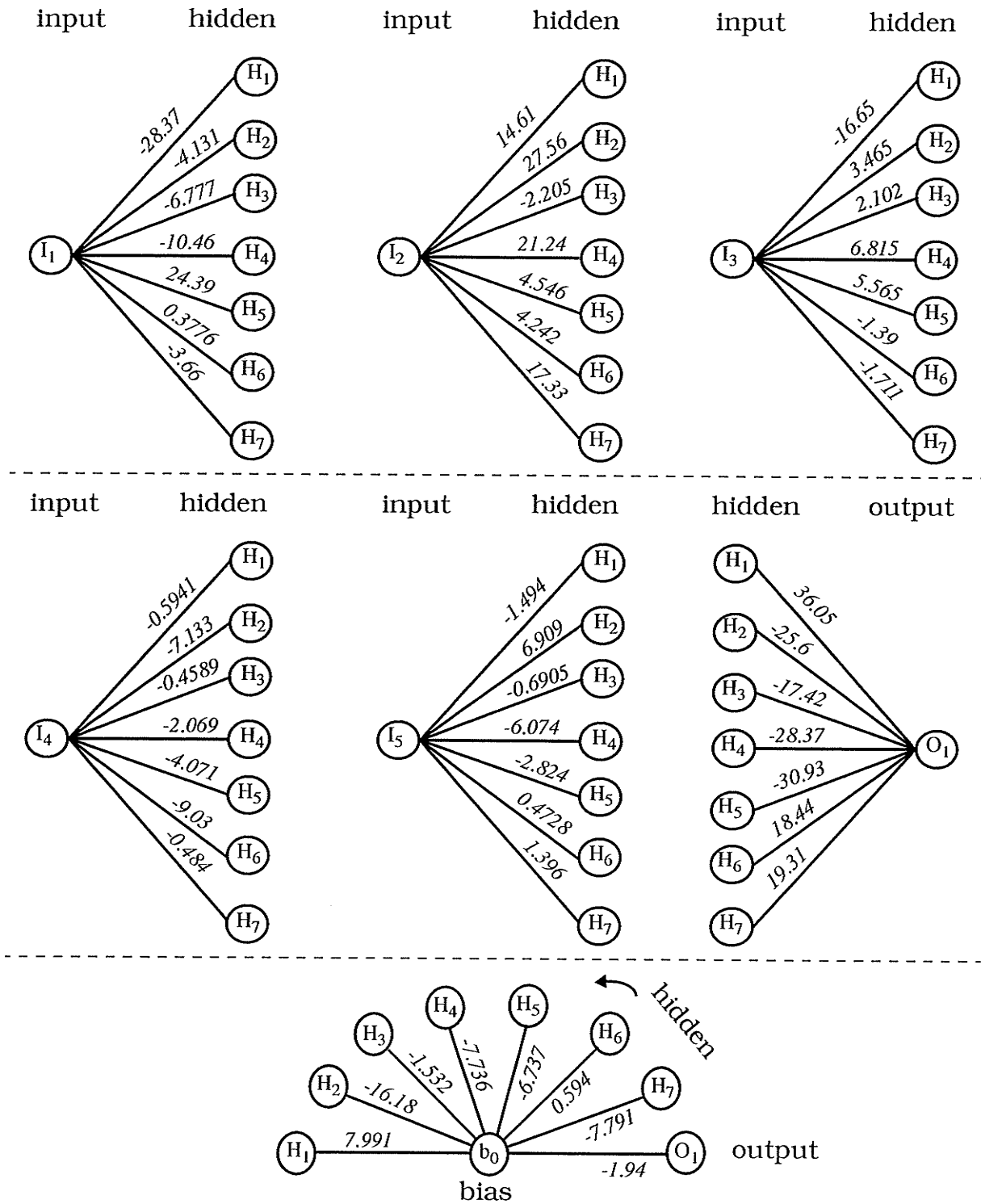
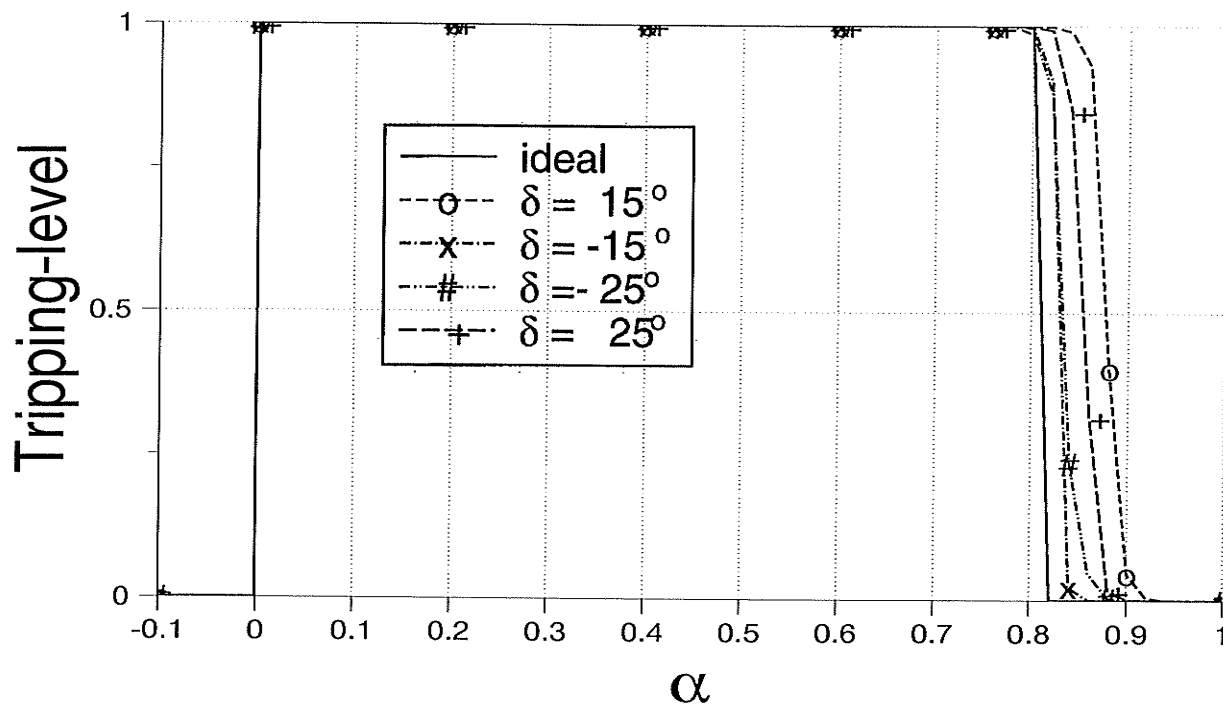


Fig. 6.7 Link weights of a successful training

of power system parameters for running is listed on Table 6.1 and running results are shown in Fig. 6.8, Fig. 6.9 and Fig. 6.10. The performance of the distance relay based on ANN strategy is very good.



**Fig. 6.8** ANN distance relay performance with varying transmitted load  
Run #1 ( $R_F = 6 \Omega$ )

Fig. 6.8 and Fig. 6.9 show the excellent operation performance of the ANN distance relay along the transmission line. The actual outputs of the neural network, corresponding to faults along the line, are quite close to the ideal operating characteristic, especially for high fault resistance.



For the single line-to-ground faults with lower fault resistance, Fig. 6.8, the neural network's ability to classify the input patterns into proper categories seems more stable if the ANN relay is at the power-sending end, i.e., negative  $\delta$ . There might be some overreach problems if this relay is at the power-receiving end (positive  $\delta$ ) with light load (for example,  $\delta = 15^\circ$ ).

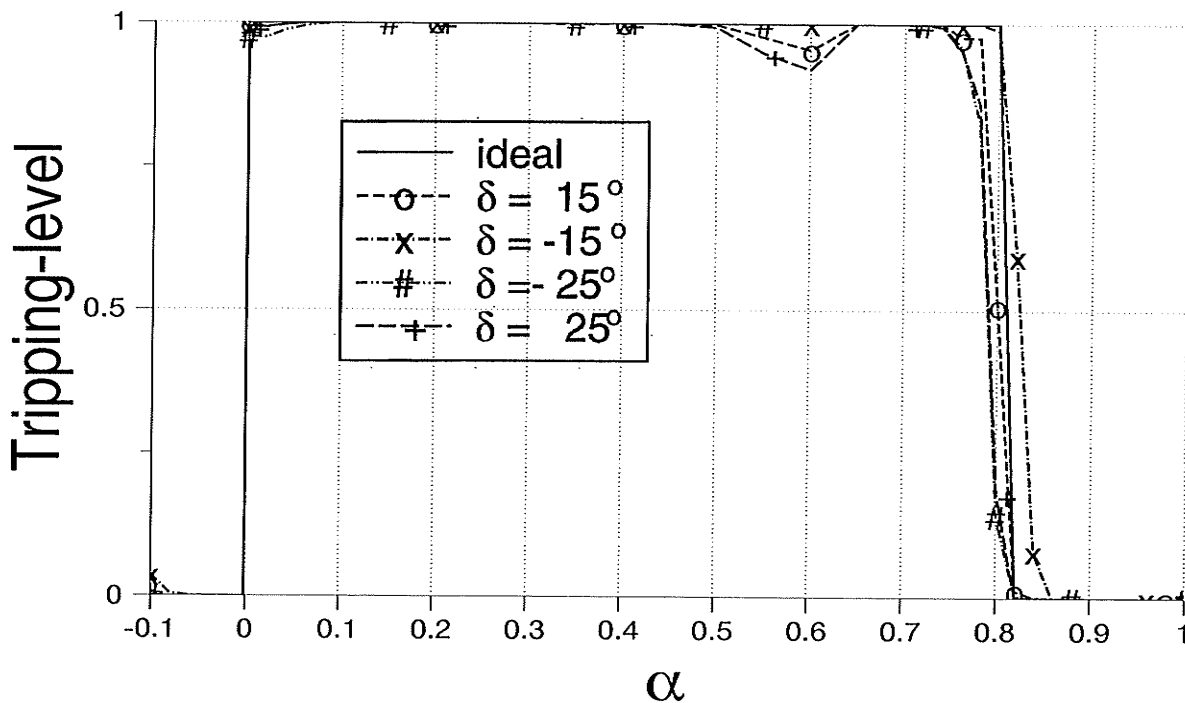


**Fig. 6.9** ANN distance relay performance with varying transmitted load  
Run #2 ( $R_F = 16 \Omega$ )

For the faults with higher fault resistance, Fig. 6.9, the neural network's ability to classify the input patterns into proper categories seems perfect for the varying load conditions. The neural network's tripping traces are very close to the expected line. The tripping for the faults around 60% of the line seems a little bit

unstable but it does not hurt the performance if outputs greater than 0.5 are considered as tripping.

Fig. 6.10 shows the good performance of the ANN distance relay to identify a  $20 \Omega$  fault resistance. The relatively higher errors appear when the ANN relay is sited on the power-sending end, i.e., negative  $\delta$ . The relay's ability of fault resistance identification is very satisfactory if relay is at the power-receiving end, i.e., positive  $\delta$ .

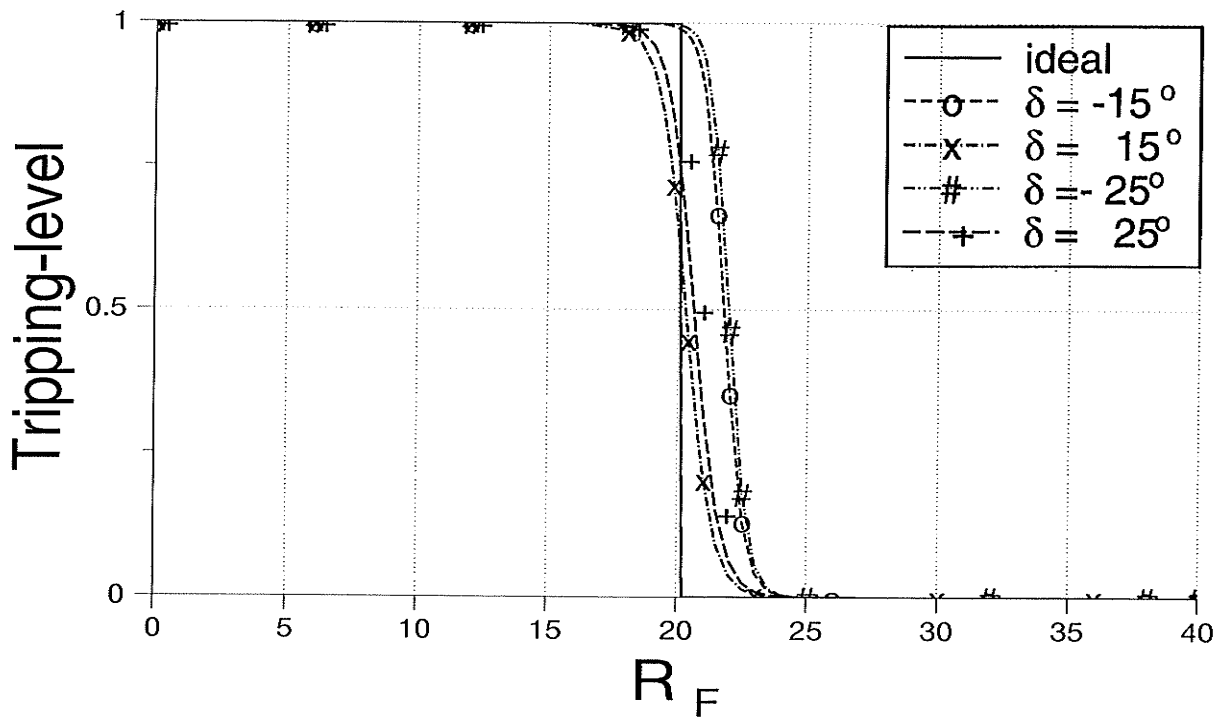


**Fig. 6.10** ANN distance relay performance with varying transmitted load  
Run #3 ( $\alpha = 0.4$ )

### 6.9 Comparison Concerning Underreach/Overreach Error

For the actual transmission line in Fig. 4.1, let us consider underreach/overreach problems for both the conventional distance relay and the ANN distance relay. Suppose that the system simulated is the same as that in the running cases, i.e., Kelsey end:  $Z_{S1} = 20.66 \angle 86.3^\circ$ ,  $Z_{S0} = 11.94 \angle 87.5^\circ$ ;  $Z_{R1} = 29.89 \angle 84.0^\circ$ ,  $Z_{R0} = 4.70 \angle 86.4^\circ$ . Assume that the conventional distance relay with a quadrilateral operating characteristic detects the fault location by Eq. ( 2.5 ), and it was set at 80% of the line length. Based on the simulation of Fig. 4.1, the reactance setting will be  $X_{set} = 34.8 \Omega$ . If there is no power flow through the line (load angle  $\delta = 0^\circ$ ), the conventional relay measures the correct distance: 80 km. In the case  $\delta = -25^\circ$ ,  $R_F = 6 \Omega$ , power out of relay location, the measured reactance by Eq. ( 2.5 ) reaches  $X_{set}$  at 86.5 km. The overreach error, thus, is  $(86.5-80)/80 = 8.125\%$ . In the case  $\delta = 25^\circ$ ,  $R_F = 6 \Omega$ , power into relay location, the measured reactance reaches  $X_{set}$  at 74 km. The underreach error is  $(80-74)/80 = 7.5\%$ . From Fig. 6.8, it is clear that the largest error of the ANN distance relay for  $\delta = 25^\circ$  and  $R_F = 6 \Omega$  is about 5 km. The maximum overreach error for the ANN relay, therefore, is only  $5/80=6.25\%$ .

Referring to Fig. 6.9, in the case  $\delta = -25^\circ$ ,  $R_F = 16 \Omega$ , the measured reactance by Eq. ( 2.5 ) can not reach  $X_{set}$  in the transmission line. The overreach error, thus, is at least  $(100-80)/80 = 25\%$ . In the case  $\delta = 25^\circ$ ,  $R_F = 16 \Omega$ , the measured reactance reaches  $X_{set}$  at 66 km. The underreach error is  $(80-66)/80 = 17.5\%$ . From Fig. 6.9, it is obvious that the errors of the ANN distance relay for

any load conditions are less than 3 km. The maximum underreach/overreach error for the ANN relay, therefore, is only  $3/80=3.75\%$ .

### **6.10 Summary**

As was well-known, the suitability of conventional distance relays to adapt to variations of source impedance and pre-fault load is still a problem. An ANN-based distance relay has been proposed. The performance of the ANN distance relay, based on the simulation of an actual transmission line of Manitoba Hydro in PSCAD/EMTDC, is very good. The following conclusions can be drawn through the training of a neural network as a distance relay:

1. The prospective ANN distance relay demonstrates a great potential to separate the single line-to-ground faults along the transmission line into proper categories.
2. The prospective ANN distance relay has a great potential to identify the fault resistances around the specified protection zone.
3. The prospective ANN distance relay can adapt to pre-fault load conditions, variable source impedance and variable ground fault resistance.
4. The prospective ANN distance relay can reduce under-reach/overreach errors.

It appears that the ANN strategy is a good solution for a distance relay to adapt to varying pre-fault load, source impedance and ground resistance. Although a great deal of study still needs to be done, the preliminary result shows an exciting future in the application of artificial neural networks to power system protection.

## Chapter Seven

# Application of ANNs to Distance Protection

### Part II : The Suitability to The Problem of Non-linear Arcing Fault Resistance

---

#### 7.1 Introduction

It is a well-accepted fact that arcing fault resistance is nonlinear. It is essentially a constant voltage component rather than a constant resistance component. It results in a setting problem for distance relays as described in Chapter 3. The research results given in Chapter 6 are limited by the fact that the investigation was based on a linear arcing fault resistance model. Artificial neural networks are also well-suited to problems of inherent nonlinear nature and therefore, it was decided to build up a nonlinear arcing fault resistance model and apply ANN methodology.

Based on the nature of the arcing fault resistance, a nonlinear arcing fault model has been applied in PSCAD/EMTDC to create the training, testing and running cases with varying system parameters. The simulation system was an actual Manitoba Hydro transmission line, the same one used in Chapter 6 except for the arcing fault resistance model. An ANN was *trained* using many load and fault cases, *tested* using cases with different system conditions and *run* using more detailed fault cases along the whole transmission line.

The research here was focused on creating more selective detection in the presence of arcing faults, especially for radial distribution lines where arc

resistance can be a significant part of the zero sequence impedance. The effectiveness was to be in spite of pre-fault loading in either direction, variable source impedance, and variable ground fault resistance. Also, a new operating characteristic was devised, and the comparison with a conventional distance relay showed that the prospective ANN distance relay had very good performance.

## **7.2 Investigation of Arcing Fault Resistance Nonlinearity**

The investigation of the nature of arcing fault resistance is an old topic and was studied by researchers as early as a half century ago. The characteristics of fault resistance are described and the neutral-current wave traces are presented in [36]. Based largely on statistical and oscillographic study of power system fault currents for five power systems, reasonable values of fault resistance for a line-to-ground fault are given by [37].

Volt-ampere characteristics of 60-cycle arcs in still air with lengths and currents have been studied under laboratory conditions [38]. Research showed that the arcs varied in peak current from 68 to 21,750 amperes and in length from 1/8 to 48 inches; the voltage gradient in an arc is affected very little by current magnitude and all gradients, throughout the entire range of currents, remained between 21.5 and 50 volts per inch. The average voltage gradients at current peak for 60-cycle arcs in air lie between 31 and 38 volts per inch for currents over the entire range from less than 100 to over 20,000 peak amperes. Typical oscillogram is shown in Fig. 7.1, illustrating the current through the arc and the voltage across the arc with a flat-top. Fig. 7.2 has shown the volt-ampere

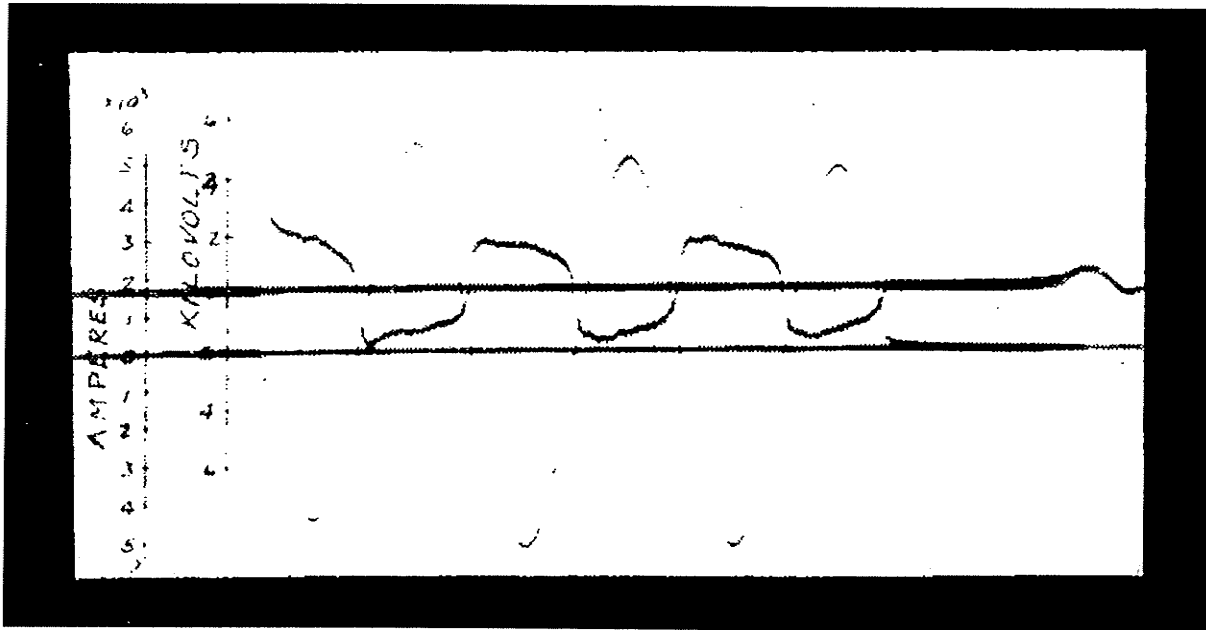


**Fig. 7.1** Current and arc voltage with 48-inch series arc [38]  
(maximum peak current 5,440 amperes)

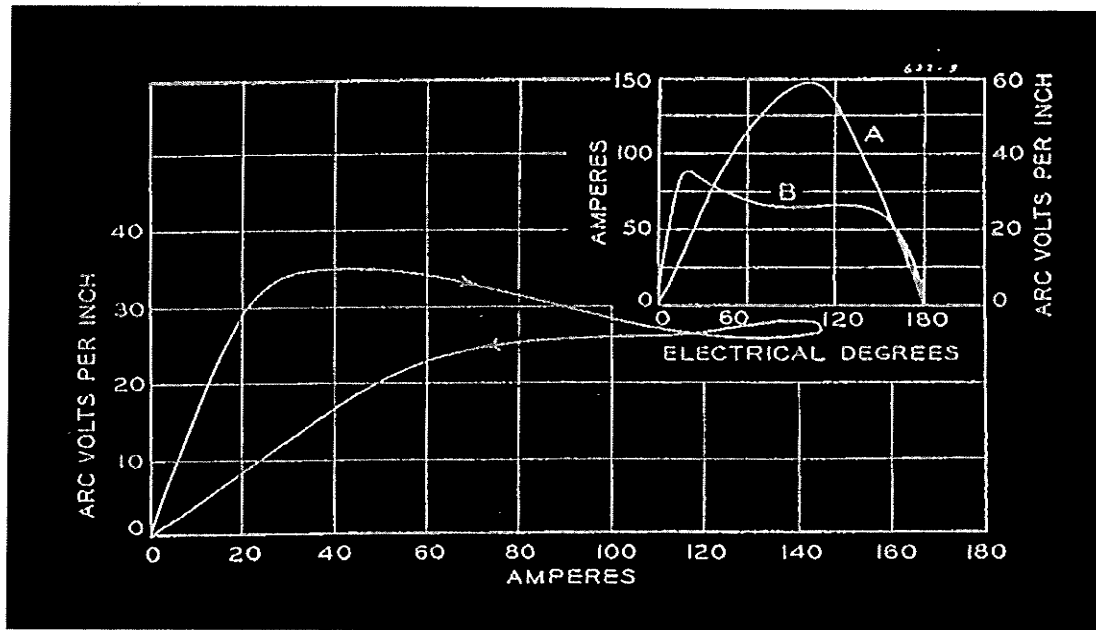


**Fig. 7.2** Volt-ampere characteristic of an arc with length 48 inches [38]  
A - Amperes      B - Volts



characteristic of an arc. Voltage and current waveshapes are illustrated on the right-top of Fig. 7.2.

Continuous conduction of a fault arc needs a certain voltage gradient applied. Research shows that the voltage across the arc has a flat-top waveform. The magnitude of the arc voltage may vary depending on arc length but it is independent of current through the arc. For example, in a simple distribution system as shown in Fig. 7.3, the current through the arc is determined only by source  $E_S$  and system impedance  $Z_S$  because the arcing resistance  $R_F$  is small.

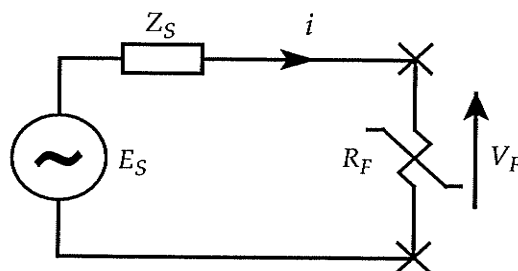


**Fig. 7.3** Independence of current through the arc in a simple system

### 7.3 Arc Length of A Ground Fault

The length of an arc in a single line-to-ground fault basically depends on the length of suspension insulator strings. Porcelain insulators have been used at all transmission line voltages from 115 through 765 kV and up to UHV [48]. Manufacturers supply catalogs which provide a physical description of the insulator's mechanical characteristics. The dimension of a typical standard porcelain disk insulator is  $10 \times 5\frac{3}{4}$  in, i.e., 10 inch of disk diameter and  $5\frac{3}{4}$  inch of height.

The electrical strength of line insulation may be determined by power frequency, switching surge, or lightning performance requirements. At different line voltages, different parameters tend to dominate. Table 7.1 shows typical line insulation levels.

**Table 7.1** Typical line insulation

Line voltage, kV	No. of standard disks	Creepage length with strong wind, in	Voltage across the arc, kV	Percentage of rated voltage
115	7 - 9	241.5 - 310.5	8.453 - 10.868	7.350 - 9.450
138	7 - 10	241.5 - 345.0	8.453 - 12.075	6.125 - 8.750
230	11 - 12	379.5 - 414.0	13.283 - 14.490	5.775 - 6.300
345	16 - 18	552.0 - 621.0	19.320 - 21.735	5.600 - 6.300
500	24 - 26	828.0 - 897.0	28.980 - 31.395	5.796 - 6.279
765	30 - 37	1035.0 - 1276.5	36.225 - 44.678	4.735 - 5.840

Design for contamination is usually expressed as inches of creepage per kilovolt, where the creepage distance is the length of the shortest path for a current over the insulator surface and is up to 2 inches per kilovolt or more for heavy contamination. Standard insulator disks ( $10 \times 5\frac{3}{4}$  in) have a typical creepage length of 11.5 inches per disk. Another criteria for insulation design is usually that flashover shall not occur for normal operating conditions, including reduced clearances to the structure from high wind which occurs only once in 50 or 100 years [48]. The velocity of this wind may be typically 80 to 100 mi/h. The third column of Table 7.1 shows the total creepage length along the insulator strings.

The data above shows that the average voltage gradient is about 35 volts per inch and this is used in what follows. The typical voltages across the arc in different voltage levels are shown in the fourth column of Table 7.1. The fifth

column of Table 7.1 gives the voltage across the arc in terms of percentages of rating voltage. The voltage across the arc lies between 4.735% and 9.45% of the rating voltage, so 10% of the rating voltage would be a good 'worst case' to use.

#### **7.4 The Model for Arc Resistance**

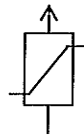
The nature of the arcing fault resistance has been described in the previous section.

It is well known that a surge arrester is a nonlinear element. Once the voltage breaks down the arrester, it will conduct and the voltage is constant no matter how large the current through it. In PSCAD/EMTDC, metal oxide surge arresters are mathematically modelled by using a large resistive branch specified with positive node numbers in the data file. The resistance of the branch is changed in a piece-wise linear fashion to represent the slope of the arrester characteristic. Fig. 7.4(a) shows the Draft icon for a metal oxide surge arrester. It has a default I-V characteristic listed in Table 7.2 which is based on the ASEA XAP-A, a gapless metal oxide surge arrester. When the default arrester voltage rating is set at 40 kV, Fig. 7.4(b) shows an actual I-V characteristic driven by a 138 kV AC source through a resistor, and Fig. 7.4(c) shows the current and voltage waveforms, respectively.

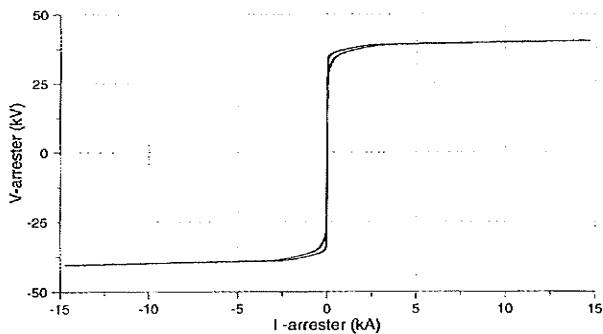
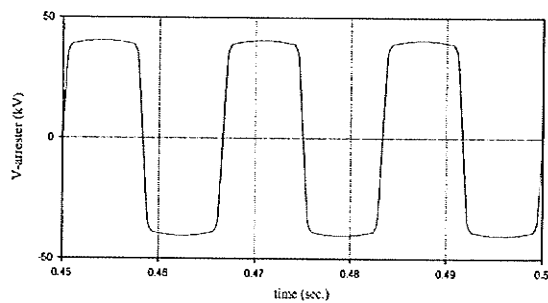
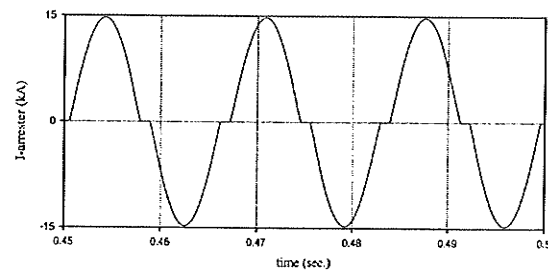
Obviously, the surge arrester model is well-suited for the simulation of this nonlinearity. Based on the same transmission line studied in Chapter 6, the simulating system structure of Fig. 7.5 is used.

**Table 7.2** ASEA XAP-A I-V characteristic

Voltage, (p.u.)	Current, (kA)
1.100	0.001
1.600	0.010
1.700	0.100
1.739	0.200
1.777	0.380
1.815	0.650
1.853	1.110
1.881	1.500
1.910	2.000
1.948	2.800
3.200	200.000



(a) Draft icon for surge arrester



(b) I-V characteristic of default arrester

(c) Current and voltage waveforms

**Fig. 7.4** Modelling metal oxide surge arrester

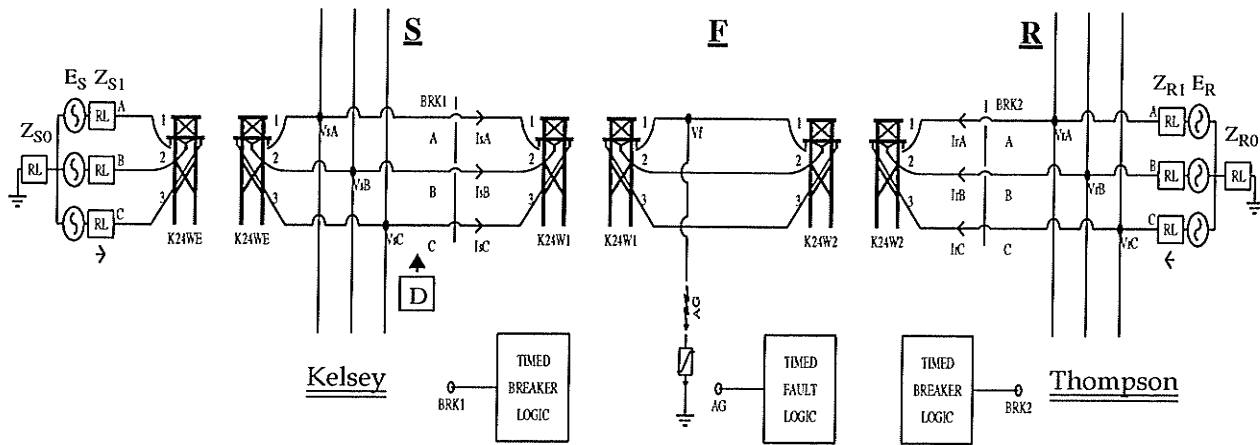


**Fig. 7.5** Simulation system considering nonlinear arc resistance

Fig. 7.6 shows the simulation outcomes at the system settings:

$$\text{Kelsey} \quad : \quad E_S = 138 \angle 0^0 \text{ kV}, Z_{S1} = 20.66 \angle 86.3^0, Z_{S0} = 11.94 \angle 87.5^0$$

$$\text{Thompson} \quad : \quad E_S = 138 \angle 25^0 \text{ kV}, Z_{R1} = 29.89 \angle 84.0^0, Z_{R0} = 4.70 \angle 86.4^0$$

$$\text{Fault} \quad : \quad \alpha = 0.20, V_F = 0.08 V_{Rating}$$

### 7.5 Structure of The Suggested ANN

Based on the same consideration in Chapter 6, the neural network in Fig. 7.7 is proposed for the prospective ANN distance relay to create more selective arcing fault detection. It is a fully connected three-layer feedforward neural network using a classifier working on the input patterns.

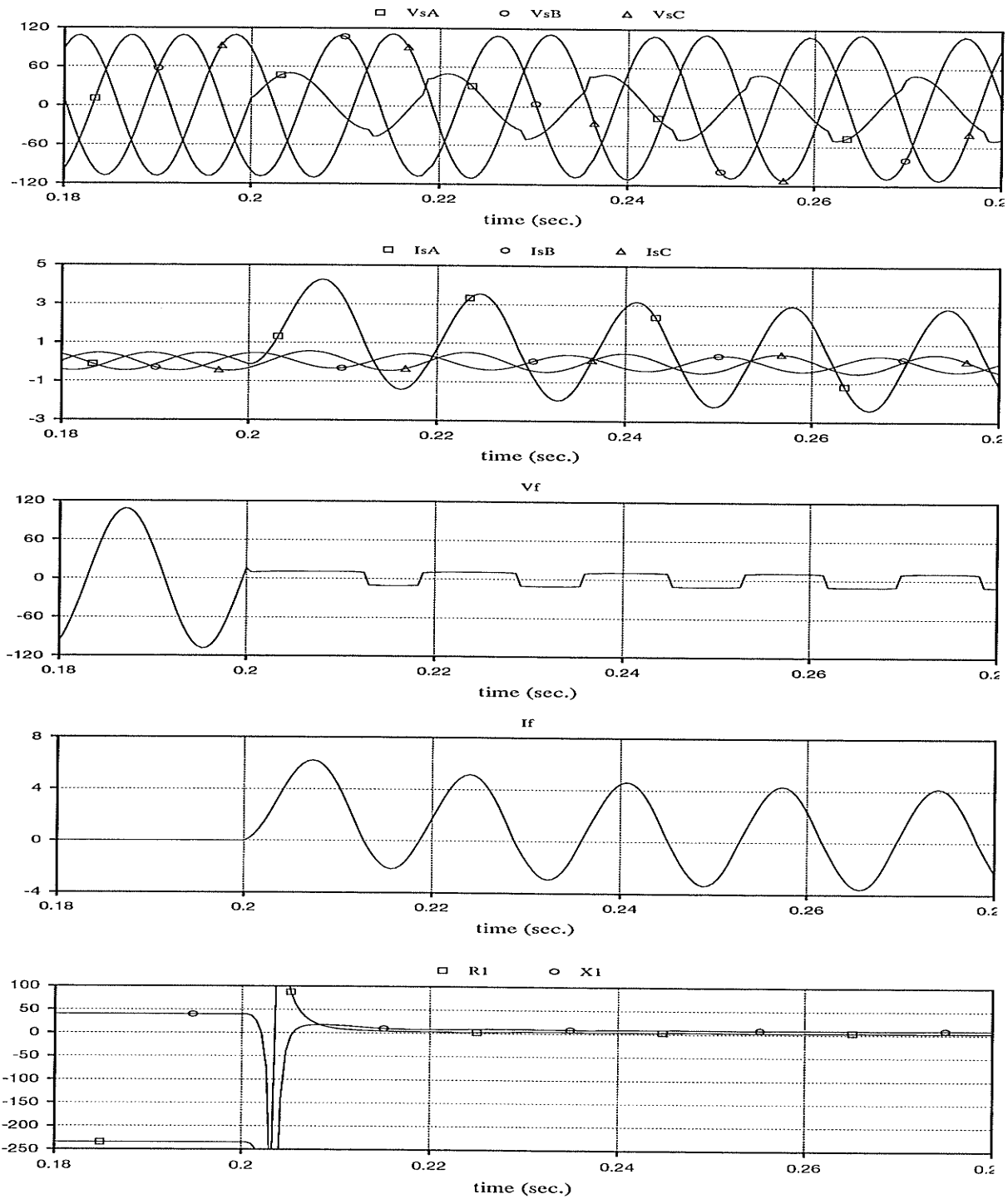


**Fig. 7.6** Simulation outcomes

(The variables are defined in Fig. 7.5, except for R1 and X1, which are the resistance and reactance seen by the relay "D".)

There are five neurons required in the input layer:  $R$ ,  $X$ ,  $X_{SO}$ ,  $R_{mem}$  and  $X_{mem}$ . Six hidden neurons are assigned at the hidden layer because dynamic training showed that six hidden neurons achieved an excellent generalizing ability. The output layer consists of only one neuron which has a continuous-value output in region  $[0, 1]$  that allow us to check the output decisiveness.

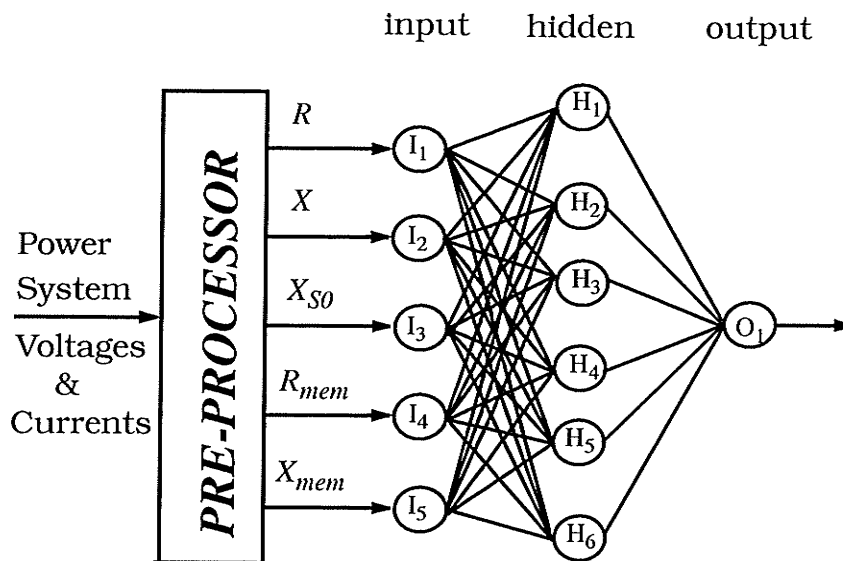


**Fig. 7.7** Proposed neural network structure

## 7.6 Operating Characteristic Defining for ANN Distance Relay

Because of the nonlinear arcing fault resistance model, the operating characteristic of the ANN distance relay is quite different from that of Chapter 6. The fractional distance along the line from the relay location,  $\alpha$ , is still one of the axes in order to identify the fault location easily. Consider that once the flashover occurs, a certain amount of voltage must be kept across the arc for a fixed length

of arc. Therefore, the cut-off voltage in the surge arrester,  $V_F$ , is chosen as another axis, as shown in Fig. 7.8.

Similarly, it is expected that the relay trips if the faults are located within 80% of the transmission line length ( $\alpha = 0.8$ ) and does not trip if beyond 80%. As was suggested above the worst case is considered to be when the arc is 10% of the system voltage rating, 10% of the system voltage rating is therefore a reasonable right hand boundary of the tripping region. A quadrilateral protection zone is, therefore, assigned to the prospective ANN distance relay as indicated by the shaded area in Fig. 7.8:

$$0 < \alpha \leq 0.80 \quad (7.1)$$

$$0.0 < V_F \leq 0.1 \quad (7.2)$$

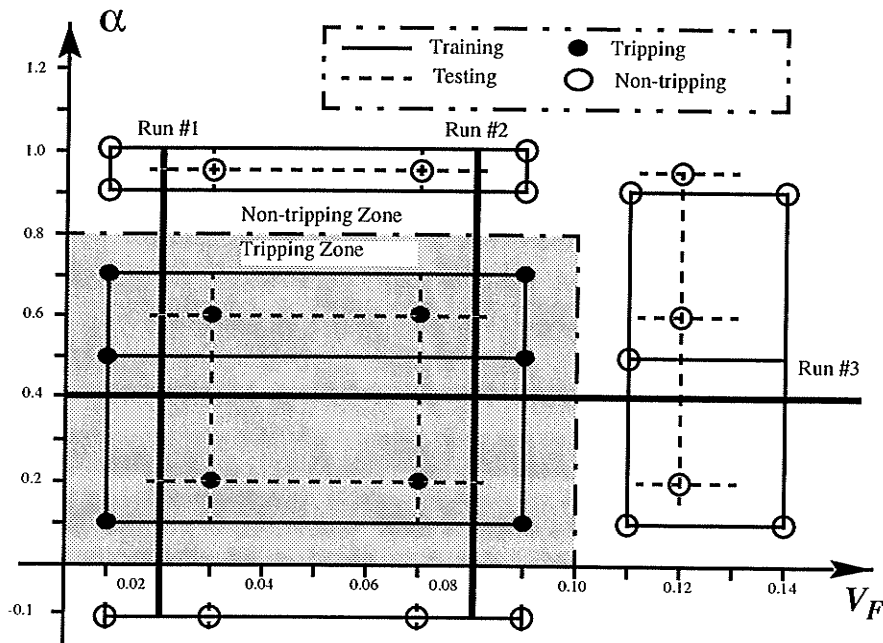


**Fig. 7.8** ANN training and testing patterns



Note that the target of the ANN output is set to 1 if a training pattern is located in the tripping-zone, otherwise to 0.

## 7.7 Selection of Training, Testing and Running Patterns

Training, testing and running patterns come from the PSCAD/EMTDC simulation of the system shown in Fig. 7.5. In the simulation, five variables, including varying source impedances, pre-fault load conditions, fault locations and the cut-off voltage of arcing fault resistances, are chosen to be adjustable, as listed in Table 7.3. Totally, 296 training cases, 22 testing cases and 508 running

**Table 7.3 : Selection of system parameters**

$E_S = E_R = 138.0 \angle 0^\circ$  kV,  $E_R = 138.0 \angle \delta$  kV  
 Source Impedance : Kelsey :  $Z_{S-maxG} = 18.45 \angle 86.3^\circ$ ,  $Z_{S-minG} = 26.16 \angle 86.3^\circ$ ,  $Z_{S-zero} = 11.94 \angle 87.5^\circ$   
 Thompson :  $Z_{R-maxG} = 25.90 \angle 84.0^\circ$ ,  $Z_{R-minG} = 31.19 \angle 86.3^\circ$ ,  $Z_{R-zero} = 4.70 \angle 86.4^\circ$

	TRAINING	TESTING	RUNNING		
			Run #1	Run #2	Run #3
$\alpha$	-0.1, 0.1, 0.5, 0.7, 0.9, 1.0	-0.1, 0.2, 0.6, 0.95	-0.1 ~ 1.0		0.4
$V_F$	0.01, 0.09, 0.11, 0.14	0.03, 0.07, 0.12	0.02	0.08	0.0 ~ 0.15
<i>Kelsey</i>	$Z_{S1} = Z_{S-maxG}$ , $Z_{S0} = Z_{S-zero}$ ; $Z_{S1} = Z_{S-minG}$ , $Z_{S0} = Z_{S-zero}$ .	$Z_{S1} = 24.50 \angle 86.3^\circ$ , $Z_{S0} = Z_{S-zero}$	$Z_{S1} = 20.66 \angle 86.3^\circ$ , $Z_{S0} = Z_{S-zero}$		
<i>Thompson</i>	$Z_{R1} = Z_{R-maxG}$ , $Z_{R0} = Z_{R-zero}$ ; $Z_{R1} = Z_{R-minG}$ , $Z_{R0} = Z_{R-zero}$ .	$Z_{R1} = 27.40 \angle 84.0^\circ$ , $Z_{R0} = Z_{R-zero}$	$Z_{R1} = 29.89 \angle 84.0^\circ$ , $Z_{R0} = Z_{R-zero}$		
$\delta$	$-30^\circ$ , $-10^\circ$ , $10^\circ$ , $30^\circ$	$-20^\circ$ , $20^\circ$	$-25^\circ$ , $-15^\circ$ , $15^\circ$ , $25^\circ$		

$\alpha$  the fractional distance along the line from the relay location.

$V_F$  the cut-off voltage of arcing fault resistance model.

$Z_S$  the source impedance at the relay end (Kelsey).

$Z_R$  the source impedance at the remote end (Thompson).

$\delta$  the load angle of Thompson end with respect to Kelsey end.

cases are created from the simulation. All the cases are listed in APPENDIX D. Testing patterns are sparsely distributed in the interested area to test the training efficiency. Three running lines, *Run #1*, *Run #2* and *Run #3* in Fig. 7.8, go through the whole tripping region and non-tripping region with many more samples than training and testing to check the ANN's performance. From Table 7.3 and Fig. 7.8, it can be seen that the training patterns are selected near the boundary to define the tripping region, and the testing patterns are scattered in tripping and non-tripping zone to sample acceptability of the training procedure. *Run #1* and *Run #2* are set close to the boundaries where the worst cases for the ANN distance relay are located. *Run #3* is set at  $\alpha = 0.4$  only for checking of sensitivity of the prospective relay on the cut-off voltage of arc resistance.

## 7.8 Training and Testing Details

The proposed neural network is trained by above 296 input/output patterns under the *error backpropagation learning algorithm*. The initial weights and biases of the network are randomly selected. Input vectors are normalized such that each element value lies in the range [0,1]. The input/output vectors are presented to the network randomly and repeatedly until all mapping examples from the training set are learned within an acceptable overall error.

The training patterns are re-presented to the ANN to inspect its operation after training. A solid node ● represents a tripping output and an oval ○ represents a non-tripping output in Fig. 7.8. The training cases all behaved correctly.

Fig. 7.9 shows the set of weights arrived here.

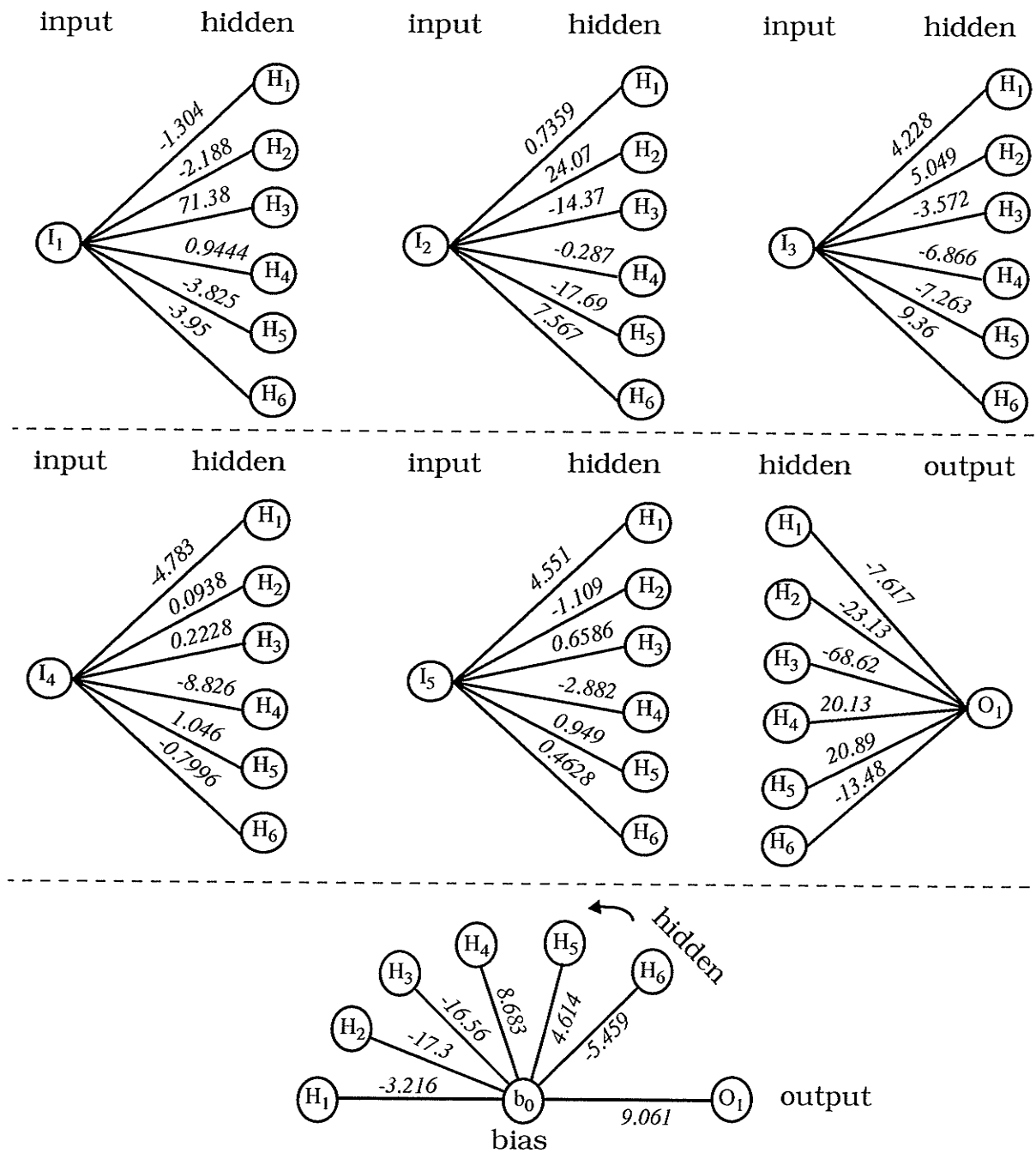
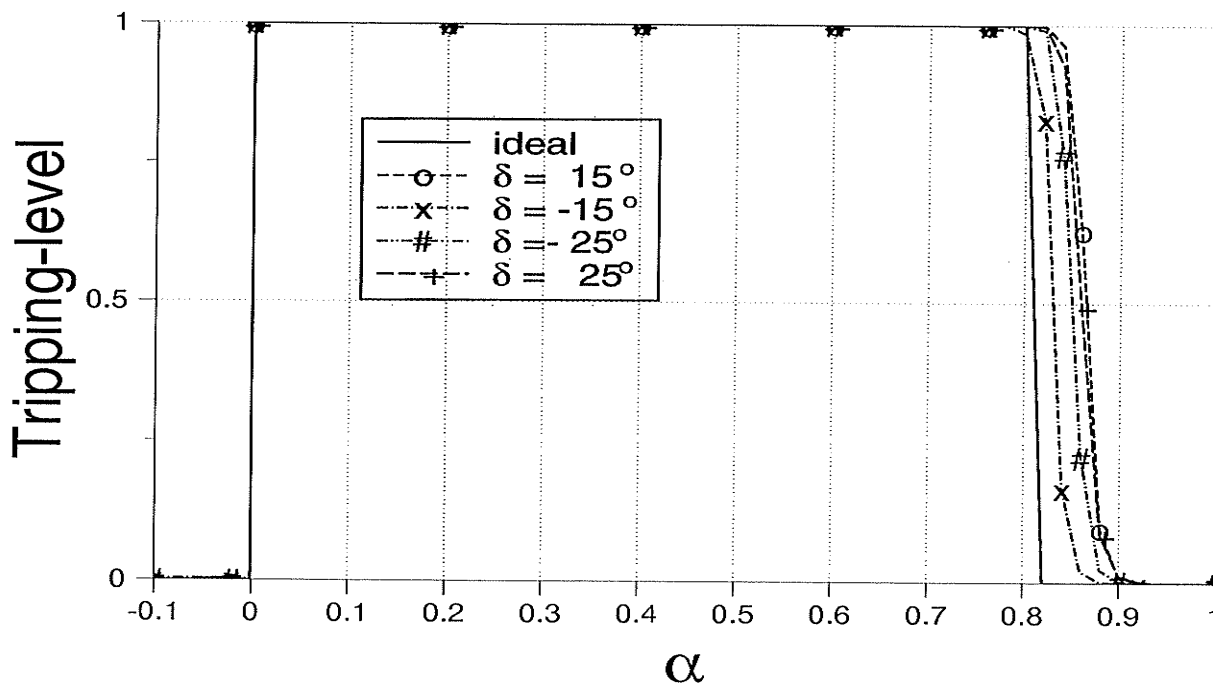


Fig. 7.9 The final weights and biases of a successful training

Twenty-two **testing patterns** (which were never presented to the network before) were applied to the ANN as well. The performance of the network on these testing patterns is shown in Fig. 7.8 and it is acceptable.

### 7.9 Running Performance of The Proposed ANN

The third set of patterns, **running data**, was presented to the proposed network to determine whether or not the trained network met our acceptance criteria. The running results are shown in Fig. 7.10, Fig. 7.11 and Fig. 7.12. The performance of the distance relay is very good.



**Fig. 7.10** ANN distance relay performance with varying transmitted load  
Run #1 ( $V_F = 0.02$ )

For the single line-to-ground faults with a short arc, i.e., low cut-off voltage  $V_F$ , shown in Fig. 7.10, the neural network's ability to classify the input patterns into proper categories is very good. There are slight overreach errors, the maximum error being around  $(86-80)/80 = 7.5\%$  and the minimum at around  $(83-80)/80 = 3.75\%$ . It seems that the ANN relay has less overreach error if it is located at the power-sending end, i.e., negative  $\delta$ .

For faults with a long arc high cut-off voltage  $V_F$ , as shown in Fig. 7.11, the neural network's ability to classify the input patterns into proper categories seems perfect for varying load conditions. The neural network's tripping traces

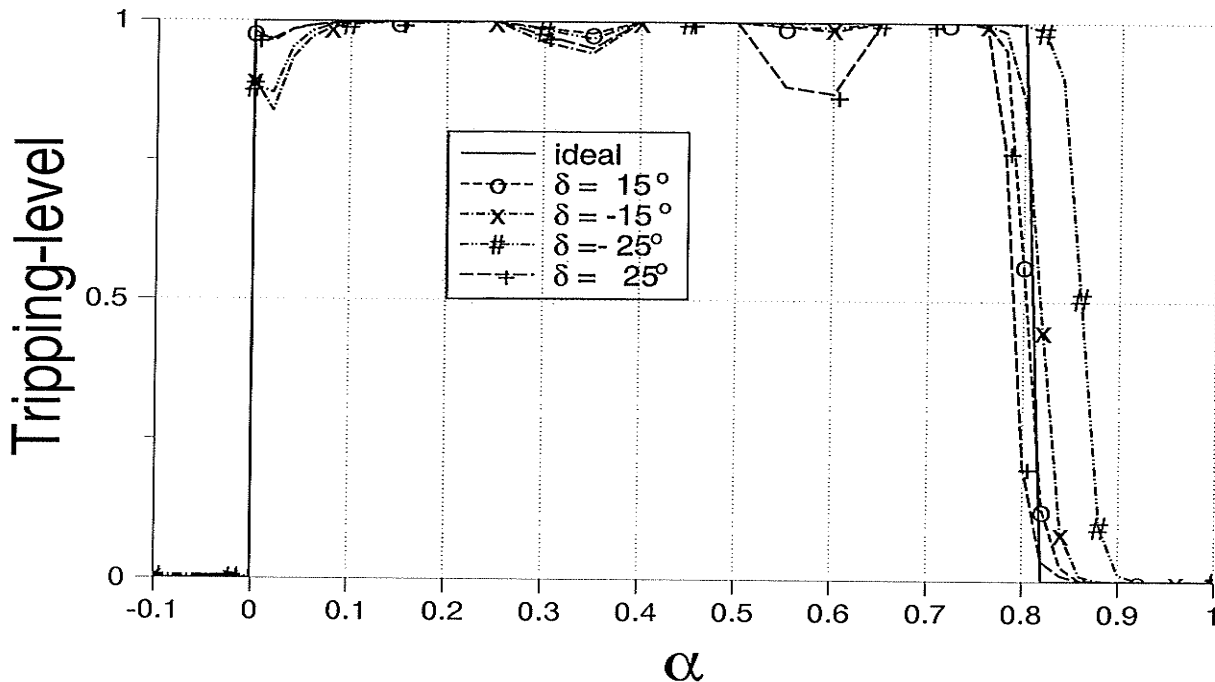


**Fig. 7.11** ANN distance relay performance with varying transmitted load

Run #2 ( $V_F = 0.08$ )

are very close to the expected ideal line when the load angle  $\delta$  is set at  $-15^\circ$ ,  $15^\circ$  and  $25^\circ$ . For  $\delta = -25^\circ$ , there are slightly more overreach errors, approximately  $(86-80)/80 = 7.5\%$ . The tripping for the faults at the beginning of the line or around 60% of the line seems a bit unstable but it does not affect the performance since outputs greater than 0.5 are considered as tripping.

Fig. 7.12 shows the performance of the ANN distance relay for case of different nonlinear arcing fault voltage. There seem to be relative higher errors appearing here. As can be seen, all the tripping traces with varying load conditions are very close, and will cover higher arcing fault voltages than the settings. This

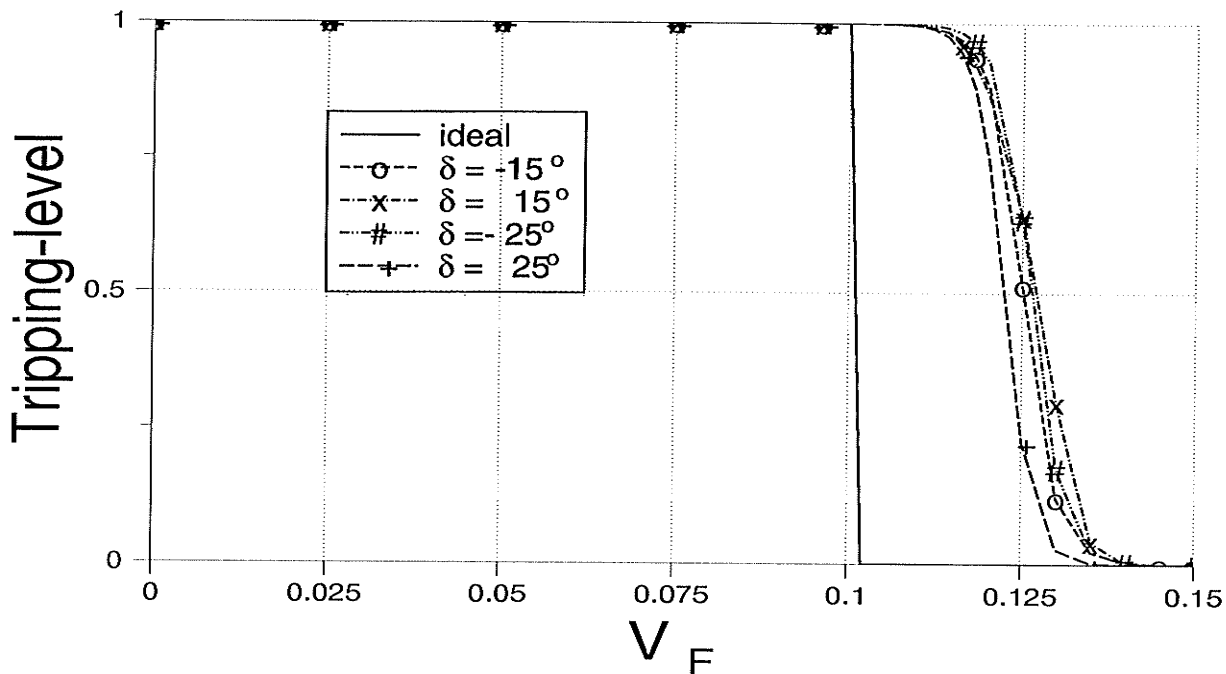


**Fig. 7.12** ANN distance relay performance with varying transmitted load  
Run #3 ( $\alpha = 0.4$ )

does not have a negative effect on the relay performance as long as the allowed fault voltage does not encroach on the load region. This load encroachment will not occur in terms of arcing faults.

### 7.10 Comparison with Conventional Distance Relay

In Chapter 4, an actual Manitoba Hydro transmission line, a 138kV line from Kelsey to Thompson in northern Manitoba, is modelled on PSCAD/EMTDC. The per kilometer impedance parameters of this line are given in Table 7.4.

**Table 7.4** Per km impedance of Kelsey - Thompson line

Impedance Element	Resistance R ( $\Omega$ )	Reactance X ( $\Omega$ )	Susceptance B ( S )
Positive Sequence	0.043	0.490	3.374
Negative Sequence	0.043	0.490	3.374
Zero Sequence	0.362	1.764	2.271

Supposing there is a conventional distance relay with a quadrilateral operating characteristic shown as in Fig. 7.13. Consider the system in Fig. 7.5, with this conventional distance relay located at the Kelsey end. Let us set its operating border based on an ANN distance relay first. Assuming that this conventional relay uses a reactance boundary of 80% of the transmission line length and has 5.5  $\Omega$  fault resistance extension, then the operating zone is defined by

$$r < R \leq 5.5 + r \quad (7.4)$$

$$0 < X \leq 39.24 \quad (7.5)$$

where  $r$  is the resistance of the line between the relay location to fault location. With this assumption, the operating zones of the conventional distance relay and

the ANN distance relay are almost the same at certain system conditions.

Let us consider that a single line-to-ground fault occurs in the middle of the line ( $\alpha = 0.5$ ) and  $V_F = 0.09$  (at daytime, for example, under maximum generation conditions),  $Z_{S1} = 18.45\angle 86.3^\circ$ ,  $Z_{R1} = 25.90\angle 83.7^\circ$  and heavy load  $\delta = -30^\circ$ . The measured impedance by the conventional distance relay using Eq. ( 2.5 ) is  $\alpha Z_{L1} = 7.26 + j20.62$  and the location of the fault on the impedance plane and on the  $\alpha$ - $V_F$  plane are shown in Fig. 7.13. In this case, both the conventional distance relay and the ANN distance relay operate well.

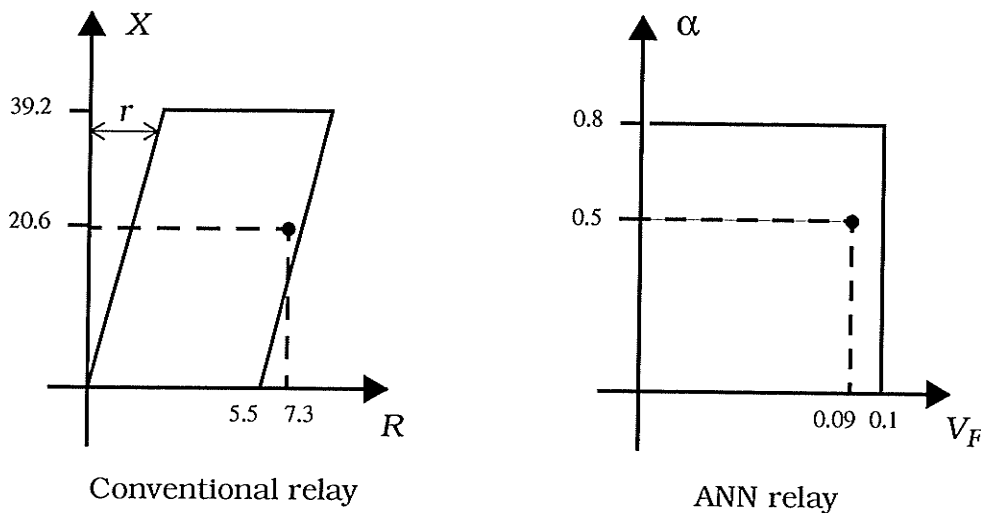


**Fig. 7.13** Comparison of conventional relay and ANN relay for low source impedance and  $\delta = -30^\circ$

However, if the system situation is changed, say at night time when the sources are in the minimum generation mode, the system parameters could be:  $Z_{S1} = 26.16\angle 86.3^\circ$ ,  $Z_{R1} = 31.19\angle 84.1^\circ$  and load flow reversed (positive  $\delta$ ). The impedance measured by a conventional distance relay is  $\alpha Z_{L1} = 8.47 + j22.31$  at  $\delta = 10^\circ$



and  $\alpha Z_{L1} = 8.82 + j23.14$  at  $\delta = 30^\circ$ . The locations of the fault on the impedance plane and on the  $\alpha$ - $V_F$  plane are shown in Fig. 7.14. The location of the fault on the impedance plane is outside of the tripping zone but the location of the fault on the  $\alpha$ - $V_F$  plane is the same as before. In this case, the conventional distance relay mis-operates but the ANN distance relay operates correctly. In other words, the ANN relay adapts to source impedance changes and responds correctly, whereas the conventional relay fails to see the fault.

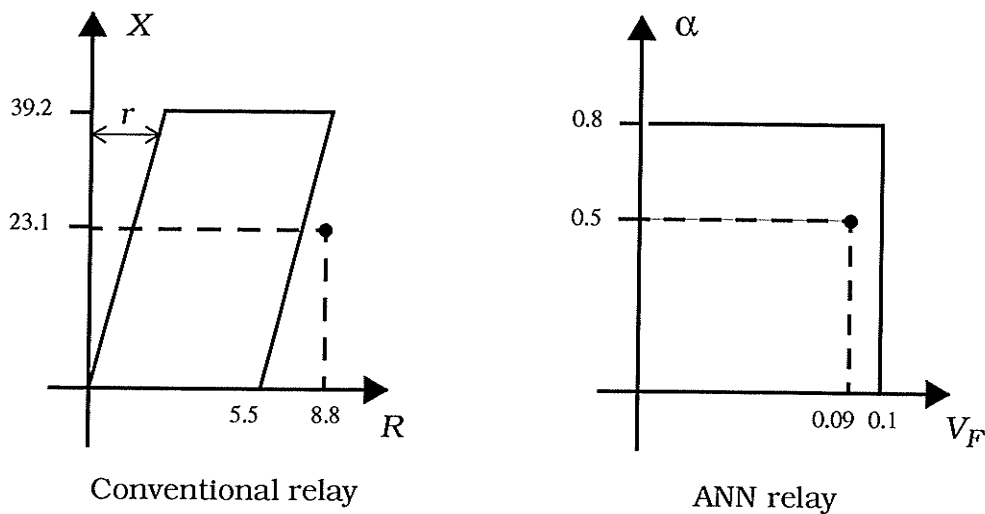


**Fig. 7.14** Comparison of conventional relay and ANN relay for high source impedance and  $\delta = 30^\circ$

## 7.11 Summary

Conventional distance relays may not operate correctly under conditions of nonlinear arcing fault resistance and variable source impedance. An ANN-based distance relay has been presented here. The performance of the ANN distance relay, based on the simulation of an actual transmission line of Manitoba Hydro with a nonlinear arc resistance model in PSCAD/EMTDC, is very good. The fol-

lowing conclusions can be drawn through the training of a neural network as a distance relay:

1. The prospective ANN distance relay demonstrates a good potential for separating the single line-to-ground faults along the transmission line into proper categories, even with nonlinear elements present in the system.
2. The prospective ANN distance relay has a good ability to identify nonlinear arcing fault resistance in the protected zone, even though the errors are little on the *reliable side*.
3. The prospective ANN distance relay can adapt to pre-fault load conditions, variable source impedance and variable arc length, i.e., varying arcing fault resistance.

Although a great deal of study still needs to be done, the preliminary result shows the exciting future for application of artificial neural networks to problems like nonlinear ground fault resistance, in power system protection.

## Chapter Eight

# Conclusions

---

The work done in this thesis has accomplished its original goals. The main achievements and contribution of this research can be summarized as follows:

- ( 1 ). Artificial neural networks have been applied to distance protection to overcome some problems of conventional distance relays.
- ( 2 ). The suitability of ANN's to handle traditional problems, such as variation of source impedance and remote infeed effects, have been investigated and the results are very promising.
- ( 3 ). The suitability of ANN's to adapt to arcing fault resistance has been investigated and the outcome is encouraging.
- ( 4 ). DRAFT icons of the conventional distance relays and their FORTRAN programs was developed in the PSCAD/EMTDC environment.
- ( 5 ). Successful simulation of thousands of cases for an actual Manitoba Hydro transmission line has been done in the PSCAD/EMTDC environment.

- ( 6 ). A set of proper input quantities to ANN's has been found and defined. The research shows that they are very effective.
- ( 7 ). The appropriate construction of an ANN used for distance protection purposes has been determined.
- ( 8 ). A functional set of weights and biases for the ANN has been found and has good recalling ability as well as a good generalizing ability.
- ( 9 ). A new kind of operating characteristic has been defined: one which uses constant fault voltage rather than constant fault resistance.

## Chapter Nine

### Future Work

---

There are still many refinements that interest the author but time is not available. These refinements are very important and critical for the implementation of real distance protection based on artificial neural networks. They are follows:

1. Examination of the behavior of the ANN distance relay under transient conditions.
2. Examination of the behavior of the ANN distance relay during power swings.
3. Application of artificial neural networks to detection of single line-to-ground faults with nonlinear ground fault resistance.
4. Application of artificial neural networks to detection of phase-to-phase faults and multiphase-to-ground faults.

## References

---

- [1.] M. A. El-Sharkawi, R. J. Marks II, S. Weerasooriya, *Control and Dynamic Systems*, Vol. 41, Academic Press, Inc., 1991.
- [2.] A. F. Sultan, G. W. Swift, D. J. Fedirchuk, "Detection of High Impedance Arcing Faults Using a Multi-Layer Perceptron," *IEEE Transactions on Power Delivery*, vol. 7, no. 4, October 1992, pp. 1871-1877.
- [3.] A. F. Sultan, *High Impedance Arcing Faults Detection Using An Artificial Neural Network*, Ph.D thesis, The University of Manitoba, 1992.
- [4.] Dehua Zhen, *A High Impedance Arcing Faults Detector*, M.Sc. thesis, The University of Manitoba, 1995.
- [5.] S. Ebron, D. L. Lubkeman, M. White, "A Neural Network Approach to The Detection of Incipient Faults on Power Distribution Feeders," *IEEE Transactions on Power Delivery*, vol. 5, no. 2, April 1990, pp. 905-914.
- [6.] A. M. Sharaf, L. A. Snider, K. Debnath, "A Neural Network Based Back Error Propagation Relay algorithm for Distribution System High Impedance Fault Detection," *IEE Conference Publication*, Vol. 2, No. 388, 1994, pp. 613-620.
- [7.] A. G. Jongepier, L. van der Sluis, "Adaptive Distance Protection of A Double-Circuit Line Using Artificial Neural Nets," *Fifth International Conference on Developments in Power System Protection*, IEE no. 368, pp. 157-160.

- 
- [8.] S. A. Khaparde, P. B. Kale, S. H. Agarwal, "Application of Artificial Neural Network in Protective Relaying of Transmission Lines," *Proceedings of The First International Forum on Applications of Neural Networks to Power Systems*, 91TH0374-9, pp. 122-125.
- [9.] Q. Y. Xuan, R. Morgan, D. Williams, Y. H. Song, A. T. Johns, "Adaptive Protection for Series Compensated EHV Transmission Systems Using Neural Networks," *IEE Conference Publication*, vol. 1, no. 389, 1994, pp. 728-732.
- [10.] Q. Y. Xuan, A. T. Johns, Y. H. Song, "Adaptive Protection Technique for Controllable Series Compensated EHV Transmission Systems Using Neural Networks," *IEE Conference Publication*, vol. 2, no. 388, 1994, pp. 621-625.
- [11.] K. Feser, U. Braun, F. Engler, A. Maier, "Application of Neural Networks in Numerical Busbar Protection Systems," *Proceedings of The First International Forum on Applications of Neural Networks to Power Systems*, 91TH0374-9, pp. 117-121.
- [12.] D. S. Fitton, R. W. Dunn, R. K. Aggarwal, A. T. Johns, Y. H. Song, "The Application of Neural Network Techniques to Adaptive Autoreclosure in Protection Equipment," *Fifth International Conference on Developments in Power System Protection*, IEE no. 368, pp. 161-164.
- [13.] R. K. Aggarwal, A. T. Johns, Y. H. Song, R. W. Dunn, D. S. Fitton, "Neural-network Based Adaptive Single-pole Autoreclosure Technique for EHV Transmission Systems," *IEE Proceedings -- Generation, Transmission and Distribution*, Vol. 141, No. 2, March 1994, pp. 155-160.
- [14.] N. Kandil, V. K. Sood, K. Khorasani, R. V. Patel, "Fault Identification in An AC-DC Transmission System Using Neural Networks," *IEEE Transactions on Power Systems*, vol. 7, no. 2, May 1992, pp. 812-819.

- 
- [15.] P. Chan, "Application of Neural-Network Computing in Intelligent Alarm Processing," *PICA conference proceedings*, Seattle, WA, May, 1989.
- [16.] K. S. Swarup, H. S. Chandrasekharaiah, "Fault Detection and Diagnosis of Power Systems Using Artificial Neural Networks," *Proceedings of The First International Forum on Applications of Neural Networks to Power Systems*, 91TH0374-9, pp. 102-106.
- [17.] H. Yang, W. Chang, C. Huang, "A New Neural Networks Approach to On-line Fault Section Estimation Using Information of Protective Relays and Circuit Breakers," *IEEE Transactions on Power Delivery*, vol. 9, no. 1, January 1994, pp. 220-229.
- [18.] C. N. Lu, M. T. Tsay, Y. J. Hwang, Y. C. Lin, "An Artificial Neural Network Based Trouble Call Analysis," *IEEE Transactions on Power Delivery*, vol. 9, no. 3, July 1994, pp. 1663-1668.
- [19.] H. Mori, H. Uematsu, S. Tsuzuki, T. Sakurai, Y. Kojima, K. Suzuki, "Identification of Harmonic Loads in Power Systems using an Artificial Neural Network," *The 2nd Symposium on Expert System Applications to Power Systems*, Seattle, July, 1989.
- [20.] A. Cichochi, T. Lobos, "Artificial Neural Networks for Real-time Estimation of Basic Waveforms of Voltages and Currents," *IEEE Transactions on Power Systems*, vol. 9, no. 2, May 1994, pp. 612-618.
- [21.] L. G. Perez, A. J. Flechsig, J. L. Meador, Z. Obradovic, "Training An Artificial Neural Network to Discriminate Between Magnetizing Inrush And Internal Faults," *IEEE Transactions on Power Delivery*, vol. 9, no. 1, January 1994, pp. 434-441.
- [22.] A. E. Guile, W. Paterson, *Electrical Power Systems*, Vol. 1, 2, Pergamon Press



- Ltd., England, 1977.
- [23.] Charles A. Gross, *Power System Analysis*, John Wiley & Sons, New York, 1979.
- [24.] A. R. van C. Warrington, *Protective Relays -- Their Theory and Practice*, Chapman & Hall Ltd., 1971.
- [25.] The Electricity Council, *Power System Protection -- 1 Principles and Components*, Peter Peregrinus Ltd., 1981.
- [26.] The Electricity Council, *Power System Protection -- 2 Systems and Models*, Peter Peregrinus Ltd., 1981.
- [27.] The Electricity Council, *Power System Protection -- 3 Application*, Peter Peregrinus Ltd., 1981.
- [28.] T. S. Madhava Rao, *Power System Protection -- Static Relays*, McGRAW-HILL BOOK COMPANY, 1981.
- [29.] A. G. Phadke, J. S. Thorp, *Computer Relaying for Power Systems*, John Wiley & Sons Inc., 1988.
- [30.] G. D. Rockefeller, C. L. Wagner, J. R. Linders, K. L. Hicks, D. T. Rizy, "Adaptive Transmission Relaying Concepts for Improved Performance," *IEEE Transactions on Power Delivery*, Vol. 3, No. 4, October 1988, pp. 1446-1458.
- [31.] J. S. Thorp, A. G. Phadke, S. H. Horowitz, M. M. Begovic, "Some Application of Phasor Measurements to Adaptive Protection," *PICA*, 1987, pp. 467-474.
- [32.] Sunny L. K. Chan, *Adaptive Impedance Relays*, M.Sc. thesis, The University of Manitoba, 1992.
- [33.] Z. Zhang and D. Chen, "An Adaptive Approach in Digital Distance Protection,"

Paper No. 88 WM 126-5, IEEE PES Winter Meeting, January 1988, New York.

- [34.] D. I. Jeerings, J. R. Linders, "Ground Resistance - Revisited," *IEEE Transactions on Power Delivery*, Vol. 4, No. 2, April 1989, pp. 949-956.
- [35.] J. R. Dunki-Jacobs, "The Effects of Arcing Ground Faults on Low-Voltage System Design," *IEEE Transactions on Industry Applications*, Vol. 1A-8, No. 3, May/June 1972, pp. 223-230.
- [36.] C. L. Gilkeson, P. A. Jeanne, J. C. Davenport, "Power System Faults to Ground, Part I : Characteristics," *AIEE Transactions*, Vol. 56, April 1937, pp. 421-428.
- [37.] C. L. Gilkeson, P. A. Jeanne, J. C. Davenport, "Power System Faults to Ground, Part II : Fault Resistance," *AIEE Transactions*, Vol. 56, April 1937, pp. 428-433.
- [38.] A. P. Strom, "Long 60-Cycle Arcs in Air," *AIEE Transactions*, Vol. 65, March 1946, pp. 113-117.
- [39.] J. Hertz, A. Krogh, R. G. Palmer, *Introduction to The Theory of Neural Computation*, Addison-Wesley, 1991.
- [40.] H. White, *Artificial Neural Networks -- Approximation and Learning Theory*, Blackwell, 1992.
- [41.] J. M. Zurada, *Introduction of Artificial Neural Systems*, West Publishing Company, 1992.
- [42.] H. Wechsler, *Neural Networks for Perception*, Vol. 1 & 2, Academic Press, Inc., 1992.
- [43.] R. Eckmiller, *Advanced Neural Computers*, North-Holland, 1990.
- [44.] Drew van Camp, *Xerion Neural Network Simulator User's Guide*, University of

---

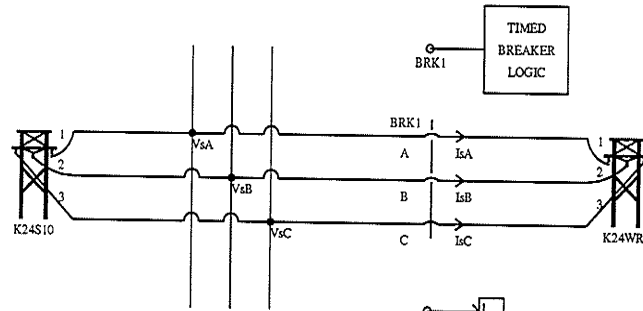
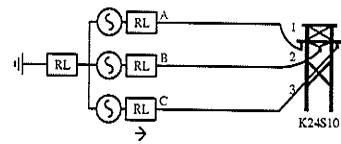
Toronto, 1992.

- [45.] Manitoba HVDC Research Centre, *EMTDC User's Manual*, 1988.
- [46.] Manitoba HVDC Research Centre, *EMTDC Reference -- Theory Manual*, 1988.
- [47.] P. G. McLaren, G. W. Swift, Z. Zhang, E. Dirks, R. P. Jayasinghe, I. Fernando, "A New Directional Element for Numerical Distance Relays," *IEEE PES Summer Meeting*, July 1994, San Francisco, 94 SM 429-1-PWRD.
- [48.] D. G. Fink, H. W. Beaty, *Standard Handbook For Electrical Engineers*, McGraw-Hill Book Company, 1987.

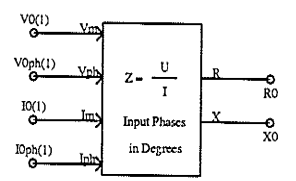
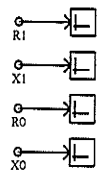
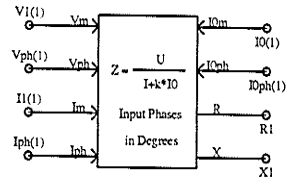
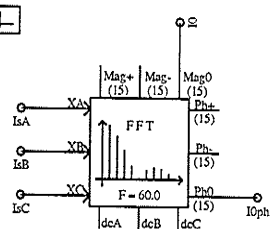
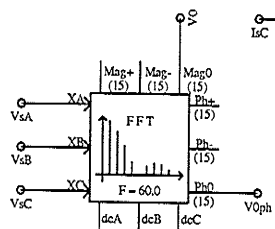
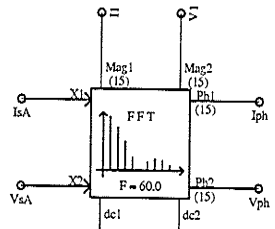
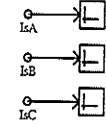
# Appendix A

## DRAFTs of Simulation Systems

---



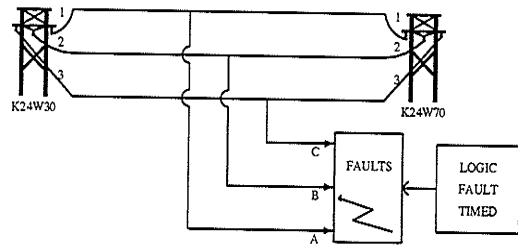
TIMED  
BREAKER  
LOGIC



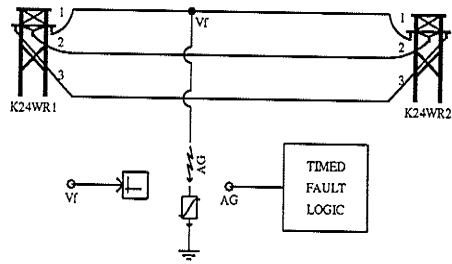
University of Manitoba, EE Dept.  
casel

Created: November 21, 1994 (wgqi)  
Last Modified: October 20, 1995 (wgqi)  
Printed On: October 20, 1995 (wgqi)

Sending End  
Subsystem #1 of 3



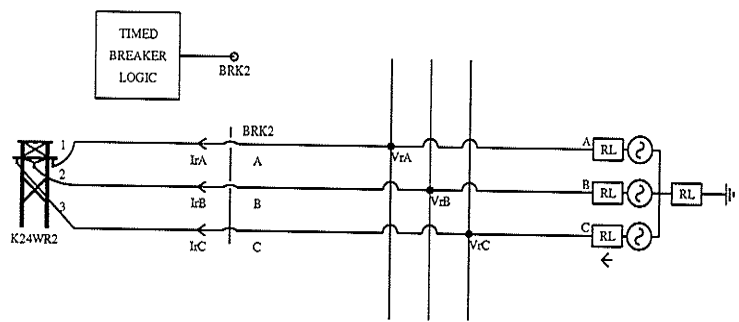
<p>University of Manitoba, EE Dept. <i>case1</i></p>	<p>Created: November 21, 1994 (wgqi)                  Last Modified: August 16, 1995 (wgqi)                  Printed On: October 20, 1995 (wgqi)</p>	<p><i>Fault Location</i>                   Subsystem #2 of 3</p>
--	--	--



University of Manitoba, EE Dept.  
casel

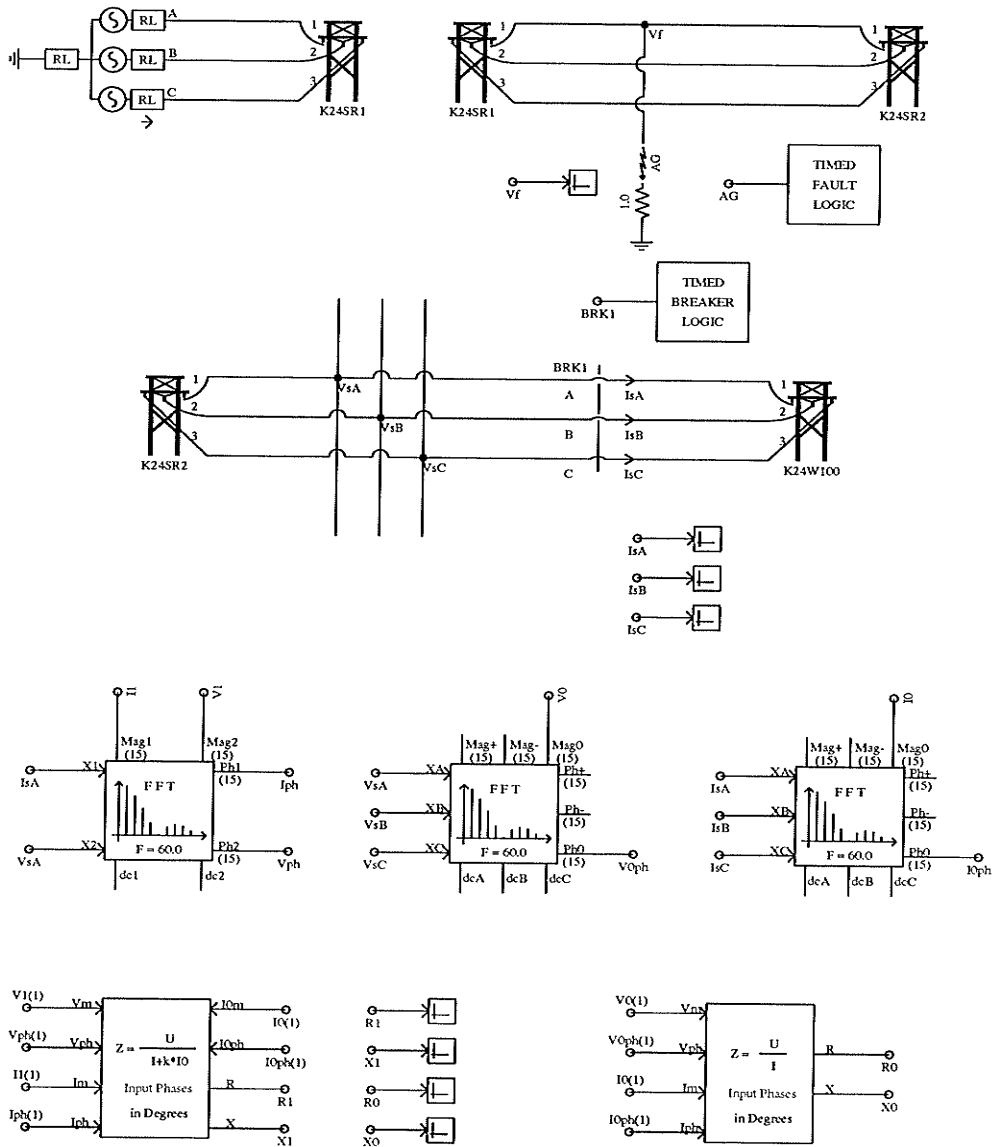
Created: November 21, 1994 (wgqi)  
Last Modified: October 20, 1995 (wgqi)  
Printed On: October 20, 1995 (wgqi)

*Fault Location*  
Subsystem #2 of 3



<p>University of Manitoba, EE Dept. casel</p>	<p>Created: November 21, 1994 (wgqi) Last Modified: October 20, 1995 (wgqi) Printed On: October 20, 1995 (wgqi)</p>	<p>Receiving End Subsystem #3 of 3</p>
---	---	--

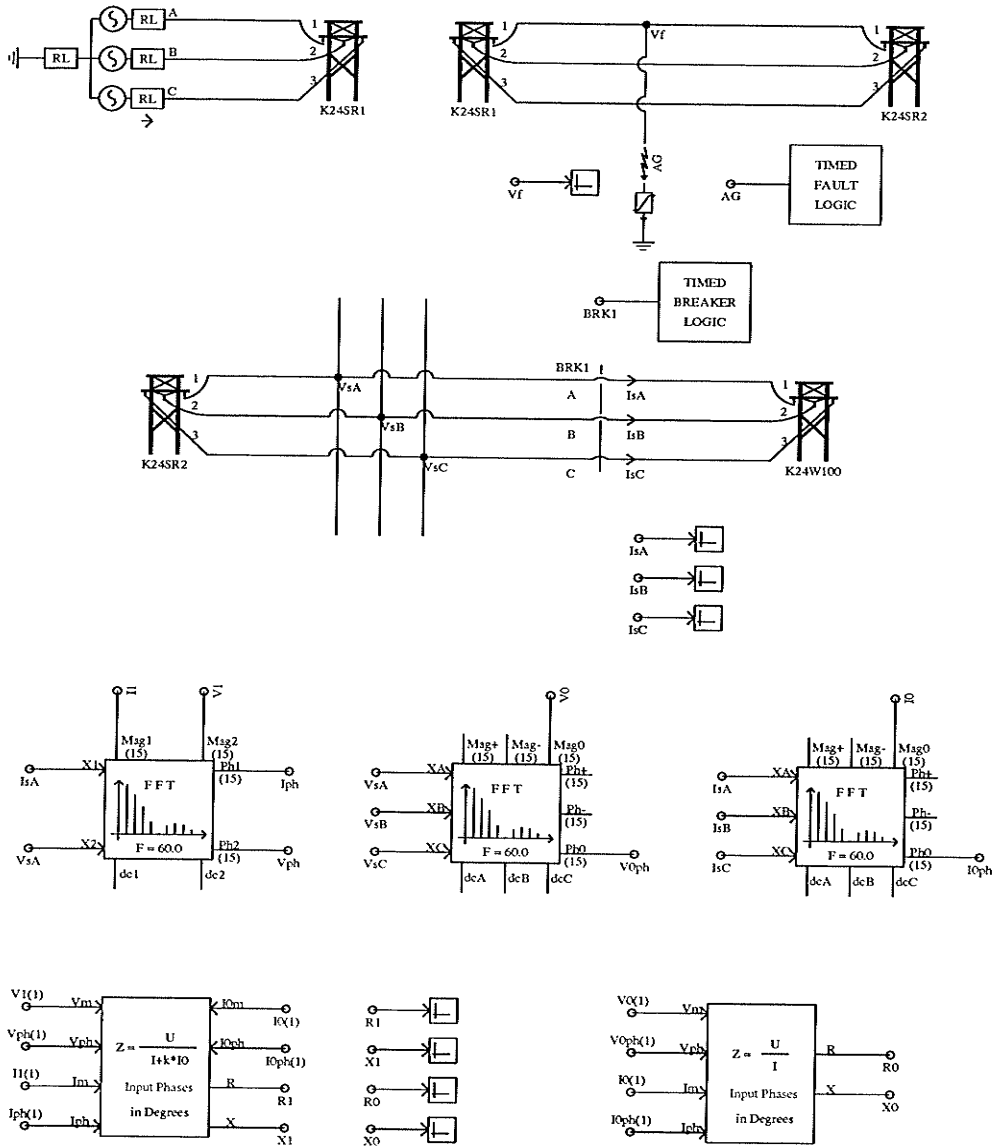


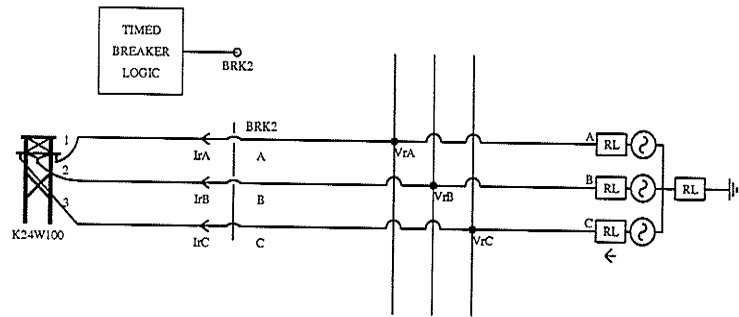


University of Manitoba, EE Dept.  
case1

Created: November 21, 1994 (wgqi)  
Last Modified: October 20, 1995 (wgqi)  
Printed On: October 20, 1995 (wgqi)

Sending End  
Subsystem #1 of 2





University of Manitoba, EE Dept.  
casel

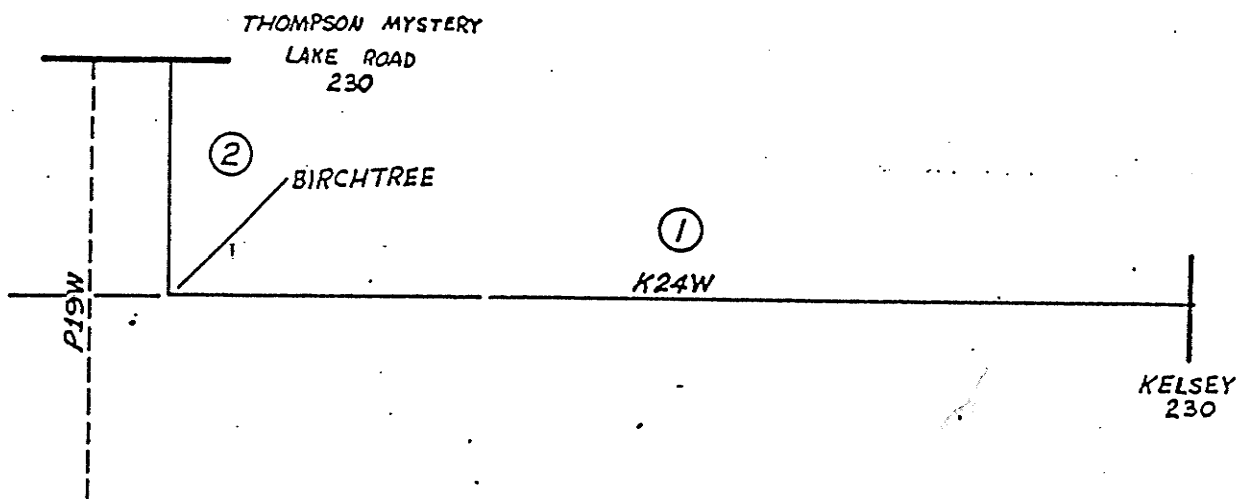
Created: November 21, 1994 (wgqi)  
Last Modified: October 11, 1995 (wgqi)  
Printed On: October 20, 1995 (wgqi)

Receiving End  
Subsystem #2 of 2

## **Appendix B**

# **Transmission Line Parameters**

---



SECTION ② - K24W TOWER & TO P19W TOWER & = 24.39m

LINE NO. K24W

NOM VOLT 230.0 KV

LINE NO. K24W

KELSEY TO THOMPSON

SEC	LENGTH KM	PHASE CONDUCTOR	YEAR	SPAN M	TOWER TYPE	GROUND CONDUCTOR	*****PER KM*****			*****			INTERMEDIATE POINTS
							R11	X11	B11	R00	X00	B00	
1	97.77	1272 ACSR SD T 5	1972	472	77 3/8 GALV STEEL	OHMS. MICROMHOS PER UNIT	0.04305	0.49048	3.37439	0.36175	1.76368	2.27063	
		RHO =3000.00					0.00008	0.00093	0.00179	0.00068	0.00333	0.00120	
2	4.09	1272 ACSR SD T 5	1972	214	74 3/8 GALV STEEL	OHMS. MICROMHOS PER UNIT	0.04336	0.47639	3.50168	0.45269	1.64087	2.51886	BIRCHTREE
		RHO =3000.00					0.00008	0.00090	0.00185	0.00086	0.00310	0.00133	
T	101.86												

TOTAL PER UNIT SELF VALUES

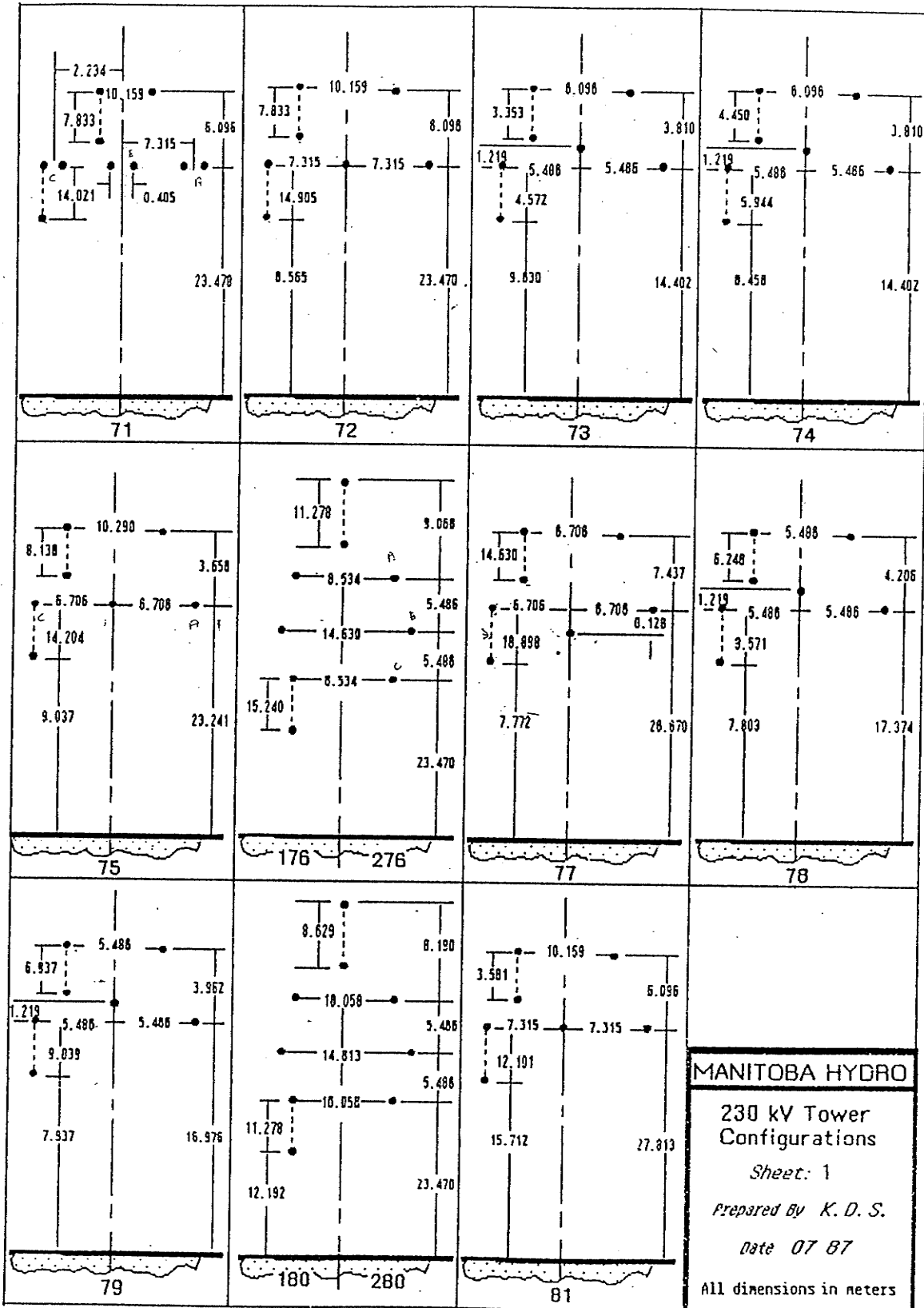
BASE KV	MVA	POSITIVE SEQUENCE			ZERO SEQUENCE SELF		
		R11	X11	B11	R00	X00	B00
230.00	100	0.0082	0.0941	0.1828	0.0694	0.3364	0.1241

TOTAL PER UNIT ZERO SEQUENCE MUTUAL VALUES

BASE	LINE RMO	K24W TO P19W		BMO
		XMO	BMO	
230.00	100	0.0031	0.0069	0.1017

JUL 1987

GENERATION & TRANSMISSION PLANNING DEPARTMENT



1.....

PSS/E SHORT CIRCUIT OUTPUT WED, AUG 02 1995 15:11 HOME BUS IS :

MANITOBA HYDRO SYSTEM - MAX.GEN (X'D) - FAMJ 95 05 08 358 [KELSEY D 138]

GRNWAY, HUBBAY, LUSINAP, GOULET, STVITAL, ROSSLAKE, DUNLOP, HERBELT

\*\*\* FAULTED BUS IS : 358 [KELSEY D 138] \*\*\* 0 LEVELS AWAY

.....

AT BUS 358 [KELSEY D 138] AREA 4 (PU) V+: / 0.0000/ 0.00 (PU) VA: / 0.0000/ 0.00 V0: / 0.2790/ -150.04

V+: / 0.6748/ 29.21 V-: / 0.3958/ -151.31

THEV. R, X, X/R: POSITIVE 0.00558 0.08539 15.293 NEGATIVE 0.00587 0.08876 15.122 ZERO 0.00274 0.06265 22.834

		T H R E E P H A S E F A U L T						O N E P H A S E F A U L T				
FROM	AREA CKT I/Z	/I+/ AN(I+)	/Z+/ AN(Z+)	APP X/R	/IA/ AN(IA)	/ZA/ AN(ZA)	APP X/R	/3I0/ AN(3I0)	/Z0/ AN(Z0)	APP X/R		
351 [RADISSON 138]	4 1 PU/PU	1.4415	-60.04	0.3376	84.95	11.318	1.2520	-58.35	0.4834	84.80	10.983	
352 [KELSEY 138]	4 1 PU/PU	10.8960	-56.85	0.0000	0.00	0.000	0.5965	-49.43	0.1712	-92.01	28.507	
TOTAL FAULT CURRENT (P.U.)		12.3355	-57.22				12.0976	-57.45	0.0000	0.00	0.000	
							12.7591	-57.91	0.0656	-92.13	26.887	
							13.3494	-57.53				

1.....

PSS/E SHORT CIRCUIT OUTPUT WED, AUG 02 1995 15:11 HOME BUS IS :

MANITOBA HYDRO SYSTEM - MAX.GEN (X'D) - FAMJ 95 05 08 360 [THOMPYS 138]

GRNWAY, HUBBAY, LUSINAP, GOULET, STVITAL, ROSSLAKE, DUNLOP, HERBELT

\*\*\* FAULTED BUS IS : 360 [THOMPYS 138] \*\*\* 0 LEVELS AWAY

.....

AT BUS 360 [THOMPYS 138] AREA 4 (PU) V+: / 0.0000/ 0.00 (PU) VA: / 0.0000/ 0.00 V0: / 0.0954/ -149.58

V+: / 0.6004/ 27.99 V-: / 0.5051/ -152.46

THEV. R, X, X/R: POSITIVE 0.01483 0.12859 8.668 NEGATIVE 0.01479 0.12982 8.778 ZERO 0.00156 0.02462 15.803

		T H R E E P H A S E F A U L T						O N E P H A S E F A U L T				
FROM	AREA CKT I/Z	/I+/ AN(I+)	/Z+/ AN(Z+)	APP X/R	/IA/ AN(IA)	/ZA/ AN(ZA)	APP X/R	/3I0/ AN(3I0)	/Z0/ AN(Z0)	APP X/R		
104 [THOMYSLK 230]	3 1 PU/PU	2.1592	-56.89	0.0944	86.73	17.509	2.1763	-57.12	0.0943	87.00	19.094	
355 [INCO 138]	4 1 PU/PU	6.3453	-55.26	0.0031	82.65	7.750	0.5426	-56.07	0.4332	-94.27	13.386	
							8.7047	-55.37	0.0057	81.45	6.650	



362 [BRNTWD-D 138]	4 1	PU/PU	0.0000	0.00	0.0000	0.00	0.000	8.9042	-55.08	0.0215	-92.05	27.946
								0.0001	-62.09	0.0000	0.00	0.000
								0.0005	120.54	0.0000	0.00	0.000
		TO SHUNT (P.U.)	0.0000	0.00				0.7189	120.42			
								2.1568	120.42			
TOTAL FAULT CURRENT		(P.U.)	8.5039	-55.67				11.5978	-55.96			

```

1.....
PSS/E SHORT CIRCUIT OUTPUT          THU, AUG 03 1995 10:22      HOME BUS IS :
MANITOBA HYDRO SYSTEM - MIN.GEN (X'D) - FAMJ 95 05 08      358 [KELSEY D 138]
GRNWAY, HUBBAY, LUSINAP, GOULET, STVITAL, ROSSLAKE, DUNLOP, HERBELT
*** FAULTED BUS IS : 358 [KELSEY D 138] ***                0 LEVELS AWAY
.....

```

```

AT BUS 358 [KELSEY D 138] AREA 4      (PU) V+: / 0.0000/ 0.00      (PU) VA: / 0.0000/ 0.00      V0: / 0.2466/ -150.63
                                           V+: / 0.6958/ 28.31      V-: / 0.4492/ -152.26

```

```

THEV. R, X, X/R: POSITIVE 0.00678 0.10034 14.792      NEGATIVE 0.00824 0.11393 13.831      ZERO 0.00274 0.06265 22.834

```

T H R E E P H A S E F A U L T							O N E P H A S E F A U L T						
FROM	AREA	CKT	I/Z	/I+/	AN(I+)	/Z+/	AN(Z+)	APP X/R	/IA/	AN(IA)	/ZA/	AN(ZA)	APP X/R
									/3I0/	AN(3I0)	/Z0/	AN(Z0)	APP X/R
351 [RADISSON 138]	4	1	PU/PU	1.4415	-60.04	0.3376	84.95	11.318	1.2748	-58.49	0.4640	84.69	10.757
352 [KELSEY 138]	4	1	PU/PU	9.4109	-57.61	0.0000	0.00	0.000	0.5272	-50.02	0.1712	-92.01	28.507
									10.5236	-58.08	0.0000	0.00	0.000
									11.2766	-58.50	0.0656	-92.13	26.887
									11.7984	-58.13			
TOTAL FAULT CURRENT (P.U.)				10.8512	-57.93								

```

1.....
PSS/E SHORT CIRCUIT OUTPUT          THU, AUG 03 1995 10:22      HOME BUS IS :
MANITOBA HYDRO SYSTEM - MIN.GEN (X'D) - FAMJ 95 05 08      360 [THOMPYS 138]
GRNWAY, HUBBAY, LUSINAP, GOULET, STVITAL, ROSSLAKE, DUNLOP, HERBELT
*** FAULTED BUS IS : 360 [THOMPYS 138] ***                0 LEVELS AWAY
.....

```

```

AT BUS 360 [THOMPYS 138] AREA 4      (PU) V+: / 0.0000/ 0.00      (PU) VA: / 0.0000/ 0.00      V0: / 0.0902/ -151.14
                                           V+: / 0.6359/ 26.54      V-: / 0.5457/ -153.84

```

```

THEV. R, X, X/R: POSITIVE 0.01615 0.14192 8.789      NEGATIVE 0.01643 0.14823 9.024      ZERO 0.00156 0.02462 15.803

```

T H R E E P H A S E F A U L T							O N E P H A S E F A U L T						
FROM	AREA	CKT	I/Z	/I+/	AN(I+)	/Z+/	AN(Z+)	APP X/R	/IA/	AN(IA)	/ZA/	AN(ZA)	APP X/R
									/3I0/	AN(3I0)	/Z0/	AN(Z0)	APP X/R
104 [THOMYSLK 230]	3	1	PU/PU	2.1804	-60.09	0.0944	86.73	17.509	2.2139	-60.27	0.0943	86.98	18.971
355 [INCO 138]	4	1	PU/PU	5.9342	-56.16	0.0031	82.65	7.750	0.5135	-57.63	0.4332	-94.27	13.386
									8.0881	-56.46	0.0058	81.22	6.475

362 [BRNTWD-D 138]	4 1	PU/PU	0.0000	0.00	0.0000	0.00	0.000	8.4278	-56.63	0.0215	-92.05	27.946
								0.0001	-62.85	0.0000	0.00	0.000
								0.0004	119.01	0.0000	0.00	0.000
		TO SHUNT (P.U.)	0.0000	0.00				0.6805	118.86			
								2.0414	118.86			
TOTAL FAULT CURRENT		(P.U.)	8.1108	-57.21				10.9773	-57.52			

```

1.....
.
.           PSS/E SHORT CIRCUIT OUTPUT           WED, AUG 02 1995 14:49           HOME BUS IS :
.
.   MANITOBA HYDRO SYSTEM - MAX.GEN (X'D) - FAMJ 95 05 08           358 [KELSEY D 138]
.   GRNWAY, HUSBAY, LUSINAP, GOULET, STVITAL, ROSSLAKE, DUNLOP, HERBELT
.
.           *** FAULTED BUS IS : 358 [KELSEY D 138] ***           0 LEVELS AWAY
.
1.....

```

```

AT BUS 358 [KELSEY D 138] AREA 4          (PU) V+: / 0.0000/ 0.00          (PU) VA: / 0.0000/ 0.00          V0: / 0.2697/ -150.40
                                           V+: / 0.6525/ 28.86          V-: / 0.3828/ -151.66

```

```

THEV. R, X, X/R: POSITIVE 0.00624 0.09666 15.491          NEGATIVE 0.00586 0.08881 15.149          ZERO 0.00274 0.06265 22.834

```

T H R E E P H A S E F A U L T									O N E P H A S E F A U L T				
FROM	AREA	CKT	I/Z	/I+/ AN(I+)	/Z+/ AN(Z+)	APP	X/R		/IA/ AN(IA)	/ZA/ AN(ZA)	APP	X/R	
									/3I0/ AN(3I0)	/Z0/ AN(Z0)		APP X/R	
351 [RADISSON 138]	4	1	PU/PU	1.3383	-60.46	0.3376	84.95	11.318	1.2228	-58.54	0.4819	84.75	10.878
352 [KELSEY 138]	4	1	PU/PU	9.7006	-57.23	0.0000	0.00	0.000	0.5766	-49.78	0.1712	-92.01	28.507
TOTAL FAULT CURRENT (P.U.)				11.0371	-57.62				12.3329	-58.27	0.0656	-92.13	26.887
									12.9035	-57.89			

```

1.....
.
.           PSS/E SHORT CIRCUIT OUTPUT           WED, AUG 02 1995 14:49           HOME BUS IS :
.
.   MANITOBA HYDRO SYSTEM - MAX.GEN (X'D) - FAMJ 95 05 08           360 [THOMPYS 138]
.   GRNWAY, HUSBAY, LUSINAP, GOULET, STVITAL, ROSSLAKE, DUNLOP, HERBELT
.
.           *** FAULTED BUS IS : 360 [THOMPYS 138] ***           0 LEVELS AWAY
.
1.....

```

```

AT BUS 360 [THOMPYS 138] AREA 4          (PU) V+: / 0.0000/ 0.00          (PU) VA: / 0.0000/ 0.00          V0: / 0.0946/ -150.23
                                           V+: / 0.5960/ 27.36          V-: / 0.5015/ -153.10

```

```

THEV. R, X, X/R: POSITIVE 0.01503 0.13519 8.997          NEGATIVE 0.01478 0.12994 8.795          ZERO 0.00156 0.02462 15.803

```

T H R E E P H A S E F A U L T									O N E P H A S E F A U L T				
FROM	AREA	CKT	I/Z	/I+/ AN(I+)	/Z+/ AN(Z+)	APP	X/R		/IA/ AN(IA)	/ZA/ AN(ZA)	APP	X/R	
									/3I0/ AN(3I0)	/Z0/ AN(Z0)		APP X/R	
104 [THOMYSLK 230]	3	1	PU/PU	2.1633	-57.88	0.0944	86.73	17.509	2.2014	-58.08	0.0943	87.00	19.060
355 [INCO 138]	4	1	PU/PU	6.0546	-55.94	0.0031	82.65	7.750	0.5382	-56.72	0.4332	-94.27	13.386
									8.5930	-55.94	0.0057	81.41	6.616

362 [BRNTWD-D 138]	4 1	PU/PU	0.0000	0.00	0.0000	0.00	0.000	8.8330	-55.73	0.0215	-92.05	27.946
								0.0001	-59.25	0.0000	0.00	0.000
								0.0005	119.89	0.0000	0.00	0.000
		TO SHUNT (P.U.)	0.0000	0.00				0.7132	119.77			
								2.1396	119.77			
TOTAL FAULT CURRENT (P.U.)			8.2169	-56.45				11.5050	-56.61			

1.....

PSS/E SHORT CIRCUIT OUTPUT THU, AUG 03 1995 10:27 HOME BUS IS :

MANITOBA HYDRO SYSTEM - MIN.GEN (X'D) - FAMJ 95 05 08 358 [KELSEY D 138]

GRNWAY, HUSBAY, LUSINAP, GOULET, STVITAL, ROSSLAKE, DUNLOP, HERBELT

\*\*\* FAULTED BUS IS : 358 [KELSEY D 138] \*\*\* 0 LEVELS AWAY

1.....

AT BUS 358 [KELSEY D 138] AREA 4 (PU) V+: / 0.0000/ 0.00 (PU) VA: / 0.0000/ 0.00 V0: / 0.2222/ -152.11

V+: / 0.6554/ 27.10 V-: / 0.4332/ -153.31

THEV. R, X, X/R: POSITIVE 0.00880 0.13707 15.582 NEGATIVE 0.00791 0.12201 15.434 ZERO 0.00274 0.06265 22.834

FROM		AREA CKT		I/Z	T H R E E P H A S E F A U L T				O N E P H A S E F A U L T					
					/I+/ AN(I+)	/Z+/ AN(Z+)	APP X/R	/IA/ AN(IA)	/ZA/ AN(ZA)	APP X/R	/3I0/ AN(3I0)	/Z0/ AN(Z0)	APP X/R	
351	[RADISSON 138]	4	1	PU/PU	1.0149	-61.77	0.3376	84.95	11.318	1.0148	-59.65	0.4808	84.57	10.517
352	[KELSEY 138]	4	1	PU/PU	7.3007	-59.05	0.0000	0.00	0.000	0.4750	-51.49	0.1712	-92.01	28.507
TOTAL FAULT CURRENT (P.U.)					8.3146	-59.39				10.1594	-59.98	0.0656	-92.13	26.887
										10.6295	-59.60			

1.....

PSS/E SHORT CIRCUIT OUTPUT THU, AUG 03 1995 10:27 HOME BUS IS :

MANITOBA HYDRO SYSTEM - MIN.GEN (X'D) - FAMJ 95 05 08 360 [THOMPYS 138]

GRNWAY, HUSBAY, LUSINAP, GOULET, STVITAL, ROSSLAKE, DUNLOP, HERBELT

\*\*\* FAULTED BUS IS : 360 [THOMPYS 138] \*\*\* 0 LEVELS AWAY

1.....

AT BUS 360 [THOMPYS 138] AREA 4 (PU) V+: / 0.0000/ 0.00 (PU) VA: / 0.0000/ 0.00 V0: / 0.0874/ -152.98

V+: / 0.6296/ 24.94 V-: / 0.5422/ -155.40

THEV. R, X, X/R: POSITIVE 0.01672 0.16292 9.744 NEGATIVE 0.01610 0.15211 9.447 ZERO 0.00156 0.02462 15.803

FROM		AREA CKT		I/Z	T H R E E P H A S E F A U L T				O N E P H A S E F A U L T					
					/I+/ AN(I+)	/Z+/ AN(Z+)	APP X/R	/IA/ AN(IA)	/ZA/ AN(ZA)	APP X/R	/3I0/ AN(3I0)	/Z0/ AN(Z0)	APP X/R	
104	[THOMYSLK 230]	3	1	PU/PU	2.2084	-62.06	0.0944	86.73	17.509	2.2779	-62.16	0.0943	86.97	18.879
355	[INCO 138]	4	1	PU/PU	5.1845	-58.10	0.0031	82.65	7.750	0.4975	-59.47	0.4332	-94.27	13.386
										7.7030	-58.22	0.0058	81.17	6.438

362 [BRNTWD-D 138]	4 1	PU/PU	0.0000	0.00	0.0000	0.00	0.000	8.1648	-58.47	0.0215	-92.05	27.946
								0.0001	-63.55	0.0000	0.00	0.000
		TO SHUNT (P.U.)	0.0000	0.00				0.0004	117.10	0.0000	0.00	0.000
								0.6592	117.02			
								1.9777	117.02			
TOTAL FAULT CURRENT		(P.U.)	7.3892	-59.28				10.6347	-59.36			

# Appendix C

## FORTRAN Programs

---



**A. DEFINITION AND SUBROUTINE OF  
CONVENTION DISTANCE RELAY**

## PARAMETERS:

PMod "Phase Input Units:" "Radians;Degrees" 7 TOGGLE 1  
 K0m "Magnitude of Zero-Seq Factor K0" "" 10 REAL 1.0 0.0 1.0e3  
 K0ph "Phase of Zero-Seq Factor K0" "" 10 REAL 0.0 -360.0 360.0

## GRAPHICS:

```

BOX(-40,-72,40,40)
LINE(-64,-64,-40,-64) ARROW_R(-40,-64)
FTEXT(-56,-68,"Vm")
LINE(-64,-32,-40,-32) ARROW_R(-40,-32)
FTEXT(-56,-36,"Vph")
LINE(-64,0,-40,0) ARROW_R(-40,0)
FTEXT(-56,-4,"Im")
LINE(-64,32,-40,32) ARROW_R(-40,32)
FTEXT(-56,28,"Iph")
LINE(40,-64,64,-64) ARROW_L(40,-64)
FTEXT(56,-68,"I0m")
LINE(40,-32,64,-32) ARROW_L(40,-32)
FTEXT(56,-36,"I0ph")
LINE(40,0,64,0)
FTEXT(56,-4,"R")
LINE(40,32,64,32)
FTEXT(56,28,"X")
FTEXT(-23,-32,"Z =") FTEXT(10,-40,"U") FTEXT(10,-22,"I+k*I0")
LINE(-12,-32,30,-32)
FTEXT(2,0,"Input Phases")
If (PMod,1)
FTEXT(3,20,"in Degrees")
Else
FTEXT(3,20,"in Radians")
EndIf

```

## NODES:

VM	-2	-2	INPUT	REAL
VPH	-2	-1	INPUT	REAL
IM	-2	0	INPUT	REAL
IPH	-2	1	INPUT	REAL
I0M	2	-2	INPUT	REAL
I0PH	2	-1	INPUT	REAL
R	2	0	OUTPUT	REAL
X	2	1	OUTPUT	REAL

FORTRAN: DSD

```
C
C RELAY FUNCTION : Z=U/(I+k*I0)
C
#DEFINE REAL IO_PH
#DEFINE REAL IA_PH
#DEFINE REAL VA_PH
#DEFINE REAL I_REAL
#DEFINE REAL I_IMAG
#DEFINE REAL I_SQUAR
  IF((ABS($IM).LT.1E-6).AND.(ABS($I0M*$K0m).LT.1E-6)) THEN
    $R = 0.0
    $X = 0.0
  ELSE
    IO_PH = $I0PH+$K0ph
    IA_PH = $IPH
    VA_PH = $VPH
#IF PMod=1
    IO_PH = IO_PH*0.01745329
    IA_PH = IA_PH*0.01745329
    VA_PH = VA_PH*0.01745329
#END
    I_REAL = $IM*COS(IA_PH)+$K0m*$I0M*COS(IO_PH)
    I_IMAG = $IM*SIN(IA_PH)+$K0m*$I0M*SIN(IO_PH)
    I_SQUAR = I_REAL*I_REAL+I_IMAG*I_IMAG
    $R = ($VM*COS(VA_PH)*I_REAL+$VM*SIN(VA_PH)*I_IMAG)/I_SQUAR
    $X = ($VM*SIN(VA_PH)*I_REAL-$VM*COS(VA_PH)*I_IMAG)/I_SQUAR
  ENDIF
C
```

**B. DEFINITION AND SUBROUTINE OF ZERO SEQUENCE  
IMPEDANCE RELAY**

PARAMETERS:

PMOD "Phase Input Units:" "Radians;Degrees" 4 TOGGLE 0

GRAPHICS:

```

BOX(-40,-72,40,40)
LINE(-64,0,-40,0)  ARROW_R(-40,0)
LINE(-64,-32,-40,-32) ARROW_R(-40,-32)
LINE(-64,32,-40,32)  ARROW_R(-40,32)
LINE(-64,-64,-40,-64) ARROW_R(-40,-64)
LINE(40,-32,64,-32)  LINE(40,0,64,0)

FTEXT(-52,-36,"Vph") FTEXT(-52,-4,"Im")  FTEXT(-52,28,"Iph")
FTEXT(52,-36,"R")   FTEXT(52,-4,"X")
FTEXT(-52,-68,"Vm")

FTEXT(-15,-32,"Z =") FTEXT(10,-40,"U") FTEXT(10,-22,"I")
LINE(0,-32,20,-32)

FTEXT(2,0,"Input Phases")
If (PMOD,1)
FTEXT(3,20,"in Degrees")
Else
FTEXT(3,20,"in Radians")
EndIf

```

NODES:

VM	-2	-2	INPUT	REAL
VPH	-2	-1	INPUT	REAL
IM	-2	0	INPUT	REAL
IPH	-2	1	INPUT	REAL
R	2	-1	OUTPUT	REAL
X	2	0	OUTPUT	REAL

FORTRAN: DSD

```

C
C FUNDAMENTAL IMPEDANCE CALCULATION
C
#DEFINE REAL Z_MAG
#DEFINE REAL Z_PHA
  IF(ABS($IM).LT.1E-6) THEN
    $R = 0.0

```

---

```
$X = 0.0
ELSE
  Z_MAG = $VM/$IM
  Z_PHA = $VPH-$IPH
#IF PMod=1
  Z_PHA = Z_PHA*0.01745329
#END
  $R = Z_MAG*COS(Z_PHA)
  $X = Z_MAG*SIN(Z_PHA)
ENDIF
C
```

**C. INPUT PATTERN NORMALIZATION SUBROUTINE**

```
c
c
c =====
c
c UPDATE AT : April 17, 1995
c
c =====
c
c character c*90
c dimension xx1(700,11)
c
c -----
c Training data file
c -----
c
c open (7,file='train.yes')
c open (8,file='train.no')
c open (9,file='load.ex')
c open (10,file='train.ex')
c open (11,file='new_run15.case')
c open (17,file='new_run25.case')
c open (12,file='test.ex')
c open (13,file='validate.case')
c open (16,file='validate.ex')
c
c xplus=90.0
c xminus=-30.0
c yplus= 50.0
c yminus=-10.0
c zplus=138.0
c zminus=-34.0
c splus=619.0
c sminus=-642.0
c dplus=42.0
c dminus=-97.0
c
c
c iyes = 24*4
c ino = 44*4
c iload = 24
c
c read (7,100) ((xx1(i,j), j=1,11), i=1, iyes)
c read (8,100) ((xx1(i,j), j=1,11), i=iyes+1, iyes+ino)
```

```

read (9,150) c
read (9,150) c
100 read (9,100) ((xx1(i,j), j=1,11), i=iyes+ino+1, iyes+ino+iload)
150 format(f5.1,f7.3,3f9.3,5f10.4, f7.2)
c format(a90)

do 500 k=1,iyes+ino+iload,1
r=1.0-(xx1(k,6)-xplus)/(xminus-xplus)
x=1.0-(xx1(k,7)-yplus)/(yminus-yplus)
z=1.0-(xx1(k,8)-zplus)/(zminus-zplus)
w=1.0-(xx1(k,9)-splus)/(sminus-splus)
u=1.0-(xx1(k,10)-dplus)/(dminus-dplus)
200 write(10,200) r,x,z,w,u,xx1(k,11)
500 format(5f10.5, ' ', 'f7.2, ' ;')
c continue

read (11,100) ((xx1(i,j), j=1,11), i=1, 254)
c

do 600 k=1,254,1
r=1.0-(xx1(k,6)-xplus)/(xminus-xplus)
x=1.0-(xx1(k,7)-yplus)/(yminus-yplus)
z=1.0-(xx1(k,8)-zplus)/(zminus-zplus)
w=1.0-(xx1(k,9)-splus)/(sminus-splus)
u=1.0-(xx1(k,10)-dplus)/(dminus-dplus)
600 write(12,200) r,x,z,w,u,xx1(k,11)
c continue

read (17,100) ((xx1(i,j), j=1,11), i=1, 254)
c

do 650 k=1,254,1
r=1.0-(xx1(k,6)-xplus)/(xminus-xplus)
x=1.0-(xx1(k,7)-yplus)/(yminus-yplus)
z=1.0-(xx1(k,8)-zplus)/(zminus-zplus)
w=1.0-(xx1(k,9)-splus)/(sminus-splus)
u=1.0-(xx1(k,10)-dplus)/(dminus-dplus)
650 write(12,200) r,x,z,w,u,xx1(k,11)
c continue

read (13,100) ((xx1(i,j), j=1,11), i=1, 22)
c

do 700 k=1,22,1
r=1.0-(xx1(k,6)-xplus)/(xminus-xplus)
x=1.0-(xx1(k,7)-yplus)/(yminus-yplus)

```

---

```
z=1.0-(xx1(k,8)-zplus)/(zminus-zplus)
w=1.0-(xx1(k,9)-splus)/(sminus-splus)
u=1.0-(xx1(k,10)-dplus)/(dminus-dplus)
write(16,200) r,x,z,w,u,xx1(k,11)
700 continue
c
close (7)
close (8)
close (9)
close (10)
close (11)
close (12)
close (13)
close (14)
close (15)
close (16)
close (17)
c
stop
end
c
```

## **Appendix D**

# **Taining, Testing and Running Patterns**

---



**PART A : TRAINING, TESTING AND RUNNING PATTERNS  
FOR LINEAR ARCING FAULT RESISTANCE MODEL**

**TRAINING CASES**

$f = 1.06738$        $|g| = 0.0224386$   
error = 0.146159      cost = 0.921217

No.	$\delta$	$\alpha$	$R_F$	$X_{SI}$	$X_{RI}$	$R_I$	$X_I$	$X_{SO}$	$R_{mem}$	$X_{mem}$	Target	Output
1	-30.0	0.1	2.0	18.446	25.904	1.479	3.879	-23.884	184.094	2.611	1.0	1.000
2	-30.0	0.3	2.0	18.446	25.904	3.101	12.624	-23.883	184.050	2.649	1.0	1.000
3	-30.0	0.5	2.0	18.446	25.904	4.723	20.951	-23.883	184.009	2.629	1.0	1.000
4	-30.0	0.7	2.0	18.446	25.904	6.271	29.257	-23.883	184.094	2.626	1.0	1.000
5	-30.0	0.1	10.0	18.446	25.904	6.797	3.998	-23.850	184.094	2.611	1.0	1.000
6	-30.0	0.3	10.0	18.446	25.904	9.596	12.419	-23.852	184.050	2.649	1.0	1.000
7	-30.0	0.5	10.0	18.446	25.904	12.943	20.240	-23.853	184.009	2.629	1.0	1.000
8	-30.0	0.7	10.0	18.446	25.904	17.595	27.490	-23.849	184.094	2.626	1.0	1.000
9	-30.0	0.1	18.0	18.446	25.904	11.820	4.106	-23.848	184.094	2.611	1.0	0.969
10	-30.0	0.3	18.0	18.446	25.904	15.652	12.229	-23.851	184.050	2.649	1.0	0.997
11	-30.0	0.5	18.0	18.446	25.904	20.460	19.593	-23.849	184.009	2.629	1.0	0.999
12	-30.0	0.7	18.0	18.446	25.904	27.589	25.970	-23.851	184.094	2.626	1.0	0.959
13	-30.0	0.1	2.0	18.446	31.189	1.475	3.889	-23.883	194.369	3.205	1.0	1.000
14	-30.0	0.3	2.0	18.446	31.189	3.093	12.653	-23.882	194.359	3.195	1.0	1.000
15	-30.0	0.5	2.0	18.446	31.189	4.702	21.024	-23.880	194.209	3.229	1.0	1.000
16	-30.0	0.7	2.0	18.446	31.189	6.216	29.420	-23.875	194.372	3.215	1.0	1.000
17	-30.0	0.1	10.0	18.446	31.189	6.770	4.024	-23.850	194.369	3.205	1.0	1.000
18	-30.0	0.3	10.0	18.446	31.189	9.535	12.481	-23.853	194.359	3.195	1.0	1.000
19	-30.0	0.5	10.0	18.446	31.189	12.813	20.369	-23.853	194.209	3.229	1.0	1.000
20	-30.0	0.7	10.0	18.446	31.189	17.276	27.778	-23.853	194.372	3.215	1.0	1.000
21	-30.0	0.1	18.0	18.446	31.189	11.788	4.148	-23.847	194.369	3.205	1.0	0.975
22	-30.0	0.3	18.0	18.446	31.189	15.571	12.323	-23.851	194.359	3.195	1.0	0.998
23	-30.0	0.5	18.0	18.446	31.189	20.273	19.778	-23.848	194.209	3.229	1.0	1.000
24	-30.0	0.7	18.0	18.446	31.189	27.132	26.348	-23.849	194.372	3.215	1.0	0.986
25	-30.0	0.1	2.0	26.157	25.904	1.504	3.851	-23.885	198.103	-2.617	1.0	1.000
26	-30.0	0.3	2.0	26.157	25.904	3.156	12.570	-23.883	198.066	-2.602	1.0	1.000
27	-30.0	0.5	2.0	26.157	25.904	4.818	20.852	-23.883	198.066	-2.609	1.0	1.000
28	-30.0	0.7	2.0	26.157	25.904	6.415	29.093	-23.878	198.150	-2.611	1.0	1.000
29	-30.0	0.1	10.0	26.157	25.904	6.978	3.958	-23.851	198.103	-2.617	1.0	1.000

30	-30.0	0.3	10.0	26.157	25.904	9.864	12.356	-23.854	198.066	-2.602	1.0	1.000
31	-30.0	0.5	10.0	26.157	25.904	13.340	20.128	-23.853	198.066	-2.609	1.0	1.000
32	-30.0	0.7	10.0	26.157	25.904	18.223	27.285	-23.854	198.150	-2.611	1.0	1.000
33	-30.0	0.1	18.0	26.157	25.904	12.160	4.049	-23.852	198.103	-2.617	1.0	0.921
34	-30.0	0.3	18.0	26.157	25.904	16.137	12.147	-23.847	198.066	-2.602	1.0	0.971
35	-30.0	0.5	18.0	26.157	25.904	21.162	19.454	-23.850	198.066	-2.609	1.0	0.992
36	-30.0	0.7	18.0	26.157	25.904	28.685	25.694	-23.849	198.150	-2.611	1.0	0.869
37	-30.0	0.1	2.0	26.157	31.189	1.499	3.862	-23.885	208.259	-2.073	1.0	1.000
38	-30.0	0.3	2.0	26.157	31.189	3.143	12.601	-23.886	208.259	-2.016	1.0	1.000
39	-30.0	0.5	2.0	26.157	31.189	4.790	20.929	-23.883	208.244	-2.017	1.0	1.000
40	-30.0	0.7	2.0	26.157	31.189	6.346	29.265	-23.883	208.256	-2.044	1.0	1.000
41	-30.0	0.1	10.0	26.157	31.189	6.942	3.984	-23.853	208.259	-2.073	1.0	1.000
42	-30.0	0.3	10.0	26.157	31.189	9.788	12.416	-23.850	208.259	-2.016	1.0	1.000
43	-30.0	0.5	10.0	26.157	31.189	13.186	20.260	-23.854	208.244	-2.017	1.0	1.000
44	-30.0	0.7	10.0	26.157	31.189	17.861	27.568	-23.854	208.256	-2.044	1.0	1.000
45	-30.0	0.1	18.0	26.157	31.189	12.110	4.090	-23.849	208.259	-2.073	1.0	0.941
46	-30.0	0.3	18.0	26.157	31.189	16.030	12.237	-23.851	208.259	-2.016	1.0	0.987
47	-30.0	0.5	18.0	26.157	31.189	20.934	19.634	-23.848	208.244	-2.017	1.0	0.998
48	-30.0	0.7	18.0	26.157	31.189	28.160	26.066	-23.852	208.256	-2.044	1.0	0.970
49	-10.0	0.1	2.0	18.446	25.904	1.545	3.928	-23.881	545.794	-76.507	1.0	1.000
50	-10.0	0.3	2.0	18.446	25.904	3.297	12.755	-23.878	545.825	-76.502	1.0	1.000
51	-10.0	0.5	2.0	18.446	25.904	5.164	21.202	-23.878	545.803	-76.484	1.0	1.000
52	-10.0	0.7	2.0	18.446	25.904	7.059	29.673	-23.873	545.922	-76.452	1.0	1.000
53	-10.0	0.1	10.0	18.446	25.904	7.040	4.340	-23.850	545.794	-76.507	1.0	1.000
54	-10.0	0.3	10.0	18.446	25.904	10.116	13.102	-23.852	545.825	-76.502	1.0	1.000
55	-10.0	0.5	10.0	18.446	25.904	13.961	21.413	-23.856	545.803	-76.484	1.0	1.000
56	-10.0	0.7	10.0	18.446	25.904	19.513	29.470	-23.853	545.922	-76.452	1.0	1.000
57	-10.0	0.1	18.0	18.446	25.904	12.437	4.725	-23.850	545.794	-76.507	1.0	0.995
58	-10.0	0.3	18.0	18.446	25.904	16.785	13.418	-23.847	545.825	-76.502	1.0	0.987
59	-10.0	0.5	18.0	18.446	25.904	22.509	21.575	-23.850	545.803	-76.484	1.0	0.994
60	-10.0	0.7	18.0	18.446	25.904	31.459	29.209	-23.853	545.922	-76.452	1.0	0.998
61	-10.0	0.1	2.0	18.446	31.189	1.538	3.935	-23.881	574.122	-85.346	1.0	1.000
62	-10.0	0.3	2.0	18.446	31.189	3.277	12.776	-23.878	574.153	-85.351	1.0	1.000
63	-10.0	0.5	2.0	18.446	31.189	5.116	21.259	-23.877	573.912	-85.288	1.0	1.000
64	-10.0	0.7	2.0	18.446	31.189	6.946	29.808	-23.876	574.569	-85.359	1.0	1.000
65	-10.0	0.1	10.0	18.446	31.189	7.000	4.347	-23.851	574.122	-85.346	1.0	1.000
66	-10.0	0.3	10.0	18.446	31.189	10.026	13.127	-23.852	574.153	-85.351	1.0	1.000
67	-10.0	0.5	10.0	18.446	31.189	13.766	21.472	-23.853	573.912	-85.288	1.0	1.000
68	-10.0	0.7	10.0	18.446	31.189	19.049	29.618	-23.847	574.569	-85.359	1.0	1.000
69	-10.0	0.1	18.0	18.446	31.189	12.370	4.734	-23.850	574.122	-85.346	1.0	0.997

---

70	-10.0	0.3	18.0	18.446	31.189	16.639	13.446	-23.849	574.153	-85.351	1.0	0.991
71	-10.0	0.5	18.0	18.446	31.189	22.191	21.645	-23.852	573.912	-85.288	1.0	0.995
72	-10.0	0.7	18.0	18.446	31.189	19.049	29.618	-23.847	574.569	-85.359	1.0	1.000
73	-10.0	0.1	2.0	26.157	25.904	1.573	3.907	-23.881	588.541	-86.282	1.0	1.000
74	-10.0	0.3	2.0	26.157	25.904	3.353	12.714	-23.878	588.641	-86.296	1.0	1.000
75	-10.0	0.5	2.0	26.157	25.904	5.259	21.128	-23.876	588.534	-86.084	1.0	1.000
76	-10.0	0.7	2.0	26.157	25.904	7.204	29.548	-23.874	588.450	-86.598	1.0	1.000
77	-10.0	0.1	10.0	26.157	25.904	7.210	4.339	-23.852	588.541	-86.282	1.0	1.000
78	-10.0	0.3	10.0	26.157	25.904	10.363	13.089	-23.852	588.641	-86.296	1.0	1.000
79	-10.0	0.5	10.0	26.157	25.904	14.327	21.373	-23.856	588.534	-86.084	1.0	1.000
80	-10.0	0.7	10.0	26.157	25.904	20.108	29.377	-23.848	588.450	-86.598	1.0	1.000
81	-10.0	0.1	18.0	26.157	25.904	12.750	4.743	-23.852	588.541	-86.282	1.0	0.990
82	-10.0	0.3	18.0	26.157	25.904	17.229	13.435	-23.851	588.641	-86.296	1.0	0.952
83	-10.0	0.5	18.0	26.157	25.904	23.148	21.573	-23.850	588.534	-86.084	1.0	0.972
84	-10.0	0.7	18.0	26.157	25.904	32.502	29.149	-23.854	588.450	-86.598	1.0	0.961
85	-10.0	0.1	2.0	26.157	31.189	1.565	3.915	-23.882	616.966	-95.674	1.0	1.000
86	-10.0	0.3	2.0	26.157	31.189	3.331	12.737	-23.881	617.219	-95.706	1.0	1.000
87	-10.0	0.5	2.0	26.157	31.189	5.206	21.185	-23.876	616.969	-95.614	1.0	1.000
88	-10.0	0.7	2.0	26.157	31.189	7.086	29.682	-23.871	617.478	-95.867	1.0	1.000
89	-10.0	0.1	10.0	26.157	31.189	7.163	4.345	-23.852	616.966	-95.674	1.0	1.000
90	-10.0	0.3	10.0	26.157	31.189	10.263	13.111	-23.852	617.219	-95.706	1.0	1.000
91	-10.0	0.5	10.0	26.157	31.189	14.116	21.430	-23.852	616.969	-95.614	1.0	1.000
92	-10.0	0.7	10.0	26.157	31.189	19.614	29.531	-23.853	617.478	-95.867	1.0	0.993
93	-10.0	0.1	18.0	26.157	31.189	12.670	4.749	-23.852	616.966	-95.674	1.0	0.993
94	-10.0	0.3	18.0	26.157	31.189	17.062	13.457	-23.848	617.219	-95.706	1.0	0.967
95	-10.0	0.5	18.0	26.157	31.189	22.804	21.634	-23.852	616.969	-95.614	1.0	0.974
96	-10.0	0.7	18.0	26.157	31.189	31.685	29.311	-23.847	617.478	-95.867	1.0	0.930
97	10.0	0.1	2.0	18.446	25.904	1.595	3.991	-23.877	-564.837	26.397	1.0	1.000
98	10.0	0.3	2.0	18.446	25.904	3.450	12.930	-23.872	-564.153	26.606	1.0	1.000
99	10.0	0.5	2.0	18.446	25.904	5.524	21.557	-23.870	-564.463	26.686	1.0	1.000
100	10.0	0.7	2.0	18.446	25.904	7.719	30.283	-23.866	-564.403	26.756	1.0	1.000
101	10.0	0.1	10.0	18.446	25.904	7.188	4.745	-23.850	-564.837	26.397	1.0	1.000
102	10.0	0.3	10.0	18.446	25.904	10.453	13.936	-23.852	-564.153	26.606	1.0	1.000
103	10.0	0.5	10.0	18.446	25.904	14.688	22.903	-23.853	-564.463	26.686	1.0	1.000
104	10.0	0.7	10.0	18.446	25.904	21.011	32.136	-23.856	-564.403	26.756	1.0	1.000
105	10.0	0.1	18.0	18.446	25.904	12.895	5.537	-23.852	-564.837	26.397	1.0	0.990
106	10.0	0.3	18.0	18.446	25.904	17.641	15.007	-23.851	-564.153	26.606	1.0	0.982
107	10.0	0.5	18.0	18.446	25.904	24.170	24.358	-23.852	-564.463	26.686	1.0	0.976
108	10.0	0.7	18.0	18.446	25.904	34.958	34.181	-23.847	-564.403	26.756	1.0	0.976
109	10.0	0.1	2.0	18.446	31.189	1.586	3.995	-23.877	-595.859	24.216	1.0	1.000

110	10.0	0.3	2.0	18.446	31.189	3.422	12.940	-23.874	-595.594	24.403	1.0	1.000
111	10.0	0.5	2.0	18.446	31.189	5.454	21.592	-23.871	-595.491	24.278	1.0	1.000
112	10.0	0.7	2.0	18.446	31.189	7.559	30.372	-23.865	-595.638	24.240	1.0	1.000
113	10.0	0.1	10.0	18.446	31.189	7.139	4.730	-23.849	-595.859	24.216	1.0	1.000
114	10.0	0.3	10.0	18.446	31.189	10.339	13.911	-23.852	-595.594	24.403	1.0	1.000
115	10.0	0.5	10.0	18.446	31.189	14.437	22.868	-23.851	-595.491	24.278	1.0	1.000
116	10.0	0.7	10.0	18.446	31.189	20.401	32.088	-23.855	-595.638	24.240	1.0	1.000
117	10.0	0.1	18.0	18.446	31.189	12.799	5.502	-23.851	-595.859	24.216	1.0	0.991
118	10.0	0.3	18.0	18.446	31.189	17.432	14.941	-23.852	-595.594	24.403	1.0	0.987
119	10.0	0.5	18.0	18.446	31.189	23.713	24.243	-23.852	-595.491	24.278	1.0	0.989
120	10.0	0.7	18.0	18.446	31.189	33.827	33.968	-23.844	-595.638	24.240	1.0	0.994
121	10.0	0.1	2.0	26.157	25.904	1.626	3.976	-23.877	-609.963	22.969	1.0	1.000
122	10.0	0.3	2.0	26.157	25.904	3.510	12.897	-23.872	-609.600	22.683	1.0	1.000
123	10.0	0.5	2.0	26.157	25.904	5.623	21.492	-23.869	-609.769	22.956	1.0	1.000
124	10.0	0.7	2.0	26.157	25.904	7.876	30.175	-23.869	-610.000	22.804	1.0	1.000
125	10.0	0.1	10.0	26.157	25.904	7.349	4.773	-23.851	-609.963	22.969	1.0	1.000
126	10.0	0.3	10.0	26.157	25.904	10.688	13.955	-23.853	-609.600	22.683	1.0	1.000
127	10.0	0.5	10.0	26.157	25.904	15.038	22.900	-23.849	-609.769	22.956	1.0	1.000
128	10.0	0.7	10.0	26.157	25.904	21.586	32.103	-23.852	-610.000	22.804	1.0	1.000
129	10.0	0.1	18.0	26.157	25.904	13.182	5.607	-23.850	-609.963	22.969	1.0	0.973
130	10.0	0.3	18.0	26.157	25.904	18.049	15.077	-23.852	-609.600	22.683	1.0	0.957
131	10.0	0.5	18.0	26.157	25.904	24.764	24.416	-23.853	-609.769	22.956	1.0	0.963
132	10.0	0.7	18.0	26.157	25.904	35.947	34.225	-23.845	-610.000	22.804	1.0	0.915
133	10.0	0.1	2.0	26.157	31.189	1.616	3.980	-23.876	-640.997	19.435	1.0	1.000
134	10.0	0.3	2.0	26.157	31.189	3.480	12.910	-23.873	-641.053	19.574	1.0	1.000
135	10.0	0.5	2.0	26.157	31.189	5.549	21.529	-23.870	-640.734	19.683	1.0	1.000
136	10.0	0.7	2.0	26.157	31.189	7.710	30.272	-23.872	-640.650	19.792	1.0	1.000
137	10.0	0.1	10.0	26.157	31.189	7.293	4.758	-23.851	-640.997	19.435	1.0	1.000
138	10.0	0.3	10.0	26.157	31.189	10.566	13.929	-23.852	-641.053	19.574	1.0	1.000
139	10.0	0.5	10.0	26.157	31.189	14.775	22.870	-23.852	-640.734	19.683	1.0	1.000
140	10.0	0.7	10.0	26.157	31.189	20.955	32.069	-23.854	-640.650	19.792	1.0	1.000
141	10.0	0.1	18.0	26.157	31.189	13.075	5.570	-23.849	-640.997	19.435	1.0	0.975
142	10.0	0.3	18.0	26.157	31.189	17.824	15.008	-23.853	-641.053	19.574	1.0	0.976
143	10.0	0.5	18.0	26.157	31.189	24.286	24.305	-23.853	-640.734	19.683	1.0	0.984
144	10.0	0.7	18.0	26.157	31.189	34.781	34.030	-23.847	-640.650	19.792	1.0	0.981
145	30.0	0.1	2.0	18.446	25.904	1.627	4.067	-23.872	-181.209	37.412	1.0	1.000
146	30.0	0.3	2.0	18.446	25.904	3.554	13.145	-23.868	-181.125	37.392	1.0	1.000
147	30.0	0.5	2.0	18.446	25.904	5.788	22.007	-23.865	-181.038	37.342	1.0	1.000
148	30.0	0.7	2.0	18.446	25.904	8.215	31.076	-23.859	-181.103	37.381	1.0	1.000
149	30.0	0.1	10.0	18.446	25.904	7.221	5.199	-23.852	-181.209	37.412	1.0	1.000

150	30.0	0.3	10.0	18.446	25.904	10.553	14.894	-23.851	-181.125	37.392	1.0	1.000
151	30.0	0.5	10.0	18.446	25.904	14.996	24.702	-23.853	-181.038	37.342	1.0	1.000
152	30.0	0.7	10.0	18.446	25.904	21.765	35.535	-23.849	-181.103	37.381	1.0	1.000
153	30.0	0.1	18.0	18.446	25.904	13.120	6.537	-23.851	-181.209	37.412	1.0	0.973
154	30.0	0.3	18.0	18.446	25.904	18.035	17.001	-23.850	-181.125	37.392	1.0	0.999
155	30.0	0.5	18.0	18.446	25.904	25.044	28.056	-23.852	-181.038	37.342	1.0	0.926
156	30.0	0.7	18.0	18.446	25.904	37.131	41.510	-23.846	-181.103	37.381	1.0	0.948
157	30.0	0.1	2.0	18.446	31.189	1.616	4.066	-23.872	-191.269	40.226	1.0	1.000
158	30.0	0.3	2.0	18.446	31.189	3.518	13.142	-23.868	-191.175	40.208	1.0	1.000
159	30.0	0.5	2.0	18.446	31.189	5.696	22.014	-23.865	-191.087	40.179	1.0	1.000
160	30.0	0.7	2.0	18.446	31.189	8.010	31.110	-23.861	-191.150	40.179	1.0	1.000
161	30.0	0.1	10.0	18.446	31.189	7.166	5.158	-23.850	-191.269	40.226	1.0	1.000
162	30.0	0.3	10.0	18.446	31.189	10.426	14.809	-23.850	-191.175	40.208	1.0	1.000
163	30.0	0.5	10.0	18.446	31.189	14.704	24.540	-23.850	-191.087	40.179	1.0	1.000
164	30.0	0.7	10.0	18.446	31.189	21.040	35.196	-23.848	-191.150	40.179	1.0	1.000
165	30.0	0.1	18.0	18.446	31.189	13.000	6.440	-23.851	-191.269	40.226	1.0	0.984
166	30.0	0.3	18.0	18.446	31.189	17.782	16.798	-23.849	-191.175	40.208	1.0	0.999
167	30.0	0.5	18.0	18.446	31.189	24.475	27.652	-23.848	-191.087	40.179	1.0	0.947
168	30.0	0.7	18.0	18.446	31.189	35.669	40.581	-23.853	-191.150	40.179	1.0	0.988
169	30.0	0.1	2.0	26.157	25.904	1.663	4.057	-23.872	-195.950	34.294	1.0	1.000
170	30.0	0.3	2.0	26.157	25.904	3.622	13.117	-23.869	-195.853	34.220	1.0	1.000
171	30.0	0.5	2.0	26.157	25.904	5.902	21.948	-23.863	-195.803	34.225	1.0	1.000
172	30.0	0.7	2.0	26.157	25.904	8.397	30.974	-23.860	-195.847	34.199	1.0	1.000
173	30.0	0.1	10.0	26.157	25.904	7.380	5.253	-23.851	-195.950	34.294	1.0	1.000
174	30.0	0.3	10.0	26.157	25.904	10.798	14.938	-23.853	-195.853	34.220	1.0	1.000
175	30.0	0.5	10.0	26.157	25.904	15.373	24.722	-23.853	-195.803	34.225	1.0	1.000
176	30.0	0.7	10.0	26.157	25.904	22.404	35.540	-23.850	-195.847	34.199	1.0	1.000
177	30.0	0.1	18.0	26.157	25.904	13.398	6.644	-23.852	-195.950	34.294	1.0	0.938
178	30.0	0.3	18.0	26.157	25.904	18.452	17.098	-23.850	-195.853	34.220	1.0	0.998
179	30.0	0.5	18.0	26.157	25.904	25.681	28.122	-23.851	-195.803	34.225	1.0	0.906
180	30.0	0.7	18.0	26.157	25.904	38.244	41.554	-23.851	-195.847	34.199	1.0	0.877
181	30.0	0.1	2.0	26.157	31.189	1.650	4.057	-23.873	-206.022	36.999	1.0	1.000
182	30.0	0.3	2.0	26.157	31.189	3.583	13.119	-23.867	-205.894	36.930	1.0	1.000
183	30.0	0.5	2.0	26.157	31.189	5.807	21.959	-23.863	-205.772	37.007	1.0	1.000
184	30.0	0.7	2.0	26.157	31.189	8.185	31.018	-23.859	-205.828	36.965	1.0	1.000
185	30.0	0.1	10.0	26.157	31.189	7.318	5.213	-23.849	-206.022	36.999	1.0	1.000
186	30.0	0.3	10.0	26.157	31.189	10.660	14.858	-23.851	-205.894	36.930	1.0	1.000
187	30.0	0.5	10.0	26.157	31.189	15.064	24.574	-23.853	-205.772	37.007	1.0	1.000
188	30.0	0.7	10.0	26.157	31.189	21.645	35.233	-23.854	-205.828	36.965	1.0	1.000
189	30.0	0.1	18.0	26.157	31.189	13.268	6.549	-23.850	-206.022	36.999	1.0	0.964

190	30.0	0.3	18.0	26.157	31.189	18.179	16.907	-23.850	-205.894	36.930	1.0	0.998
191	30.0	0.5	18.0	26.157	31.189	25.083	27.742	-23.847	-205.772	37.007	1.0	0.935
192	30.0	0.7	18.0	26.157	31.189	36.718	40.676	-23.847	-205.828	36.965	1.0	0.974
193	-30.0	0.9	2.0	18.446	25.904	9.513	38.419	-23.869	184.147	2.622	0.0	0.001
194	-30.0	1.0	2.0	18.446	25.904	12.895	43.634	-23.863	184.481	2.629	0.0	0.000
195	-30.0	0.9	10.0	18.446	25.904	28.503	33.013	-23.845	184.147	2.622	0.0	0.056
196	-30.0	1.0	10.0	18.446	25.904	39.804	34.461	-23.848	184.481	2.629	0.0	0.000
197	-30.0	0.9	18.0	18.446	25.904	43.822	28.970	-23.856	184.147	2.622	0.0	0.000
198	-30.0	1.0	18.0	18.446	25.904	59.496	28.459	-23.856	184.481	2.629	0.0	0.000
199	-30.0	0.1	22.0	18.446	25.904	14.228	4.155	-23.853	184.094	2.611	0.0	0.059
200	-30.0	0.3	22.0	18.446	25.904	18.527	12.138	-23.850	184.050	2.649	0.0	0.006
201	-30.0	0.5	22.0	18.446	25.904	23.975	19.288	-23.847	184.009	2.629	0.0	0.021
202	-30.0	0.7	22.0	18.446	25.904	32.156	25.279	-23.857	184.094	2.626	0.0	0.001
203	-30.0	0.9	22.0	18.446	25.904	50.408	27.298	-23.857	184.147	2.622	0.0	0.000
204	-30.0	0.1	30.0	18.446	25.904	18.840	4.244	-23.850	184.094	2.611	0.0	0.000
205	-30.0	0.5	30.0	18.446	25.904	30.575	18.709	-23.846	184.009	2.629	0.0	0.000
206	-30.0	0.9	30.0	18.446	25.904	61.894	24.502	-23.868	184.147	2.622	0.0	0.000
207	-30.0	-0.1	2.0	18.446	25.904	-10.087	-7.150	137.959	184.469	2.634	0.0	0.000
208	-30.0	-0.1	10.0	18.446	25.904	-59.002	-26.945	137.934	184.469	2.634	0.0	0.000
209	-30.0	-0.1	18.0	18.446	25.904	-133.519	-75.091	137.959	184.469	2.634	0.0	0.000
210	-30.0	0.9	2.0	18.446	31.189	9.234	38.822	-23.881	194.400	3.253	0.0	0.000
211	-30.0	1.0	2.0	18.446	31.189	12.134	44.265	-23.866	194.684	3.275	0.0	0.000
212	-30.0	0.9	10.0	18.446	31.189	27.343	33.847	-23.856	194.400	3.253	0.0	0.058
213	-30.0	1.0	10.0	18.446	31.189	37.163	36.042	-23.847	194.684	3.275	0.0	0.000
214	-30.0	0.9	18.0	18.446	31.189	42.271	30.037	-23.846	194.400	3.253	0.0	0.000
215	-30.0	1.0	18.0	18.446	31.189	56.230	30.401	-23.844	194.684	3.275	0.0	0.000
216	-30.0	0.1	22.0	18.446	31.189	14.196	4.205	-23.849	194.369	3.205	0.0	0.079
217	-30.0	0.3	22.0	18.446	31.189	18.444	12.244	-23.847	194.359	3.195	0.0	0.012
218	-30.0	0.5	22.0	18.446	31.189	23.781	19.498	-23.852	194.209	3.229	0.0	0.069
219	-30.0	0.7	22.0	18.446	31.189	31.658	25.695	-23.845	194.372	3.215	0.0	0.003
220	-30.0	0.9	22.0	18.446	31.189	48.785	28.440	-23.846	194.400	3.253	0.0	0.000
221	-30.0	0.1	30.0	18.446	31.189	18.830	4.310	-23.852	194.369	3.205	0.0	0.000
222	-30.0	0.5	30.0	18.446	31.189	30.388	18.967	-23.853	194.209	3.229	0.0	0.000
223	-30.0	0.9	30.0	18.446	31.189	60.288	25.729	-23.871	194.400	3.253	0.0	0.000
224	-30.0	-0.1	2.0	18.446	31.189	-10.418	-7.158	137.947	194.675	3.227	0.0	0.000
225	-30.0	-0.1	10.0	18.446	31.189	-60.875	-26.920	137.922	194.675	3.227	0.0	0.000
226	-30.0	-0.1	18.0	18.446	31.189	-137.591	-74.042	137.928	194.675	3.227	0.0	0.022
227	-30.0	0.9	2.0	26.157	25.904	9.803	38.157	-23.865	198.203	-2.598	0.0	0.000
228	-30.0	1.0	2.0	26.157	25.904	13.435	43.273	-23.863	198.500	-2.543	0.0	0.000
229	-30.0	0.9	10.0	26.157	25.904	29.864	32.420	-23.846	198.203	-2.598	0.0	0.062

230 -30.0	1.0	10.0	26.157	25.904	42.188	33.307	-23.855	198.500	-2.543	0.0	0.000
231 -30.0	0.9	18.0	26.157	25.904	46.104	28.061	-23.846	198.203	-2.598	0.0	0.000
232 -30.0	1.0	18.0	26.157	25.904	63.281	26.727	-23.844	198.500	-2.543	0.0	0.000
233 -30.0	0.1	22.0	26.157	25.904	14.648	4.087	-23.851	198.103	-2.617	0.0	0.017
234 -30.0	0.3	22.0	26.157	25.904	19.122	12.039	-23.849	198.066	-2.602	0.0	0.001
235 -30.0	0.5	22.0	26.157	25.904	24.833	19.133	-23.854	198.066	-2.609	0.0	0.001
236 -30.0	0.7	22.0	26.157	25.904	33.478	24.962	-23.855	198.150	-2.611	0.0	0.000
237 -30.0	0.9	22.0	26.157	25.904	53.114	26.255	-23.855	198.203	-2.598	0.0	0.000
238 -30.0	0.1	30.0	26.157	25.904	19.430	4.151	-23.853	198.103	-2.617	0.0	0.000
239 -30.0	0.5	30.0	26.157	25.904	31.728	18.506	-23.847	198.066	-2.609	0.0	0.000
240 -30.0	0.9	30.0	26.157	25.904	65.347	23.193	-23.844	198.203	-2.598	0.0	0.000
241 -30.0	-0.1	2.0	26.157	25.904	-8.426	-6.672	137.978	198.541	-2.609	0.0	0.000
242 -30.0	-0.1	10.0	26.157	25.904	-46.430	-20.881	137.916	198.541	-2.609	0.0	0.000
243 -30.0	-0.1	18.0	26.157	25.904	-98.374	-48.717	137.944	198.541	-2.609	0.0	0.000
244 -30.0	0.9	2.0	26.157	31.189	9.495	38.572	-23.875	208.400	-2.063	0.0	0.000
245 -30.0	1.0	2.0	26.157	31.189	12.604	43.942	-23.859	208.713	-2.003	0.0	0.000
246 -30.0	0.9	10.0	26.157	31.189	28.578	33.281	-23.853	208.400	-2.063	0.0	0.069
247 -30.0	1.0	10.0	26.157	31.189	39.260	34.996	-23.842	208.713	-2.003	0.0	0.000
248 -30.0	0.9	18.0	26.157	31.189	44.378	29.167	-23.863	208.400	-2.063	0.0	0.000
249 -30.0	1.0	18.0	26.157	31.189	59.616	28.807	-23.840	208.713	-2.003	0.0	0.000
250 -30.0	0.1	22.0	26.157	31.189	14.596	4.136	-23.849	208.259	-2.073	0.0	0.025
251 -30.0	0.3	22.0	26.157	31.189	19.007	12.146	-23.851	208.259	-2.016	0.0	0.001
252 -30.0	0.5	22.0	26.157	31.189	24.584	19.335	-23.850	208.244	-2.017	0.0	0.004
253 -30.0	0.7	22.0	26.157	31.189	32.904	25.378	-23.852	208.256	-2.044	0.0	0.000
254 -30.0	0.9	22.0	26.157	31.189	51.275	27.433	-23.850	208.400	-2.063	0.0	0.000
255 -30.0	0.1	30.0	26.157	31.189	19.381	4.217	-23.851	208.259	-2.073	0.0	0.000
256 -30.0	0.5	30.0	26.157	31.189	31.477	18.756	-23.855	208.244	-2.017	0.0	0.000
257 -30.0	0.9	30.0	26.157	31.189	63.483	24.471	-23.860	208.400	-2.063	0.0	0.000
258 -30.0	-0.1	2.0	26.157	31.189	-8.705	-6.707	137.984	208.728	-2.067	0.0	0.000
259 -30.0	-0.1	10.0	26.157	31.189	-47.964	-21.119	137.903	208.728	-2.067	0.0	0.000
260 -30.0	-0.1	18.0	26.157	31.189	-101.488	-49.036	137.947	208.728	-2.067	0.0	0.000
261 -10.0	0.9	2.0	18.446	25.904	10.691	39.445	-23.868	546.028	-76.202	0.0	0.000
262 -10.0	1.0	2.0	18.446	25.904	14.308	45.539	-23.860	547.228	-76.739	0.0	0.000
263 -10.0	0.9	10.0	18.446	25.904	33.189	37.083	-23.843	546.028	-76.202	0.0	0.046
264 -10.0	1.0	10.0	18.446	25.904	48.545	40.998	-23.848	547.228	-76.739	0.0	0.000
265 -10.0	0.9	18.0	18.446	25.904	53.951	34.762	-23.860	546.028	-76.202	0.0	0.000
266 -10.0	1.0	18.0	18.446	25.904	78.723	36.663	-23.846	547.228	-76.739	0.0	0.000
267 -10.0	0.1	22.0	18.446	25.904	15.096	4.905	-23.851	545.794	-76.507	0.0	0.030
268 -10.0	0.3	22.0	18.446	25.904	20.062	13.563	-23.848	545.825	-76.502	0.0	0.002
269 -10.0	0.5	22.0	18.446	25.904	26.684	21.635	-23.847	545.803	-76.484	0.0	0.036

---

270	-10.0	0.7	22.0	18.446	25.904	37.236	29.038	-23.846	545.922	-76.452	0.0	0.011
271	-10.0	0.9	22.0	18.446	25.904	63.712	33.605	-23.856	546.028	-76.202	0.0	0.000
272	-10.0	0.1	30.0	18.446	25.904	20.340	5.246	-23.852	545.794	-76.507	0.0	0.000
273	-10.0	0.5	30.0	18.446	25.904	34.852	21.719	-23.852	545.803	-76.484	0.0	0.000
274	-10.0	0.9	30.0	18.446	25.904	82.136	31.297	-23.852	546.028	-76.202	0.0	0.000
275	-10.0	-0.1	2.0	18.446	25.904	-9.978	-4.740	137.953	547.809	-76.982	0.0	0.000
276	-10.0	-0.1	10.0	18.446	25.904	-51.618	-7.853	137.913	547.809	-76.982	0.0	0.000
277	-10.0	-0.1	18.0	18.446	25.904	-99.667	-12.899	137.900	547.809	-76.982	0.0	0.005
278	-10.0	0.9	2.0	18.446	31.189	10.290	39.740	-23.867	574.978	-85.567	0.0	0.001
279	-10.0	1.0	2.0	18.446	31.189	13.329	45.916	-23.866	575.350	-85.711	0.0	0.000
280	-10.0	0.9	10.0	18.446	31.189	31.466	37.602	-23.849	574.978	-85.567	0.0	0.009
281	-10.0	1.0	10.0	18.446	31.189	44.395	41.982	-23.838	575.350	-85.711	0.0	0.000
282	-10.0	0.9	18.0	18.446	31.189	51.177	35.472	-23.838	574.978	-85.567	0.0	0.000
283	-10.0	1.0	18.0	18.446	31.189	72.290	38.177	-23.846	575.350	-85.711	0.0	0.000
284	-10.0	0.1	22.0	18.446	31.189	15.019	4.916	-23.849	574.122	-85.346	0.0	0.038
285	-10.0	0.3	22.0	18.446	31.189	19.892	13.591	-23.851	574.153	-85.351	0.0	0.005
286	-10.0	0.5	22.0	18.446	31.189	26.312	21.708	-23.847	573.912	-85.288	0.0	0.089
287	-10.0	0.7	22.0	18.446	31.189	36.350	29.230	-23.854	574.569	-85.359	0.0	0.046
288	-10.0	0.9	22.0	18.446	31.189	60.518	34.414	-23.847	574.978	-85.567	0.0	0.000
289	-10.0	0.1	30.0	18.446	31.189	20.243	5.260	-23.850	574.122	-85.346	0.0	0.000
290	-10.0	0.5	30.0	18.446	31.189	34.384	21.802	-23.848	573.912	-85.288	0.0	0.000
291	-10.0	0.9	30.0	18.446	31.189	78.243	32.290	-23.855	574.978	-85.567	0.0	0.000
292	-10.0	-0.1	2.0	18.446	31.189	-10.271	-4.707	137.956	575.828	-85.950	0.0	0.000
293	-10.0	-0.1	10.0	18.446	31.189	-53.129	-7.793	137.938	575.828	-85.950	0.0	0.000
294	-10.0	-0.1	18.0	18.446	31.189	-102.428	-12.823	137.938	575.828	-85.950	0.0	0.000
295	-10.0	0.9	2.0	26.157	25.904	11.017	39.258	-23.872	588.772	-86.507	0.0	0.004
296	-10.0	1.0	2.0	26.157	25.904	14.943	45.340	-23.865	590.028	-86.702	0.0	0.000
297	-10.0	0.9	10.0	26.157	25.904	34.654	36.802	-23.854	588.772	-86.507	0.0	0.032
298	-10.0	1.0	10.0	26.157	25.904	51.441	40.460	-23.840	590.028	-86.702	0.0	0.000
299	-10.0	0.9	18.0	26.157	25.904	56.499	34.370	-23.845	588.772	-86.507	0.0	0.000
300	-10.0	1.0	18.0	26.157	25.904	83.662	35.837	-23.849	590.028	-86.702	0.0	0.000
301	-10.0	0.1	22.0	26.157	25.904	15.483	4.933	-23.851	588.541	-86.282	0.0	0.010
302	-10.0	0.3	22.0	26.157	25.904	20.604	13.589	-23.853	588.641	-86.296	0.0	0.001
303	-10.0	0.5	22.0	26.157	25.904	27.466	21.647	-23.850	588.534	-86.084	0.0	0.006
304	-10.0	0.7	22.0	26.157	25.904	38.506	28.999	-23.847	588.450	-86.598	0.0	0.000
305	-10.0	0.9	22.0	26.157	25.904	66.797	33.164	-23.846	588.772	-86.507	0.0	0.000
306	-10.0	0.1	30.0	26.157	25.904	20.875	5.293	-23.849	588.541	-86.282	0.0	0.000
307	-10.0	0.5	30.0	26.157	25.904	35.915	21.763	-23.853	588.534	-86.084	0.0	0.000
308	-10.0	0.9	30.0	26.157	25.904	86.257	30.768	-23.846	588.772	-86.507	0.0	0.000
309	-10.0	-0.1	2.0	26.157	25.904	-8.448	-4.768	137.944	590.537	-86.938	0.0	0.000



310	-10.0	-0.1	10.0	26.157	25.904	-42.701	-7.285	137.919	590.537	-86.938	0.0	0.000
311	-10.0	-0.1	18.0	26.157	25.904	-80.930	-10.997	137.950	590.537	-86.938	0.0	0.014
312	-10.0	0.9	2.0	26.157	31.189	10.589	39.564	-23.870	617.566	-95.706	0.0	0.016
313	-10.0	1.0	2.0	26.157	31.189	13.878	45.740	-23.853	618.010	-96.196	0.0	0.000
314	-10.0	0.9	10.0	26.157	31.189	32.814	37.327	-23.848	617.566	-95.706	0.0	0.009
315	-10.0	1.0	10.0	26.157	31.189	46.928	41.514	-23.845	618.010	-96.196	0.0	0.000
316	-10.0	0.9	18.0	26.157	31.189	53.540	35.097	-23.844	617.566	-95.706	0.0	0.000
317	-10.0	1.0	18.0	26.157	31.189	76.634	37.431	-23.844	618.010	-96.196	0.0	0.000
318	-10.0	0.1	22.0	26.157	31.189	15.388	4.941	-23.851	616.966	-95.674	0.0	0.013
319	-10.0	0.3	22.0	26.157	31.189	20.410	13.615	-23.853	617.219	-95.706	0.0	0.001
320	-10.0	0.5	22.0	26.157	31.189	27.057	21.712	-23.849	616.969	-95.614	0.0	0.016
321	-10.0	0.7	22.0	26.157	31.189	37.550	29.179	-23.850	617.478	-95.867	0.0	0.001
322	-10.0	0.9	22.0	26.157	31.189	63.377	33.983	-23.853	617.566	-95.706	0.0	0.000
323	-10.0	0.1	30.0	26.157	31.189	20.757	5.300	-23.853	616.966	-95.674	0.0	0.000
324	-10.0	0.5	30.0	26.157	31.189	35.398	21.833	-23.847	616.969	-95.614	0.0	0.000
325	-10.0	0.9	30.0	26.157	31.189	82.054	31.766	-23.857	617.566	-95.706	0.0	0.000
326	-10.0	-0.1	2.0	26.157	31.189	-8.704	-4.750	137.950	618.594	-96.207	0.0	0.000
327	-10.0	-0.1	10.0	26.157	31.189	-44.021	-7.280	137.919	618.594	-96.207	0.0	0.000
328	-10.0	-0.1	18.0	26.157	31.189	-83.334	-11.052	137.897	618.594	-96.207	0.0	0.002
329	10.0	0.9	2.0	18.446	25.904	11.571	40.808	-23.865	-564.341	26.714	0.0	0.001
330	10.0	1.0	2.0	18.446	25.904	15.115	47.937	-23.859	-565.062	26.393	0.0	0.000
331	10.0	0.9	10.0	18.446	25.904	37.362	43.427	-23.847	-564.341	26.714	0.0	0.068
332	10.0	1.0	10.0	18.446	25.904	57.314	53.064	-23.850	-565.062	26.393	0.0	0.000
333	10.0	0.9	18.0	18.446	25.904	65.623	46.542	-23.851	-564.341	26.714	0.0	0.000
334	10.0	1.0	18.0	18.446	25.904	106.147	59.639	-23.853	-565.062	26.393	0.0	0.000
335	10.0	0.1	22.0	18.446	25.904	15.790	5.948	-23.852	-564.837	26.397	0.0	0.044
336	10.0	0.3	22.0	18.446	25.904	21.300	15.564	-23.847	-564.153	26.606	0.0	0.013
337	10.0	0.5	22.0	18.446	25.904	29.026	25.124	-23.853	-564.463	26.686	0.0	0.020
338	10.0	0.7	22.0	18.446	25.904	42.185	35.279	-23.851	-564.403	26.756	0.0	0.000
339	10.0	0.9	22.0	18.446	25.904	80.765	48.282	-23.847	-564.341	26.714	0.0	0.000
340	10.0	0.1	30.0	18.446	25.904	21.664	6.796	-23.851	-564.837	26.397	0.0	0.000
341	10.0	0.5	30.0	18.446	25.904	38.976	26.733	-23.850	-564.463	26.686	0.0	0.000
342	10.0	0.9	30.0	18.446	25.904	113.319	52.241	-23.853	-564.341	26.714	0.0	0.000
343	10.0	-0.1	2.0	18.446	25.904	-9.322	-2.652	137.941	-564.691	26.306	0.0	0.000
344	10.0	-0.1	10.0	18.446	25.904	-42.802	2.825	137.925	-564.691	26.306	0.0	0.000
345	10.0	-0.1	18.0	18.446	25.904	-72.518	7.280	137.909	-564.691	26.306	0.0	0.000
346	10.0	0.9	2.0	18.446	31.189	11.065	40.962	-23.858	-595.541	24.198	0.0	0.000
347	10.0	1.0	2.0	18.446	31.189	13.985	47.966	-23.862	-596.222	23.775	0.0	0.000
348	10.0	0.9	10.0	18.446	31.189	34.960	43.285	-23.849	-595.541	24.198	0.0	0.021
349	10.0	1.0	10.0	18.446	31.189	51.067	52.237	-23.859	-596.222	23.775	0.0	0.000

350	10.0	0.9	18.0	18.446	31.189	60.886	45.987	-23.856	-595.541	24.198	0.0	0.000
351	10.0	1.0	18.0	18.446	31.189	92.992	57.482	-23.844	-596.222	23.775	0.0	0.000
352	10.0	0.1	22.0	18.446	31.189	15.668	5.900	-23.853	-595.859	24.216	0.0	0.055
353	10.0	0.3	22.0	18.446	31.189	21.039	15.474	-23.848	-595.594	24.403	0.0	0.022
354	10.0	0.5	22.0	18.446	31.189	28.452	24.964	-23.847	-595.491	24.278	0.0	0.064
355	10.0	0.7	22.0	18.446	31.189	40.763	34.974	-23.848	-595.638	24.240	0.0	0.004
356	10.0	0.9	22.0	18.446	31.189	74.632	47.469	-23.843	-595.541	24.198	0.0	0.000
357	10.0	0.1	30.0	18.446	31.189	21.484	6.720	-23.852	-595.859	24.216	0.0	0.000
358	10.0	0.5	30.0	18.446	31.189	38.159	26.473	-23.851	-595.491	24.278	0.0	0.000
359	10.0	0.9	30.0	18.446	31.189	103.988	50.815	-23.858	-595.541	24.198	0.0	0.000
360	10.0	-0.1	2.0	18.446	31.189	-9.603	-2.583	137.953	-595.916	24.239	0.0	0.000
361	10.0	-0.1	10.0	18.446	31.189	-44.205	3.063	137.916	-595.916	24.239	0.0	0.000
362	10.0	-0.1	18.0	18.446	31.189	-75.007	7.635	137.969	-595.916	24.239	0.0	0.000
363	10.0	0.9	2.0	26.157	25.904	11.930	40.678	-23.863	-609.675	22.897	0.0	0.000
364	10.0	1.0	2.0	26.157	25.904	15.807	47.917	-23.853	-609.831	22.907	0.0	0.000
365	10.0	0.9	10.0	26.157	25.904	38.921	43.423	-23.849	-609.675	22.897	0.0	0.018
366	10.0	1.0	10.0	26.157	25.904	60.681	53.430	-23.841	-609.831	22.907	0.0	0.000
367	10.0	0.9	18.0	26.157	25.904	68.424	46.656	-23.855	-609.675	22.897	0.0	0.000
368	10.0	1.0	18.0	26.157	25.904	60.681	53.430	-23.841	-609.831	22.907	0.0	0.000
369	10.0	0.1	22.0	26.157	25.904	16.139	6.037	-23.848	-609.963	22.969	0.0	0.023
370	10.0	0.3	22.0	26.157	25.904	21.793	15.657	-23.852	-609.600	22.683	0.0	0.006
371	10.0	0.5	22.0	26.157	25.904	29.744	25.210	-23.856	-609.769	22.956	0.0	0.010
372	10.0	0.7	22.0	26.157	25.904	43.377	35.363	-23.847	-610.000	22.804	0.0	0.000
373	10.0	0.9	22.0	26.157	25.904	84.186	48.447	-23.841	-609.675	22.897	0.0	0.000
374	10.0	0.1	30.0	26.157	25.904	22.137	6.925	-23.851	-609.963	22.969	0.0	0.000
375	10.0	0.5	30.0	26.157	25.904	39.922	26.871	-23.849	-609.769	22.956	0.0	0.000
376	10.0	0.9	30.0	26.157	25.904	118.044	52.497	-23.847	-609.675	22.897	0.0	0.000
377	10.0	-0.1	2.0	26.157	25.904	-7.980	-3.069	137.925	-609.522	23.172	0.0	0.000
378	10.0	-0.1	10.0	26.157	25.904	-36.824	1.388	137.906	-609.522	23.172	0.0	0.000
379	10.0	-0.1	18.0	26.157	25.904	-63.068	5.148	137.950	-609.522	23.172	0.0	0.000
380	10.0	0.9	2.0	26.157	31.189	11.398	40.850	-23.865	-640.591	19.636	0.0	0.000
381	10.0	1.0	2.0	26.157	31.189	14.580	47.955	-23.855	-641.338	18.900	0.0	0.000
382	10.0	0.9	10.0	26.157	31.189	36.407	43.306	-23.860	-640.591	19.636	0.0	0.006
383	10.0	1.0	10.0	26.157	31.189	53.954	52.579	-23.848	-641.338	18.900	0.0	0.000
384	10.0	0.9	18.0	26.157	31.189	63.465	46.125	-23.854	-640.591	19.636	0.0	0.000
385	10.0	1.0	18.0	26.157	31.189	98.440	58.242	-23.860	-641.338	18.900	0.0	0.000
386	10.0	0.1	22.0	26.157	31.189	16.003	5.988	-23.850	-640.997	19.435	0.0	0.029
387	10.0	0.3	22.0	26.157	31.189	21.512	15.565	-23.848	-641.053	19.574	0.0	0.014
388	10.0	0.5	22.0	26.157	31.189	29.146	25.053	-23.852	-640.734	19.683	0.0	0.036
389	10.0	0.7	22.0	26.157	31.189	41.917	35.075	-23.849	-640.650	19.792	0.0	0.001

390	10.0	0.9	22.0	26.157	31.189	77.803	47.682	-23.842	-640.591	19.636	0.0	0.000
391	10.0	0.1	30.0	26.157	31.189	21.938	6.848	-23.850	-640.997	19.435	0.0	0.000
392	10.0	0.5	30.0	26.157	31.189	39.075	26.617	-23.848	-640.734	19.683	0.0	0.000
393	10.0	0.9	30.0	26.157	31.189	108.334	51.149	-23.854	-640.591	19.636	0.0	0.000
394	10.0	-0.1	2.0	26.157	31.189	-8.223	-3.004	137.934	-640.094	19.244	0.0	0.000
395	10.0	-0.1	10.0	26.157	31.189	-38.033	1.613	137.919	-640.094	19.244	0.0	0.000
396	10.0	-0.1	18.0	26.157	31.189	-38.033	1.613	137.919	-640.094	19.244	0.0	0.000
397	30.0	0.9	2.0	18.446	25.904	12.037	42.461	-23.858	-181.128	37.378	0.0	0.011
398	30.0	1.0	2.0	18.446	25.904	15.081	50.667	-23.854	-181.381	37.408	0.0	0.000
399	30.0	0.9	10.0	18.446	25.904	39.646	52.809	-23.856	-181.128	37.378	0.0	0.000
400	30.0	1.0	10.0	18.446	25.904	61.667	74.103	-23.853	-181.381	37.408	0.0	0.000
401	30.0	0.9	18.0	18.446	25.904	75.033	70.355	-23.852	-181.128	37.378	0.0	0.000
402	30.0	1.0	18.0	18.446	25.904	127.916	128.122	-23.875	-181.381	37.408	0.0	0.000
403	30.0	0.1	22.0	18.446	25.904	16.188	7.291	-23.852	-181.209	37.412	0.0	0.008
404	30.0	0.3	22.0	18.446	25.904	21.963	18.204	-23.847	-181.125	37.392	0.0	0.047
405	30.0	0.5	22.0	18.446	25.904	30.397	30.023	-23.850	-181.038	37.342	0.0	0.081
406	30.0	0.7	22.0	18.446	25.904	45.577	45.231	-23.853	-181.103	37.381	0.0	0.006
407	30.0	0.9	22.0	18.446	25.904	96.350	83.549	-23.837	-181.128	37.378	0.0	0.000
408	30.0	0.1	30.0	18.446	25.904	22.572	8.989	-23.850	-181.209	37.412	0.0	0.000
409	30.0	0.5	30.0	18.446	25.904	41.824	34.650	-23.848	-181.038	37.342	0.0	0.000
410	30.0	0.9	30.0	18.446	25.904	147.288	125.631	-23.847	-181.128	37.378	0.0	0.000
411	30.0	-0.1	2.0	18.446	25.904	-8.264	-0.895	137.938	-181.372	37.428	0.0	0.000
412	30.0	-0.1	10.0	18.446	25.904	-34.716	9.050	137.925	-181.372	37.428	0.0	0.000
413	30.0	-0.1	18.0	18.446	25.904	-54.278	15.381	137.934	-181.372	37.428	0.0	0.000
414	30.0	0.9	10.0	18.446	31.189	11.456	42.437	-23.856	-191.178	40.171	0.0	0.033
415	30.0	1.0	10.0	18.446	31.189	13.903	50.258	-23.848	-191.447	40.211	0.0	0.000
416	30.0	0.9	10.0	18.446	31.189	36.667	51.341	-23.851	-191.178	40.171	0.0	0.000
417	30.0	1.0	10.0	18.446	31.189	53.795	68.588	-23.846	-191.447	40.211	0.0	0.000
418	30.0	0.9	18.0	18.446	31.189	45.669	54.581	-23.853	-191.150	40.179	0.0	0.000
419	30.0	1.0	18.0	18.446	31.189	68.009	65.594	-23.843	-191.178	40.171	0.0	0.000
420	30.0	0.1	22.0	18.446	31.189	16.030	7.158	-23.850	-191.269	40.226	0.0	0.014
421	30.0	0.3	22.0	18.446	31.189	21.632	17.927	-23.847	-191.175	40.208	0.0	0.041
422	30.0	0.5	22.0	18.446	31.189	29.660	29.461	-23.847	-191.087	40.179	0.0	0.104
423	30.0	0.7	22.0	18.446	31.189	43.655	43.862	-23.854	-191.150	40.179	0.0	0.083
424	30.0	0.9	22.0	18.446	31.189	86.527	75.853	-23.857	-191.178	40.171	0.0	0.000
425	30.0	0.1	30.0	18.446	31.189	22.318	8.767	-23.851	-191.269	40.226	0.0	0.000
426	30.0	0.5	30.0	18.446	31.189	40.683	33.673	-23.847	-191.087	40.179	0.0	0.000
427	30.0	0.9	30.0	18.446	31.189	130.150	106.366	-23.848	-191.178	40.171	0.0	0.000
428	30.0	-0.1	2.0	18.446	31.189	-8.543	-0.779	137.931	-191.384	40.194	0.0	0.000
429	30.0	-0.1	10.0	18.446	31.189	-36.026	9.528	137.919	-191.384	40.194	0.0	0.000

430	30.0	-0.1	18.0	18.446	31.189	-56.447	16.166	137.931	-191.384	40.194	0.0	0.000
431	30.0	0.9	2.0	26.157	25.904	12.446	42.400	-23.858	-195.872	34.199	0.0	0.004
432	30.0	1.0	2.0	26.157	25.904	15.786	50.863	-23.856	-196.125	34.251	0.0	0.000
433	30.0	0.9	10.0	26.157	25.904	41.419	53.098	-23.854	-195.872	34.199	0.0	0.000
434	30.0	1.0	10.0	26.157	25.904	65.381	75.842	-23.848	-196.125	34.251	0.0	0.000
435	30.0	0.9	18.0	26.157	25.904	78.446	70.875	-23.846	-195.872	34.199	0.0	0.000
436	30.0	1.0	18.0	26.157	25.904	136.075	132.512	-23.833	-196.125	34.251	0.0	0.000
437	30.0	0.1	22.0	26.157	25.904	16.524	7.421	-23.851	-195.950	34.294	0.0	0.003
438	30.0	0.3	22.0	26.157	25.904	22.468	18.319	-23.852	-195.853	34.220	0.0	0.031
439	30.0	0.5	22.0	26.157	25.904	31.167	30.094	-23.849	-195.803	34.225	0.0	0.044
440	30.0	0.7	22.0	26.157	25.904	46.931	45.245	-23.848	-195.847	34.199	0.0	0.001
441	30.0	0.9	22.0	26.157	25.904	100.816	84.098	-23.853	-195.872	34.199	0.0	0.000
442	30.0	0.1	30.0	26.157	25.904	23.023	9.151	-23.852	-195.950	34.294	0.0	0.000
443	30.0	0.5	30.0	26.157	25.904	42.850	34.700	-23.849	-195.803	34.225	0.0	0.000
444	30.0	0.9	30.0	26.157	25.904	154.622	125.591	-23.851	-195.872	34.199	0.0	0.000
445	30.0	-0.1	2.0	26.157	25.904	-7.132	-1.623	137.925	-196.078	34.209	0.0	0.000
446	30.0	-0.1	10.0	26.157	25.904	-30.667	6.852	137.922	-196.078	34.209	0.0	0.000
447	30.0	-0.1	18.0	26.157	25.904	-49.107	12.631	137.925	-196.078	34.209	0.0	0.000
448	30.0	0.9	2.0	26.157	31.189	11.834	42.395	-23.855	-205.891	36.916	0.0	0.011
449	30.0	1.0	2.0	26.157	31.189	14.505	50.437	-23.851	-206.100	36.997	0.0	0.000
450	30.0	0.9	10.0	26.157	31.189	38.250	51.688	-23.852	-205.891	36.916	0.0	0.000
451	30.0	1.0	10.0	26.157	31.189	56.877	70.102	-23.859	-206.100	36.997	0.0	0.000
452	30.0	0.9	18.0	26.157	31.189	71.048	66.308	-23.858	-205.891	36.916	0.0	0.000
453	30.0	1.0	18.0	26.157	31.189	114.481	109.069	-23.842	-206.100	36.997	0.0	0.000
454	30.0	0.1	22.0	26.157	31.189	16.350	7.292	-23.852	-206.022	36.999	0.0	0.005
455	30.0	0.3	22.0	26.157	31.189	22.111	18.056	-23.851	-205.894	36.930	0.0	0.029
456	30.0	0.5	22.0	26.157	31.189	30.392	29.573	-23.851	-205.772	37.007	0.0	0.066
457	30.0	0.7	22.0	26.157	31.189	44.925	43.979	-23.851	-205.828	36.965	0.0	0.013
458	30.0	0.9	22.0	26.157	31.189	90.369	76.688	-23.858	-205.891	36.916	0.0	0.000
459	30.0	0.1	30.0	26.157	31.189	22.746	8.937	-23.848	-206.022	36.999	0.0	0.000
460	30.0	0.5	30.0	26.157	31.189	41.658	33.790	-23.850	-205.772	37.007	0.0	0.000
461	30.0	0.9	30.0	26.157	31.189	136.128	107.203	-23.848	-205.891	36.916	0.0	0.000
462	30.0	-0.1	2.0	26.157	31.189	-7.364	-1.510	137.925	-206.056	37.039	0.0	0.000
463	30.0	-0.1	10.0	26.157	31.189	-31.770	7.314	137.900	-206.056	37.039	0.0	0.000
464	30.0	-0.1	18.0	26.157	31.189	-50.962	13.384	137.966	-206.056	37.039	0.0	0.000
465	-30.0	0.5	0.0	26.157	31.189	208.247	-1.812	0.220	208.244	-2.017	0.0	0.000
466	-30.0	0.5	0.0	26.157	25.904	198.100	-2.360	-0.145	198.066	-2.609	0.0	0.000
467	-30.0	0.5	0.0	18.446	25.904	184.000	2.859	-0.014	184.009	2.629	0.0	0.000
468	-30.0	0.5	0.0	18.446	31.189	194.259	3.417	-0.055	194.209	3.229	0.0	0.000
469	-20.0	0.5	0.0	26.157	31.189	313.300	-20.415	0.076	313.212	-20.749	0.0	0.000

470	-20.0	0.5	0.0	26.157	25.904	298.331	-19.193	0.023	298.169	-19.492	0.0	0.000
471	-20.0	0.5	0.0	18.446	25.904	276.938	-12.964	0.150	276.931	-13.259	0.0	0.000
472	-20.0	0.5	0.0	18.446	31.189	292.006	-14.048	-0.276	291.741	-14.388	0.0	0.000
473	-10.0	0.5	0.0	18.446	31.189	574.459	-84.165	0.065	573.912	-85.288	0.0	0.000
474	-10.0	0.5	0.0	18.446	25.904	545.731	-75.564	0.085	545.803	-76.484	0.0	0.000
475	-10.0	0.5	0.0	26.157	25.904	588.969	-85.536	-0.269	588.534	-86.084	0.0	0.000
476	-10.0	0.5	0.0	26.157	31.189	617.281	-94.448	-0.132	616.969	-95.614	0.0	0.000
477	10.0	0.5	0.0	26.157	31.189	-640.369	19.187	-0.104	-640.734	19.683	0.0	0.006
478	10.0	0.5	0.0	26.157	25.904	-609.413	22.518	-0.087	-609.769	22.956	0.0	0.010
479	10.0	0.5	0.0	18.446	25.904	-564.550	26.117	0.097	-564.463	26.686	0.0	0.014
480	10.0	0.5	0.0	18.446	31.189	-595.625	23.073	0.220	-595.491	24.278	0.0	0.009
481	20.0	0.5	0.0	26.157	31.189	-315.175	37.864	-0.008	-315.159	38.133	0.0	0.008
482	20.0	0.5	0.0	26.157	25.904	-299.647	35.791	0.039	-299.666	36.172	0.0	0.004
483	20.0	0.5	0.0	18.446	25.904	-277.359	38.970	-0.102	-277.319	39.221	0.0	0.007
484	20.0	0.5	0.0	18.446	31.189	-292.688	41.049	-0.134	-292.681	41.346	0.0	0.014
485	30.0	0.5	0.0	18.446	31.189	-191.100	39.943	-0.068	-191.087	40.179	0.0	0.002
486	30.0	0.5	0.0	18.446	25.904	-181.081	37.027	0.007	-181.038	37.342	0.0	0.001
487	30.0	0.5	0.0	26.157	25.904	-195.891	33.930	0.101	-195.803	34.225	0.0	0.000
488	30.0	0.5	0.0	26.157	31.189	-205.878	36.713	-0.047	-205.772	37.007	0.0	0.001

**TESTING CASES****error = 0.00      cost = 0.921217**

No.	$\delta$	$\alpha$	$R_F$	$X_{SI}$	$X_{RI}$	$R_I$	$X_I$	$X_{SO}$	$R_{mem}$	$X_{mem}$	Target	Output
1	-20.0	-0.10	4.0	24.500	27.400	-17.686	-7.401	137.906	298.906	-18.603	0.0	0.000
2	-20.0	-0.10	14.0	24.500	27.400	-70.075	-19.724	137.947	298.906	-18.603	0.0	0.000
3	-20.0	0.20	4.0	24.500	27.400	3.596	8.339	-23.875	298.819	-18.557	1.0	1.000
4	-20.0	0.20	14.0	24.500	27.400	11.118	8.631	-23.851	298.819	-18.557	1.0	1.000
5	-20.0	0.20	26.0	24.500	27.400	19.668	8.909	-23.851	298.819	-18.557	0.0	0.000
6	-20.0	0.60	4.0	24.500	27.400	9.132	24.238	-23.863	297.812	-18.463	1.0	1.000
7	-20.0	0.60	14.0	24.500	27.400	21.695	22.836	-23.849	297.812	-18.463	1.0	1.000
8	-20.0	0.60	26.0	24.500	27.400	35.416	21.277	-23.849	297.812	-18.463	0.0	0.000
9	-20.0	0.80	26.0	24.500	27.400	50.408	27.417	-23.855	298.828	-18.596	0.0	0.000
10	-20.0	0.95	4.0	24.500	27.400	18.560	39.847	-23.853	298.091	-18.481	0.0	0.000
11	-20.0	0.95	14.0	24.500	27.400	48.278	33.485	-23.850	298.091	-18.481	0.0	0.000

12	20.0	-0.10	4.0	24.500	27.400	-15.150	-0.214	137.931	-299.484	37.487	0.0	0.000
13	20.0	-0.10	14.0	24.500	27.400	-46.722	7.726	137.941	-299.484	37.487	0.0	0.000
14	20.0	0.20	4.0	24.500	27.400	3.789	8.749	-23.867	-300.081	37.416	1.0	1.000
15	20.0	0.20	14.0	24.500	27.400	11.779	10.338	-23.851	-300.081	37.416	1.0	1.000
16	20.0	0.20	26.0	24.500	27.400	21.898	12.537	-23.848	-300.081	37.416	0.0	0.000
17	20.0	0.60	4.0	24.500	27.400	10.503	26.044	-23.856	-299.028	37.335	1.0	1.000
18	20.0	0.60	14.0	24.500	27.400	25.532	28.445	-23.851	-299.028	37.335	1.0	0.995
19	20.0	0.60	26.0	24.500	27.400	45.556	32.080	-23.849	-299.028	37.335	0.0	0.000
20	20.0	0.80	26.0	24.500	27.400	72.889	49.816	-23.851	-299.969	37.336	0.0	0.000
21	20.0	0.95	4.0	24.500	27.400	21.499	46.674	-23.853	-299.094	37.383	0.0	0.000
22	20.0	0.95	14.0	24.500	27.400	68.127	58.917	-23.854	-299.094	37.383	0.0	0.000

RUNNING CASES

No.	$\delta$	$\alpha$	$R_F$	$X_{SI}$	$X_{RI}$	$R_I$	$X_I$	$X_{SO}$	$R_{mem}$	$X_{mem}$	Target	Output
1	-15.0	-0.10	6.0	20.660	29.890	-27.287	-7.449	137.925	395.666	-37.185	0.0	0.000
2	-15.0	-0.08	6.0	20.660	29.890	-26.569	-6.490	137.928	392.244	-36.798	0.0	0.000
3	-15.0	-0.06	6.0	20.660	29.890	-24.126	-5.306	137.944	392.263	-36.556	0.0	0.000
4	-15.0	-0.04	6.0	20.660	29.890	-22.013	-4.200	137.925	392.263	-36.558	0.0	0.000
5	-15.0	-0.02	6.0	20.660	29.890	-20.229	-3.179	137.925	392.234	-36.770	0.0	0.000
6	-15.0	-0.00	6.0	20.660	29.890	-18.731	-2.936	137.922	395.678	-37.205	0.0	0.000
7	-15.0	0.00	6.0	20.660	29.890	3.878	0.921	-23.854	394.769	-37.063	1.0	1.000
8	-15.0	0.02	6.0	20.660	29.890	3.923	0.997	-23.854	391.184	-36.473	1.0	1.000
9	-15.0	0.04	6.0	20.660	29.890	4.006	1.728	-23.855	391.169	-36.378	1.0	1.000
10	-15.0	0.06	6.0	20.660	29.890	4.095	2.482	-23.856	391.538	-36.427	1.0	1.000
11	-15.0	0.08	6.0	20.660	29.890	4.178	3.236	-23.855	391.166	-36.400	1.0	1.000
12	-15.0	0.10	6.0	20.660	29.890	4.288	4.086	-23.857	391.169	-36.482	1.0	1.000
13	-15.0	0.15	6.0	20.660	29.890	4.507	5.891	-23.858	391.175	-36.451	1.0	1.000
14	-15.0	0.20	6.0	20.660	29.890	5.102	8.492	-23.862	392.169	-36.503	1.0	1.000
15	-15.0	0.25	6.0	20.660	29.890	5.289	10.466	-23.862	391.053	-36.313	1.0	1.000
16	-15.0	0.30	6.0	20.660	29.890	6.659	12.832	-23.861	391.172	-36.433	1.0	1.000
17	-15.0	0.35	6.0	20.660	29.890	7.527	15.004	-23.861	390.778	-36.363	1.0	1.000
18	-15.0	0.40	6.0	39.389	59.084	6.379	16.516	-23.867	390.822	-36.325	1.0	1.000
19	-15.0	0.45	6.0	20.660	29.890	7.270	18.716	-23.866	390.778	-36.357	1.0	1.000
20	-15.0	0.50	6.0	20.660	29.890	9.422	21.146	-23.862	391.134	-36.362	1.0	1.000

---

21	-15.0	0.55	6.0	20.660	29.890	10.814	22.703	-23.856	390.822	-36.327	1.0	1.000
22	-15.0	0.60	6.0	20.660	29.890	11.747	24.337	-23.857	391.041	-36.312	1.0	1.000
23	-15.0	0.65	6.0	20.660	29.890	11.542	27.225	-23.859	390.987	-36.301	1.0	1.000
24	-15.0	0.70	6.0	20.660	29.890	12.959	29.322	-23.859	391.231	-36.492	1.0	1.000
25	-15.0	0.72	6.0	20.660	29.890	13.196	30.305	-23.859	391.212	-36.423	1.0	1.000
26	-15.0	0.74	6.0	20.660	29.890	13.649	31.120	-23.857	391.191	-36.479	1.0	1.000
27	-15.0	0.76	6.0	20.660	29.890	14.738	31.681	-23.856	391.125	-36.372	1.0	1.000
28	-15.0	0.78	6.0	20.660	29.890	15.353	32.498	-23.855	391.556	-36.430	1.0	1.000
29	-15.0	0.80	6.0	20.660	29.890	16.304	33.321	-23.854	392.237	-36.684	1.0	0.997
30	-15.0	0.82	6.0	20.660	29.890	17.275	33.985	-23.853	391.328	-36.515	0.0	0.904
31	-15.0	0.84	6.0	20.660	29.890	17.922	35.101	-23.851	391.225	-36.524	0.0	0.023
32	-15.0	0.86	6.0	20.660	29.890	19.204	35.789	-23.851	391.303	-36.522	0.0	0.001
33	-15.0	0.88	6.0	20.660	29.890	19.942	36.842	-23.851	391.384	-36.449	0.0	0.000
34	-15.0	0.90	6.0	20.660	29.890	20.995	37.760	-23.854	391.337	-36.517	0.0	0.000
35	-15.0	0.92	6.0	20.660	29.890	22.346	38.606	-23.850	391.297	-36.452	0.0	0.000
36	-15.0	0.94	6.0	20.660	29.890	23.805	39.508	-23.852	391.756	-36.340	0.0	0.000
37	-15.0	0.96	6.0	20.660	29.890	25.406	40.384	-23.853	391.284	-36.464	0.0	0.000
38	-15.0	0.98	6.0	20.660	29.890	27.164	41.401	-23.857	391.334	-36.515	0.0	0.000
39	-15.0	1.00	6.0	20.660	29.890	27.753	42.283	-23.859	395.597	-37.313	0.0	0.000
40	-15.0	0.40	0.0	20.660	29.890	0.643	16.145	-23.872	390.822	-36.325	1.0	1.000
41	-15.0	0.40	0.2	20.660	29.890	0.835	16.160	-23.877	390.822	-36.325	1.0	1.000
42	-15.0	0.40	0.4	20.660	29.890	1.031	16.176	-23.878	390.822	-36.325	1.0	1.000
43	-15.0	0.40	0.6	20.660	29.890	1.226	16.190	-23.882	390.822	-36.325	1.0	1.000
44	-15.0	0.40	0.8	20.660	29.890	1.421	16.204	-23.884	390.822	-36.325	1.0	1.000
45	-15.0	0.40	1.0	20.660	29.890	1.615	16.219	-23.886	390.822	-36.325	1.0	1.000
46	-15.0	0.40	1.2	20.660	29.890	1.809	16.233	-23.885	390.822	-36.325	1.0	1.000
47	-15.0	0.40	1.4	20.660	29.890	2.003	16.245	-23.889	390.822	-36.325	1.0	1.000
48	-15.0	0.40	1.6	20.660	29.890	2.196	16.257	-23.887	390.822	-36.325	1.0	1.000
49	-15.0	0.40	1.8	20.660	29.890	2.389	16.271	-23.887	390.822	-36.325	1.0	1.000
50	-15.0	0.40	2.0	20.660	29.890	2.581	16.283	-23.887	390.822	-36.325	1.0	1.000
51	-15.0	0.40	2.5	20.660	29.890	3.061	16.313	-23.885	390.822	-36.325	1.0	1.000
52	-15.0	0.40	3.0	20.660	29.890	3.539	16.345	-23.885	390.822	-36.325	1.0	1.000
53	-15.0	0.40	3.5	20.660	29.890	4.015	16.373	-23.880	390.822	-36.325	1.0	1.000
54	-15.0	0.40	4.0	20.660	29.890	4.490	16.402	-23.877	390.822	-36.325	1.0	1.000
55	-15.0	0.40	6.0	20.660	29.890	6.379	16.516	-23.867	390.822	-36.325	1.0	1.000
56	-15.0	0.40	8.0	20.660	29.890	8.252	16.627	-23.858	390.822	-36.325	1.0	1.000
57	-15.0	0.40	10.0	20.660	29.890	10.110	16.734	-23.855	390.822	-36.325	1.0	1.000
58	-15.0	0.40	12.0	20.660	29.890	11.951	16.840	-23.853	390.822	-36.325	1.0	1.000
59	-15.0	0.40	14.0	20.660	29.890	13.777	16.941	-23.851	390.822	-36.325	1.0	1.000

60	-15.0	0.40	16.0	20.660	29.890	15.585	17.037	-23.852	390.822	-36.325	1.0	1.000
61	-15.0	0.40	18.0	20.660	29.890	17.377	17.132	-23.849	390.822	-36.325	1.0	1.000
62	-15.0	0.40	18.5	20.660	29.890	17.824	17.155	-23.851	390.822	-36.325	1.0	1.000
63	-15.0	0.40	19.0	20.660	29.890	18.267	17.176	-23.850	390.822	-36.325	1.0	0.999
64	-15.0	0.40	19.2	20.660	29.890	18.445	17.186	-23.850	390.822	-36.325	1.0	0.999
65	-15.0	0.40	19.4	20.660	29.890	18.624	17.196	-23.852	390.822	-36.325	1.0	0.998
66	-15.0	0.40	19.6	20.660	29.890	18.801	17.204	-23.851	390.822	-36.325	1.0	0.996
67	-15.0	0.40	19.8	20.660	29.890	18.977	17.213	-23.851	390.822	-36.325	1.0	0.994
68	-15.0	0.40	20.0	20.660	29.890	19.154	17.220	-23.848	390.822	-36.325	1.0	0.990
69	-15.0	0.40	20.2	20.660	29.890	19.331	17.229	-23.851	390.822	-36.325	0.0	0.983
70	-15.0	0.40	20.4	20.660	29.890	19.507	17.238	-23.850	390.822	-36.325	0.0	0.972
71	-15.0	0.40	20.6	20.660	29.890	19.684	17.247	-23.851	390.822	-36.325	0.0	0.954
72	-15.0	0.40	20.8	20.660	29.890	19.859	17.256	-23.850	390.822	-36.325	0.0	0.926
73	-15.0	0.40	21.0	20.660	29.890	20.036	17.264	-23.850	390.822	-36.325	0.0	0.881
74	-15.0	0.40	21.5	20.660	29.890	20.476	17.286	-23.852	390.822	-36.325	0.0	0.669
75	-15.0	0.40	22.0	20.660	29.890	20.914	17.307	-23.851	390.822	-36.325	0.0	0.355
76	-15.0	0.40	22.5	20.660	29.890	21.351	17.327	-23.850	390.822	-36.325	0.0	0.132
77	-15.0	0.40	23.0	20.660	29.890	21.787	17.346	-23.850	390.822	-36.325	0.0	0.041
78	-15.0	0.40	23.5	20.660	29.890	22.223	17.367	-23.849	390.822	-36.325	0.0	0.012
79	-15.0	0.40	24.0	20.660	29.890	22.658	17.387	-23.851	390.822	-36.325	0.0	0.003
80	-15.0	0.40	24.5	20.660	29.890	23.093	17.406	-23.850	390.822	-36.325	0.0	0.001
81	-15.0	0.40	25.0	20.660	29.890	23.525	17.427	-23.852	390.822	-36.325	0.0	0.000
82	-15.0	0.40	26.0	20.660	29.890	24.386	17.466	-23.852	390.822	-36.325	0.0	0.000
83	-15.0	0.40	28.0	20.660	29.890	26.098	17.541	-23.850	390.822	-36.325	0.0	0.000
84	-15.0	0.40	30.0	20.660	29.890	27.796	17.610	-23.850	390.822	-36.325	0.0	0.000
85	-15.0	0.40	32.0	20.660	29.890	29.478	17.677	-23.852	390.822	-36.325	0.0	0.000
86	-15.0	0.40	34.0	20.660	29.890	31.145	17.740	-23.850	390.822	-36.325	0.0	0.000
87	-15.0	0.40	36.0	20.660	29.890	32.797	17.800	-23.849	390.822	-36.325	0.0	0.000
88	-15.0	0.40	38.0	20.660	29.890	34.436	17.857	-23.850	390.822	-36.325	0.0	0.000
89	-15.0	0.40	40.0	20.660	29.890	36.058	17.909	-23.850	390.822	-36.325	0.0	0.000
90	15.0	-0.10	6.0	20.660	29.890	-23.289	0.754	137.919	-401.319	37.353	0.0	0.001
91	15.0	-0.08	6.0	20.660	29.890	-22.730	1.475	137.925	-397.734	37.787	0.0	0.000
92	15.0	-0.06	6.0	20.660	29.890	-20.903	1.813	137.909	-397.850	37.859	0.0	0.000
93	15.0	-0.04	6.0	20.660	29.890	-19.290	2.193	137.916	-397.853	37.866	0.0	0.000
94	15.0	-0.02	6.0	20.660	29.890	-17.914	2.620	137.928	-397.709	37.817	0.0	0.000
95	15.0	0.00	6.0	20.660	29.890	-16.714	2.344	137.922	-401.325	37.368	0.0	0.000
96	15.0	0.00	6.0	20.660	29.890	3.919	1.194	-23.853	-401.953	37.478	1.0	1.000
97	15.0	0.02	6.0	20.660	29.890	3.961	1.275	-23.853	-397.747	37.840	1.0	1.000
98	15.0	0.04	6.0	20.660	29.890	4.060	2.017	-23.854	-397.706	37.913	1.0	1.000



99	15.0	0.06	6.0	20.660	29.890	4.165	2.784	-23.853	-398.250	37.997	1.0	1.000
100	15.0	0.08	6.0	20.660	29.890	4.270	3.551	-23.854	-397.737	37.958	1.0	1.000
101	15.0	0.10	6.0	20.660	29.890	4.391	4.419	-23.855	-397.713	37.874	1.0	1.000
102	15.0	0.15	6.0	20.660	29.890	4.673	6.254	-23.856	-397.744	37.886	1.0	1.000
103	15.0	0.20	6.0	20.660	29.890	5.267	8.955	-23.860	-398.788	37.760	1.0	1.000
104	15.0	0.25	6.0	20.660	29.890	5.514	10.968	-23.860	-397.531	38.083	1.0	1.000
105	15.0	0.30	6.0	20.660	29.890	6.946	13.547	-23.858	-397.731	37.929	1.0	1.000
106	15.0	0.35	6.0	20.660	29.890	7.890	15.879	-23.858	-397.225	37.971	1.0	1.000
107	15.0	0.40	6.0	20.660	29.890	6.834	17.217	-23.862	-397.197	37.975	1.0	1.000
108	15.0	0.45	6.0	20.660	29.890	7.810	19.586	-23.859	-397.316	37.914	1.0	1.000
109	15.0	0.50	6.0	20.660	29.890	10.089	22.451	-23.859	-397.537	38.087	1.0	1.000
110	15.0	0.55	6.0	20.660	29.890	11.757	24.303	-23.855	-397.250	37.945	1.0	1.000
111	15.0	0.60	6.0	20.660	29.890	12.948	26.154	-23.853	-397.331	37.942	1.0	1.000
112	15.0	0.65	6.0	20.660	29.890	12.613	29.112	-23.856	-397.284	37.918	1.0	1.000
113	15.0	0.70	6.0	20.660	29.890	14.253	31.617	-23.855	-397.625	37.953	1.0	1.000
114	15.0	0.72	6.0	20.660	29.890	14.490	32.703	-23.856	-397.297	38.006	1.0	1.000
115	15.0	0.74	6.0	20.660	29.890	15.030	33.665	-23.853	-397.331	37.966	1.0	1.000
116	15.0	0.76	6.0	20.660	29.890	16.361	34.550	-23.853	-397.312	37.961	1.0	1.000
117	15.0	0.78	6.0	20.660	29.890	17.110	35.543	-23.854	-397.841	37.779	1.0	1.000
118	15.0	0.80	6.0	20.660	29.890	18.264	36.685	-23.852	-398.572	37.917	1.0	1.000
119	15.0	0.82	6.0	20.660	29.890	19.378	37.713	-23.852	-397.697	37.870	0.0	0.999
120	15.0	0.84	6.0	20.660	29.890	20.060	39.134	-23.848	-397.603	38.024	0.0	0.990
121	15.0	0.86	6.0	20.660	29.890	21.605	40.304	-23.849	-397.728	37.877	0.0	0.931
122	15.0	0.88	6.0	20.660	29.890	22.419	41.711	-23.855	-397.753	37.839	0.0	0.403
123	15.0	0.90	6.0	20.660	29.890	23.632	43.091	-23.851	-397.741	37.875	0.0	0.047
124	15.0	0.92	6.0	20.660	29.890	25.215	44.559	-23.850	-397.572	37.978	0.0	0.005
125	15.0	0.94	6.0	20.660	29.890	27.002	46.125	-23.851	-397.841	37.798	0.0	0.001
126	15.0	0.96	6.0	20.660	29.890	28.855	47.824	-23.848	-397.609	38.021	0.0	0.000
127	15.0	0.98	6.0	20.660	29.890	30.914	49.802	-23.847	-397.638	37.946	0.0	0.000
128	15.0	1.00	6.0	20.660	29.890	31.667	50.922	-23.846	-401.831	37.539	0.0	0.000
129	15.0	0.40	0.0	20.660	29.890	1.126	16.037	-23.868	-397.197	37.975	1.0	1.000
130	15.0	0.40	0.2	20.660	29.890	1.311	16.076	-23.870	-397.197	37.975	1.0	1.000
131	15.0	0.40	0.4	20.660	29.890	1.502	16.115	-23.872	-397.197	37.975	1.0	1.000
132	15.0	0.40	0.6	20.660	29.890	1.692	16.156	-23.872	-397.197	37.975	1.0	1.000
133	15.0	0.40	0.8	20.660	29.890	1.882	16.195	-23.875	-397.197	37.975	1.0	1.000
134	15.0	0.40	1.0	20.660	29.890	2.072	16.234	-23.875	-397.197	37.975	1.0	1.000
135	15.0	0.40	1.2	20.660	29.890	2.262	16.274	-23.878	-397.197	37.975	1.0	1.000
136	15.0	0.40	1.4	20.660	29.890	2.451	16.312	-23.878	-397.197	37.975	1.0	1.000
137	15.0	0.40	1.6	20.660	29.890	2.641	16.352	-23.878	-397.197	37.975	1.0	1.000

---

138	15.0	0.40	1.8	20.660	29.890	2.831	16.391	-23.878	-397.197	37.975	1.0	1.000
139	15.0	0.40	2.0	20.660	29.890	3.020	16.429	-23.878	-397.197	37.975	1.0	1.000
140	15.0	0.40	2.5	20.660	29.890	3.494	16.527	-23.876	-397.197	37.975	1.0	1.000
141	15.0	0.40	3.0	20.660	29.890	3.969	16.624	-23.875	-397.197	37.975	1.0	1.000
142	15.0	0.40	3.5	20.660	29.890	4.444	16.722	-23.873	-397.197	37.975	1.0	1.000
143	15.0	0.40	4.0	20.660	29.890	4.920	16.820	-23.872	-397.197	37.975	1.0	1.000
144	15.0	0.40	6.0	20.660	29.890	6.834	17.217	-23.862	-397.197	37.975	1.0	1.000
145	15.0	0.40	8.0	20.660	29.890	8.768	17.625	-23.856	-397.197	37.975	1.0	1.000
146	15.0	0.40	10.0	20.660	29.890	10.722	18.044	-23.853	-397.197	37.975	1.0	1.000
147	15.0	0.40	12.0	20.660	29.890	12.696	18.473	-23.852	-397.197	37.975	1.0	1.000
148	15.0	0.40	14.0	20.660	29.890	14.686	18.913	-23.852	-397.197	37.975	1.0	1.000
149	15.0	0.40	16.0	20.660	29.890	16.696	19.362	-23.851	-397.197	37.975	1.0	1.000
150	15.0	0.40	18.0	20.660	29.890	18.725	19.821	-23.852	-397.197	37.975	1.0	0.987
151	15.0	0.40	18.5	20.660	29.890	19.234	19.936	-23.851	-397.197	37.975	1.0	0.967
152	15.0	0.40	19.0	20.660	29.890	19.745	20.054	-23.850	-397.197	37.975	1.0	0.921
153	15.0	0.40	19.2	20.660	29.890	19.949	20.098	-23.850	-397.197	37.975	1.0	0.888
154	15.0	0.40	19.4	20.660	29.890	20.155	20.148	-23.853	-397.197	37.975	1.0	0.845
155	15.0	0.40	19.6	20.660	29.890	20.359	20.195	-23.851	-397.197	37.975	1.0	0.788
156	15.0	0.40	19.8	20.660	29.890	20.565	20.243	-23.850	-397.197	37.975	1.0	0.718
157	15.0	0.40	20.0	20.660	29.890	20.771	20.286	-23.850	-397.197	37.975	1.0	0.634
158	15.0	0.40	20.2	20.660	29.890	20.976	20.335	-23.850	-397.197	37.975	0.0	0.543
159	15.0	0.40	20.4	20.660	29.890	21.183	20.385	-23.851	-397.197	37.975	0.0	0.448
160	15.0	0.40	20.6	20.660	29.890	21.388	20.432	-23.850	-397.197	37.975	0.0	0.357
161	15.0	0.40	20.8	20.660	29.890	21.594	20.478	-23.850	-397.197	37.975	0.0	0.274
162	15.0	0.40	21.0	20.660	29.890	21.802	20.526	-23.849	-397.197	37.975	0.0	0.204
163	15.0	0.40	21.5	20.660	29.890	22.316	20.646	-23.850	-397.197	37.975	0.0	0.090
164	15.0	0.40	22.0	20.660	29.890	22.836	20.767	-23.852	-397.197	37.975	0.0	0.037
165	15.0	0.40	22.5	20.660	29.890	23.355	20.887	-23.850	-397.197	37.975	0.0	0.014
166	15.0	0.40	23.0	20.660	29.890	23.875	21.008	-23.848	-397.197	37.975	0.0	0.006
167	15.0	0.40	23.5	20.660	29.890	24.396	21.134	-23.850	-397.197	37.975	0.0	0.002
168	15.0	0.40	24.0	20.660	29.890	24.920	21.257	-23.851	-397.197	37.975	0.0	0.001
169	15.0	0.40	24.5	20.660	29.890	25.444	21.377	-23.848	-397.197	37.975	0.0	0.000
170	15.0	0.40	25.0	20.660	29.890	25.972	21.505	-23.852	-397.197	37.975	0.0	0.000
171	15.0	0.40	26.0	20.660	29.890	27.026	21.755	-23.851	-397.197	37.975	0.0	0.000
172	15.0	0.40	28.0	20.660	29.890	29.147	22.265	-23.850	-397.197	37.975	0.0	0.000
173	15.0	0.40	30.0	20.660	29.890	31.291	22.786	-23.850	-397.197	37.975	0.0	0.000
174	15.0	0.40	32.0	20.660	29.890	33.455	23.319	-23.851	-397.197	37.975	0.0	0.000
175	15.0	0.40	34.0	20.660	29.890	35.636	23.862	-23.849	-397.197	37.975	0.0	0.000
176	15.0	0.40	36.0	20.660	29.890	37.842	24.419	-23.851	-397.197	37.975	0.0	0.000
177	15.0	0.40	38.0	20.660	29.890	40.065	24.985	-23.849	-397.197	37.975	0.0	0.000

178	15.0	0.40	40.0	20.660	29.890	42.312	25.568	-23.852	-397.197	37.975	0.0	0.000
179	-15.0	-0.10	16.0	20.660	29.890	-80.663	-20.096	137.953	395.666	-37.185	0.0	0.036
180	-15.0	-0.08	16.0	20.660	29.890	-74.521	-14.893	137.931	392.244	-36.798	0.0	0.005
181	-15.0	-0.06	16.0	20.660	29.890	-68.699	-12.609	137.944	392.263	-36.556	0.0	0.000
182	-15.0	-0.04	16.0	20.660	29.890	-64.054	-10.594	137.922	392.263	-36.558	0.0	0.000
183	-15.0	-0.02	16.0	20.660	29.890	-58.578	-8.864	137.941	392.234	-36.770	0.0	0.000
184	-15.0	0.00	16.0	20.660	29.890	-53.894	-8.053	137.916	395.678	-37.205	0.0	0.000
185	-15.0	0.00	16.0	20.660	29.890	10.180	1.314	-23.851	394.769	-37.063	1.0	0.992
186	-15.0	0.02	16.0	20.660	29.890	10.246	1.384	-23.851	391.184	-36.473	1.0	0.992
187	-15.0	0.04	16.0	20.660	29.890	10.420	2.126	-23.850	391.169	-36.378	1.0	0.996
188	-15.0	0.06	16.0	20.660	29.890	10.610	2.886	-23.850	391.538	-36.427	1.0	0.998
189	-15.0	0.08	16.0	20.660	29.890	10.796	3.638	-23.852	391.166	-36.400	1.0	0.999
190	-15.0	0.10	16.0	20.660	29.890	11.020	4.490	-23.851	391.169	-36.482	1.0	1.000
191	-15.0	0.15	16.0	20.660	29.890	11.520	6.298	-23.851	391.175	-36.451	1.0	1.000
192	-15.0	0.20	16.0	20.660	29.890	12.531	8.904	-23.850	392.169	-36.503	1.0	1.000
193	-15.0	0.25	16.0	20.660	29.890	13.086	10.912	-23.852	391.053	-36.313	1.0	1.000
194	-15.0	0.30	16.0	20.660	29.890	14.938	13.075	-23.850	391.172	-36.433	1.0	1.000
195	-15.0	0.35	16.0	20.660	29.890	16.322	15.118	-23.851	390.778	-36.363	1.0	1.000
196	-15.0	0.40	16.0	20.660	29.890	15.585	17.037	-23.852	390.822	-36.325	1.0	1.000
197	-15.0	0.45	16.0	20.660	29.890	17.045	19.126	-23.850	390.778	-36.357	1.0	1.000
198	-15.0	0.50	16.0	20.660	29.890	19.952	21.095	-23.851	391.134	-36.362	1.0	1.000
199	-15.0	0.55	16.0	20.660	29.890	22.304	22.036	-23.850	390.822	-36.327	1.0	1.000
200	-15.0	0.60	16.0	20.660	29.890	24.161	23.324	-23.850	391.041	-36.312	1.0	1.000
201	-15.0	0.65	16.0	20.660	29.890	24.716	26.875	-23.850	390.987	-36.301	1.0	1.000
202	-15.0	0.70	16.0	20.660	29.890	27.503	28.561	-23.852	391.231	-36.492	1.0	1.000
203	-15.0	0.72	16.0	20.660	29.890	27.503	28.561	-23.852	391.231	-36.492	1.0	1.000
204	-15.0	0.74	16.0	20.660	29.890	29.325	30.326	-23.851	391.191	-36.479	1.0	1.000
205	-15.0	0.76	16.0	20.660	29.890	31.596	29.935	-23.850	391.125	-36.372	1.0	1.000
206	-15.0	0.78	16.0	20.660	29.890	32.392	31.032	-23.852	391.556	-36.430	1.0	1.000
207	-15.0	0.80	16.0	20.660	29.890	34.556	31.257	-23.852	392.237	-36.684	1.0	0.988
208	-15.0	0.82	16.0	20.660	29.890	36.782	31.461	-23.851	391.328	-36.515	0.0	0.595
209	-15.0	0.84	16.0	20.660	29.890	38.587	32.396	-23.850	391.225	-36.524	0.0	0.081
210	-15.0	0.86	16.0	20.660	29.890	41.282	32.662	-23.845	391.303	-36.522	0.0	0.001
211	-15.0	0.88	16.0	20.660	29.890	43.201	33.517	-23.853	391.384	-36.449	0.0	0.000
212	-15.0	0.90	16.0	20.660	29.890	45.544	34.108	-23.852	391.337	-36.517	0.0	0.000
213	-15.0	0.92	16.0	20.660	29.890	48.623	34.534	-23.853	391.297	-36.452	0.0	0.000
214	-15.0	0.94	16.0	20.660	29.890	51.781	34.960	-23.853	391.756	-36.340	0.0	0.000
215	-15.0	0.96	16.0	20.660	29.890	55.332	35.320	-23.853	391.284	-36.464	0.0	0.000
216	-15.0	0.98	16.0	20.660	29.890	59.283	35.768	-23.843	391.334	-36.515	0.0	0.000

217	-15.0	1.00	16.0	20.660	29.890	60.480	36.420	-23.850	395.597	-37.313	0.0	0.000
218	15.0	-0.10	16.0	20.660	29.890	-56.400	7.319	137.925	-401.319	37.353	0.0	0.000
219	15.0	-0.08	16.0	20.660	29.890	-55.184	7.833	137.947	-397.734	37.787	0.0	0.000
220	15.0	-0.06	16.0	20.660	29.890	-51.145	7.565	137.956	-397.850	37.859	0.0	0.000
221	15.0	-0.04	16.0	20.660	29.890	-47.529	7.415	137.934	-397.853	37.866	0.0	0.000
222	15.0	-0.02	16.0	20.660	29.890	-44.417	7.398	137.934	-397.709	37.817	0.0	0.000
223	15.0	0.00	16.0	20.660	29.890	-41.710	6.693	137.922	-401.325	37.368	0.0	0.000
224	15.0	0.00	16.0	20.660	29.890	10.580	2.142	-23.851	-401.953	37.478	1.0	0.999
225	15.0	0.02	16.0	20.660	29.890	10.650	2.229	-23.851	-397.747	37.840	1.0	0.999
226	15.0	0.04	16.0	20.660	29.890	10.850	3.012	-23.850	-397.706	37.913	1.0	0.999
227	15.0	0.06	16.0	20.660	29.890	11.063	3.816	-23.851	-398.250	37.997	1.0	1.000
228	15.0	0.08	16.0	20.660	29.890	11.279	4.611	-23.852	-397.737	37.958	1.0	1.000
229	15.0	0.10	16.0	20.660	29.890	11.523	5.524	-23.851	-397.713	37.874	1.0	1.000
230	15.0	0.15	16.0	20.660	29.890	12.110	7.445	-23.852	-397.744	37.886	1.0	1.000
231	15.0	0.20	16.0	20.660	29.890	13.170	10.331	-23.851	-398.788	37.760	1.0	1.000
232	15.0	0.25	16.0	20.660	29.890	13.808	12.508	-23.850	-397.531	38.083	1.0	1.000
233	15.0	0.30	16.0	20.660	29.890	15.900	15.089	-23.850	-397.731	37.929	1.0	1.000
234	15.0	0.35	16.0	20.660	29.890	17.503	17.499	-23.850	-397.225	37.971	1.0	0.997
235	15.0	0.40	16.0	20.660	29.890	16.696	19.362	-23.851	-397.197	37.975	1.0	1.000
236	15.0	0.45	16.0	20.660	29.890	18.389	21.865	-23.852	-397.316	37.914	1.0	0.999
237	15.0	0.50	16.0	20.660	29.890	21.845	24.615	-23.852	-397.537	38.087	1.0	0.997
238	15.0	0.55	16.0	20.660	29.890	24.994	26.107	-23.851	-397.250	37.945	1.0	0.976
239	15.0	0.60	16.0	20.660	29.890	27.530	27.901	-23.850	-397.331	37.942	1.0	0.954
240	15.0	0.65	16.0	20.660	29.890	27.771	32.125	-23.851	-397.284	37.918	1.0	1.000
241	15.0	0.70	16.0	20.660	29.890	31.426	34.818	-23.853	-397.625	37.953	1.0	1.000
242	15.0	0.72	16.0	20.660	29.890	32.330	36.303	-23.849	-397.297	38.006	1.0	1.000
243	15.0	0.74	16.0	20.660	29.890	33.699	37.448	-23.851	-397.331	37.966	1.0	0.999
244	15.0	0.76	16.0	20.660	29.890	37.157	37.696	-23.851	-397.312	37.961	1.0	0.977
245	15.0	0.78	16.0	20.660	29.890	38.134	39.200	-23.851	-397.841	37.779	1.0	0.976
246	15.0	0.80	16.0	20.660	29.890	41.355	40.209	-23.855	-398.572	37.917	0.0	0.510
247	15.0	0.82	16.0	20.660	29.890	44.621	41.366	-23.850	-397.697	37.870	0.0	0.013
248	15.0	0.84	16.0	20.660	29.890	47.101	43.338	-23.849	-397.603	38.024	0.0	0.001
249	15.0	0.86	16.0	20.660	29.890	51.254	44.845	-23.848	-397.728	37.877	0.0	0.000
250	15.0	0.88	16.0	20.660	29.890	54.051	46.870	-23.852	-397.753	37.839	0.0	0.000
251	15.0	0.90	16.0	20.660	29.890	57.679	48.829	-23.848	-397.741	37.875	0.0	0.000
252	15.0	0.92	16.0	20.660	29.890	62.619	51.116	-23.854	-397.572	37.978	0.0	0.000
253	15.0	0.94	16.0	20.660	29.890	67.959	53.451	-23.841	-397.841	37.798	0.0	0.000
254	15.0	0.96	16.0	20.660	29.890	74.068	56.365	-23.848	-397.609	38.021	0.0	0.000
255	15.0	0.98	16.0	20.660	29.890	81.119	59.896	-23.850	-397.638	37.946	0.0	0.000

256	15.0	1.00	16.0	20.660	29.890	83.197	61.157	-23.857	-401.831	37.539	0.0	0.000
1	-25.0	-0.10	6.0	20.660	29.890	-28.009	-11.099	137.928	238.316	-5.595	0.0	0.000
2	-25.0	-0.08	6.0	20.660	29.890	-27.263	-10.020	137.925	236.066	-5.118	0.0	0.000
3	-25.0	-0.06	6.0	20.660	29.890	-24.677	-8.390	137.909	236.003	-5.133	0.0	0.000
4	-25.0	-0.04	6.0	20.660	29.890	-22.455	-6.918	137.925	236.003	-5.134	0.0	0.000
5	-25.0	-0.02	6.0	20.660	29.890	-20.581	-5.604	137.928	236.100	-5.128	0.0	0.000
6	-25.0	0.00	6.0	20.660	29.890	-19.027	-5.111	137.925	238.306	-5.574	0.0	0.000
7	-25.0	0.00	6.0	20.660	29.890	3.841	0.837	-23.855	237.947	-5.016	1.0	1.000
8	-25.0	0.02	6.0	20.660	29.890	3.887	0.911	-23.853	235.500	-5.108	1.0	1.000
9	-25.0	0.04	6.0	20.660	29.890	3.964	1.640	-23.855	235.497	-5.143	1.0	1.000
10	-25.0	0.06	6.0	20.660	29.890	4.046	2.391	-23.855	235.869	-5.086	1.0	1.000
11	-25.0	0.08	6.0	20.660	29.890	4.121	3.143	-23.856	235.491	-5.151	1.0	1.000
12	-25.0	0.10	6.0	20.660	29.890	4.227	3.988	-23.857	235.509	-5.093	1.0	1.000
13	-25.0	0.15	6.0	20.660	29.890	4.422	5.788	-23.858	235.503	-5.108	1.0	1.000
14	-25.0	0.20	6.0	20.660	29.890	5.009	8.358	-23.861	236.131	-5.105	1.0	1.000
15	-25.0	0.25	6.0	20.660	29.890	5.174	10.324	-23.864	235.441	-5.083	1.0	1.000
16	-25.0	0.30	6.0	20.660	29.890	6.507	12.630	-23.863	235.447	-5.111	1.0	1.000
17	-25.0	0.35	6.0	20.660	29.890	7.338	14.758	-23.864	235.409	-5.134	1.0	1.000
18	-25.0	0.40	6.0	20.660	29.890	6.174	16.328	-23.868	235.365	-5.137	1.0	1.000
19	-25.0	0.45	6.0	20.660	29.890	7.025	18.484	-23.866	235.409	-5.135	1.0	1.000
20	-25.0	0.50	6.0	20.660	29.890	9.106	20.794	-23.865	235.459	-5.115	1.0	1.000
21	-25.0	0.55	6.0	20.660	29.890	10.392	22.286	-23.858	235.391	-5.148	1.0	1.000
22	-25.0	0.60	6.0	20.660	29.890	11.231	23.873	-23.855	235.428	-5.111	1.0	1.000
23	-25.0	0.65	6.0	20.660	29.890	11.058	26.728	-23.862	235.375	-5.120	1.0	1.000
24	-25.0	0.70	6.0	20.660	29.890	12.375	28.725	-23.860	235.506	-5.078	1.0	1.000
25	-25.0	0.72	6.0	20.660	29.890	12.601	29.677	-23.860	235.481	-5.122	1.0	1.000
26	-25.0	0.74	6.0	20.660	29.890	13.020	30.456	-23.861	235.462	-5.104	1.0	1.000
27	-25.0	0.76	6.0	20.660	29.890	14.012	30.947	-23.856	235.462	-5.105	1.0	1.000
28	-25.0	0.78	6.0	20.660	29.890	14.577	31.724	-23.854	235.947	-5.128	1.0	0.999
29	-25.0	0.80	6.0	20.660	29.890	15.445	32.474	-23.853	236.200	-5.060	1.0	0.986
30	-25.0	0.82	6.0	20.660	29.890	16.347	33.052	-23.855	235.644	-5.042	0.0	0.883
31	-25.0	0.84	6.0	20.660	29.890	16.957	34.092	-23.851	235.531	-5.066	0.0	0.239
32	-25.0	0.86	6.0	20.660	29.890	18.129	34.673	-23.851	235.647	-5.029	0.0	0.047
33	-25.0	0.88	6.0	20.660	29.890	18.816	35.641	-23.851	235.675	-4.998	0.0	0.004
34	-25.0	0.90	6.0	20.660	29.890	19.785	36.451	-23.852	235.638	-5.047	0.0	0.000
35	-25.0	0.92	6.0	20.660	29.890	21.023	37.164	-23.852	235.606	-5.080	0.0	0.000
36	-25.0	0.94	6.0	20.660	29.890	22.342	37.926	-23.856	235.953	-5.089	0.0	0.000
37	-25.0	0.96	6.0	20.660	29.890	23.799	38.623	-23.850	235.622	-5.071	0.0	0.000
38	-25.0	0.98	6.0	20.660	29.890	25.398	39.437	-23.852	235.634	-5.048	0.0	0.000

---

39	-25.0	1.00	6.0	20.660	29.890	25.923	40.271	-23.847	238.109	-5.051	0.0	0.000
40	-25.0	0.40	0.0	20.660	29.890	0.492	16.222	-23.875	235.365	-5.137	1.0	1.000
41	-25.0	0.40	0.2	20.660	29.890	0.683	16.228	-23.878	235.365	-5.137	1.0	1.000
42	-25.0	0.40	0.4	20.660	29.890	0.879	16.235	-23.880	235.365	-5.137	1.0	1.000
43	-25.0	0.40	0.6	20.660	29.890	1.074	16.241	-23.883	235.365	-5.137	1.0	1.000
44	-25.0	0.40	0.8	20.660	29.890	1.268	16.247	-23.885	235.365	-5.137	1.0	1.000
45	-25.0	0.40	1.0	20.660	29.890	1.462	16.252	-23.888	235.365	-5.137	1.0	1.000
46	-25.0	0.40	1.2	20.660	29.890	1.656	16.256	-23.888	235.365	-5.137	1.0	1.000
47	-25.0	0.40	1.4	20.660	29.890	1.848	16.260	-23.887	235.365	-5.137	1.0	1.000
48	-25.0	0.40	1.6	20.660	29.890	2.041	16.264	-23.890	235.365	-5.137	1.0	1.000
49	-25.0	0.40	1.8	20.660	29.890	2.232	16.268	-23.889	235.365	-5.137	1.0	1.000
50	-25.0	0.40	2.0	20.660	29.890	2.424	16.272	-23.890	235.365	-5.137	1.0	1.000
51	-25.0	0.40	2.5	20.660	29.890	2.901	16.281	-23.889	235.365	-5.137	1.0	1.000
52	-25.0	0.40	3.0	20.660	29.890	3.375	16.289	-23.887	235.365	-5.137	1.0	1.000
53	-25.0	0.40	3.5	20.660	29.890	3.846	16.295	-23.882	235.365	-5.137	1.0	1.000
54	-25.0	0.40	4.0	20.660	29.890	4.315	16.302	-23.879	235.365	-5.137	1.0	1.000
55	-25.0	0.40	6.0	20.660	29.890	6.174	16.328	-23.868	235.365	-5.137	1.0	1.000
56	-25.0	0.40	8.0	20.660	29.890	8.006	16.354	-23.860	235.365	-5.137	1.0	1.000
57	-25.0	0.40	10.0	20.660	29.890	9.811	16.378	-23.855	235.365	-5.137	1.0	1.000
58	-25.0	0.40	12.0	20.660	29.890	11.589	16.399	-23.854	235.365	-5.137	1.0	1.000
59	-25.0	0.40	14.0	20.660	29.890	13.340	16.417	-23.851	235.365	-5.137	1.0	1.000
60	-25.0	0.40	16.0	20.660	29.890	15.065	16.433	-23.850	235.365	-5.137	1.0	1.000
61	-25.0	0.40	18.0	20.660	29.890	16.764	16.446	-23.852	235.365	-5.137	1.0	1.000
62	-25.0	0.40	18.5	20.660	29.890	17.184	16.447	-23.849	235.365	-5.137	1.0	1.000
63	-25.0	0.40	19.0	20.660	29.890	17.603	16.452	-23.849	235.365	-5.137	1.0	1.000
64	-25.0	0.40	19.2	20.660	29.890	17.769	16.454	-23.851	235.365	-5.137	1.0	1.000
65	-25.0	0.40	19.4	20.660	29.890	17.937	16.454	-23.851	235.365	-5.137	1.0	0.999
66	-25.0	0.40	19.6	20.660	29.890	18.103	16.455	-23.849	235.365	-5.137	1.0	0.999
67	-25.0	0.40	19.8	20.660	29.890	18.269	16.456	-23.850	235.365	-5.137	1.0	0.998
68	-25.0	0.40	20.0	20.660	29.890	18.436	16.456	-23.851	235.365	-5.137	1.0	0.996
69	-25.0	0.40	20.2	20.660	29.890	18.603	16.456	-23.850	235.365	-5.137	0.0	0.993
70	-25.0	0.40	20.4	20.660	29.890	18.767	16.458	-23.851	235.365	-5.137	0.0	0.987
71	-25.0	0.40	20.6	20.660	29.890	18.934	16.458	-23.851	235.365	-5.137	0.0	0.978
72	-25.0	0.40	20.8	20.660	29.890	19.097	16.460	-23.850	235.365	-5.137	0.0	0.962
73	-25.0	0.40	21.0	20.660	29.890	19.263	16.461	-23.851	235.365	-5.137	0.0	0.934
74	-25.0	0.40	21.5	20.660	29.890	19.674	16.463	-23.850	235.365	-5.137	0.0	0.778
75	-25.0	0.40	22.0	20.660	29.890	20.084	16.464	-23.850	235.365	-5.137	0.0	0.465
76	-25.0	0.40	22.5	20.660	29.890	20.492	16.465	-23.850	235.365	-5.137	0.0	0.180
77	-25.0	0.40	23.0	20.660	29.890	20.897	16.467	-23.850	235.365	-5.137	0.0	0.054

78	-25.0	0.40	23.5	20.660	29.890	21.304	16.468	-23.852	235.365	-5.137	0.0	0.015
79	-25.0	0.40	24.0	20.660	29.890	21.707	16.468	-23.851	235.365	-5.137	0.0	0.004
80	-25.0	0.40	24.5	20.660	29.890	22.108	16.470	-23.849	235.365	-5.137	0.0	0.001
81	-25.0	0.40	25.0	20.660	29.890	22.509	16.470	-23.851	235.365	-5.137	0.0	0.000
82	-25.0	0.40	26.0	20.660	29.890	23.305	16.472	-23.850	235.365	-5.137	0.0	0.000
83	-25.0	0.40	28.0	20.660	29.890	24.881	16.473	-23.851	235.365	-5.137	0.0	0.000
84	-25.0	0.40	30.0	20.660	29.890	26.434	16.467	-23.849	235.365	-5.137	0.0	0.000
85	-25.0	0.40	32.0	20.660	29.890	27.965	16.464	-23.850	235.365	-5.137	0.0	0.000
86	-25.0	0.40	34.0	20.660	29.890	29.472	16.459	-23.850	235.365	-5.137	0.0	0.000
87	-25.0	0.40	36.0	20.660	29.890	30.958	16.448	-23.849	235.365	-5.137	0.0	0.000
88	-25.0	0.40	38.0	20.660	29.890	32.426	16.438	-23.851	235.365	-5.137	0.0	0.000
89	-25.0	0.40	40.0	20.660	29.890	33.870	16.426	-23.851	235.365	-5.137	0.0	0.000
90	25.0	-0.10	6.0	20.660	29.890	-21.639	2.763	137.950	-236.409	39.131	0.0	0.000
91	25.0	-0.08	6.0	20.660	29.890	-21.142	3.434	137.941	-234.297	39.587	0.0	0.000
92	25.0	-0.06	6.0	20.660	29.890	-19.532	3.608	137.931	-234.216	39.580	0.0	0.000
93	25.0	-0.04	6.0	20.660	29.890	-18.098	3.840	137.922	-234.213	39.581	0.0	0.000
94	25.0	-0.02	6.0	20.660	29.890	-16.871	4.144	137.919	-234.303	39.587	0.0	0.000
95	25.0	0.00	6.0	20.660	29.890	-15.790	3.754	137.922	-236.406	39.138	0.0	0.000
96	25.0	0.00	6.0	20.660	29.890	3.907	1.289	-23.853	-236.619	39.782	1.0	1.000
97	25.0	0.02	6.0	20.660	29.890	3.948	1.371	-23.853	-234.156	39.598	1.0	1.000
98	25.0	0.04	6.0	20.660	29.890	4.051	2.119	-23.854	-234.087	39.629	1.0	1.000
99	25.0	0.06	6.0	20.660	29.890	4.160	2.891	-23.854	-234.409	39.573	1.0	1.000
100	25.0	0.08	6.0	20.660	29.890	4.272	3.664	-23.854	-234.087	39.622	1.0	1.000
101	25.0	0.10	6.0	20.660	29.890	4.395	4.540	-23.855	-234.150	39.592	1.0	1.000
102	25.0	0.15	6.0	20.660	29.890	4.697	6.391	-23.855	-234.122	39.592	1.0	1.000
103	25.0	0.20	6.0	20.660	29.890	5.281	9.124	-23.857	-234.722	39.653	1.0	1.000
104	25.0	0.25	6.0	20.660	29.890	5.544	11.155	-23.858	-233.956	39.546	1.0	1.000
105	25.0	0.30	6.0	20.660	29.890	6.978	13.813	-23.858	-234.044	39.563	1.0	1.000
106	25.0	0.35	6.0	20.660	29.890	7.933	16.212	-23.858	-233.825	39.549	1.0	1.000
107	25.0	0.40	6.0	20.660	29.890	6.925	17.493	-23.860	-233.825	39.544	1.0	1.000
108	25.0	0.45	6.0	20.660	29.890	7.914	19.928	-23.857	-233.803	39.521	1.0	1.000
109	25.0	0.50	6.0	20.660	29.890	10.196	22.959	-23.856	-233.988	39.541	1.0	1.000
110	25.0	0.55	6.0	20.660	29.890	11.932	24.947	-23.854	-233.822	39.524	1.0	1.000
111	25.0	0.60	6.0	20.660	29.890	13.199	26.902	-23.853	-233.828	39.507	1.0	1.000
112	25.0	0.65	6.0	20.660	29.890	12.805	29.868	-23.853	-233.822	39.525	1.0	1.000
113	25.0	0.70	6.0	20.660	29.890	14.486	32.542	-23.854	-233.962	39.536	1.0	1.000
114	25.0	0.72	6.0	20.660	29.890	14.708	33.669	-23.853	-233.959	39.563	1.0	1.000
115	25.0	0.74	6.0	20.660	29.890	15.267	34.694	-23.855	-233.941	39.529	1.0	1.000
116	25.0	0.76	6.0	20.660	29.890	16.648	35.726	-23.851	-233.941	39.525	1.0	1.000

117	25.0	0.78	6.0	20.660	29.890	17.432	36.800	-23.853	-234.284	39.589	1.0	1.000
118	25.0	0.80	6.0	20.660	29.890	18.619	38.088	-23.853	-234.663	39.637	1.0	0.999
119	25.0	0.82	6.0	20.660	29.890	19.748	39.273	-23.850	-234.138	39.511	0.0	0.992
120	25.0	0.84	6.0	20.660	29.890	20.391	40.817	-23.849	-233.997	39.496	0.0	0.854
121	25.0	0.86	6.0	20.660	29.890	21.982	42.205	-23.849	-234.062	39.539	0.0	0.322
122	25.0	0.88	6.0	20.660	29.890	22.770	43.754	-23.848	-234.125	39.520	0.0	0.018
123	25.0	0.90	6.0	20.660	29.890	23.985	45.344	-23.851	-234.044	39.526	0.0	0.001
124	25.0	0.92	6.0	20.660	29.890	25.562	47.089	-23.846	-234.000	39.521	0.0	0.000
125	25.0	0.94	6.0	20.660	29.890	27.381	48.969	-23.848	-234.294	39.629	0.0	0.000
126	25.0	0.96	6.0	20.660	29.890	29.198	51.052	-23.852	-234.000	39.506	0.0	0.000
127	25.0	0.98	6.0	20.660	29.890	31.209	53.469	-23.850	-234.050	39.525	0.0	0.000
128	25.0	1.00	6.0	20.660	29.890	31.995	54.708	-23.846	-236.581	39.772	0.0	0.000
129	25.0	0.40	0.0	20.660	29.890	1.291	16.039	-23.865	-233.825	39.544	1.0	1.000
130	25.0	0.40	0.2	20.660	29.890	1.473	16.086	-23.867	-233.825	39.544	1.0	1.000
131	25.0	0.40	0.4	20.660	29.890	1.660	16.133	-23.870	-233.825	39.544	1.0	1.000
132	25.0	0.40	0.6	20.660	29.890	1.846	16.181	-23.869	-233.825	39.544	1.0	1.000
133	25.0	0.40	0.8	20.660	29.890	2.033	16.230	-23.872	-233.825	39.544	1.0	1.000
134	25.0	0.40	1.0	20.660	29.890	2.219	16.277	-23.873	-233.825	39.544	1.0	1.000
135	25.0	0.40	1.2	20.660	29.890	2.406	16.324	-23.873	-233.825	39.544	1.0	1.000
136	25.0	0.40	1.4	20.660	29.890	2.593	16.372	-23.875	-233.825	39.544	1.0	1.000
137	25.0	0.40	1.6	20.660	29.890	2.779	16.419	-23.873	-233.825	39.544	1.0	1.000
138	25.0	0.40	1.8	20.660	29.890	2.965	16.467	-23.874	-233.825	39.544	1.0	1.000
139	25.0	0.40	2.0	20.660	29.890	3.151	16.514	-23.874	-233.825	39.544	1.0	1.000
140	25.0	0.40	2.5	20.660	29.890	3.618	16.633	-23.873	-233.825	39.544	1.0	1.000
141	25.0	0.40	3.0	20.660	29.890	4.087	16.753	-23.871	-233.825	39.544	1.0	1.000
142	25.0	0.40	3.5	20.660	29.890	4.556	16.874	-23.869	-233.825	39.544	1.0	1.000
143	25.0	0.40	4.0	20.660	29.890	5.026	16.995	-23.867	-233.825	39.544	1.0	1.000
144	25.0	0.40	6.0	20.660	29.890	6.925	17.493	-23.860	-233.825	39.544	1.0	1.000
145	25.0	0.40	8.0	20.660	29.890	8.853	18.013	-23.856	-233.825	39.544	1.0	1.000
146	25.0	0.40	10.0	20.660	29.890	10.810	18.552	-23.851	-233.825	39.544	1.0	1.000
147	25.0	0.40	12.0	20.660	29.890	12.797	19.115	-23.852	-233.825	39.544	1.0	1.000
148	25.0	0.40	14.0	20.660	29.890	14.812	19.698	-23.853	-233.825	39.544	1.0	1.000
149	25.0	0.40	16.0	20.660	29.890	16.855	20.304	-23.851	-233.825	39.544	1.0	1.000
150	25.0	0.40	18.0	20.660	29.890	18.929	20.928	-23.850	-233.825	39.544	1.0	0.995
151	25.0	0.40	18.5	20.660	29.890	19.453	21.089	-23.850	-233.825	39.544	1.0	0.986
152	25.0	0.40	19.0	20.660	29.890	19.976	21.252	-23.849	-233.825	39.544	1.0	0.961
153	25.0	0.40	19.2	20.660	29.890	20.188	21.316	-23.851	-233.825	39.544	1.0	0.942
154	25.0	0.40	19.4	20.660	29.890	20.398	21.384	-23.850	-233.825	39.544	1.0	0.916
155	25.0	0.40	19.6	20.660	29.890	20.609	21.447	-23.849	-233.825	39.544	1.0	0.879



156	25.0	0.40	19.8	20.660	29.890	20.823	21.515	-23.853	-233.825	39.544	1.0	0.830
157	25.0	0.40	20.0	20.660	29.890	21.034	21.579	-23.851	-233.825	39.544	1.0	0.765
158	25.0	0.40	20.2	20.660	29.890	21.244	21.646	-23.848	-233.825	39.544	0.0	0.688
159	25.0	0.40	20.4	20.660	29.890	21.455	21.714	-23.848	-233.825	39.544	0.0	0.598
160	25.0	0.40	20.6	20.660	29.890	21.668	21.782	-23.851	-233.825	39.544	0.0	0.502
161	25.0	0.40	20.8	20.660	29.890	21.883	21.847	-23.851	-233.825	39.544	0.0	0.403
162	25.0	0.40	21.0	20.660	29.890	22.095	21.915	-23.850	-233.825	39.544	0.0	0.314
163	25.0	0.40	21.5	20.660	29.890	22.631	22.085	-23.852	-233.825	39.544	0.0	0.148
164	25.0	0.40	22.0	20.660	29.890	23.165	22.256	-23.851	-233.825	39.544	0.0	0.062
165	25.0	0.40	22.5	20.660	29.890	23.704	22.426	-23.848	-233.825	39.544	0.0	0.025
166	25.0	0.40	23.0	20.660	29.890	24.245	22.602	-23.850	-233.825	39.544	0.0	0.010
167	25.0	0.40	23.5	20.660	29.890	24.786	22.776	-23.851	-233.825	39.544	0.0	0.004
168	25.0	0.40	24.0	20.660	29.890	25.330	22.955	-23.850	-233.825	39.544	0.0	0.002
169	25.0	0.40	24.5	20.660	29.890	25.875	23.135	-23.850	-233.825	39.544	0.0	0.001
170	25.0	0.40	25.0	20.660	29.890	26.423	23.316	-23.850	-233.825	39.544	0.0	0.000
171	25.0	0.40	26.0	20.660	29.890	27.526	23.683	-23.852	-233.825	39.544	0.0	0.000
172	25.0	0.40	28.0	20.660	29.890	29.753	24.436	-23.852	-233.825	39.544	0.0	0.000
173	25.0	0.40	30.0	20.660	29.890	32.011	25.215	-23.851	-233.825	39.544	0.0	0.000
174	25.0	0.40	32.0	20.660	29.890	34.304	26.025	-23.851	-233.825	39.544	0.0	0.000
175	25.0	0.40	34.0	20.660	29.890	36.630	26.864	-23.852	-233.825	39.544	0.0	0.000
176	25.0	0.40	36.0	20.660	29.890	38.987	27.734	-23.851	-233.825	39.544	0.0	0.000
177	25.0	0.40	38.0	20.660	29.890	41.378	28.638	-23.851	-233.825	39.544	0.0	0.000
178	25.0	0.40	40.0	20.660	29.890	43.803	29.572	-23.848	-233.825	39.544	0.0	0.000
179	-25.0	-0.10	16.0	20.660	29.890	-89.493	-32.472	137.906	238.316	-5.595	0.0	0.000
180	-25.0	-0.08	16.0	20.660	29.890	-86.979	-30.628	137.913	236.066	-5.118	0.0	0.000
181	-25.0	-0.06	16.0	20.660	29.890	-77.491	-25.735	137.934	236.003	-5.133	0.0	0.000
182	-25.0	-0.04	16.0	20.660	29.890	-69.583	-21.712	137.928	236.003	-5.134	0.0	0.000
183	-25.0	-0.02	16.0	20.660	29.890	-63.141	-18.457	137.931	236.100	-5.128	0.0	0.000
184	-25.0	0.00	16.0	20.660	29.890	-57.691	-16.390	137.922	238.306	-5.574	0.0	0.000
185	-25.0	0.00	16.0	20.660	29.890	9.984	1.094	-23.851	237.947	-5.016	1.0	0.975
186	-25.0	0.02	16.0	20.660	29.890	10.050	1.160	-23.851	235.500	-5.108	1.0	0.974
187	-25.0	0.04	16.0	20.660	29.890	10.217	1.891	-23.850	235.497	-5.143	1.0	0.987
188	-25.0	0.06	16.0	20.660	29.890	10.398	2.639	-23.851	235.869	-5.086	1.0	0.994
189	-25.0	0.08	16.0	20.660	29.890	10.567	3.381	-23.851	235.491	-5.151	1.0	0.997
190	-25.0	0.10	16.0	20.660	29.890	10.780	4.216	-23.851	235.509	-5.093	1.0	0.999
191	-25.0	0.15	16.0	20.660	29.890	11.241	5.996	-23.850	235.503	-5.108	1.0	1.000
192	-25.0	0.20	16.0	20.660	29.890	12.218	8.524	-23.849	236.131	-5.105	1.0	1.000
193	-25.0	0.25	16.0	20.660	29.890	12.733	10.488	-23.851	235.441	-5.083	1.0	1.000
194	-25.0	0.30	16.0	20.660	29.890	14.484	12.552	-23.851	235.447	-5.111	1.0	1.000

195	-25.0	0.35	16.0	20.660	29.890	15.777	14.508	-23.850	235.409	-5.134	1.0	1.000
196	-25.0	0.40	16.0	20.660	29.890	15.065	16.433	-23.850	235.365	-5.137	1.0	1.000
197	-25.0	0.45	16.0	20.660	29.890	16.426	18.422	-23.851	235.409	-5.135	1.0	1.000
198	-25.0	0.50	16.0	20.660	29.890	19.124	20.225	-23.853	235.459	-5.115	1.0	1.000
199	-25.0	0.55	16.0	20.660	29.890	21.226	21.084	-23.851	235.391	-5.148	1.0	1.000
200	-25.0	0.60	16.0	20.660	29.890	22.873	22.287	-23.849	235.428	-5.111	1.0	1.000
201	-25.0	0.65	16.0	20.660	29.890	23.449	25.635	-23.851	235.375	-5.120	1.0	1.000
202	-25.0	0.70	16.0	20.660	29.890	25.946	27.137	-23.850	235.506	-5.078	1.0	1.000
203	-25.0	0.72	16.0	20.660	29.890	26.672	28.093	-23.851	235.481	-5.122	1.0	1.000
204	-25.0	0.74	16.0	20.660	29.890	27.591	28.722	-23.848	235.462	-5.104	1.0	0.997
205	-25.0	0.76	16.0	20.660	29.890	29.536	28.278	-23.849	235.462	-5.105	1.0	0.959
206	-25.0	0.78	16.0	20.660	29.890	30.260	29.291	-23.851	235.947	-5.128	1.0	0.827
207	-25.0	0.80	16.0	20.660	29.890	32.129	29.414	-23.851	236.200	-5.060	0.0	0.143
208	-25.0	0.82	16.0	20.660	29.890	34.059	29.487	-23.851	235.644	-5.042	0.0	0.004
209	-25.0	0.84	16.0	20.660	29.890	35.639	30.255	-23.848	235.531	-5.066	0.0	0.000
210	-25.0	0.86	16.0	20.660	29.890	37.951	30.370	-23.851	235.647	-5.029	0.0	0.000
211	-25.0	0.88	16.0	20.660	29.890	39.600	31.052	-23.850	235.675	-4.998	0.0	0.000
212	-25.0	0.90	16.0	20.660	29.890	41.592	31.477	-23.848	235.638	-5.047	0.0	0.000
213	-25.0	0.92	16.0	20.660	29.890	44.183	31.692	-23.853	235.606	-5.080	0.0	0.000
214	-25.0	0.94	16.0	20.660	29.890	46.807	31.935	-23.854	235.953	-5.089	0.0	0.000
215	-25.0	0.96	16.0	20.660	29.890	49.743	32.042	-23.845	235.622	-5.071	0.0	0.000
216	-25.0	0.98	16.0	20.660	29.890	52.972	32.212	-23.842	235.634	-5.048	0.0	0.000
217	-25.0	1.00	16.0	20.660	29.890	53.974	32.818	-23.850	238.109	-5.051	0.0	0.000
218	25.0	-0.10	16.0	20.660	29.890	-50.006	11.020	137.947	-236.409	39.131	0.0	0.000
219	25.0	-0.08	16.0	20.660	29.890	-48.993	11.466	137.941	-234.297	39.587	0.0	0.000
220	25.0	-0.06	16.0	20.660	29.890	-45.727	11.002	137.913	-234.216	39.580	0.0	0.000
221	25.0	-0.04	16.0	20.660	29.890	-42.773	10.653	137.925	-234.213	39.581	0.0	0.000
222	25.0	-0.02	16.0	20.660	29.890	-40.204	10.454	137.922	-234.303	39.587	0.0	0.000
223	25.0	-0.00	16.0	20.660	29.890	-37.963	9.590	137.919	-236.406	39.138	0.0	0.000
224	25.0	0.00	16.0	20.660	29.890	10.638	2.469	-23.851	-236.619	39.782	1.0	0.993
225	25.0	0.02	16.0	20.660	29.890	10.708	2.563	-23.850	-234.156	39.598	1.0	0.993
226	25.0	0.04	16.0	20.660	29.890	10.910	3.363	-23.850	-234.087	39.629	1.0	0.996
227	25.0	0.06	16.0	20.660	29.890	11.130	4.185	-23.852	-234.409	39.573	1.0	0.998
228	25.0	0.08	16.0	20.660	29.890	11.350	4.997	-23.851	-234.087	39.622	1.0	0.999
229	25.0	0.10	16.0	20.660	29.890	11.597	5.934	-23.850	-234.150	39.592	1.0	1.000
230	25.0	0.15	16.0	20.660	29.890	12.206	7.904	-23.850	-234.122	39.592	1.0	1.000
231	25.0	0.20	16.0	20.660	29.890	13.251	10.897	-23.852	-234.722	39.653	1.0	1.000
232	25.0	0.25	16.0	20.660	29.890	13.903	13.144	-23.851	-233.956	39.546	1.0	1.000
233	25.0	0.30	16.0	20.660	29.890	16.035	15.905	-23.849	-234.044	39.563	1.0	1.000

---

234	25.0	0.35	16.0	20.660	29.890	17.681	18.477	-23.850	-233.825	39.549	1.0	1.000
235	25.0	0.40	16.0	20.660	29.890	16.855	20.304	-23.851	-233.825	39.544	1.0	1.000
236	25.0	0.45	16.0	20.660	29.890	18.593	22.989	-23.853	-233.803	39.521	1.0	0.999
237	25.0	0.50	16.0	20.660	29.890	22.165	26.109	-23.851	-233.988	39.541	1.0	0.993
238	25.0	0.55	16.0	20.660	29.890	25.560	27.927	-23.850	-233.822	39.524	1.0	0.948
239	25.0	0.60	16.0	20.660	29.890	28.312	30.013	-23.850	-233.828	39.507	1.0	0.920
240	25.0	0.65	16.0	20.660	29.890	28.332	34.456	-23.850	-233.822	39.525	1.0	1.000
241	25.0	0.70	16.0	20.660	29.890	32.205	37.697	-23.851	-233.962	39.536	1.0	0.999
242	25.0	0.72	16.0	20.660	29.890	33.095	39.377	-23.852	-233.959	39.563	1.0	0.998
243	25.0	0.74	16.0	20.660	29.890	34.543	40.756	-23.852	-233.941	39.529	1.0	0.995
244	25.0	0.76	16.0	20.660	29.890	38.414	41.481	-23.850	-233.941	39.525	1.0	0.954
245	25.0	0.78	16.0	20.660	29.890	39.417	43.183	-23.847	-234.284	39.589	1.0	0.859
246	25.0	0.80	16.0	20.660	29.890	42.978	44.734	-23.851	-234.663	39.637	0.0	0.182
247	25.0	0.82	16.0	20.660	29.890	46.548	46.542	-23.852	-234.138	39.511	0.0	0.003
248	25.0	0.84	16.0	20.660	29.890	49.145	49.128	-23.849	-233.997	39.496	0.0	0.000
249	25.0	0.86	16.0	20.660	29.890	53.750	51.537	-23.850	-234.062	39.539	0.0	0.000
250	25.0	0.88	16.0	20.660	29.890	56.731	54.315	-23.850	-234.125	39.520	0.0	0.000
251	25.0	0.90	16.0	20.660	29.890	60.698	57.261	-23.851	-234.044	39.526	0.0	0.000
252	25.0	0.92	16.0	20.660	29.890	66.151	60.957	-23.848	-234.000	39.521	0.0	0.000
253	25.0	0.94	16.0	20.660	29.890	72.158	64.907	-23.847	-234.294	39.629	0.0	0.000
254	25.0	0.96	16.0	20.660	29.890	78.946	69.987	-23.856	-234.000	39.506	0.0	0.000
255	25.0	0.98	16.0	20.660	29.890	86.735	76.296	-23.853	-234.050	39.525	0.0	0.000
256	25.0	1.00	16.0	20.660	29.890	89.142	78.149	-23.857	-236.581	39.772	0.0	0.000

**PART B : TRAINING, TESTING AND RUNNING PATTERNS  
FOR NONLINEAR ARCING FAULT RESISTANCE MODEL**

TRAINING CASES

f = 2.22408      |g| = 0.0521562  
error = 0.146159      cost = 1.37857

No.	$\delta$	$\alpha$	$V_F$	$X_{SI}$	$X_{RI}$	$R_I$	$X_I$	$X_{SO}$	$R_{mem}$	$X_{mem}$	Target	Output
1	-30.0	0.1	0.01	18.446	25.904	0.331	3.850	-23.882	184.184	2.617	1.0	1.000
2	-30.0	0.5	0.01	18.446	25.904	3.032	21.084	-23.878	184.041	2.633	1.0	1.000
3	-30.0	0.7	0.01	18.446	25.904	3.824	29.627	-23.855	184.113	2.636	1.0	1.000
4	-30.0	0.1	0.09	18.446	25.904	2.358	3.986	-23.719	184.184	2.616	1.0	0.984
5	-30.0	0.5	0.09	18.446	25.904	7.263	20.625	-24.404	184.041	2.633	1.0	0.998
6	-30.0	0.7	0.09	18.446	25.904	9.235	29.065	-23.270	184.113	2.636	1.0	1.000
7	-30.0	0.1	0.01	18.446	31.189	0.337	3.865	-23.856	194.369	3.227	1.0	1.000
8	-30.0	0.5	0.01	18.446	31.189	3.051	21.139	-23.898	194.350	3.229	1.0	1.000
9	-30.0	0.7	0.01	18.446	31.189	3.864	29.754	-23.878	194.400	3.243	1.0	1.000
10	-30.0	0.1	0.09	18.446	31.189	2.375	3.971	-23.793	194.369	3.227	1.0	0.972
11	-30.0	0.5	0.09	18.446	31.189	7.316	20.681	-24.556	194.350	3.229	1.0	0.996
12	-30.0	0.7	0.09	18.446	31.189	9.331	29.283	-23.235	194.400	3.241	1.0	1.000
13	-30.0	0.1	0.01	26.157	25.904	0.350	3.818	-23.890	198.141	-2.575	1.0	1.000
14	-30.0	0.5	0.01	26.157	25.904	3.083	20.992	-23.846	198.069	-2.603	1.0	1.000
15	-30.0	0.7	0.01	26.157	25.904	3.889	29.476	-23.822	198.200	-2.599	1.0	1.000
16	-30.0	0.1	0.09	26.157	25.904	2.653	3.950	-23.816	198.141	-2.575	1.0	0.802
17	-30.0	0.5	0.09	26.157	25.904	7.656	20.666	-24.052	198.069	-2.603	1.0	0.980
18	-30.0	0.7	0.09	26.157	25.904	9.677	28.926	-23.192	198.200	-2.599	1.0	1.000
19	-30.0	0.1	0.01	26.157	31.189	0.352	3.834	-23.869	208.365	-2.042	1.0	1.000
20	-30.0	0.5	0.01	26.157	31.189	3.100	21.048	-23.871	208.256	-2.038	1.0	1.000
21	-30.0	0.7	0.01	26.157	31.189	3.923	29.614	-23.835	208.369	-2.050	1.0	1.000
22	-30.0	0.1	0.09	26.157	31.189	2.671	4.057	-23.559	208.365	-2.042	1.0	0.748
23	-30.0	0.5	0.09	26.157	31.189	7.698	20.671	-24.198	208.256	-2.038	1.0	0.960
24	-30.0	0.7	0.09	26.157	31.189	9.773	29.069	-23.137	208.369	-2.050	1.0	1.000
25	-10.0	0.1	0.01	18.446	25.904	0.380	3.839	-23.872	546.116	-76.289	1.0	1.000
26	-10.0	0.5	0.01	18.446	25.904	3.401	21.148	-23.852	545.813	-76.137	1.0	1.000
27	-10.0	0.7	0.01	18.446	25.904	4.486	29.691	-23.864	546.150	-76.298	1.0	1.000
28	-10.0	0.1	0.09	18.446	25.904	2.389	4.024	-23.979	546.116	-76.288	1.0	0.978

29	-10.0	0.5	0.09	18.446	25.904	7.690	21.317	-24.034	545.813	-76.138	1.0	0.991
30	-10.0	0.7	0.09	18.446	25.904	9.991	29.918	-23.327	546.150	-76.298	1.0	0.996
31	-10.0	0.1	0.01	18.446	31.189	0.384	3.846	-23.870	574.844	-85.157	1.0	1.000
32	-10.0	0.5	0.01	18.446	31.189	3.396	21.204	-23.850	574.828	-85.502	1.0	1.000
33	-10.0	0.7	0.01	18.446	31.189	4.475	29.824	-23.878	574.909	-85.508	1.0	1.000
34	-10.0	0.1	0.09	18.446	31.189	2.403	4.030	-23.989	574.844	-85.157	1.0	0.982
35	-10.0	0.5	0.09	18.446	31.189	7.712	21.365	-24.046	574.841	-85.496	1.0	0.994
36	-10.0	0.7	0.09	18.446	31.189	10.027	30.070	-23.264	574.909	-85.508	1.0	0.996
37	-10.0	0.1	0.01	26.157	25.904	0.401	3.818	-23.862	589.062	-86.218	1.0	1.000
38	-10.0	0.5	0.01	26.157	25.904	3.463	21.072	-23.840	588.625	-86.479	1.0	1.000
39	-10.0	0.7	0.01	26.157	25.904	4.560	29.562	-23.846	588.881	-86.633	1.0	1.000
40	-10.0	0.1	0.09	26.157	25.904	2.670	4.040	-23.968	589.062	-86.218	1.0	0.755
41	-10.0	0.5	0.09	26.157	25.904	8.069	21.406	-23.702	588.625	-86.479	1.0	0.932
42	-10.0	0.7	0.09	26.157	25.904	10.423	29.818	-23.254	588.881	-86.633	1.0	0.974
43	-10.0	0.1	0.01	26.157	31.189	0.406	3.824	-23.865	617.450	-95.845	1.0	1.000
44	-10.0	0.5	0.01	26.157	31.189	3.457	21.131	-23.840	617.256	-95.655	1.0	1.000
45	-10.0	0.7	0.01	26.157	31.189	4.544	29.711	-23.854	617.572	-96.067	1.0	1.000
46	-10.0	0.1	0.09	26.157	31.189	2.691	4.047	-23.982	617.485	-95.850	1.0	0.802
47	-10.0	0.5	0.09	26.157	31.189	8.102	21.452	-23.708	617.256	-95.655	1.0	0.948
48	-10.0	0.7	0.09	26.157	31.189	10.477	29.962	-23.209	617.572	-96.067	1.0	0.971
49	10.0	0.1	0.01	18.446	25.904	0.436	3.836	-23.871	-564.931	26.919	1.0	1.000
50	10.0	0.5	0.01	18.446	25.904	3.767	21.290	-23.899	-564.266	27.033	1.0	1.000
51	10.0	0.7	0.01	18.446	25.904	5.120	29.922	-23.873	-564.456	26.979	1.0	1.000
52	10.0	0.1	0.09	18.446	25.904	2.431	4.188	-23.717	-564.906	26.928	1.0	0.983
53	10.0	0.5	0.09	18.446	25.904	8.080	22.187	-23.434	-564.266	27.033	1.0	0.998
54	10.0	0.7	0.09	18.446	25.904	10.696	31.036	-23.292	-564.456	26.979	1.0	0.999
55	10.0	0.1	0.01	18.446	31.189	0.436	3.843	-23.871	-595.885	24.185	1.0	1.000
56	10.0	0.5	0.01	18.446	31.189	3.739	21.337	-23.901	-595.056	24.013	1.0	1.000
57	10.0	0.7	0.01	18.446	31.189	5.065	30.042	-23.857	-595.416	23.905	1.0	1.000
58	10.0	0.1	0.09	18.446	31.189	2.440	4.210	-23.673	-595.881	24.289	1.0	0.984
59	10.0	0.5	0.09	18.446	31.189	8.078	22.264	-23.317	-595.065	24.026	1.0	0.999
60	10.0	0.7	0.09	18.446	31.189	10.692	31.090	-23.251	-595.416	23.905	1.0	0.999
61	10.0	0.1	0.01	26.157	25.904	0.462	3.810	-23.877	-609.809	23.150	1.0	1.000
62	10.0	0.5	0.01	26.157	25.904	3.825	21.230	-23.873	-609.259	23.167	1.0	1.000
63	10.0	0.7	0.01	26.157	25.904	5.194	29.817	-23.840	-609.240	23.319	1.0	1.000
64	10.0	0.1	0.09	26.157	25.904	2.717	4.217	-23.725	-609.809	23.150	1.0	0.784
65	10.0	0.5	0.09	26.157	25.904	8.456	22.223	-23.399	-609.259	23.167	1.0	0.980
66	10.0	0.7	0.09	26.157	25.904	11.126	31.010	-23.274	-609.240	23.319	1.0	0.994
67	10.0	0.1	0.01	26.157	31.189	0.464	3.818	-23.878	-640.319	19.359	1.0	1.000
68	10.0	0.5	0.01	26.157	31.189	3.798	21.283	-23.861	-640.188	19.945	1.0	1.000

69	10.0	0.7	0.01	26.157	31.189	5.141	29.947	-23.817	-640.181	19.645	1.0	1.000
70	10.0	0.1	0.09	26.157	31.189	2.734	4.240	-23.684	-640.319	19.359	1.0	0.792
71	10.0	0.5	0.09	26.157	31.189	8.465	22.308	-23.261	-640.188	19.945	1.0	0.987
72	10.0	0.7	0.09	26.157	31.189	11.143	31.075	-23.257	-640.181	19.645	1.0	0.994
73	30.0	0.1	0.01	18.446	31.189	0.495	3.863	-23.865	-191.163	40.205	1.0	1.000
74	30.0	0.5	0.01	18.446	31.189	4.041	21.580	-23.860	-191.066	40.160	1.0	1.000
75	30.0	0.7	0.01	18.446	31.189	5.603	30.425	-23.835	-191.094	40.132	1.0	1.000
76	30.0	0.1	0.09	18.446	31.189	2.527	4.273	-23.975	-191.163	40.205	1.0	0.973
77	30.0	0.5	0.09	18.446	31.189	8.428	23.089	-23.241	-191.066	40.159	1.0	0.995
78	30.0	0.7	0.09	18.446	31.189	11.274	32.393	-23.284	-191.094	40.132	1.0	0.994
79	30.0	0.1	0.01	18.446	25.904	0.498	3.857	-23.864	-181.134	37.390	1.0	1.000
80	30.0	0.5	0.01	18.446	25.904	4.092	21.539	-23.888	-181.050	37.360	1.0	1.000
81	30.0	0.7	0.01	18.446	25.904	5.709	30.320	-23.876	-181.059	37.346	1.0	1.000
82	30.0	0.1	0.09	18.446	25.904	2.523	4.260	-24.002	-181.128	37.399	1.0	0.981
83	30.0	0.5	0.09	18.446	25.904	8.448	23.053	-23.416	-181.050	37.360	1.0	0.995
84	30.0	0.7	0.09	18.446	25.904	11.291	32.444	-23.181	-181.059	37.346	1.0	0.995
85	30.0	0.1	0.01	26.157	25.904	0.533	3.833	-23.870	-195.919	34.177	1.0	1.000
86	30.0	0.5	0.01	26.157	25.904	4.175	21.465	-23.898	-195.772	34.179	1.0	1.000
87	30.0	0.7	0.01	26.157	25.904	5.802	30.209	-23.875	-195.828	34.205	1.0	1.000
88	30.0	0.1	0.09	26.157	25.904	2.834	4.264	-24.087	-195.919	34.177	1.0	0.769
89	30.0	0.5	0.09	26.157	25.904	8.821	23.140	-23.347	-195.778	34.174	1.0	0.963
90	30.0	0.7	0.09	26.157	25.904	11.778	32.426	-23.323	-195.828	34.205	1.0	0.952
91	30.0	0.1	0.01	26.157	31.189	0.530	3.839	-23.876	-205.884	36.996	1.0	1.000
92	30.0	0.5	0.01	26.157	31.189	4.127	21.509	-23.884	-205.710	36.987	1.0	1.000
93	30.0	0.7	0.01	26.157	31.189	5.709	30.312	-23.876	-205.775	36.981	1.0	1.000
94	30.0	0.1	0.09	26.157	31.189	2.845	4.281	-24.064	-205.881	37.006	1.0	0.683
95	30.0	0.5	0.09	26.157	31.189	8.827	23.149	-23.336	-205.710	36.987	1.0	0.944
96	30.0	0.7	0.09	26.157	31.189	11.732	32.494	-23.181	-205.775	36.981	1.0	0.953
97	-30.0	0.9	0.01	18.446	25.904	4.828	39.842	-23.726	184.178	2.582	0.0	0.005
98	-30.0	1.0	0.01	18.446	25.904	5.377	46.420	-23.893	184.488	2.629	0.0	0.000
99	-30.0	0.9	0.09	18.446	25.904	11.613	38.011	-24.314	184.178	2.582	0.0	0.036
100	-30.0	1.0	0.09	18.446	25.904	13.389	43.999	-23.447	184.488	2.629	0.0	0.000
101	-30.0	0.1	0.11	18.446	25.904	2.886	4.011	-23.828	184.184	2.616	0.0	0.228
102	-30.0	0.5	0.11	18.446	25.904	8.428	20.810	-23.916	184.041	2.633	0.0	0.074
103	-30.0	0.9	0.11	18.446	25.904	11.613	38.011	-24.314	184.178	2.582	0.0	0.036
104	-30.0	0.1	0.14	18.446	25.904	3.695	4.025	-23.908	184.184	2.616	0.0	0.000
105	-30.0	0.9	0.14	18.446	25.904	15.930	37.053	-24.093	184.178	2.582	0.0	0.000
106	-30.0	-0.1	0.01	18.446	25.904	-1.357	-4.435	138.003	184.478	2.668	0.0	0.000
107	-30.0	-0.1	0.09	18.446	25.904	-9.876	-7.162	138.719	184.478	2.668	0.0	0.000
108	-30.0	0.9	0.01	18.446	31.189	4.882	40.068	-23.812	194.400	3.222	0.0	0.002

109 -30.0	1.0	0.01	18.446	31.189	5.455	46.647	-23.879	194.691	3.242	0.0	0.000
110 -30.0	0.9	0.09	18.446	31.189	11.743	38.218	-24.512	194.400	3.222	0.0	0.016
111 -30.0	1.0	0.09	18.446	31.189	13.437	44.160	-23.327	194.691	3.243	0.0	0.000
112 -30.0	0.1	0.11	18.446	31.189	2.902	4.032	-23.816	194.369	3.227	0.0	0.149
113 -30.0	0.5	0.11	18.446	31.189	8.501	20.964	-23.661	194.350	3.229	0.0	0.044
114 -30.0	0.9	0.11	18.446	31.189	13.448	37.657	-24.884	194.400	3.222	0.0	0.000
115 -30.0	0.1	0.14	18.446	31.189	3.715	4.067	-23.888	194.369	3.227	0.0	0.000
116 -30.0	0.9	0.14	18.446	31.189	16.115	37.228	-24.666	194.400	3.222	0.0	0.000
117 -30.0	-0.1	0.01	18.446	31.189	-1.352	-4.433	137.897	194.675	3.228	0.0	0.000
118 -30.0	-0.1	0.09	18.446	31.189	-10.255	-7.329	138.341	194.675	3.228	0.0	0.000
119 -30.0	0.9	0.01	26.157	25.904	4.877	39.639	-23.837	198.241	-2.563	0.0	0.007
120 -30.0	1.0	0.01	26.157	25.904	5.424	46.272	-23.857	198.500	-2.556	0.0	0.000
121 -30.0	0.9	0.09	26.157	25.904	12.212	37.764	-24.138	198.241	-2.563	0.0	0.014
122 -30.0	1.0	0.09	26.157	25.904	14.082	43.513	-24.001	198.500	-2.556	0.0	0.000
123 -30.0	0.1	0.11	26.157	25.904	3.248	4.012	-23.801	198.141	-2.575	0.0	0.010
124 -30.0	0.5	0.11	26.157	25.904	8.824	20.467	-24.458	198.069	-2.602	0.0	0.001
125 -30.0	0.9	0.11	26.157	25.904	13.977	37.072	-24.754	198.241	-2.563	0.0	0.000
126 -30.0	0.1	0.14	26.157	25.904	4.157	4.076	-23.759	198.141	-2.575	0.0	0.000
127 -30.0	0.9	0.14	26.157	25.904	16.897	36.810	-23.514	198.241	-2.563	0.0	0.000
128 -30.0	-0.1	0.01	26.157	25.904	-1.344	-4.556	137.916	198.500	-2.576	0.0	0.000
129 -30.0	-0.1	0.09	26.157	25.904	-10.018	-7.416	137.831	198.500	-2.576	0.0	0.000
130 -30.0	0.9	0.01	26.157	31.189	4.933	39.886	-23.853	208.400	-2.058	0.0	0.003
131 -30.0	1.0	0.01	26.157	31.189	5.469	46.493	-23.869	208.744	-2.033	0.0	0.000
132 -30.0	0.9	0.09	26.157	31.189	12.365	37.961	-24.370	208.400	-2.058	0.0	0.006
133 -30.0	1.0	0.09	26.157	31.189	14.283	43.876	-23.245	208.753	-2.044	0.0	0.000
134 -30.0	0.1	0.11	26.157	31.189	3.270	4.065	-23.713	208.365	-2.042	0.0	0.006
135 -30.0	0.5	0.11	26.157	31.189	8.903	20.579	-24.422	208.256	-2.038	0.0	0.000
136 -30.0	0.9	0.11	26.157	31.189	14.163	37.271	-24.858	208.400	-2.058	0.0	0.000
137 -30.0	0.1	0.14	26.157	31.189	4.189	4.094	-23.740	208.365	-2.042	0.0	0.000
138 -30.0	0.9	0.14	26.157	31.189	17.085	36.951	-24.188	208.400	-2.058	0.0	0.000
139 -30.0	-0.1	0.01	26.157	31.189	-1.383	-4.540	137.919	208.753	-2.075	0.0	0.000
140 -30.0	-0.1	0.09	26.157	31.189	-10.481	-7.471	138.100	208.753	-2.075	0.0	0.000
141 -10.0	0.9	0.01	18.446	25.904	5.571	39.955	-23.884	546.441	-76.527	0.0	0.000
142 -10.0	1.0	0.01	18.446	25.904	5.869	46.586	-23.926	547.275	-76.599	0.0	0.000
143 -10.0	0.9	0.09	18.446	25.904	12.765	39.233	-24.577	546.441	-76.527	0.0	0.000
144 -10.0	1.0	0.09	18.446	25.904	14.439	45.624	-24.275	547.275	-76.599	0.0	0.000
145 -10.0	0.1	0.11	18.446	25.904	2.911	4.080	-23.988	546.116	-76.289	0.0	0.227
146 -10.0	0.5	0.11	18.446	25.904	8.830	21.275	-24.416	545.813	-76.138	0.0	0.026
147 -10.0	0.9	0.11	18.446	25.904	14.690	39.412	-23.623	546.441	-76.527	0.0	0.000
148 -10.0	0.1	0.14	18.446	25.904	3.721	4.206	-23.982	546.116	-76.288	0.0	0.000

149 -10.0	0.9	0.14	18.446	25.904	17.503	39.025	-25.030	546.441	-76.527	0.0	0.000
150 -10.0	-0.1	0.01	18.446	25.904	-1.201	-4.233	137.969	547.625	-76.473	0.0	0.007
151 -10.0	-0.1	0.09	18.446	25.904	-9.710	-4.955	138.091	547.625	-76.471	0.0	0.024
152 -10.0	0.9	0.01	18.446	31.189	5.544	40.209	-23.837	574.956	-85.622	0.0	0.000
153 -10.0	1.0	0.01	18.446	31.189	5.888	46.827	-23.897	575.509	-85.613	0.0	0.000
154 -10.0	0.9	0.09	18.446	31.189	12.822	39.464	-24.624	574.947	-85.619	0.0	0.000
155 -10.0	1.0	0.09	18.446	31.189	14.471	45.881	-24.375	575.509	-85.613	0.0	0.000
156 -10.0	0.1	0.11	18.446	31.189	2.926	4.100	-23.950	574.844	-85.157	0.0	0.272
157 -10.0	0.5	0.11	18.446	31.189	8.860	21.325	-24.453	574.828	-85.502	0.0	0.039
158 -10.0	0.9	0.11	18.446	31.189	14.767	39.664	-23.397	574.956	-85.622	0.0	0.000
159 -10.0	0.1	0.14	18.446	31.189	3.741	4.212	-24.001	574.841	-85.161	0.0	0.000
160 -10.0	0.9	0.14	18.446	31.189	17.610	39.330	-25.050	574.969	-85.609	0.0	0.000
161 -10.0	-0.1	0.01	18.446	31.189	-1.191	-4.226	137.863	575.569	-85.638	0.0	0.009
162 -10.0	-0.1	0.09	18.446	31.189	-10.078	-4.922	138.081	575.569	-85.638	0.0	0.027
163 -10.0	0.9	0.01	26.157	25.904	5.657	39.809	-23.760	589.297	-86.802	0.0	0.000
164 -10.0	1.0	0.01	26.157	25.904	5.934	46.485	-23.899	590.125	-86.713	0.0	0.000
165 -10.0	0.9	0.09	26.157	25.904	13.396	39.033	-24.570	589.297	-86.802	0.0	0.000
166 -10.0	1.0	0.09	26.157	25.904	15.316	45.417	-24.160	590.125	-86.713	0.0	0.000
167 -10.0	0.1	0.11	26.157	25.904	3.263	4.042	-24.100	589.062	-86.218	0.0	0.008
168 -10.0	0.5	0.11	26.157	25.904	9.255	21.253	-24.296	588.625	-86.479	0.0	0.001
169 -10.0	0.9	0.11	26.157	25.904	15.436	39.119	-24.087	589.297	-86.802	0.0	0.000
170 -10.0	0.1	0.14	26.157	25.904	4.171	4.252	-23.915	589.062	-86.218	0.0	0.000
171 -10.0	0.9	0.14	26.157	25.904	18.462	38.744	-25.065	589.297	-86.802	0.0	0.000
172 -10.0	-0.1	0.01	26.157	25.904	-1.224	-4.347	137.975	590.366	-86.551	0.0	0.009
173 -10.0	-0.1	0.09	26.157	25.904	-9.975	-5.173	137.944	590.366	-86.551	0.0	0.029
174 -10.0	0.9	0.01	26.157	31.189	5.632	40.064	-23.660	617.862	-95.989	0.0	0.000
175 -10.0	1.0	0.01	26.157	31.189	5.931	46.665	-23.937	617.994	-96.365	0.0	0.000
176 -10.0	0.9	0.09	26.157	31.189	13.474	39.266	-24.608	617.862	-95.989	0.0	0.000
177 -10.0	1.0	0.09	26.157	31.189	15.357	45.666	-24.294	617.994	-96.363	0.0	0.000
178 -10.0	0.1	0.11	26.157	31.189	3.288	4.048	-24.105	617.450	-95.845	0.0	0.010
179 -10.0	0.5	0.11	26.157	31.189	9.299	21.298	-24.352	617.256	-95.655	0.0	0.001
180 -10.0	0.9	0.11	26.157	31.189	15.547	39.377	-23.911	617.862	-95.989	0.0	0.000
181 -10.0	0.1	0.14	26.157	31.189	4.203	4.260	-23.942	617.485	-95.850	0.0	0.000
182 -10.0	0.9	0.14	26.157	31.189	18.615	39.038	-25.175	617.862	-95.989	0.0	0.000
183 -10.0	-0.1	0.01	26.157	31.189	-1.254	-4.329	137.969	618.153	-96.474	0.0	0.010
184 -10.0	-0.1	0.09	26.157	31.189	-10.398	-5.153	137.941	618.153	-96.474	0.0	0.031
185 10.0	0.9	0.01	18.446	25.904	6.276	40.293	-23.833	-564.591	26.860	0.0	0.013
186 10.0	1.0	0.01	18.446	25.904	6.325	46.955	-23.802	-565.041	26.233	0.0	0.000
187 10.0	0.9	0.09	18.446	25.904	13.755	41.105	-24.098	-564.591	26.860	0.0	0.000
188 10.0	1.0	0.09	18.446	25.904	15.209	48.135	-23.766	-565.041	26.233	0.0	0.000



---

189	10.0	0.1	0.11	18.446	25.904	2.957	4.270	-23.834	-564.906	26.928	0.0	0.245
190	10.0	0.5	0.11	18.446	25.904	9.253	22.194	-23.939	-564.266	27.033	0.0	0.029
191	10.0	0.9	0.11	18.446	25.904	15.680	41.726	-23.403	-564.591	26.860	0.0	0.000
192	10.0	0.1	0.14	18.446	25.904	3.774	4.384	-23.893	-564.931	26.919	0.0	0.000
193	10.0	0.9	0.14	18.446	25.904	18.780	42.254	-23.070	-564.591	26.860	0.0	0.000
194	10.0	-0.1	0.01	18.446	25.904	-1.021	-4.083	137.947	-564.872	26.302	0.0	0.000
195	10.0	-0.1	0.09	18.446	25.904	-9.065	-2.897	138.316	-564.872	26.302	0.0	0.001
196	10.0	0.9	0.01	18.446	31.189	6.176	40.508	-23.825	-595.319	24.024	0.0	0.008
197	10.0	1.0	0.01	18.446	31.189	6.226	47.143	-23.800	-595.956	23.720	0.0	0.000
198	10.0	0.9	0.09	18.446	31.189	13.729	41.270	-24.421	-595.319	24.023	0.0	0.000
199	10.0	1.0	0.09	18.446	31.189	15.139	48.353	-23.588	-595.931	23.656	0.0	0.000
200	10.0	0.1	0.11	18.446	31.189	2.971	4.274	-23.836	-595.894	24.197	0.0	0.230
201	10.0	0.5	0.11	18.446	31.189	9.249	22.263	-23.802	-595.065	24.026	0.0	0.052
202	10.0	0.9	0.11	18.446	31.189	15.681	41.907	-23.268	-595.319	24.024	0.0	0.000
203	10.0	0.1	0.14	18.446	31.189	3.790	4.394	-23.870	-595.885	24.185	0.0	0.000
204	10.0	0.9	0.14	18.446	31.189	18.796	42.371	-23.203	-595.319	24.029	0.0	0.000
205	10.0	-0.1	0.01	18.446	31.189	-1.043	-4.061	137.950	-596.097	23.767	0.0	0.001
206	10.0	-0.1	0.09	18.446	31.189	-9.403	-2.823	138.294	-596.097	23.767	0.0	0.003
207	10.0	0.9	0.01	26.157	25.904	6.387	40.126	-23.904	-609.469	23.195	0.0	0.015
208	10.0	1.0	0.01	26.157	25.904	6.436	46.880	-23.826	-609.797	22.867	0.0	0.000
209	10.0	0.9	0.09	26.157	25.904	14.417	41.019	-23.762	-609.469	23.194	0.0	0.000
210	10.0	1.0	0.09	26.157	25.904	16.132	48.153	-23.897	-609.797	22.867	0.0	0.000
211	10.0	0.1	0.11	26.157	25.904	3.304	4.344	-23.773	-609.794	23.142	0.0	0.012
212	10.0	0.5	0.11	26.157	25.904	9.698	22.205	-23.956	-609.259	23.167	0.0	0.001
213	10.0	0.9	0.11	26.157	25.904	16.494	41.704	-23.173	-609.469	23.194	0.0	0.000
214	10.0	0.1	0.14	26.157	25.904	4.232	4.431	-23.950	-609.809	23.150	0.0	0.000
215	10.0	0.9	0.14	26.157	25.904	19.821	42.270	-22.940	-609.469	23.194	0.0	0.000
216	10.0	-0.1	0.01	26.157	25.904	-1.074	-4.177	138.019	-609.566	23.156	0.0	0.002
217	10.0	-0.1	0.09	26.157	25.904	-9.391	-3.004	138.297	-609.566	23.156	0.0	0.005
218	10.0	0.9	0.01	26.157	31.189	6.296	40.360	-23.896	-640.150	19.515	0.0	0.009
219	10.0	1.0	0.01	26.157	31.189	6.360	47.058	-23.780	-641.331	19.108	0.0	0.000
220	10.0	0.9	0.09	26.157	31.189	14.417	41.204	-24.008	-640.150	19.518	0.0	0.000
221	10.0	1.0	0.09	26.157	31.189	6.360	47.058	-23.780	-641.331	19.108	0.0	0.000
222	10.0	0.1	0.11	26.157	31.189	3.328	4.345	-23.794	-640.319	19.359	0.0	0.011
223	10.0	0.5	0.11	26.157	31.189	9.712	22.294	-23.793	-640.188	19.945	0.0	0.001
224	10.0	0.9	0.11	26.157	31.189	16.527	41.927	-23.039	-640.150	19.518	0.0	0.000
225	10.0	0.1	0.14	26.157	31.189	4.259	4.446	-23.917	-640.319	19.357	0.0	0.000
226	10.0	0.9	0.14	26.157	31.189	19.883	42.418	-22.994	-640.150	19.515	0.0	0.000
227	10.0	-0.1	0.01	26.157	31.189	-1.097	-4.155	137.969	-641.066	19.457	0.0	0.007
228	10.0	-0.1	0.09	26.157	31.189	-9.785	-2.914	138.350	-641.066	19.457	0.0	0.018

229	30.0	0.9	0.01	18.446	31.189	6.739	41.009	-23.839	-191.153	40.179	0.0	0.010
230	30.0	1.0	0.01	18.446	31.189	6.530	47.554	-23.842	-191.444	40.212	0.0	0.000
231	30.0	0.9	0.09	18.446	31.189	14.208	43.905	-21.726	-191.153	40.179	0.0	0.000
232	30.0	1.0	0.09	18.446	31.189	15.237	51.086	-23.879	-191.444	40.212	0.0	0.000
233	30.0	0.1	0.11	18.446	31.189	3.058	4.424	-23.902	-191.163	40.205	0.0	0.180
234	30.0	0.5	0.11	18.446	31.189	9.620	23.343	-23.666	-191.066	40.159	0.0	0.014
235	30.0	0.9	0.11	18.446	31.189	16.261	44.553	-23.477	-191.153	40.179	0.0	0.000
236	30.0	0.1	0.14	18.446	31.189	3.900	4.623	-24.009	-191.163	40.205	0.0	0.000
237	30.0	0.9	0.14	18.446	31.189	19.558	45.674	-23.564	-191.153	40.179	0.0	0.000
238	30.0	-0.1	0.01	18.446	31.189	-0.906	-3.947	138.006	-191.372	40.220	0.0	0.000
239	30.0	-0.1	0.09	18.446	31.189	-8.478	-0.840	138.591	-191.372	40.220	0.0	0.000
240	30.0	0.9	0.01	18.446	25.904	6.910	40.817	-23.889	-181.097	37.384	0.0	0.017
241	30.0	1.0	0.01	18.446	25.904	6.686	47.408	-23.884	-181.384	37.411	0.0	0.000
242	30.0	0.9	0.09	18.446	25.904	14.290	43.714	-23.171	-181.097	37.381	0.0	0.000
243	30.0	1.0	0.09	18.446	25.904	15.238	51.523	-23.242	-181.384	37.412	0.0	0.000
244	30.0	0.1	0.11	18.446	25.904	3.038	4.497	-23.724	-181.134	37.390	0.0	0.320
245	30.0	0.5	0.11	18.446	25.904	9.631	23.347	-23.635	-181.050	37.360	0.0	0.019
246	30.0	0.9	0.11	18.446	25.904	16.335	44.498	-23.436	-181.097	37.381	0.0	0.000
247	30.0	0.1	0.14	18.446	25.904	3.893	4.605	-24.062	-181.134	37.391	0.0	0.000
248	30.0	0.9	0.14	18.446	25.904	19.604	45.774	-24.367	-181.097	37.381	0.0	0.000
249	30.0	-0.1	0.01	18.446	25.904	-0.889	-3.972	137.984	-181.387	37.377	0.0	0.000
250	30.0	-0.1	0.09	18.446	25.904	-8.157	-0.989	138.591	-181.387	37.377	0.0	0.000
251	30.0	0.9	0.01	26.157	25.904	7.070	40.668	-23.941	-195.812	34.206	0.0	0.030
252	30.0	1.0	0.01	26.157	25.904	6.810	47.357	-23.837	-196.116	34.239	0.0	0.000
253	30.0	0.9	0.09	26.157	25.904	14.998	43.803	-23.309	-195.812	34.206	0.0	0.000
254	30.0	1.0	0.09	26.157	25.904	6.810	47.357	-23.837	-196.116	34.239	0.0	0.000
255	30.0	0.1	0.11	26.157	25.904	3.420	4.536	-23.750	-195.919	34.177	0.0	0.016
256	30.0	0.5	0.11	26.157	25.904	10.129	23.345	-23.743	-195.778	34.174	0.0	0.000
257	30.0	0.9	0.11	26.157	25.904	17.244	44.583	-23.460	-195.812	34.206	0.0	0.000
258	30.0	0.1	0.14	26.157	25.904	4.387	4.666	-24.150	-195.919	34.177	0.0	0.000
259	30.0	0.9	0.14	26.157	25.904	20.621	46.308	-23.397	-195.812	34.206	0.0	0.000
260	30.0	-0.1	0.01	26.157	25.904	-0.972	-4.048	138.034	-196.128	34.185	0.0	0.000
261	30.0	-0.1	0.09	26.157	25.904	-8.763	-1.468	137.303	-196.128	34.185	0.0	0.000
262	30.0	0.9	0.01	26.157	31.189	6.903	40.876	-23.920	-205.819	36.951	0.0	0.017
263	30.0	1.0	0.01	26.157	31.189	6.683	47.495	-23.862	-206.050	37.028	0.0	0.000
264	30.0	0.9	0.09	26.157	31.189	14.936	44.051	-22.243	-205.822	36.965	0.0	0.000
265	30.0	1.0	0.09	26.157	31.189	16.122	51.670	-23.622	-206.050	37.028	0.0	0.000
266	30.0	0.1	0.11	26.157	31.189	3.431	4.573	-23.653	-205.881	37.006	0.0	0.011
267	30.0	0.5	0.11	26.157	31.189	10.101	23.437	-23.564	-205.710	36.987	0.0	0.000
268	30.0	0.9	0.11	26.157	31.189	17.152	44.778	-23.581	-205.822	36.965	0.0	0.000

269	30.0	0.1	0.14	26.157	31.189	4.410	4.669	-24.151	-205.884	36.996	0.0	0.000
270	30.0	0.9	0.14	26.157	31.189	20.757	45.864	-24.376	-205.822	36.965	0.0	0.000
271	30.0	-0.1	0.01	26.157	31.189	-0.984	-4.016	138.034	-206.059	37.020	0.0	0.000
272	30.0	-0.1	0.09	26.157	31.189	-9.156	-1.361	137.175	-206.059	37.020	0.0	0.000
LOAD												
273	-30.0	0.5	0.00	26.157	31.189	208.247	-1.812	0.220	208.244	-2.017	0.0	0.000
274	-30.0	0.5	0.00	26.157	25.904	198.100	-2.360	-0.145	198.066	-2.609	0.0	0.000
275	-30.0	0.5	0.00	18.446	25.904	184.000	2.859	-0.014	184.009	2.629	0.0	0.000
276	-30.0	0.5	0.00	18.446	31.189	194.259	3.417	-0.055	194.209	3.229	0.0	0.000
277	-20.0	0.5	0.00	26.157	31.189	313.300	-20.415	0.076	313.212	-20.749	0.0	0.000
278	-20.0	0.5	0.00	26.157	25.904	298.331	-19.193	0.023	298.169	-19.492	0.0	0.000
279	-20.0	0.5	0.00	18.446	25.904	276.938	-12.964	0.150	276.931	-13.259	0.0	0.000
280	-20.0	0.5	0.00	18.446	31.189	292.006	-14.048	-0.276	291.741	-14.388	0.0	0.000
281	-10.0	0.5	0.00	18.446	31.189	574.459	-84.165	0.065	573.912	-85.288	0.0	0.000
282	-10.0	0.5	0.00	18.446	25.904	545.731	-75.564	0.085	545.803	-76.484	0.0	0.000
283	-10.0	0.5	0.00	26.157	25.904	588.969	-85.536	-0.269	588.534	-86.084	0.0	0.000
284	-10.0	0.5	0.00	26.157	31.189	617.281	-94.448	-0.132	616.969	-95.614	0.0	0.000
285	10.0	0.5	0.00	26.157	31.189	-640.369	19.187	-0.104	-640.734	19.683	0.0	0.013
286	10.0	0.5	0.00	26.157	25.904	-609.413	22.518	-0.087	-609.769	22.956	0.0	0.009
287	10.0	0.5	0.00	18.446	25.904	-564.550	26.117	0.097	-564.463	26.686	0.0	0.007
288	10.0	0.5	0.00	18.446	31.189	-595.625	23.073	0.220	-595.491	24.278	0.0	0.008
289	20.0	0.5	0.00	26.157	31.189	-315.175	37.864	-0.008	-315.159	38.133	0.0	0.000
290	20.0	0.5	0.00	26.157	25.904	-299.647	35.791	0.039	-299.666	36.172	0.0	0.000
291	20.0	0.5	0.00	18.446	25.904	-277.359	38.970	-0.102	-277.319	39.221	0.0	0.000
292	20.0	0.5	0.00	18.446	31.189	-292.688	41.049	-0.134	-292.681	41.346	0.0	0.000
293	30.0	0.5	0.00	18.446	31.189	-191.100	39.943	-0.068	-191.087	40.179	0.0	0.000
294	30.0	0.5	0.00	18.446	25.904	-181.081	37.027	0.007	-181.038	37.342	0.0	0.000
295	30.0	0.5	0.00	26.157	25.904	-195.891	33.930	0.101	-195.803	34.225	0.0	0.000
296	30.0	0.5	0.00	26.157	31.189	-205.878	36.713	-0.047	-205.772	37.007	0.0	0.000

**TESTING CASES**

**error = 0.002      cost = 0.921217**

No.	$\delta$	$\alpha$	$V_F$	$X_{SI}$	$X_{RI}$	$R_I$	$X_I$	$X_{SO}$	$R_{mem}$	$X_{mem}$	Target	Output
1	-20.0	-0.10	0.03	24.500	27.400	-3.307	-4.703	138.144	298.734	-18.664	0.0	0.001
2	-20.0	-0.10	0.07	24.500	27.400	-7.839	-5.608	138.556	298.734	-18.664	0.0	0.001

3	-20.0	0.20	0.03	24.500	27.400	1.474	8.238	-23.921	298.769	-18.538	1.0	1.000
4	-20.0	0.20	0.07	24.500	27.400	2.885	8.297	-24.018	298.769	-18.538	1.0	1.000
5	-20.0	0.20	0.12	24.500	27.400	4.703	8.511	-23.887	298.769	-18.538	0.0	0.000
6	-20.0	0.60	0.03	24.500	27.400	5.614	24.596	-23.983	297.866	-18.518	1.0	1.000
7	-20.0	0.60	0.07	24.500	27.400	8.167	24.450	-23.887	297.866	-18.518	1.0	1.000
8	-20.0	0.60	0.12	24.500	27.400	11.435	24.294	-23.622	297.866	-18.518	0.0	0.000
9	-20.0	0.95	0.03	24.500	27.400	7.520	42.331	-23.745	298.200	-18.443	0.0	0.000
10	-20.0	0.95	0.07	24.500	27.400	11.537	41.579	-24.279	298.200	-18.443	0.0	0.000
11	-20.0	0.95	0.12	24.500	27.400	16.690	40.994	-23.537	298.200	-18.443	0.0	0.000
12	20.0	-0.10	0.03	24.500	27.400	-2.921	-3.604	138.041	-299.503	37.472	0.0	0.000
13	20.0	-0.10	0.07	24.500	27.400	-7.067	-2.619	137.722	-299.509	37.473	0.0	0.000
14	20.0	0.20	0.03	24.500	27.400	1.685	8.349	-23.921	-299.884	37.498	1.0	1.000
15	20.0	0.20	0.07	24.500	27.400	3.078	8.672	-23.929	-299.884	37.498	1.0	1.000
16	20.0	0.20	0.12	24.500	27.400	4.896	9.233	-23.488	-299.884	37.498	0.0	0.001
17	20.0	0.60	0.03	24.500	27.400	6.763	25.464	-23.971	-298.925	37.344	1.0	1.000
18	20.0	0.60	0.07	24.500	27.400	9.431	26.030	-23.799	-298.925	37.344	1.0	0.998
19	20.0	0.60	0.12	24.500	27.400	12.981	26.847	-23.369	-298.925	37.344	0.0	0.000
20	20.0	0.95	0.03	24.500	27.400	8.850	43.905	-23.964	-299.066	37.282	0.0	0.000
21	20.0	0.95	0.07	24.500	27.400	13.268	45.097	-23.518	-299.066	37.282	0.0	0.000
22	20.0	0.95	0.12	24.500	27.400	19.063	46.661	-23.974	-299.066	37.282	0.0	0.000

**RUNNING CASES**f

No.	$\delta$	$\alpha$	$V_F$	$X_{SI}$	$X_{RI}$	$R_I$	$X_I$	$X_{SO}$	$R_{mem}$	$X_{mem}$	Target	Output
1	-15.0	-0.10	0.020	20.660	29.890	-2.217	-4.359	138.006	395.516	-37.362	0.0	0.002
2	-15.0	-0.02	0.020	20.660	29.890	-2.132	-3.502	138.038	392.244	-36.597	0.0	0.002
3	-15.0	-0.06	0.020	20.660	29.890	-2.006	-2.586	138.056	392.091	-36.466	0.0	0.002
4	-15.0	-0.04	0.020	20.660	29.890	-1.944	-1.829	137.913	392.091	-36.467	0.0	0.002
5	-15.0	-0.02	0.020	20.660	29.890	-1.809	-1.023	137.925	392.244	-36.598	0.0	0.002
6	-15.0	-0.00	0.020	20.660	29.890	-1.751	-0.945	137.934	395.516	-37.363	0.0	0.002
7	-15.0	0.00	0.020	20.660	29.890	0.385	0.697	-23.868	395.444	-37.364	1.0	1.000
8	-15.0	0.02	0.020	20.660	29.890	0.421	0.772	-23.888	391.284	-36.378	1.0	1.000
9	-15.0	0.04	0.020	20.660	29.890	0.472	1.495	-23.888	391.212	-36.406	1.0	1.000
10	-15.0	0.06	0.020	20.660	29.890	0.519	2.247	-23.877	391.850	-36.403	1.0	1.000
11	-15.0	0.08	0.020	20.660	29.890	0.563	3.000	-23.886	391.212	-36.406	1.0	1.000
12	-15.0	0.10	0.020	20.660	29.890	0.624	3.852	-23.878	391.300	-36.385	1.0	1.000

13	-15.0	0.15	0.020	20.660	29.890	0.719	5.663	-23.874	391.291	-36.385	1.0	1.000
14	-15.0	0.20	0.020	20.660	29.890	1.134	8.247	-23.912	392.175	-36.782	1.0	1.000
15	-15.0	0.25	0.020	20.660	29.890	1.152	10.189	-23.934	391.134	-36.450	1.0	1.000
16	-15.0	0.30	0.020	20.660	29.890	2.289	12.658	-23.916	391.222	-36.405	1.0	1.000
17	-15.0	0.35	0.020	20.660	29.890	2.895	14.903	-23.902	391.022	-36.461	1.0	1.000
18	-15.0	0.40	0.020	20.660	29.890	1.525	16.197	-23.903	391.125	-36.377	1.0	1.000
19	-15.0	0.45	0.020	20.660	29.890	2.116	18.448	-23.933	391.056	-36.466	1.0	1.000
20	-15.0	0.50	0.020	20.660	29.890	3.854	21.116	-23.958	391.175	-36.476	1.0	1.000
21	-15.0	0.55	0.020	20.660	29.890	4.683	23.062	-23.815	391.056	-36.466	1.0	1.000
22	-15.0	0.60	0.020	20.660	29.890	5.071	24.862	-23.892	391.159	-36.411	1.0	1.000
23	-15.0	0.65	0.020	20.660	29.890	4.438	27.410	-23.817	391.125	-36.426	1.0	1.000
24	-15.0	0.70	0.020	20.660	29.890	5.008	29.735	-23.805	391.303	-36.454	1.0	1.000
25	-15.0	0.72	0.020	20.660	29.890	4.899	30.675	-23.797	391.178	-36.476	1.0	1.000
26	-15.0	0.74	0.020	20.660	29.890	4.991	31.550	-23.782	391.178	-36.479	1.0	1.000
27	-15.0	0.76	0.020	20.660	29.890	5.315	32.653	-23.866	391.178	-36.479	1.0	1.000
28	-15.0	0.78	0.020	20.660	29.890	5.825	33.326	-23.819	391.828	-36.480	1.0	0.999
29	-15.0	0.80	0.020	20.660	29.890	5.947	34.436	-23.954	392.256	-36.818	1.0	0.985
30	-15.0	0.82	0.020	20.660	29.890	6.068	35.403	-23.905	391.506	-36.469	0.0	0.831
31	-15.0	0.84	0.020	20.660	29.890	5.941	36.640	-23.914	391.306	-36.482	0.0	0.169
32	-15.0	0.86	0.020	20.660	29.890	6.234	37.608	-23.894	391.472	-36.435	0.0	0.021
33	-15.0	0.88	0.020	20.660	29.890	6.155	38.793	-23.957	391.478	-36.452	0.0	0.002
34	-15.0	0.90	0.020	20.660	29.890	6.267	39.902	-24.033	391.475	-36.405	0.0	0.000
35	-15.0	0.92	0.020	20.660	29.890	6.352	41.081	-23.999	391.331	-36.457	0.0	0.000
36	-15.0	0.94	0.020	20.660	29.890	6.566	42.373	-23.481	392.175	-36.467	0.0	0.000
37	-15.0	0.96	0.020	20.660	29.890	6.604	43.509	-23.923	391.337	-36.458	0.0	0.000
38	-15.0	0.98	0.020	20.660	29.890	6.648	44.928	-23.989	391.459	-36.435	0.0	0.000
39	-15.0	1.00	0.020	20.660	29.890	6.805	45.989	-23.952	395.466	-37.358	0.0	0.000
40	-15.0	0.40	0.000	20.660	29.890	0.649	16.146	-23.874	391.125	-36.377	1.0	1.000
41	-15.0	0.40	0.002	20.660	29.890	0.733	16.157	-23.862	391.125	-36.377	1.0	1.000
42	-15.0	0.40	0.004	20.660	29.890	0.818	16.163	-23.871	391.125	-36.377	1.0	1.000
43	-15.0	0.40	0.006	20.660	29.890	0.906	16.162	-23.889	391.125	-36.377	1.0	1.000
44	-15.0	0.40	0.008	20.660	29.890	0.993	16.165	-23.900	391.125	-36.377	1.0	1.000
45	-15.0	0.40	0.010	20.660	29.890	1.079	16.171	-23.903	391.125	-36.377	1.0	1.000
46	-15.0	0.40	0.012	20.660	29.890	1.168	16.178	-23.892	391.125	-36.377	1.0	1.000
47	-15.0	0.40	0.014	20.660	29.890	1.255	16.180	-23.895	391.125	-36.377	1.0	1.000
48	-15.0	0.40	0.016	20.660	29.890	1.344	16.184	-23.906	391.125	-36.377	1.0	1.000
49	-15.0	0.40	0.018	20.660	29.890	1.434	16.192	-23.909	391.125	-36.377	1.0	1.000
50	-15.0	0.40	0.020	20.660	29.890	1.525	16.197	-23.903	391.125	-36.377	1.0	1.000
51	-15.0	0.40	0.025	20.660	29.890	1.750	16.210	-23.955	391.125	-36.377	1.0	1.000

52	-15.0	0.40	0.030	20.660	29.890	1.987	16.306	-23.732	391.125	-36.377	1.0	1.000
53	-15.0	0.40	0.035	20.660	29.890	2.206	16.305	-23.791	391.125	-36.377	1.0	1.000
54	-15.0	0.40	0.040	20.660	29.890	2.430	16.306	-23.850	391.125	-36.377	1.0	1.000
55	-15.0	0.40	0.045	20.660	29.890	2.662	16.334	-23.841	391.125	-36.377	1.0	1.000
56	-15.0	0.40	0.050	20.660	29.890	2.891	16.325	-23.913	391.125	-36.377	1.0	1.000
57	-15.0	0.40	0.055	20.660	29.890	3.128	16.341	-23.936	391.125	-36.377	1.0	1.000
58	-15.0	0.40	0.060	20.660	29.890	3.366	16.364	-23.922	391.125	-36.377	1.0	1.000
59	-15.0	0.40	0.065	20.660	29.890	3.602	16.377	-24.024	391.141	-36.388	1.0	1.000
60	-15.0	0.40	0.070	20.660	29.890	3.841	16.536	-23.797	391.125	-36.377	1.0	1.000
61	-15.0	0.40	0.075	20.660	29.890	4.080	16.622	-23.497	391.125	-36.377	1.0	1.000
62	-15.0	0.40	0.080	20.660	29.890	4.310	16.605	-23.613	391.125	-36.377	1.0	1.000
63	-15.0	0.40	0.082	20.660	29.890	4.402	16.598	-23.668	391.125	-36.377	1.0	1.000
64	-15.0	0.40	0.084	20.660	29.890	4.495	16.597	-23.700	391.125	-36.377	1.0	1.000
65	-15.0	0.40	0.086	20.660	29.890	4.589	16.605	-23.705	391.125	-36.377	1.0	1.000
66	-15.0	0.40	0.088	20.660	29.890	4.683	16.618	-23.689	391.125	-36.377	1.0	1.000
67	-15.0	0.40	0.090	20.660	29.890	4.778	16.625	-23.673	391.125	-36.377	1.0	1.000
68	-15.0	0.40	0.092	20.660	29.890	4.873	16.628	-23.669	391.125	-36.377	1.0	1.000
69	-15.0	0.40	0.094	20.660	29.890	4.968	16.628	-23.682	391.125	-36.377	1.0	1.000
70	-15.0	0.40	0.096	20.660	29.890	5.063	16.627	-23.698	391.125	-36.377	1.0	1.000
71	-15.0	0.40	0.098	20.660	29.890	5.160	16.626	-23.716	391.141	-36.388	1.0	1.000
72	-15.0	0.40	0.100	20.660	29.890	5.256	16.622	-23.733	391.125	-36.377	1.0	1.000
73	-15.0	0.40	0.102	20.660	29.890	5.352	16.618	-23.750	391.125	-36.377	0.0	1.000
74	-15.0	0.40	0.104	20.660	29.890	5.450	16.614	-23.765	391.125	-36.377	0.0	0.999
75	-15.0	0.40	0.106	20.660	29.890	5.548	16.610	-23.783	391.125	-36.377	0.0	0.999
76	-15.0	0.40	0.108	20.660	29.890	5.645	16.611	-23.796	391.125	-36.377	0.0	0.998
77	-15.0	0.40	0.110	20.660	29.890	5.744	16.614	-23.805	391.125	-36.377	0.0	0.996
78	-15.0	0.40	0.112	20.660	29.890	5.844	16.621	-23.812	391.125	-36.377	0.0	0.992
79	-15.0	0.40	0.114	20.660	29.890	5.944	16.630	-23.810	391.125	-36.377	0.0	0.984
80	-15.0	0.40	0.116	20.660	29.890	6.045	16.639	-23.804	391.141	-36.388	0.0	0.969
81	-15.0	0.40	0.118	20.660	29.890	6.147	16.649	-23.803	391.125	-36.377	0.0	0.939
82	-15.0	0.40	0.120	20.660	29.890	6.247	16.654	-23.811	391.125	-36.377	0.0	0.881
83	-15.0	0.40	0.125	20.660	29.890	6.500	16.665	-23.900	391.141	-36.388	0.0	0.516
84	-15.0	0.40	0.130	20.660	29.890	6.751	16.687	-24.047	391.125	-36.377	0.0	0.123
85	-15.0	0.40	0.135	20.660	29.890	6.997	16.811	-23.925	391.141	-36.388	0.0	0.024
86	-15.0	0.40	0.140	20.660	29.890	7.244	16.962	-23.618	391.141	-36.388	0.0	0.004
87	-15.0	0.40	0.145	20.660	29.890	7.496	17.049	-23.385	391.141	-36.388	0.0	0.001
88	-15.0	0.40	0.150	20.660	29.890	7.751	17.033	-23.429	391.125	-36.377	0.0	0.000
89	15.0	-0.10	0.020	20.660	29.890	-1.915	-3.774	138.244	-401.384	37.414	0.0	0.000
90	15.0	-0.02	0.020	20.660	29.890	-1.927	-2.988	137.903	-397.778	37.706	0.0	0.000

91	15.0	-0.06	0.020	20.660	29.890	-1.810	-2.109	137.984	-397.681	37.722	0.0	0.000
92	15.0	-0.04	0.020	20.660	29.890	-1.765	-1.235	138.141	-397.675	37.721	0.0	0.000
93	15.0	-0.02	0.020	20.660	29.890	-1.680	-0.442	138.062	-397.766	37.708	0.0	0.000
94	15.0	-0.00	0.020	20.660	29.890	-1.681	-0.486	137.831	-401.347	37.372	0.0	0.000
95	15.0	0.00	0.020	20.660	29.890	0.404	0.730	-23.837	-401.884	37.453	1.0	1.000
96	15.0	0.02	0.020	20.660	29.890	0.435	0.804	-23.851	-397.841	37.983	1.0	1.000
97	15.0	0.04	0.020	20.660	29.890	0.496	1.532	-23.839	-397.663	37.927	1.0	1.000
98	15.0	0.06	0.020	20.660	29.890	0.561	2.281	-23.856	-397.775	37.809	1.0	1.000
99	15.0	0.08	0.020	20.660	29.890	0.636	3.019	-23.906	-397.663	37.927	1.0	1.000
100	15.0	0.10	0.020	20.660	29.890	0.712	3.868	-23.907	-397.841	38.019	1.0	1.000
101	15.0	0.15	0.020	20.660	29.890	0.877	5.671	-23.892	-397.638	37.915	1.0	1.000
102	15.0	0.20	0.020	20.660	29.890	1.286	8.279	-23.918	-398.516	37.939	1.0	1.000
103	15.0	0.25	0.020	20.660	29.890	1.370	10.214	-23.922	-397.206	37.882	1.0	1.000
104	15.0	0.30	0.020	20.660	29.890	2.518	12.791	-23.910	-397.516	37.936	1.0	1.000
105	15.0	0.35	0.020	20.660	29.890	3.170	15.109	-23.952	-396.934	37.812	1.0	1.000
106	15.0	0.40	0.020	20.660	29.890	1.989	16.197	-23.944	-396.934	37.809	1.0	1.000
107	15.0	0.45	0.020	20.660	29.890	2.643	18.536	-23.937	-396.919	37.794	1.0	1.000
108	15.0	0.50	0.020	20.660	29.890	4.382	21.495	-23.834	-397.269	37.860	1.0	1.000
109	15.0	0.55	0.020	20.660	29.890	5.333	23.440	-24.001	-396.916	37.783	1.0	1.000
110	15.0	0.60	0.020	20.660	29.890	5.866	25.318	-24.002	-396.922	37.806	1.0	1.000
111	15.0	0.65	0.020	20.660	29.890	5.246	27.715	-24.003	-396.934	37.809	1.0	1.000
112	15.0	0.70	0.020	20.660	29.890	5.914	30.148	-24.016	-397.497	37.938	1.0	1.000
113	15.0	0.72	0.020	20.660	29.890	5.818	31.074	-23.942	-397.172	37.829	1.0	1.000
114	15.0	0.74	0.020	20.660	29.890	5.953	31.961	-23.902	-397.078	37.837	1.0	1.000
115	15.0	0.76	0.020	20.660	29.890	6.285	33.147	-23.947	-397.072	37.845	1.0	1.000
116	15.0	0.78	0.020	20.660	29.890	6.903	33.923	-23.883	-397.709	37.767	1.0	1.000
117	15.0	0.80	0.020	20.660	29.890	7.085	35.126	-23.951	-398.372	37.818	1.0	1.000
118	15.0	0.82	0.020	20.660	29.890	7.174	36.112	-23.969	-397.569	37.893	0.0	0.998
119	15.0	0.84	0.020	20.660	29.890	6.990	37.308	-23.986	-397.431	37.900	0.0	0.963
120	15.0	0.86	0.020	20.660	29.890	7.298	38.365	-23.983	-397.591	37.934	0.0	0.632
121	15.0	0.88	0.020	20.660	29.890	7.175	39.542	-23.780	-397.675	38.000	0.0	0.097
122	15.0	0.90	0.020	20.660	29.890	7.278	40.727	-23.556	-397.522	38.021	0.0	0.011
123	15.0	0.92	0.020	20.660	29.890	7.351	41.891	-23.574	-397.494	37.928	0.0	0.002
124	15.0	0.94	0.020	20.660	29.890	7.529	43.037	-24.053	-397.731	37.765	0.0	0.001
125	15.0	0.96	0.020	20.660	29.890	7.478	44.357	-23.819	-397.494	37.928	0.0	0.000
126	15.0	0.98	0.020	20.660	29.890	7.403	45.781	-23.881	-397.519	37.953	0.0	0.000
127	15.0	1.00	0.020	20.660	29.890	7.569	46.827	-24.019	-401.659	37.406	0.0	0.000
128	15.0	0.40	0.000	20.660	29.890	1.132	16.037	-23.868	-396.934	37.817	1.0	1.000
129	15.0	0.40	0.002	20.660	29.890	1.212	16.055	-23.865	-396.934	37.817	1.0	1.000

130	15.0	0.40	0.004	20.660	29.890	1.294	16.073	-23.866	-396.934	37.817	1.0	1.000
131	15.0	0.40	0.006	20.660	29.890	1.376	16.089	-23.867	-396.934	37.817	1.0	1.000
132	15.0	0.40	0.008	20.660	29.890	1.460	16.110	-23.863	-396.934	37.817	1.0	1.000
133	15.0	0.40	0.010	20.660	29.890	1.545	16.125	-23.877	-396.934	37.817	1.0	1.000
134	15.0	0.40	0.012	20.660	29.890	1.636	16.133	-23.914	-396.934	37.814	1.0	1.000
135	15.0	0.40	0.014	20.660	29.890	1.727	16.145	-23.916	-396.934	37.817	1.0	1.000
136	15.0	0.40	0.016	20.660	29.890	1.814	16.165	-23.912	-396.934	37.817	1.0	1.000
137	15.0	0.40	0.018	20.660	29.890	1.901	16.181	-23.929	-396.934	37.817	1.0	1.000
138	15.0	0.40	0.020	20.660	29.890	1.989	16.197	-23.944	-396.934	37.809	1.0	1.000
139	15.0	0.40	0.025	20.660	29.890	2.213	16.299	-23.778	-396.934	37.817	1.0	1.000
140	15.0	0.40	0.030	20.660	29.890	2.433	16.318	-23.867	-396.934	37.817	1.0	1.000
141	15.0	0.40	0.035	20.660	29.890	2.658	16.344	-23.925	-396.934	37.817	1.0	1.000
142	15.0	0.40	0.040	20.660	29.890	2.885	16.394	-23.911	-396.934	37.817	1.0	1.000
143	15.0	0.40	0.045	20.660	29.890	3.110	16.432	-23.935	-396.934	37.817	1.0	1.000
144	15.0	0.40	0.050	20.660	29.890	3.340	16.497	-23.886	-396.934	37.817	1.0	1.000
145	15.0	0.40	0.055	20.660	29.890	3.572	16.558	-23.901	-396.934	37.817	1.0	1.000
146	15.0	0.40	0.060	20.660	29.890	3.798	16.660	-23.906	-396.934	37.817	1.0	1.000
147	15.0	0.40	0.065	20.660	29.890	4.017	16.847	-23.486	-396.934	37.817	1.0	1.000
148	15.0	0.40	0.070	20.660	29.890	4.252	16.866	-23.540	-396.934	37.817	1.0	1.000
149	15.0	0.40	0.075	20.660	29.890	4.489	16.871	-23.688	-396.934	37.817	1.0	1.000
150	15.0	0.40	0.080	20.660	29.890	4.726	16.907	-23.736	-396.934	37.817	1.0	1.000
151	15.0	0.40	0.082	20.660	29.890	4.823	16.922	-23.745	-396.934	37.817	1.0	1.000
152	15.0	0.40	0.084	20.660	29.890	4.921	16.930	-23.770	-396.934	37.817	1.0	1.000
153	15.0	0.40	0.086	20.660	29.890	5.018	16.938	-23.801	-396.934	37.817	1.0	1.000
154	15.0	0.40	0.088	20.660	29.890	5.117	16.946	-23.838	-396.934	37.817	1.0	1.000
155	15.0	0.40	0.090	20.660	29.890	5.215	16.953	-23.874	-396.934	37.817	1.0	1.000
156	15.0	0.40	0.092	20.660	29.890	5.313	16.961	-23.907	-396.934	37.817	1.0	1.000
157	15.0	0.40	0.094	20.660	29.890	5.412	16.968	-23.938	-396.934	37.817	1.0	1.000
158	15.0	0.40	0.096	20.660	29.890	5.511	16.978	-23.964	-396.934	37.817	1.0	1.000
159	15.0	0.40	0.098	20.660	29.890	5.611	16.994	-23.982	-396.934	37.817	1.0	1.000
160	15.0	0.40	0.100	20.660	29.890	5.710	17.014	-23.993	-396.934	37.817	1.0	1.000
161	15.0	0.40	0.102	20.660	29.890	5.810	17.040	-23.996	-396.934	37.817	0.0	1.000
162	15.0	0.40	0.104	20.660	29.890	5.910	17.064	-23.989	-396.934	37.817	0.0	1.000
163	15.0	0.40	0.106	20.660	29.890	6.011	17.090	-23.980	-396.934	37.817	0.0	0.999
164	15.0	0.40	0.108	20.660	29.890	6.112	17.116	-23.974	-396.934	37.817	0.0	0.998
165	15.0	0.40	0.110	20.660	29.890	6.213	17.140	-23.987	-396.934	37.817	0.0	0.996
166	15.0	0.40	0.112	20.660	29.890	6.314	17.161	-24.014	-396.934	37.814	0.0	0.992
167	15.0	0.40	0.114	20.660	29.890	6.417	17.181	-24.061	-396.934	37.817	0.0	0.983
168	15.0	0.40	0.116	20.660	29.890	6.519	17.198	-24.123	-396.934	37.817	0.0	0.963
169	15.0	0.40	0.118	20.660	29.890	6.619	17.229	-24.177	-396.934	37.814	0.0	0.923



170	15.0	0.40	0.120	20.660	29.890	6.712	17.286	-24.166	-396.934	37.817	0.0	0.867
171	15.0	0.40	0.125	20.660	29.890	6.937	17.487	-23.887	-396.934	37.817	0.0	0.642
172	15.0	0.40	0.130	20.660	29.890	7.169	17.668	-23.534	-396.934	37.817	0.0	0.299
173	15.0	0.40	0.135	20.660	29.890	7.429	17.717	-23.483	-396.934	37.817	0.0	0.042
174	15.0	0.40	0.140	20.660	29.890	7.698	17.713	-23.643	-396.934	37.817	0.0	0.003
175	15.0	0.40	0.145	20.660	29.890	7.970	17.706	-23.832	-396.934	37.817	0.0	0.000
176	15.0	0.40	0.150	20.660	29.890	8.247	17.703	-23.991	-396.934	37.817	0.0	0.000
177	-15.0	-0.10	0.080	20.660	29.890	-8.840	-4.916	139.028	395.516	-37.362	0.0	0.005
178	-15.0	-0.08	0.080	20.660	29.890	-8.630	-4.517	137.744	392.244	-36.597	0.0	0.005
179	-15.0	-0.06	0.080	20.660	29.890	-8.293	-3.662	137.706	392.091	-36.466	0.0	0.004
180	-15.0	-0.04	0.080	20.660	29.890	-7.979	-2.764	137.775	392.091	-36.467	0.0	0.003
181	-15.0	-0.02	0.080	20.660	29.890	-7.690	-1.902	137.778	392.244	-36.598	0.0	0.003
182	-15.0	-0.00	0.080	20.660	29.890	-7.535	-1.793	137.788	395.516	-37.363	0.0	0.003
183	-15.0	0.00	0.080	20.660	29.890	1.674	0.850	-23.826	323.178	-23.504	1.0	0.893
184	-15.0	0.02	0.080	20.660	29.890	1.709	0.902	-23.841	391.284	-36.378	1.0	0.839
185	-15.0	0.04	0.080	20.660	29.890	1.823	1.640	-23.832	391.212	-36.406	1.0	0.933
186	-15.0	0.06	0.080	20.660	29.890	1.943	2.407	-23.826	391.850	-36.403	1.0	0.971
187	-15.0	0.08	0.080	20.660	29.890	2.058	3.168	-23.846	391.212	-36.406	1.0	0.987
188	-15.0	0.10	0.080	20.660	29.890	2.204	4.020	-23.871	391.300	-36.385	1.0	0.993
189	-15.0	0.15	0.080	20.660	29.890	2.468	5.839	-23.872	391.291	-36.383	1.0	0.998
190	-15.0	0.20	0.080	20.660	29.890	3.141	8.446	-23.944	392.187	-36.786	1.0	0.997
191	-15.0	0.25	0.080	20.660	29.890	3.340	10.445	-23.880	391.134	-36.450	1.0	1.000
192	-15.0	0.30	0.080	20.660	29.890	4.743	12.861	-23.920	391.237	-36.450	1.0	0.962
193	-15.0	0.35	0.080	20.660	29.890	5.577	15.103	-23.789	391.022	-36.461	1.0	0.943
194	-15.0	0.40	0.080	20.660	29.890	4.310	16.605	-23.613	391.125	-36.377	1.0	1.000
195	-15.0	0.45	0.080	20.660	29.890	5.143	18.888	-23.415	391.056	-36.466	1.0	1.000
196	-15.0	0.50	0.080	20.660	29.890	7.200	21.488	-23.197	391.175	-36.476	1.0	0.999
197	-15.0	0.55	0.080	20.660	29.890	8.220	23.036	-23.777	391.056	-36.466	1.0	0.992
198	-15.0	0.60	0.080	20.660	29.890	8.736	24.342	-24.754	391.159	-36.411	1.0	0.990
199	-15.0	0.65	0.080	20.660	29.890	8.380	27.269	-24.218	391.125	-36.426	1.0	1.000
200	-15.0	0.70	0.080	20.660	29.890	9.241	29.378	-24.581	391.303	-36.455	1.0	1.000
201	-15.0	0.72	0.080	20.660	29.890	9.246	30.373	-24.550	391.178	-36.476	1.0	1.000
202	-15.0	0.74	0.080	20.660	29.890	9.445	31.219	-24.517	391.178	-36.478	1.0	1.000
203	-15.0	0.76	0.080	20.660	29.890	9.894	32.265	-24.190	391.178	-36.479	1.0	0.998
204	-15.0	0.78	0.080	20.660	29.890	10.470	32.903	-24.303	391.828	-36.480	1.0	0.983
205	-15.0	0.80	0.080	20.660	29.890	10.762	34.049	-24.146	392.256	-36.840	1.0	0.866
206	-15.0	0.82	0.080	20.660	29.890	11.012	34.965	-24.072	391.541	-36.438	0.0	0.449
207	-15.0	0.84	0.080	20.660	29.890	11.033	36.181	-24.151	391.294	-36.479	0.0	0.086
208	-15.0	0.86	0.080	20.660	29.890	11.452	37.068	-24.196	391.469	-36.435	0.0	0.010

209	-15.0	0.88	0.080	20.660	29.890	11.517	38.247	-24.052	391.478	-36.452	0.0	0.001
210	-15.0	0.90	0.080	20.660	29.890	11.807	39.393	-23.677	391.475	-36.405	0.0	0.000
211	-15.0	0.92	0.080	20.660	29.890	12.112	40.568	-23.035	391.331	-36.457	0.0	0.000
212	-15.0	0.94	0.080	20.660	29.890	12.501	41.787	-22.789	392.175	-36.467	0.0	0.000
213	-15.0	0.96	0.080	20.660	29.890	12.757	42.825	-23.969	391.337	-36.459	0.0	0.000
214	-15.0	0.98	0.080	20.660	29.890	12.920	43.864	-24.504	391.459	-36.435	0.0	0.000
215	-15.0	1.00	0.080	20.660	29.890	13.178	44.874	-24.440	395.466	-37.358	0.0	0.000
216	15.0	-0.10	0.080	20.660	29.890	-8.090	-2.805	137.725	-401.384	37.413	0.0	0.000
217	15.0	-0.08	0.080	20.660	29.890	-7.917	-1.945	137.722	-397.775	37.707	0.0	0.000
218	15.0	-0.06	0.080	20.660	29.890	-7.659	-1.111	137.688	-397.681	37.725	0.0	0.000
219	15.0	-0.04	0.080	20.660	29.890	-7.395	-0.297	137.762	-397.681	37.722	0.0	0.000
220	15.0	-0.02	0.080	20.660	29.890	-7.171	0.467	137.837	-397.775	37.709	0.0	0.000
221	15.0	-0.00	0.080	20.660	29.890	-7.024	0.490	137.922	-401.347	37.373	0.0	0.000
222	15.0	0.00	0.080	20.660	29.890	1.673	1.040	-23.702	-323.969	37.162	1.0	0.981
223	15.0	0.02	0.080	20.660	29.890	1.702	1.050	-23.731	-397.841	37.983	1.0	0.963
224	15.0	0.04	0.080	20.660	29.890	1.832	1.841	-23.602	-397.663	37.927	1.0	0.984
225	15.0	0.06	0.080	20.660	29.890	1.969	2.614	-23.577	-397.775	37.808	1.0	0.992
226	15.0	0.08	0.080	20.660	29.890	2.109	3.378	-23.593	-397.663	37.927	1.0	0.995
227	15.0	0.10	0.080	20.660	29.890	2.265	4.240	-23.616	-397.841	38.019	1.0	0.997
228	15.0	0.15	0.080	20.660	29.890	2.605	6.047	-23.687	-397.638	37.915	1.0	0.999
229	15.0	0.20	0.080	20.660	29.890	3.267	8.733	-23.784	-398.516	37.939	1.0	0.999
230	15.0	0.25	0.080	20.660	29.890	3.529	10.743	-23.796	-397.206	37.882	1.0	1.000
231	15.0	0.30	0.080	20.660	29.890	4.978	13.297	-23.949	-397.516	37.936	1.0	0.988
232	15.0	0.35	0.080	20.660	29.890	5.875	15.624	-23.902	-396.934	37.812	1.0	0.979
233	15.0	0.40	0.080	20.660	29.890	4.726	16.907	-23.736	-396.934	37.817	1.0	1.000
234	15.0	0.45	0.080	20.660	29.890	5.619	19.244	-23.773	-396.919	37.794	1.0	1.000
235	15.0	0.50	0.080	20.660	29.890	7.726	22.124	-23.870	-397.244	37.850	1.0	1.000
236	15.0	0.55	0.080	20.660	29.890	8.958	24.252	-23.302	-396.916	37.783	1.0	0.992
237	15.0	0.60	0.080	20.660	29.890	9.718	26.153	-23.153	-396.934	37.806	1.0	0.985
238	15.0	0.65	0.080	20.660	29.890	9.278	28.743	-23.481	-396.934	37.809	1.0	1.000
239	15.0	0.70	0.080	20.660	29.890	10.235	31.205	-23.420	-397.497	37.938	1.0	1.000
240	15.0	0.72	0.080	20.660	29.890	10.235	32.172	-23.529	-397.172	37.829	1.0	1.000
241	15.0	0.74	0.080	20.660	29.890	10.474	33.078	-23.532	-397.078	37.837	1.0	1.000
242	15.0	0.76	0.080	20.660	29.890	10.988	34.173	-22.998	-397.072	37.845	1.0	0.998
243	15.0	0.78	0.080	20.660	29.890	11.697	34.964	-23.342	-397.709	37.767	1.0	0.951
244	15.0	0.80	0.080	20.660	29.890	12.039	36.219	-22.856	-398.375	37.821	1.0	0.566
245	15.0	0.82	0.080	20.660	29.890	12.295	37.228	-22.862	-397.569	37.941	0.0	0.129
246	15.0	0.84	0.080	20.660	29.890	12.267	38.498	-22.954	-397.437	37.897	0.0	0.026
247	15.0	0.86	0.080	20.660	29.890	12.767	39.537	-23.122	-397.591	37.934	0.0	0.002

248	15.0	0.88	0.080	20.660	29.890	12.799	40.729	-23.412	-397.675	38.000	0.0	0.001
249	15.0	0.90	0.080	20.660	29.890	13.068	41.850	-23.744	-397.522	38.021	0.0	0.000
250	15.0	0.92	0.080	20.660	29.890	13.312	42.918	-23.849	-397.494	37.928	0.0	0.000
251	15.0	0.94	0.080	20.660	29.890	13.698	44.166	-23.747	-397.731	37.765	0.0	0.000
252	15.0	0.96	0.080	20.660	29.890	13.891	45.509	-23.802	-397.494	37.928	0.0	0.000
253	15.0	0.98	0.080	20.660	29.890	14.036	47.007	-24.048	-397.519	37.953	0.0	0.000
254	15.0	1.00	0.080	20.660	29.890	14.342	48.095	-24.161	-401.659	37.406	0.0	0.000
1	-25.0	-0.10	0.020	20.660	29.890	-2.274	-4.631	137.887	238.172	-5.628	0.0	0.000
2	-25.0	-0.02	0.020	20.660	29.890	-2.164	-3.704	137.891	236.134	-5.158	0.0	0.000
3	-25.0	-0.06	0.020	20.660	29.890	-2.083	-2.798	138.072	235.950	-5.052	0.0	0.000
4	-25.0	-0.04	0.020	20.660	29.890	-1.927	-1.949	138.044	235.950	-5.051	0.0	0.000
5	-25.0	-0.02	0.020	20.660	29.890	-1.816	-1.245	137.859	236.131	-5.159	0.0	0.000
6	-25.0	-0.00	0.020	20.660	29.890	-1.793	-1.130	137.972	238.172	-5.647	0.0	0.000
7	-25.0	0.00	0.020	20.660	29.890	0.387	0.690	-23.861	238.122	-5.058	1.0	1.000
8	-25.0	0.02	0.020	20.660	29.890	0.422	0.770	-23.860	235.588	-5.025	1.0	1.000
9	-25.0	0.04	0.020	20.660	29.890	0.462	1.497	-23.865	235.572	-5.057	1.0	1.000
10	-25.0	0.06	0.020	20.660	29.890	0.502	2.254	-23.865	235.956	-5.104	1.0	1.000
11	-25.0	0.08	0.020	20.660	29.890	0.547	2.994	-23.915	235.572	-5.049	1.0	1.000
12	-25.0	0.10	0.020	20.660	29.890	0.606	3.847	-23.912	235.581	-5.013	1.0	1.000
13	-25.0	0.15	0.020	20.660	29.890	0.685	5.663	-23.899	235.559	-5.035	1.0	1.000
14	-25.0	0.20	0.020	20.660	29.890	1.098	8.264	-23.875	236.206	-5.022	1.0	1.000
15	-25.0	0.25	0.020	20.660	29.890	1.088	10.241	-23.846	235.434	-5.070	1.0	1.000
16	-25.0	0.30	0.020	20.660	29.890	2.215	12.670	-23.871	235.572	-5.064	1.0	1.000
17	-25.0	0.35	0.020	20.660	29.890	2.799	14.890	-23.873	235.447	-5.115	1.0	1.000
18	-25.0	0.40	0.020	20.660	29.890	1.382	16.243	-23.911	235.441	-5.128	1.0	1.000
19	-25.0	0.45	0.020	20.660	29.890	1.952	18.495	-23.891	235.437	-5.122	1.0	1.000
20	-25.0	0.50	0.020	20.660	29.890	3.684	21.098	-23.862	235.478	-5.095	1.0	1.000
21	-25.0	0.55	0.020	20.660	29.890	4.473	23.010	-23.709	235.437	-5.122	1.0	1.000
22	-25.0	0.60	0.020	20.660	29.890	4.800	24.762	-23.934	235.441	-5.127	1.0	1.000
23	-25.0	0.65	0.020	20.660	29.890	4.163	27.352	-23.903	235.447	-5.114	1.0	1.000
24	-25.0	0.70	0.020	20.660	29.890	4.690	29.565	-24.022	235.613	-5.058	1.0	1.000
25	-25.0	0.72	0.020	20.660	29.890	4.584	30.518	-24.024	235.491	-5.090	1.0	1.000
26	-25.0	0.74	0.020	20.660	29.890	4.658	31.397	-24.001	235.503	-5.082	1.0	1.000
27	-25.0	0.76	0.020	20.660	29.890	4.976	32.548	-23.913	235.484	-5.099	1.0	1.000
28	-25.0	0.78	0.020	20.660	29.890	5.436	33.148	-23.935	235.947	-5.082	1.0	1.000
29	-25.0	0.80	0.020	20.660	29.890	5.566	34.338	-23.928	236.253	-5.030	1.0	0.999
30	-25.0	0.82	0.020	20.660	29.890	5.698	35.299	-23.841	235.759	-5.007	0.0	0.990
31	-25.0	0.84	0.020	20.660	29.890	5.589	36.550	-23.733	235.641	-5.056	0.0	0.767
32	-25.0	0.86	0.020	20.660	29.890	5.875	37.504	-23.668	235.653	-5.020	0.0	0.226

33	-25.0	0.88	0.020	20.660	29.890	5.783	38.665	-23.971	235.772	-5.031	0.0	0.024
34	-25.0	0.90	0.020	20.660	29.890	5.887	39.738	-24.002	235.706	-5.004	0.0	0.003
35	-25.0	0.92	0.020	20.660	29.890	5.992	40.878	-24.001	235.622	-5.055	0.0	0.001
36	-25.0	0.94	0.020	20.660	29.890	6.197	42.102	-23.939	235.972	-5.104	0.0	0.000
37	-25.0	0.96	0.020	20.660	29.890	6.296	43.310	-24.064	235.609	-5.041	0.0	0.000
38	-25.0	0.98	0.020	20.660	29.890	6.385	44.851	-23.463	235.703	-5.011	0.0	0.000
39	-25.0	1.00	0.020	20.660	29.890	6.452	45.792	-23.931	238.159	-5.053	0.0	0.000
40	-25.0	0.40	0.000	20.660	29.890	0.498	16.223	-23.875	235.441	-5.128	1.0	1.000
41	-25.0	0.40	0.002	20.660	29.890	0.582	16.223	-23.877	235.441	-5.128	1.0	1.000
42	-25.0	0.40	0.004	20.660	29.890	0.669	16.225	-23.879	235.441	-5.128	1.0	1.000
43	-25.0	0.40	0.006	20.660	29.890	0.755	16.229	-23.886	235.441	-5.128	1.0	1.000
44	-25.0	0.40	0.008	20.660	29.890	0.847	16.250	-23.859	235.441	-5.128	1.0	1.000
45	-25.0	0.40	0.010	20.660	29.890	0.937	16.259	-23.831	235.441	-5.128	1.0	1.000
46	-25.0	0.40	0.012	20.660	29.890	1.025	16.254	-23.856	235.441	-5.128	1.0	1.000
47	-25.0	0.40	0.014	20.660	29.890	1.115	16.244	-23.885	235.441	-5.128	1.0	1.000
48	-25.0	0.40	0.016	20.660	29.890	1.204	16.242	-23.897	235.441	-5.128	1.0	1.000
49	-25.0	0.40	0.018	20.660	29.890	1.292	16.241	-23.906	235.441	-5.128	1.0	1.000
50	-25.0	0.40	0.020	20.660	29.890	1.382	16.243	-23.911	235.441	-5.128	1.0	1.000
51	-25.0	0.40	0.025	20.660	29.890	1.608	16.255	-23.878	235.441	-5.128	1.0	1.000
52	-25.0	0.40	0.030	20.660	29.890	1.836	16.272	-23.852	235.441	-5.128	1.0	1.000
53	-25.0	0.40	0.035	20.660	29.890	2.067	16.293	-23.852	235.441	-5.128	1.0	1.000
54	-25.0	0.40	0.040	20.660	29.890	2.309	16.362	-23.827	235.441	-5.128	1.0	1.000
55	-25.0	0.40	0.045	20.660	29.890	2.554	16.377	-23.743	235.441	-5.128	1.0	1.000
56	-25.0	0.40	0.050	20.660	29.890	2.786	16.307	-23.948	235.441	-5.128	1.0	1.000
57	-25.0	0.40	0.055	20.660	29.890	3.021	16.268	-24.054	235.441	-5.128	1.0	1.000
58	-25.0	0.40	0.060	20.660	29.890	3.258	16.270	-24.036	235.441	-5.128	1.0	1.000
59	-25.0	0.40	0.065	20.660	29.890	3.490	16.245	-24.100	235.441	-5.128	1.0	1.000
60	-25.0	0.40	0.070	20.660	29.890	3.725	16.231	-24.142	235.441	-5.128	1.0	1.000
61	-25.0	0.40	0.075	20.660	29.890	3.967	16.244	-24.122	235.441	-5.128	1.0	1.000
62	-25.0	0.40	0.080	20.660	29.890	4.211	16.255	-24.117	235.441	-5.128	1.0	1.000
63	-25.0	0.40	0.082	20.660	29.890	4.307	16.257	-24.156	235.441	-5.128	1.0	1.000
64	-25.0	0.40	0.084	20.660	29.890	4.403	16.254	-24.211	235.441	-5.128	1.0	1.000
65	-25.0	0.40	0.086	20.660	29.890	4.499	16.259	-24.260	235.441	-5.128	1.0	1.000
66	-25.0	0.40	0.088	20.660	29.890	4.597	16.302	-24.232	235.441	-5.128	1.0	1.000
67	-25.0	0.40	0.090	20.660	29.890	4.697	16.371	-24.105	235.441	-5.128	1.0	1.000
68	-25.0	0.40	0.092	20.660	29.890	4.797	16.446	-23.928	235.441	-5.128	1.0	1.000
69	-25.0	0.40	0.094	20.660	29.890	4.897	16.501	-23.755	235.441	-5.128	1.0	1.000
70	-25.0	0.40	0.096	20.660	29.890	4.995	16.517	-23.659	235.441	-5.128	1.0	1.000
71	-25.0	0.40	0.098	20.660	29.890	5.091	16.513	-23.660	235.441	-5.128	1.0	1.000

72	-25.0	0.40	0.100	20.660	29.890	5.186	16.495	-23.715	235.441	-5.128	1.0	1.000
73	-25.0	0.40	0.102	20.660	29.890	5.279	16.477	-23.795	235.441	-5.128	0.0	1.000
74	-25.0	0.40	0.104	20.660	29.890	5.374	16.461	-23.873	235.441	-5.128	0.0	1.000
75	-25.0	0.40	0.106	20.660	29.890	5.469	16.454	-23.926	235.441	-5.128	0.0	0.999
76	-25.0	0.40	0.108	20.660	29.890	5.565	16.452	-23.953	235.441	-5.128	0.0	0.999
77	-25.0	0.40	0.110	20.660	29.890	5.661	16.452	-23.966	235.441	-5.128	0.0	0.998
78	-25.0	0.40	0.112	20.660	29.890	5.758	16.451	-23.979	235.441	-5.128	0.0	0.996
79	-25.0	0.40	0.114	20.660	29.890	5.854	16.445	-24.004	235.441	-5.128	0.0	0.992
80	-25.0	0.40	0.116	20.660	29.890	5.949	16.442	-24.034	235.441	-5.128	0.0	0.983
81	-25.0	0.40	0.118	20.660	29.890	6.047	16.438	-24.061	235.441	-5.128	0.0	0.965
82	-25.0	0.40	0.120	20.660	29.890	6.143	16.438	-24.088	235.441	-5.128	0.0	0.927
83	-25.0	0.40	0.125	20.660	29.890	6.386	16.444	-24.124	235.441	-5.128	0.0	0.639
84	-25.0	0.40	0.130	20.660	29.890	6.633	16.457	-24.130	235.441	-5.128	0.0	0.178
85	-25.0	0.40	0.135	20.660	29.890	6.880	16.488	-24.100	235.441	-5.128	0.0	0.024
86	-25.0	0.40	0.140	20.660	29.890	7.131	16.558	-23.991	235.441	-5.128	0.0	0.003
87	-25.0	0.40	0.145	20.660	29.890	7.386	16.646	-23.798	235.441	-5.128	0.0	0.000
88	-25.0	0.40	0.150	20.660	29.890	7.643	16.723	-23.631	235.441	-5.128	0.0	0.000
89	25.0	-0.10	0.020	20.660	29.890	-1.865	-3.752	137.825	-236.419	39.158	0.0	0.000
90	25.0	-0.02	0.020	20.660	29.890	-1.796	-2.763	138.072	-234.356	39.565	0.0	0.000
91	25.0	-0.06	0.020	20.660	29.890	-1.747	-1.929	138.016	-234.256	39.620	0.0	0.000
92	25.0	-0.04	0.020	20.660	29.890	-1.664	-1.102	138.062	-234.256	39.621	0.0	0.000
93	25.0	-0.02	0.020	20.660	29.890	-1.685	-0.398	137.794	-234.347	39.558	0.0	0.000
94	25.0	-0.00	0.020	20.660	29.890	-1.619	-0.266	137.984	-236.412	39.132	0.0	0.000
95	25.0	0.00	0.020	20.660	29.890	0.413	0.725	-23.872	-236.622	39.798	1.0	1.000
96	25.0	0.02	0.020	20.660	29.890	0.442	0.801	-23.880	-234.038	39.531	1.0	1.000
97	25.0	0.04	0.020	20.660	29.890	0.513	1.532	-23.872	-234.031	39.570	1.0	1.000
98	25.0	0.06	0.020	20.660	29.890	0.584	2.282	-23.872	-234.290	39.599	1.0	1.000
99	25.0	0.08	0.020	20.660	29.890	0.660	3.034	-23.886	-234.031	39.568	1.0	1.000
100	25.0	0.10	0.020	20.660	29.890	0.738	3.884	-23.883	-234.038	39.540	1.0	1.000
101	25.0	0.15	0.020	20.660	29.890	0.923	5.692	-23.865	-234.025	39.562	1.0	1.000
102	25.0	0.20	0.020	20.660	29.890	1.337	8.352	-23.778	-234.700	39.611	1.0	1.000
103	25.0	0.25	0.020	20.660	29.890	1.441	10.293	-23.797	-233.878	39.538	1.0	1.000
104	25.0	0.30	0.020	20.660	29.890	2.587	12.891	-23.882	-234.022	39.571	1.0	1.000
105	25.0	0.35	0.020	20.660	29.890	3.248	15.214	-23.876	-233.828	39.571	1.0	1.000
106	25.0	0.40	0.020	20.660	29.890	2.143	16.263	-23.861	-233.828	39.535	1.0	1.000
107	25.0	0.45	0.020	20.660	29.890	2.809	18.593	-23.893	-233.759	39.544	1.0	1.000
108	25.0	0.50	0.020	20.660	29.890	4.530	21.606	-23.894	-233.847	39.521	1.0	1.000
109	25.0	0.55	0.020	20.660	29.890	5.520	23.697	-23.865	-233.759	39.542	1.0	1.000
110	25.0	0.60	0.020	20.660	29.890	6.111	25.624	-23.827	-233.822	39.529	1.0	1.000

111	25.0	0.65	0.020	20.660	29.890	5.500	27.986	-23.788	-233.812	39.566	1.0	1.000
112	25.0	0.70	0.020	20.660	29.890	6.187	30.458	-23.800	-234.006	39.539	1.0	1.000
113	25.0	0.72	0.020	20.660	29.890	6.102	31.361	-23.802	-233.837	39.514	1.0	1.000
114	25.0	0.74	0.020	20.660	29.890	6.252	32.256	-23.788	-233.844	39.535	1.0	1.000
115	25.0	0.76	0.020	20.660	29.890	6.577	33.453	-23.773	-233.828	39.510	1.0	1.000
116	25.0	0.78	0.020	20.660	29.890	7.231	34.278	-23.722	-234.262	39.602	1.0	1.000
117	25.0	0.80	0.020	20.660	29.890	7.400	35.522	-23.696	-234.625	39.571	1.0	1.000
118	25.0	0.82	0.020	20.660	29.890	7.474	36.526	-23.717	-234.006	39.514	0.0	0.997
119	25.0	0.84	0.020	20.660	29.890	7.283	37.712	-23.700	-233.978	39.510	0.0	0.927
120	25.0	0.86	0.020	20.660	29.890	7.605	38.762	-23.810	-234.019	39.502	0.0	0.497
121	25.0	0.88	0.020	20.660	29.890	7.480	39.831	-23.821	-234.062	39.525	0.0	0.088
122	25.0	0.90	0.020	20.660	29.890	7.575	40.982	-23.936	-234.012	39.490	0.0	0.013
123	25.0	0.92	0.020	20.660	29.890	7.620	42.146	-23.996	-233.991	39.520	0.0	0.003
124	25.0	0.94	0.020	20.660	29.890	7.820	43.444	-23.984	-234.284	39.577	0.0	0.001
125	25.0	0.96	0.020	20.660	29.890	7.736	44.749	-23.912	-234.006	39.539	0.0	0.000
126	25.0	0.98	0.020	20.660	29.890	7.592	46.136	-23.872	-234.019	39.501	0.0	0.000
127	25.0	1.00	0.020	20.660	29.890	7.800	47.254	-23.729	-236.538	39.798	0.0	0.000
128	25.0	0.40	0.000	20.660	29.890	1.297	16.042	-23.865	-233.828	39.534	1.0	1.000
129	25.0	0.40	0.002	20.660	29.890	1.377	16.061	-23.866	-233.828	39.534	1.0	1.000
130	25.0	0.40	0.004	20.660	29.890	1.459	16.083	-23.863	-233.828	39.534	1.0	1.000
131	25.0	0.40	0.006	20.660	29.890	1.542	16.105	-23.868	-233.828	39.535	1.0	1.000
132	25.0	0.40	0.008	20.660	29.890	1.627	16.122	-23.899	-233.828	39.535	1.0	1.000
133	25.0	0.40	0.010	20.660	29.890	1.717	16.159	-23.870	-233.828	39.535	1.0	1.000
134	25.0	0.40	0.012	20.660	29.890	1.803	16.191	-23.827	-233.828	39.534	1.0	1.000
135	25.0	0.40	0.014	20.660	29.890	1.887	16.208	-23.834	-233.828	39.534	1.0	1.000
136	25.0	0.40	0.016	20.660	29.890	1.972	16.226	-23.845	-233.828	39.534	1.0	1.000
137	25.0	0.40	0.018	20.660	29.890	2.057	16.244	-23.851	-233.828	39.534	1.0	1.000
138	25.0	0.40	0.020	20.660	29.890	2.143	16.263	-23.861	-233.828	39.535	1.0	1.000
139	25.0	0.40	0.025	20.660	29.890	2.359	16.329	-23.838	-233.828	39.534	1.0	1.000
140	25.0	0.40	0.030	20.660	29.890	2.580	16.377	-23.874	-233.828	39.534	1.0	1.000
141	25.0	0.40	0.035	20.660	29.890	2.818	16.423	-23.944	-233.828	39.534	1.0	1.000
142	25.0	0.40	0.040	20.660	29.890	3.064	16.445	-24.083	-233.828	39.530	1.0	1.000
143	25.0	0.40	0.045	20.660	29.890	3.282	16.625	-23.790	-233.828	39.534	1.0	1.000
144	25.0	0.40	0.050	20.660	29.890	3.512	16.661	-23.800	-233.828	39.536	1.0	1.000
145	25.0	0.40	0.055	20.660	29.890	3.746	16.680	-23.910	-233.828	39.534	1.0	1.000
146	25.0	0.40	0.060	20.660	29.890	3.981	16.722	-23.955	-233.828	39.536	1.0	1.000
147	25.0	0.40	0.065	20.660	29.890	4.220	16.762	-23.992	-233.828	39.534	1.0	1.000
148	25.0	0.40	0.070	20.660	29.890	4.460	16.792	-24.061	-233.828	39.534	1.0	1.000
149	25.0	0.40	0.075	20.660	29.890	4.702	16.843	-24.095	-233.831	39.535	1.0	1.000

150	25.0	0.40	0.080	20.660	29.890	4.944	16.919	-24.066	-233.828	39.536	1.0	1.000
151	25.0	0.40	0.082	20.660	29.890	5.042	16.949	-24.055	-233.828	39.534	1.0	1.000
152	25.0	0.40	0.084	20.660	29.890	5.140	16.979	-24.065	-233.828	39.534	1.0	1.000
153	25.0	0.40	0.086	20.660	29.890	5.238	17.005	-24.099	-233.828	39.536	1.0	1.000
154	25.0	0.40	0.088	20.660	29.890	5.337	17.028	-24.156	-233.828	39.536	1.0	1.000
155	25.0	0.40	0.090	20.660	29.890	5.435	17.052	-24.210	-233.828	39.537	1.0	1.000
156	25.0	0.40	0.092	20.660	29.890	5.525	17.112	-24.208	-233.828	39.534	1.0	1.000
157	25.0	0.40	0.094	20.660	29.890	5.609	17.202	-24.102	-233.828	39.535	1.0	1.000
158	25.0	0.40	0.096	20.660	29.890	5.691	17.302	-23.930	-233.828	39.536	1.0	1.000
159	25.0	0.40	0.098	20.660	29.890	5.776	17.395	-23.741	-233.828	39.534	1.0	1.000
160	25.0	0.40	0.100	20.660	29.890	5.866	17.459	-23.591	-233.828	39.534	1.0	1.000
161	25.0	0.40	0.102	20.660	29.890	5.965	17.487	-23.539	-233.828	39.534	0.0	1.000
162	25.0	0.40	0.104	20.660	29.890	6.067	17.501	-23.568	-233.828	39.536	0.0	1.000
163	25.0	0.40	0.106	20.660	29.890	6.169	17.505	-23.633	-233.828	39.534	0.0	0.999
164	25.0	0.40	0.108	20.660	29.890	6.273	17.510	-23.715	-233.828	39.534	0.0	0.998
165	25.0	0.40	0.110	20.660	29.890	6.376	17.517	-23.788	-233.828	39.535	0.0	0.995
166	25.0	0.40	0.112	20.660	29.890	6.479	17.529	-23.848	-233.828	39.536	0.0	0.989
167	25.0	0.40	0.114	20.660	29.890	6.582	17.543	-23.892	-233.828	39.534	0.0	0.976
168	25.0	0.40	0.116	20.660	29.890	6.686	17.557	-23.930	-233.828	39.530	0.0	0.946
169	25.0	0.40	0.118	20.660	29.890	6.792	17.569	-23.971	-233.828	39.530	0.0	0.878
170	25.0	0.40	0.120	20.660	29.890	6.897	17.583	-24.017	-233.828	39.534	0.0	0.748
171	25.0	0.40	0.125	20.660	29.890	7.162	17.623	-24.135	-233.828	39.534	0.0	0.226
172	25.0	0.40	0.130	20.660	29.890	7.424	17.682	-24.228	-233.828	39.534	0.0	0.028
173	25.0	0.40	0.135	20.660	29.890	7.684	17.758	-24.280	-233.828	39.535	0.0	0.003
174	25.0	0.40	0.140	20.660	29.890	7.941	17.850	-24.284	-233.828	39.530	0.0	0.000
175	25.0	0.40	0.145	20.660	29.890	8.196	17.974	-24.234	-233.828	39.534	0.0	0.000
176	25.0	0.40	0.150	20.660	29.890	8.443	18.141	-24.080	-233.828	39.534	0.0	0.000
177	-25.0	-0.10	0.080	20.660	29.890	-8.940	-6.188	138.491	238.172	-5.628	0.0	0.000
178	-25.0	-0.08	0.080	20.660	29.890	-8.715	-5.222	138.578	236.134	-5.158	0.0	0.000
179	-25.0	-0.06	0.080	20.660	29.890	-8.357	-4.252	138.631	235.950	-5.052	0.0	0.000
180	-25.0	-0.04	0.080	20.660	29.890	-7.986	-3.704	137.734	235.950	-5.053	0.0	0.000
181	-25.0	-0.02	0.080	20.660	29.890	-7.666	-3.009	137.163	236.131	-5.159	0.0	0.000
182	-25.0	-0.00	0.080	20.660	29.890	-7.524	-2.886	137.113	238.172	-5.647	0.0	0.000
183	-25.0	0.00	0.080	20.660	29.890	1.669	0.849	-23.696	238.122	-5.058	1.0	0.883
184	-25.0	0.02	0.080	20.660	29.890	1.711	0.925	-23.692	235.588	-5.025	1.0	0.870
185	-25.0	0.04	0.080	20.660	29.890	1.820	1.669	-23.651	235.572	-5.057	1.0	0.952
186	-25.0	0.06	0.080	20.660	29.890	1.935	2.441	-23.603	235.956	-5.104	1.0	0.982
187	-25.0	0.08	0.080	20.660	29.890	2.047	3.192	-23.622	235.572	-5.053	1.0	0.992
188	-25.0	0.10	0.080	20.660	29.890	2.194	4.025	-23.666	235.581	-5.013	1.0	0.996

189	-25.0	0.15	0.080	20.660	29.890	2.445	5.871	-23.550	235.559	-5.035	1.0	0.999
190	-25.0	0.20	0.080	20.660	29.890	3.118	8.485	-23.485	236.206	-5.022	1.0	0.999
191	-25.0	0.25	0.080	20.660	29.890	3.291	10.408	-23.622	235.434	-5.070	1.0	1.000
192	-25.0	0.30	0.080	20.660	29.890	4.676	12.847	-23.588	235.572	-5.064	1.0	0.985
193	-25.0	0.35	0.080	20.660	29.890	5.483	14.928	-23.921	235.447	-5.115	1.0	0.969
194	-25.0	0.40	0.080	20.660	29.890	4.211	16.255	-24.117	235.441	-5.128	1.0	1.000
195	-25.0	0.45	0.080	20.660	29.890	5.001	18.419	-24.287	235.437	-5.122	1.0	1.000
196	-25.0	0.50	0.080	20.660	29.890	6.962	20.764	-24.570	235.478	-5.095	1.0	1.000
197	-25.0	0.55	0.080	20.660	29.890	7.933	22.575	-24.061	235.437	-5.122	1.0	0.998
198	-25.0	0.60	0.080	20.660	29.890	8.497	24.494	-23.440	235.441	-5.127	1.0	0.999
199	-25.0	0.65	0.080	20.660	29.890	8.139	27.180	-23.703	235.447	-5.114	1.0	1.000
200	-25.0	0.70	0.080	20.660	29.890	8.910	29.415	-23.371	235.613	-5.058	1.0	1.000
201	-25.0	0.72	0.080	20.660	29.890	8.906	30.372	-23.404	235.488	-5.090	1.0	1.000
202	-25.0	0.74	0.080	20.660	29.890	9.071	31.218	-23.272	235.503	-5.082	1.0	1.000
203	-25.0	0.76	0.080	20.660	29.890	9.505	32.017	-23.343	235.494	-5.097	1.0	1.000
204	-25.0	0.78	0.080	20.660	29.890	10.037	32.816	-23.035	235.947	-5.082	1.0	0.999
205	-25.0	0.80	0.080	20.660	29.890	10.259	33.581	-23.821	236.253	-5.030	1.0	0.997
206	-25.0	0.82	0.080	20.660	29.890	10.483	34.343	-23.943	235.759	-5.007	0.0	0.986
207	-25.0	0.84	0.080	20.660	29.890	10.526	35.546	-24.146	235.641	-5.057	0.0	0.898
208	-25.0	0.86	0.080	20.660	29.890	10.925	36.363	-24.393	235.653	-5.010	0.0	0.509
209	-25.0	0.88	0.080	20.660	29.890	11.000	37.493	-24.485	235.772	-5.031	0.0	0.099
210	-25.0	0.90	0.080	20.660	29.890	11.276	38.544	-24.492	235.703	-5.004	0.0	0.012
211	-25.0	0.92	0.080	20.660	29.890	11.545	39.593	-24.431	235.609	-5.057	0.0	0.002
212	-25.0	0.94	0.080	20.660	29.890	11.897	40.752	-24.302	235.972	-5.104	0.0	0.000
213	-25.0	0.96	0.080	20.660	29.890	12.188	41.907	-24.387	235.609	-5.041	0.0	0.000
214	-25.0	0.98	0.080	20.660	29.890	12.432	43.222	-24.398	235.703	-5.011	0.0	0.000
215	-25.0	1.00	0.080	20.660	29.890	12.719	44.380	-23.667	238.159	-5.053	0.0	0.000
216	25.0	-0.10	0.080	20.660	29.890	-7.750	-1.850	138.466	-236.419	39.158	0.0	0.000
217	25.0	-0.08	0.080	20.660	29.890	-7.557	-0.978	138.400	-234.347	39.557	0.0	0.000
218	25.0	-0.06	0.080	20.660	29.890	-7.306	-0.168	138.553	-234.256	39.620	0.0	0.000
219	25.0	-0.04	0.080	20.660	29.890	-7.249	0.220	137.478	-234.256	39.621	0.0	0.000
220	25.0	-0.02	0.080	20.660	29.890	-7.110	0.848	137.216	-234.347	39.558	0.0	0.000
221	25.0	-0.00	0.080	20.660	29.890	-6.962	0.871	137.378	-236.412	39.132	0.0	0.000
222	25.0	0.00	0.080	20.660	29.890	1.686	1.009	-23.795	-236.622	39.797	1.0	0.971
223	25.0	0.02	0.080	20.660	29.890	1.722	1.087	-23.790	-234.038	39.532	1.0	0.968
224	25.0	0.04	0.080	20.660	29.890	1.862	1.827	-23.778	-234.031	39.570	1.0	0.984
225	25.0	0.06	0.080	20.660	29.890	2.006	2.595	-23.798	-234.287	39.598	1.0	0.991
226	25.0	0.08	0.080	20.660	29.890	2.153	3.367	-23.839	-234.031	39.566	1.0	0.995
227	25.0	0.10	0.080	20.660	29.890	2.315	4.237	-23.869	-234.038	39.540	1.0	0.997



---

228	25.0	0.15	0.080	20.660	29.890	2.677	6.079	-23.903	-234.025	39.562	1.0	0.999
229	25.0	0.20	0.080	20.660	29.890	3.353	8.761	-23.975	-234.722	39.629	1.0	0.998
230	25.0	0.25	0.080	20.660	29.890	3.644	10.761	-23.968	-233.878	39.538	1.0	1.000
231	25.0	0.30	0.080	20.660	29.890	5.090	13.385	-23.976	-234.022	39.571	1.0	0.975
232	25.0	0.35	0.080	20.660	29.890	6.005	15.749	-23.988	-233.828	39.571	1.0	0.952
233	25.0	0.40	0.080	20.660	29.890	4.944	16.919	-24.066	-233.828	39.536	1.0	1.000
234	25.0	0.45	0.080	20.660	29.890	5.869	19.311	-24.292	-233.759	39.544	1.0	1.000
235	25.0	0.50	0.080	20.660	29.890	7.968	22.312	-24.408	-233.847	39.521	1.0	0.999
236	25.0	0.55	0.080	20.660	29.890	9.245	24.174	-24.750	-233.759	39.542	1.0	0.884
237	25.0	0.60	0.080	20.660	29.890	9.976	26.138	-24.654	-233.822	39.529	1.0	0.871
238	25.0	0.65	0.080	20.660	29.890	9.623	28.848	-24.568	-233.828	39.568	1.0	1.000
239	25.0	0.70	0.080	20.660	29.890	10.639	31.386	-24.615	-234.006	39.539	1.0	1.000
240	25.0	0.72	0.080	20.660	29.890	10.614	32.444	-24.471	-233.837	39.514	1.0	1.000
241	25.0	0.74	0.080	20.660	29.890	10.860	33.400	-24.407	-233.844	39.535	1.0	0.999
242	25.0	0.76	0.080	20.660	29.890	11.423	34.453	-24.484	-233.825	39.506	1.0	0.993
243	25.0	0.78	0.080	20.660	29.890	12.159	35.385	-24.491	-234.262	39.602	1.0	0.772
244	25.0	0.80	0.080	20.660	29.890	12.540	36.544	-24.529	-234.625	39.570	1.0	0.207
245	25.0	0.82	0.080	20.660	29.890	12.764	37.593	-24.496	-234.006	39.514	0.0	0.036
246	25.0	0.84	0.080	20.660	29.890	12.712	38.874	-24.505	-233.978	39.513	0.0	0.011
247	25.0	0.86	0.080	20.660	29.890	13.216	39.993	-24.527	-234.019	39.499	0.0	0.001
248	25.0	0.88	0.080	20.660	29.890	13.232	41.235	-24.538	-234.062	39.521	0.0	0.000
249	25.0	0.90	0.080	20.660	29.890	13.484	42.483	-24.514	-234.012	39.490	0.0	0.000
250	25.0	0.92	0.080	20.660	29.890	13.693	43.779	-24.507	-233.991	39.520	0.0	0.000
251	25.0	0.94	0.080	20.660	29.890	14.029	45.274	-24.380	-234.272	39.577	0.0	0.000
252	25.0	0.96	0.080	20.660	29.890	14.105	46.777	-23.749	-234.006	39.539	0.0	0.000
253	25.0	0.98	0.080	20.660	29.890	14.142	48.391	-23.333	-234.019	39.501	0.0	0.000
254	25.0	1.00	0.080	20.660	29.890	14.451	49.473	-23.502	-236.538	39.798	0.0	0.000